8-2017

Efficient Numerical Methods for Magnetohydrodynamic Flow

Muhammad Mohebujjaman
Clemson University, mmohebu@g.clemson.edu

Efficient Numerical Methods for Magnetohydrodynamic Flow

A Thesis
Presented to
the Graduate School of
Clemson University

In Partial Fulfillment
of the Requirements for the Degree
Doctor of Philosophy
Mathematical sciences

---

by
Muhammad Mohebujjaman
August 2017

Accepted by:
Dr. Leo Rebholz, Committee Chair
Dr. Timo Heister, Co-chair
Dr. Hyesuk Lee
Dr. Qingshan Chen

Dedicated To

My Parents and Beloved Wife.

Abstract

This dissertation studies efficient numerical methods for approximating solutions to viscous, incompressible, time-dependent magnetohydrodynamic (MHD) flows and computing MHD flows ensembles.

Chapter 3 presents and analyzes a fully discrete, decoupled efficient algorithm for MHD flow that is based on the Elsässer variable formulation, proves its unconditional stability with respect to the timestep size, and proves its unconditional convergence. Numerical experiments are given which verify all predicted convergence rates of our analysis, show the results of the scheme on a set of channel flow problems match well the results found when the computation is done with MHD in primitive variables, and finally illustrate that the scheme performs well for channel flow over a step.

In chapter 4, we propose, analyze, and test a new MHD discretization which decouples the system into two Oseen problems at each timestep, yet maintains unconditional stability with respect to timestep size. The scheme is optimally accurate in space, and behaves like second order in time in practice. The proposed method chooses $\theta \in [0, 1]$, dependent on the viscosity ν and magnetic diffusivity ν_m, so that unconditionally stability is achieved, and gives temporal accuracy $O(\Delta t^2 + (1-\theta)|\nu - \nu_m|\Delta t)$. In practice, ν and ν_m are small, and so the method behaves like second order. We show the θ-method provides excellent accuracy in cases

where usual BDF2 is unstable.

Chapter 5 proposes an efficient algorithm and studies for computing flow ensembles of incompressible MHD flows under uncertainties in initial or boundary data. The ensemble average of J realizations is approximated through an efficient algorithm that, at each time step, uses the same coefficient matrix for each of the J system solves. Hence, preconditioners need to be built only once per time step, and the algorithm can take advantage of block linear solvers. Additionally, an Elsässer variable formulation is used, which allows for a stable decoupling of each MHD system at each time step. We prove stability and convergence of the algorithm, and test it with two numerical experiments.

This work concludes with chapter 6, which proposes, analyzes and tests high order algebraic splitting methods for MHD flows. The key idea is to applying Yosida-type algebraic splitting to the incremental part of the unknowns at each time step. This reduces the block Schur complement by decoupling it into two Navier-Stokes-type Schur complements, each of which is symmetric positive definite and the same at each time step. We prove the splitting is third order in Δt, and if used together with (block-)pressure correction, is fourth order. A full analysis of the solver is given, both as a linear algebraic approximation, and as a finite element discretization of an approximation to the un-split discrete system. Numerical tests are given to illustrate the theory and show the effectiveness of the method.

Finally, conclusions and future works are discussed in the final chapter.

Acknowledgments

The Ph.D. research work presented in this thesis has been carried in the Department of Mathematical Sciences at Clemson University under the supervision of Dr. Leo G. Rebholz. The author was partially supported by the National Science Foundation (NSF).

First of all, I would like to pay homage to my supervisor Dr. Rebholz for giving me the continuous motivation, support, and encouragement to explore new ideas throughout over the past five years. Dr. Rebholz, it has been a great pleasure to work with you. You have always shown much interest whatever I presented you and helped me sharing your knowledge in improving my works. I owe much of my success in this thesis to you.

I would like thank to Dr. Timo Heister, his inspiration and support helped me in learning Dealii. I learned a lot from his course, office hours and group research meeting.

I am greatly indebted to my family. My parents have supported my education. Many thanks goes to my wife Kamronnaher, without her help, support and inspiration, it would be impossible.

I am also thankful for my committee members Dr. Hyesuk Lee and Dr. Qingshan Chen. I have learned a lot from their courses as well as our conversations.

I would like to thank all of my, professors, and friends who helped me over the

past five years. Your support and encouragement made this possible.

I would like to express my gratitude to the Mathematical Sciences Department, Clemson University and Dr. Rebholz for their financial support during this study.

I recall with a deep sense of gratitude to the Clemson University for providing me the computing facilities in Palmetto Super Computer.

I would like to thank my friend Javier Ruiz Ramirez for our brainstorm conversations.

Lastly, I want to give thanks to my collaborators Mine Akbas and Mengying Xiao. Chapter 3 is a joint work with Mine Akbas and Leo Rebholz. Chapter 4 is a joint work with Timo Heister and Leo Rebholz. Chapter 6 is a collaborative work with Mine Akbas, Mengying Xiao and Leo Rebholz.

Table of Contents

List of Tables

List of Figures

Chapter 1

Introduction

1.1 Motivation

The study of fluid flow has a wide range of applications in many scientific and engineering fields such as aerodynamics, weather prediction, astrophysics, traffic engineering, petroleum engineering, and ocean current modeling. For these problems, the determination of forces and moments on aircraft, predicting weather patterns, understanding of nebulae in interstellar space and estimation the mass flow rate of petroleum through pipelines, are critically important.

The incompressible Navier-Stokes equations (NSE) are the basis for simulating flows in computational modeling, and are widely believed to be the accurate physical model. Even though from an analytical point of view, a large number of mathematicians and scientists have been investigating these equations for the last 160 years, [37, 58, 92, 93], a complete understanding of them and their fundamental solution properties is still unknown, and remains a $1 million Clay Prize Problem [4]. From the computational side, to obtain an accurate numerical simulation, very high number of degrees of freedom (dof) are needed, which is known from Kolmogorov's

1941 results [58].

Even more complex situations arise in simulating flow of an electrically conducting fluids in presence of magnetic field, which is called Magnetofluiddynamic or Magnetohydrodynamic (MHD) flow. Examples of such flows are flow of salt water, liquid metals, hot ionised gases (plasma) and strong electrolytes [24]. The word *magnetohydrodynamics* is derived from *magneto* - meaning magnetic field, *hydro* - meaning water (or liquid) and -*dynamics* referring to the movement of an object by forces. The word Magnetohydrodynamics was first introduced by Swedish physicist Hannes Alfvèn (1908-1995). He was the first who studied the existence of electromagnetic-hydrodynamic waves [11]. He described astrophysical phenomena as an independent scientific discipline. He received the Nobel Prize in Physics (1970) for fundamental work and discoveries in MHD with successful applications in different parts of plasma physics. MHD is a relatively new discipline in natural science and engineering. The official birth of incompressible MHD was 1936-1937 starting with the pioneering theoretical and experimental work of Hartmann (1937) in liquid metal duct flow under the influence of a strong external magnetic field [74]. The physical principles governing such flows are that when an electrically conducting fluid moves in a magnetic field, the magnetic field induces currents in the fluid, which in turn create forces on the fluid and also alters the magnetic field. The governing equations of the MHD model consist of a non-linear system of partial differential equations (PDEs) that couple the Navier-Stokes equations for fluid flow to Maxwell's equations for electromagnetics.

In recent years, the study of MHD flows has become important due to its applications in, e.g. engineering, physical science, geophysics and astrophysics [16, 18, 26, 28, 47, 74, 79, 80, 83], ranging from the solar wind [70], to the Sun [82], the interstellar medium [43] and beyond [103], liquid metal cooling in nuclear reactors [15, 41, 91], process metallurgy [24], and MHD propulsion [64, 72]. Geomagnetic dynamo [2],

MHD generator [1], MHD pump [5, 10], Solar wind [3], Artificial heart [81] use magnetohydrodynamic principles. Moreover, in modern metallurgical technologies, the MHD devices are ubiquitous and going to be important for power engineering in the future. Importance and use of some of them are briefly outlined next. The MHD

Figure 1.1: A modern MHD pump [5]. Photograph courtesy of Intellectual Ventures Laboratory.

pump (shown in figure 1.1) is much more efficient for blood circulation compare to the present displacement-type diaphram pump or centrifugal-type impeller pump [95]. Electromagnetic force delivers the fluid in an MHD pump. It has no mechanical moving parts, either for rotation or for reciprocation. Therefore, there is no mechanical loss which makes the operation more dependable. It has the ability to reach to full power level almost immediately. Nuclear reactor TerraPower uses MHD pump to circulate its coolant.

It is about 400,000 Americans suffer from end-stage heart disease every year. However, only an estimated 3,000 human hearts become available every year for transplantation. Due to high demand, several industries produce artificial hearts for transplantation, and their designs are mostly based on mechanical approaches that can provide only a limited time of operation before recharging or replacement is required. Employing moving parts in their designs is one of the major issues which

provide friction, wear and fatigue which further allow only a limited period of reliable use. It requires further major surgery beyond the original installation procedure, if it needs repair or replacement of an artificial heart or heart assist device. To undergo this surgery, the patient undergoes significant risk. Therefore, we require an artificial heart that is more durable and reliable than existing designs. The artificial heart (shown in figure 1.2) that uses the technology of magnetohydrodynamics to induce human blood has no moving parts, is an implantable artificial heart apparatus. As the MHD is the direct interaction between a conductive fluid, electric and magnetic fields, blood is classified as an electrolytic fluid from an electric point of view and artificial heart uses MHD propulsion.

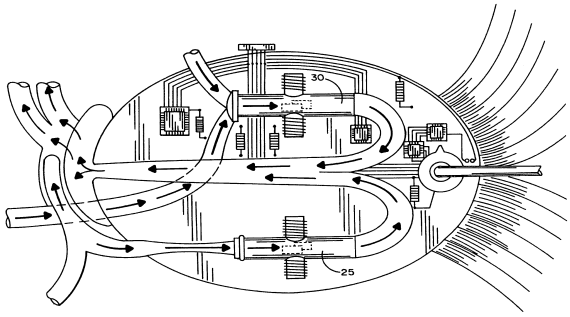

Figure 1.2: The design of an artificial heart [81]. Photograph courtesy of E. J. Peralta.

For an efficient and accurate numerical approximation for time-dependent, incompressible MHD flows at high Reynolds numbers, the problem of computing solutions u, B, p and λ for the following dimensionless system of evolution equations

gives rise [17, 24, 57, 89]

$$
\begin{aligned}
u_t + (u \cdot \nabla)u - s(B \cdot \nabla)B - \nu \Delta u + \nabla p &= f, && (1.1)\\
\nabla \cdot u &= 0, && (1.2)\\
B_t + (u \cdot \nabla)B - (B \cdot \nabla)u - \nu_m \Delta B + \nabla \lambda &= \nabla \times g, && (1.3)\\
\nabla \cdot B &= 0, && (1.4)
\end{aligned}
$$

in $\Omega \times (0, T)$. Here, Ω is convex domain of the fluid, u is velocity of the fluid, $\nabla \times g$ is the forcing on the magnetic field B, s is the coupling number, T is the simulation time, ν is the kinematic viscosity, ν_m is the magnetic diffusivity, p is a modified pressure, f is body force and λ is a Lagrange parameter. The conservation of linear momentum is given by (1.1) and the conservation of mass by (1.2). Equation (1.3) represents the induction equation (Maxwell equation) for the magnetic field B which is accompanied by the solenoidal constraint on the magnetic induction as (1.4); equation (1.4) ensures that there is no magnetic monopoles. A magnetic monopole is a hypothetical elementary particle with an isolated magnetic north pole or magnetic south pole. The modified pressure p is related to the fluid pressure, p_f, via $p = p_f/\rho + B \cdot B/2$, where density is denoted by ρ. The kinematic viscosity ν is defined by $\nu := Re^{-1}$ and the magnetic diffusivity ν_m is defined by $\nu_m : (= Re_m^{-1}) = 1/(\mu\sigma)$, where Re_m is the magnetic Reynolds number, μ is the magnetic permeability of free space and σ is the electric conductivity of the fluid. An artificial magnetic pressure λ, is a Lagrange multiplier, introduced in the induction equation to enforce the divergence free constraint on the magnetic induction equation within a variational context. In continuous case the magnetic pressure vanishes. We note that the curl formulation of the Maxwell's equation is avoided by assuming smooth domains, which is a common assumption in, e.g., applications in geophysics and astrophysics. An important property that

determines the behavior of the MHD equations is the ratio between the viscous and magnetic diffusion rates, the magnetic Prandtl number $Pr_m := Re_m/Re = \nu/\nu_m$. This ratio is crucial for the stability of certain numerical schemes, as it is used to determine a key parameter.

A fundamental difficulty in simulating MHD flow is solving large 4×4 fully coupled linear systems that arise in common discretizations of (1.1)-(1.4). The coupled system can be solved by monolithic methods, or implicit (fully coupled) methods, e.g. [100], where at each time step the fully coupled system is solved iteratively. These methods are robust and stable but they are computationally expensive in time and resources. It is an open problem how to decouple the discretized equations in an unconditionally stable way (with respect to the timestep size), and timestepping methods that decouple the equations are prone to unstable behavior without using excessively small timestep sizes. To confront this issue, an excellent idea was presented by Trenchea in [94]: if one rewrites the MHD system in terms of Elsässer variables (defined below), then an unconditionally stable and decoupled timestepping algorithm can be created.

To derive the Elsässer formulation, decompose the magnetic field into two parts, $B := B_0(t) + b$, where $B_0(t)$ is a known uniform background magnetic field and b is fluctuations in it. Defining $v := u + \sqrt{s}b$, $w := u - \sqrt{s}b$, $\tilde{B}_0 := \sqrt{s}B_0$, $f_1 := f + \nabla \times g - \frac{dB_0}{dt}$, $f_2 := f - \sqrt{s}(\nabla \times g + \frac{dB_0}{dt})$, $q := p + \sqrt{s}\lambda$ and $r := p - \sqrt{s}\lambda$,

then equation (1.1)-(1.4) produces the Elsässer formulation

$$v_t + w \cdot \nabla v - (\tilde{B}_0 \cdot \nabla)v + \nabla q - \frac{\nu + \nu_m}{2}\Delta v - \frac{\nu - \nu_m}{2}\Delta w = f_1, \quad (1.5)$$

$$\nabla \cdot v = 0, \quad (1.6)$$

$$w_t + v \cdot \nabla w + (\tilde{B}_0 \cdot \nabla)w + \nabla r - \frac{\nu + \nu_m}{2}\Delta w - \frac{\nu - \nu_m}{2}\Delta v = f_2, \quad (1.7)$$

$$\nabla \cdot w = 0. \quad (1.8)$$

We observe that the above Elsässer formulation has no self coupling nonlinear term, except the cross coupling terms of v and w. This happens due to the Alfvèn effect, that describes a fundamental interaction process [25, 31, 36, 48, 56, 63, 68, 90, 96, 97]. We also note that certain physical phenomena for MHD turbulence can be more easily described using the Elsässer formulation [23], and that the velocity u and magnetic field B are easily recoverable from simulations using Elsässer variables. Analysis of this algorithm in a semidiscrete setting (temporal discretization only) with a defect correction method was performed in [99], but no numerical experiments were performed beyond convergence rate verification. It is the goal of this thesis to explore, develop and test algorithms for MHD based on Elsässer variables, via 1) methods for (1.5)-(1.8), 2) new models and algorithms for high Re and/or Re_m, 3) uncertainty quantification using ensemble averaging for MHD simulation, and 4) finally we will propose, analyze and tests a high order algebraic splitting for MHD simulation in terms of primitive variables where at each time step, we apply Yosida-type algebraic splitting to the block saddle point problem that arises from a particular incremental formulation of MHD.

1.2 Outline of the thesis

This thesis is arranged as follows:

Chapter 2

In this chapter, we provide notations, mathematical preliminaries that will allow for a smooth analysis to follow and Elsässer formulation for our problem.

Chapter 3

This chapter discuss a fully discrete, efficient algorithm for magnetohydrodynamic (MHD) flow that is based on the Elsässer variable formulation and a timestepping scheme that decouples the MHD system but still provides unconditional stability with respect to the timestep size. We prove stability and optimal convergence of the scheme, and also connect the scheme to one based on handling each decoupled system with a penalty-projection method. Numerical experiments are given which verify all predicted convergence rates of our analysis on some analytical test problems, show the results of the scheme on a set of channel flow problems match well the results found when the computation is done with MHD in primitive variable, and finally show the scheme performs well on a channel flow over a step.

Chapter 4

In this chapter, we propose, analyze, and test a new MHD discretization which decouples the system into two Oseen problems at each timestep yet maintains unconditional stability with respect to the time step size, is optimally accurate in space, and behaves like second order in time in practice. The proposed method chooses a parameter $\theta \in [0, 1]$, dependent on the viscosity ν and magnetic diffusivity ν_m, so

that the explicit treatment of certain viscous terms does not cause instabilities, and gives temporal accuracy $O(\Delta t^2 + (1-\theta)|\nu - \nu_m|\Delta t)$. In practice, ν and ν_m are small, and so the method behaves like second order. When $\theta = 1$, the method reduces to a linearized BDF2 method, but it has been proven by Li and Trenchea that such a method is stable only in the uncommon case of $\frac{1}{2} < \frac{\nu}{\nu_m} < 2$. For the proposed method, stability and convergence are rigorously proven for appropriately chosen θ, and several numerical tests are provided that confirm the theory and show the method provides excellent accuracy in cases where usual BDF2 is unstable.

Chapter 5

In this chapter, an efficient algorithm is proposed and studied for computing flow ensembles of incompressible magnetohydrodynamic (MHD) flows under uncertainties in initial or boundary data. The ensemble average of J realizations is approximated through an algorithm (adapted from a breakthrough idea of Jiang and Layton, 2014) that, at each time step, uses the same matrix for each of the J system solves. Hence, preconditioners need built only once per time step, and the algorithm can take advantage of block linear solvers. Additionally, an Elsässer variable formulation is used, which allows for a stable decoupling of each MHD system at each time step. We prove stability and convergence of the algorithm, and test it with two numerical experiments.

Chapter 6

This chapter proposes, analyzes and tests high order algebraic splitting methods for magnetohydrodynamic (MHD) flows. The main idea is to apply, at each time step, Yosida-type algebraic splitting to a block saddle point problem that arises from a particular incremental formulation of MHD. By doing so, we dramatically reduce the

complexity of the nonsymmetric block Schur complement by decoupling it into two Stokes-type Schur complements, each of which is symmetric positive definite and also is the same at each time step. We prove the splitting is $O(\Delta t^3)$ accurate, and if used together with (block-)pressure correction, is fourth order. A full analysis of the solver is given, both as a linear algebraic approximation, but also in a finite element context that uses the natural spatial norms. Numerical tests are given to illustrate the theory and show the effectiveness of the method.

Chapter 7

General conclusions and future research directions are drawn in this chapter.

Appendix A

To study a conditional stability analysis of MHD ensemble algorithm in chapter 5, we prove Theorem 8.

1.3 List of publications

1.3.1 Published

1. M. Akbas, M. Mohebujjaman, L. Rebholz and M. Xiao, **High order algebraic splitting for magnetohydrodynamics simulation**, Journal of Computational and Applied Mathematics, 321, 128-142, 2017.

2. M. Mohebujjaman and L. Rebholz, **An efficient algorithm for computation of MHD flow ensembles**, Computational Methods in Applied Mathematics, 17(1), 121-137, 2017.

3. T. Heister, M. Mohebujjaman and L. Rebholz, **Decoupled, unconditionally**

stable, higher order discretizations for MHD flow simulation, Journal of Scientific Computing, 71(1), 21-43, 2017.

4. N. Jiang, M. Mohebujjaman, L. Rebholz and C. Trenchea, **An optimally accurate discrete regularization for second order timestepping methods for Navier-Stokes equations**[1], Computer Methods in Applied Mechanics and Engineering, 310, 388-405, 2016.

5. M. Akbas, S. Kaya, M. Mohebujjaman and L. Rebholz, **Numerical analysis and testing of a fully discrete, decoupled penalty-projection algorithm for MHD in Elsässer variable**, International Journal of Numerical Analysis and Modeling, 13(1), 90-113, 2016.

1.3.2 Accepted

1. M. Mohebujjaman, L. G. Rebholz, X. Xie, and T. Iliescu, **Energy Balance and Mass Conservation in Reduced Order Models of Fluid Flows**[1], Journal of Computational Physics, accepted.

1.3.3 Submitted

1. X. Xie, M. Mohebujjaman, L. G. Rebholz, and T. Iliescu, **Calibrated Filtered Reduced Order Modeling**[1], submitted.

1.3.4 Ongoing Work

1. M. Mohebujjaman, **High order accurate decoupled efficient algorithm for MHD flow ensembles simulation**[1], in preparation.

[1]Not part of this thesis

Chapter 2

Notation and Preliminaries

2.1 Introduction

Throughout the analysis presented in this thesis, we will assume that $\Omega \subset \mathbb{R}^d, d \in \{2, 3\}$, is a polygonal or polyhedral domain with boundary $\partial\Omega$. We denote the usual $L^2(\Omega)$ norm and its inner product by $\|.\|$ and $(.,.)$ respectively. The $L^p(\Omega)$ norms and the Sobolev $W_p^k(\Omega)$ norms are denoted by $\|.\|_{L^p}$ and $\|.\|_{W_p^k(\Omega)}$ respectively for $k \in \mathbb{N}, 1 \leq p \leq \infty$. In particular, $H^k(\Omega)$ is used to represent the Sobolev space $W_2^k(\Omega)$. $\|.\|_{H^k}$ and $|.|_k$ denote the norm and the seminorm in $H^k(\Omega)$.

For X being a normed function space in Ω, $L^p(0,t;X)$ is the space of all functions defined on $(0,t) \times \Omega$ for which the norm

$$\|u\|_{L^p(0,t;X)} = \left(\int_0^t \|u\|_X^p dx \right)^{1/p}, p \in [1, \infty)$$

is finite. For $p = \infty$, the usual modification is used in the definition of this space. The natural function spaces for our problem are

$$X := H_0^1(\Omega)^d = \{v \in (L^2(\Omega))^d : \nabla v \in L^2(\Omega)^{d \times d}, v = 0 \text{ on } \partial\Omega\},$$

$$Q := L_0^2(\Omega) = \{q \in L^2(\Omega) : \int_\Omega q \ dx = 0\}.$$

The results of this thesis also hold in the periodic setting.

For f an element in the dual space of X, its norm is defined by

$$\|f\|_{-1} = \sup_{v \in X} \frac{\|(f, v)\|}{\|\nabla v\|}.$$

The space of divergence free functions in X is given by

$$V := \{v \in X : (\nabla \cdot v, q) = 0, \forall q \in Q\}.$$

The Poincaré-Friedrichs' inequality will be used frequently throughout our analysis: For $v \in X$,

$$\|v\| \leq C\|\nabla v\|, \ \ C = C(\Omega).$$

We define the trilinear form $b^* : X \times X \times X \to \mathbb{R}$ by

$$b^*(u, v, w) := \frac{1}{2}((u \cdot \nabla v, w) - (u \cdot \nabla w, v)), \ \ \forall u, v, w \in X.$$

Note that $b^*(u, v, w)$ is skew symmetric, $b^*(u, v, v) = 0$, and if $\|\nabla \cdot u\| = 0$, then $(u \cdot \nabla v, w) = b^*(u, v, w)$. Moreover, $b^*(u, v, w)$ satisfies the following bound [35],

$$|b^*(u, v, w)| \leq C(\Omega)\|\nabla u\|\|\nabla v\|\|\nabla w\|, \ \text{ for any } \ u, v, w \in X. \tag{2.1}$$

2.2 Discrete Setting

We denote regular, conforming finite element spaces $X_h \subset X$ and $Q_h \subset Q$, defined on a triangulation $T_h(\Omega)$, where the subscript h denotes a triangle fineness measure

and is defined as

$$h := \max_{\forall K \in T_h(\Omega)} \text{diameter}(K).$$

For stability of the discrete pressures, we assume that (X_h, Q_h) satisfies the usual discrete inf-sup (LBB) condition

$$\inf_{q_h \in Q_h} \sup_{v_h \in X_h} \frac{(q_h, \nabla \cdot v_h)}{\|q_h\| \|\nabla v_h\|} \geq \beta > 0, \tag{2.2}$$

where β is independent of h. For simplicity of analysis, we will further assume that either the Scott-Vogelius finite element pair $(X_h, Q_h) = ((P_k)^d, P_{k-1}^{disc})$ with appropriate macro-element structures so that LBB holds [13, 84, 101, 102], or $((P_k)^d, P_{k-1})$ Taylor Hood elements are used throughout, where the polynomial degree $k \geq d$. Velocity and pressure as well as magnetic field and the corresponding magnetic pressure will be approximated by Scott-Vogelius or Taylor Hood elements. However, our results can be extended without major difficulty (but with more terms) to any inf-sup stable element choice.

The space of discretely divergence free functions is defined as

$$V_h := \{v_h \in X_h : (\nabla \cdot v_h, q_h) = 0, \ \forall \ q_h \in Q_h\}.$$

We also assume the mesh is sufficiently regular for the inverse inequality to hold in X_h: there exists a constant C_i, independent of the mesh width h, such that

$$\|\nabla \phi_h\| \leq C_i h^{-1} \|\phi_h\|, \ \forall \phi_h \in X_h.$$

We will formulate our equations in V_h formulation, and due to the LBB condition, this will be equivalent to the (X_h, Q_h) formulation. As is commonly done, we

analyze with the V_h formulation and compute with the (X_h, Q_h) form.

With the use of Scott-Vogelius finite element pairs, V_h is conforming to V, i.e., $V_h \subset V$ and the functions in V_h are divergence-free point wise in the L^2 sense:

$$V_h = \{v_h \in X_h : \|\nabla \cdot v_h\| = 0\}.$$

However, in MHD the enforcement of the solenoidal constraints is believed critical, so Scott-Vogelius elements are a natural choice for simulations. Thus, using Scott-Vogelius elements will provide for strongly divergence free discrete velocity and magnetic filed solutions. We note that if appropriate macro-element mesh structures are used with Scott-Vogelius elements (i.e. that provide LBB stability), strongly divergence free solutions can be found by solving the saddle point linear system, although it is also possible to use the iterative penalty method (see, e.g. [40, 85]).

We have the following approximation properties typical of piecewise polynomials of degree $(k, k-1)$ hold for (X_h, Q_h): [20]

$$\inf_{v_h \in X_h} \|u - v_h\| \leq Ch^{k+1}|u|_{k+1}, \quad u \in H^{k+1}(\Omega), \tag{2.3}$$

$$\inf_{v_h \in X_h} \|\nabla(u - v_h)\| \leq Ch^{k}|u|_{k+1}, \quad u \in H^{k+1}(\Omega), \tag{2.4}$$

$$\inf_{q_h \in Q_h} \|p - q_h\| \leq Ch^{k}|p|_{k}, \quad p \in H^{k}(\Omega). \tag{2.5}$$

where $|\cdot|_r$ denotes the H^r seminorm.

With the inverse inequality and the LBB assumption, we have the following approximation properties

$$\|\nabla(u - P_{L^2}^{V_h}(u))\| \leq Ch^{k}|u|_{k+1}, \quad u \in H^{k+1}(\Omega), \tag{2.6}$$

$$\inf_{v_h \in V_h} \|\nabla(u - v_h)\| \leq Ch^{k}|u|_{k+1}, \quad u \in H^{k+1}(\Omega), \tag{2.7}$$

where $P_{L^2}^{V_h}(u)$ is the L^2 projection of u into V_h.

The following lemma for discrete Gronwall inequality was proven in [46].

Lemma 2.2.1. *Let Δt, H, a_n, b_n, c_n, d_n be non-negative numbers for $n = 1, \cdots, M$ such that*

$$a_M + \Delta t \sum_{n=1}^{M} b_n \leq \Delta t \sum_{n=1}^{M-1} d_n a_n + \Delta t \sum_{n=1}^{M} c_n + H \quad \textit{for } M \in \mathbb{N},$$

then for all $\Delta t > 0$,

$$a_M + \Delta t \sum_{n=1}^{M} b_n \leq exp\left(\Delta t \sum_{n=1}^{M-1} d_n\right)\left(\Delta t \sum_{n=1}^{M} c_n + H\right) \quad \textit{for } M \in \mathbb{N}.$$

The ensemble mean and fluctuation are denoted by $< v >$ and $v_j^{'}$ respectively and these are defined as follows: mean $< v >:= \frac{1}{J}\sum_{j=1}^{J} v_j$ and fluctuation $v_j^{'} := v_j - < v >$, where J is the number of realization. Frobenius norm of an array and the Euclidean norm of a vector are denoted by $|\cdot|$. Approximations to $\frac{1}{J}\sum_{j=1}^{J} v_j(\cdot, t_n)$ and $v_j^{'}(\cdot, t_n)$ are denoted by $< v >^n$ and $v_j^{'n}$ respectively.

2.3 Derivation of Elsässer formulation

The Elsässer formulation of MHD was first proposed by W. Elsässer in 1950 [27], and since then has been used in several analytical studies, e.g. [25, 69, 88]. To derive it, begin by splitting the magnetic field into two parts, $\sqrt{s}B := \sqrt{s}B_0 + \sqrt{s}b$ (mean and fluctuation, respectively), with $B_0 = B_0(t)$. For boundary conditions, we assume the Dirichlet condition $B = B_0$ on $\partial\Omega$, and homogeneous Dirichlet conditions for the velocity, $u = 0$, and magnetic field fluctuations, $b = 0$. The system (1.1)-(1.4)

can now be written as

$$\begin{aligned} u_t + (u\cdot\nabla)u - s(B_0\cdot\nabla)b - s(b\cdot\nabla)b - \nu\Delta u + \nabla p &= f, && (2.8)\\ \nabla\cdot u &= 0, && (2.9)\\ b_t + (u\cdot\nabla)b - (B_0\cdot\nabla)u - (b\cdot\nabla)u - \nu_m\Delta b + \nabla\lambda &= \nabla\times g - \frac{dB_0}{dt}, && (2.10)\\ \nabla\cdot b &= 0. && (2.11) \end{aligned}$$

Rescaling (2.10) by $\sqrt{s}$, adding (subtracting) (2.8) to (from) (2.10) and setting $f_1 := f + \nabla\times g - \frac{dB_0}{dt}$, $f_2 := f - \sqrt{s}(\nabla\times g + \frac{dB_0}{dt})$, $q := p + \sqrt{s}\lambda$ and $r := p - \sqrt{s}\lambda$ gives

$$\begin{aligned} &(u+\sqrt{s}b)_t + (u\cdot\nabla)(u+\sqrt{s}b) - (\sqrt{s}B_0\cdot\nabla)(u+\sqrt{s}b)\\ &\quad -(\sqrt{s}b\cdot\nabla)(u+\sqrt{s}b) - \nu\Delta u - \nu_m\Delta(\sqrt{s}b) + \nabla q &&= f_1,\\ &\quad \nabla\cdot(u+\sqrt{s}b) &&= 0,\\ &(u-\sqrt{s}b)_t + (u\cdot\nabla)(u-\sqrt{s}b) + (\sqrt{s}B_0\cdot\nabla)(u-\sqrt{s}b)\\ &\quad +(\sqrt{s}b\cdot\nabla)(u-\sqrt{s}b) - \nu\Delta u + \nu_m\Delta(\sqrt{s}b) + \nabla r &&= f_2,\\ &\quad \nabla\cdot(u-\sqrt{s}b) &&= 0. \end{aligned}$$

Now defining $v = u + \sqrt{s}b$, $w = u - \sqrt{s}b$, $\tilde{B}_0 = \sqrt{s}B_0$ produces the Elsässer formulation (1.5)-(1.8).

Chapter 3

Analysis and testing of a first order fully discrete scheme for MHD in Elsässer variable.

3.1 Introduction

In this chapter, we propose, analyze and test a fully discrete decoupled scheme for (1.5)-(1.8) in section 3.2. We prove its stability and convergence theorems. Then we connect the scheme to one based on handling each decouple system with a penalty-projection method in section 3.3. In section 3.4, we examine the convergence of the scheme for a test problem, a comparison is shown between Elsässer variable scheme and primitive variable scheme, and finally we apply it on a benchmark channel flow problem.

3.2 An efficient and stable backward-Euler scheme for MHD

We now present and analyze an efficient fully discrete decoupled linearized scheme for MHD. In this scheme, the time derivative is approximated by the first-

order backward-Euler formula. After defining the scheme, we state and prove its unconditional stability and convergence theorems.

Algorithm 3.2.1. *Let $f_1, f_2 \in L^\infty(0,T;H^{-1}(\Omega))$ and time step $\Delta t > 0$ and end time $T > 0$ be given. Set $M = T/\Delta t$ and start with $\tilde{v}^0 = v(0), \tilde{w}^0 = w(0) \in H^2 \cup V$. For all $n = 0, 1, ..., M-1$, compute $(v_h^{n+1}, w_h^{n+1}) \in V_h \times V_h$ satisfying for all $(\chi_h,\ l_h) \in V_h \times V_h$,*

$$\left(\frac{v_h^{n+1} - v_h^n}{\Delta t}, \chi_h\right) + (w_h^n \cdot \nabla v_h^{n+1}, \chi_h) - (\tilde{B}_0(t^{n+1}) \cdot \nabla v_h^{n+1}, \chi_h) + \frac{\nu + \nu_m}{2}(\nabla v_h^{n+1}, \nabla \chi_h) + \frac{\nu - \nu_m}{2}(\nabla w_h^n, \nabla \chi_h) = (f_1(t^{n+1}), \chi_h), \quad (3.1)$$

and

$$\left(\frac{w_h^{n+1} - w_h^n}{\Delta t}, l_h\right) + (v_h^n \cdot \nabla w_h^{n+1}, l_h) + (\tilde{B}_0(t^{n+1}) \cdot \nabla w_h^{n+1}, l_h) + \frac{\nu + \nu_m}{2}(\nabla w_h^{n+1}, \nabla l_h) + \frac{\nu - \nu_m}{2}(\nabla v_h^n, \nabla l_h) = (f_2(t^{n+1}), l_h). \quad (3.2)$$

Even though the scheme is decoupled into 2 sub-problems, it is unconditionally stable with respect to the timestep size. We prove this in the following lemma.

Lemma 3.2.1. *Suppose $f_1, f_2 \in L^\infty(0,T;H^{-1}(\Omega))$, $v_h^0, w_h^0 \in H^1(\Omega)$. Then for any $\Delta t > 0$, solutions to (3.1)-(3.2) satisfy*

$$\begin{aligned}\|v_h^M\|^2 + \|w_h^M\|^2 + &\frac{(\nu - \nu_m)^2}{2(\nu + \nu_m)}\Delta t \left(\|\nabla v_h^M\|^2 + \|\nabla w_h^M\|^2\right) \\ &+ \frac{\nu\nu_m}{\nu + \nu_m}\Delta t \sum_{n=0}^{M-1}\left(\|\nabla v_h^{n+1}\|^2 + \|\nabla w_h^{n+1}\|^2\right) \\ &\le \|v_h^0\|^2 + \|w_h^0\|^2 + \frac{(\nu - \nu_m)^2}{2(\nu + \nu_m)}\left(\|\nabla v_h^0\|^2 + \|\nabla w_h^0\|^2\right) \\ &+ \frac{\nu + \nu_m}{\nu\nu_m}\Delta t \sum_{n=0}^{M-1}\left(\|f_1(t^{n+1})\|_{-1}^2 + \|f_2(t^{n+1})\|_{-1}^2\|\right).\end{aligned}$$

Proof. Taking $\chi_h = v_h^{n+1}$ in (3.1),$l_h = w_h^{n+1}$ in (3.2), and using the polarization identity

$$(b-a,b) = \frac{1}{2}(\|b-a\|^2 + \|b\|^2 - \|a\|^2),$$

gives

$$\frac{1}{2\Delta t}\big(\|v_h^{n+1} - v_h^n\|^2 + \|v_h^{n+1}\|^2 - \|v_h^n\|^2\big) + \frac{\nu+\nu_m}{2}\|\nabla v_h^{n+1}\|^2 + \frac{\nu-\nu_m}{2}(\nabla w_h^n, \nabla v_h^{n+1}) = (f_1(t^{n+1}), v_h^{n+1}), \tag{3.3}$$

and

$$\frac{1}{2\Delta t}\left(\|w_h^{n+1} - w_h^n\|^2 + \|w_h^{n+1}\|^2 - \|w_h^n\|^2\right) + \frac{\nu+\nu_m}{2}\|\nabla w_h^{n+1}\|^2 + \frac{\nu-\nu_m}{2}(\nabla v_h^n, \nabla w_h^{n+1}) = (f_2(t^{n+1}), w_h^{n+1}). \tag{3.4}$$

Adding (3.3) and (3.4) yields

$$\begin{aligned}\frac{1}{2\Delta t}&\big(\|v_h^{n+1}\|^2 - \|v_h^n\|^2 + \|w_h^{n+1}\|^2 - \|w_h^n\|^2 + \|v_h^{n+1} - v_h^n\|^2 + \|w_h^{n+1} - w_h^n\|^2\big) \\ &+ \frac{\nu+\nu_m}{2}(\|\nabla v_h^{n+1}\|^2 + \|\nabla w_h^{n+1}\|^2) + \frac{\nu-\nu_m}{2}\left((\nabla w_h^n, v_h^{n+1}) + (\nabla v_h^n, \nabla w_h^{n+1})\right) \\ &= (f_1(t^{n+1}), v_h^{n+1}) + (f_2(t^{n+1}), w_h^{n+1}),\end{aligned}$$

then using Cauchy-Schwarz's inequality on the right hand side provides

$$\begin{aligned}
&\frac{1}{2\Delta t}\Bigg(\|v_h^{n+1}\|^2+\|w_h^{n+1}\|^2-(\|v_h^n\|^2+\|w_h^n\|^2)+\|v_h^{n+1}-v_h^n\|^2\\
&+\|w_h^{n+1}-w_h^n\|^2\Bigg)+\frac{\nu+\nu_m}{2}(\|\nabla v_h^{n+1}\|^2+\|\nabla w_h^{n+1}\|^2)\\
&\leq|\frac{\nu-\nu_m}{2}|\left(\|\nabla w_h^n\|\|\nabla v_h^{n+1}\|+\|\nabla v_h^n\|\|\nabla w_h^{n+1}\|\right)\\
&+\|f_1(t^{n+1})\|_{-1}\|\nabla v_h^{n+1}\|+\|f_2(t^{n+1})\|_{-1}\|\nabla w_h^{n+1}\|. \qquad (3.5)
\end{aligned}$$

After application of Young's inequality $ab\leq\frac{\epsilon}{2}a^2+\frac{1}{2\epsilon}b^2$ with $\epsilon=\frac{\nu+\nu_m}{2}$, we obtain

$$\begin{aligned}
&\frac{1}{2\Delta t}\left(\|v_h^{n+1}\|^2+\|w_h^{n+1}\|^2-(\|v_h^n\|^2+\|w_h^n\|^2)+\|v_h^{n+1}-v_h^n\|^2+\|w_h^{n+1}-w_h^n\|^2\right)\\
&\qquad+\frac{\nu+\nu_m}{2}\left(\|\nabla v_h^{n+1}\|^2+\|\nabla w_h^{n+1}\|^2\right)\leq\frac{\nu+\nu_m}{4}\|\nabla v_h^{n+1}\|^2\\
&\qquad+\frac{(\nu-\nu_m)^2}{4(\nu+\nu_m)}\|\nabla w_h^n\|^2+\frac{\nu+\nu_m}{4}\|\nabla w_h^{n+1}\|^2+\frac{(\nu-\nu_m)^2}{4(\nu+\nu_m)}\|\nabla v_h^n\|^2\\
&\qquad+\|f_1(t^{n+1})\|_{-1}\|\nabla v_h^{n+1}\|+\|f_2(t^{n+1})\|_{-1}\|\nabla w_h^{n+1}\|. \qquad (3.6)
\end{aligned}$$

Reducing and dropping the non-negative terms $\|v_h^{n+1}-v_h^n\|^2$, $\|w_h^{n+1}-w_h^n\|^2$ on the left hand side gives us

$$\begin{aligned}
&\frac{1}{2\Delta t}\left(\|v_h^{n+1}\|^2-\|v_h^n\|^2+\|w_h^{n+1}\|^2-\|w_h^n\|^2\right)\\
&+\frac{\nu+\nu_m}{4}\left(\|\nabla v_h^{n+1}\|^2-\frac{(\nu-\nu_m)^2}{(\nu+\nu_m)^2}\|\nabla v_h^n\|^2\right)\\
&+\frac{\nu+\nu_m}{4}\left(\|\nabla w_h^{n+1}\|^2-\frac{(\nu-\nu_m)^2}{(\nu+\nu_m)^2}\|\nabla w_h^n\|^2\right)\\
&\leq\|f_1(t^{n+1})\|_{-1}\|\nabla v_h^{n+1}\|+\|f_2(t^{n+1})\|_{-1}\|\nabla w_h^{n+1}\|. \qquad (3.7)
\end{aligned}$$

Applying again Young's inequality with $\epsilon = \frac{\nu\nu_m}{\nu+\nu_m}$, we have

$$\begin{aligned}\frac{1}{2\Delta t}\big(\|v_h^{n+1}\|^2 - \|v_h^n\|^2 + \|w_h^{n+1}\|^2 - \|w_h^n\|^2\big) + \frac{\nu\nu_m}{2(\nu+\nu_m)}\big(\|\nabla v_h^{n+1}\|^2 + \|\nabla w_h^{n+1}\|^2\big) \\ + \frac{(\nu-\nu_m)^2}{4(\nu+\nu_m)}\left(\|\nabla v_h^{n+1}\|^2 - \|\nabla v_h^n\|^2 + \|\nabla w_h^{n+1}\|^2 - \|\nabla w_h^n\|^2\right) \\ \leq \frac{(\nu+\nu_m)}{2\nu\nu_m}\left(\|f_1(t^{n+1})\|_{-1}^2 + \|f_2(t^{n+1})\|_{-1}^2\right). \qquad (3.8)\end{aligned}$$

Multiplying both sides by $2\Delta t$ and summing over timesteps finishes the proof. □

The proposed algorithm also converges optimally in space in time, with assumed smoothness of the true solution.

Theorem 1. *Assume* (v, w, p) *solves* (1.5)-(1.6) *and satisfying*

$$v, w \in L^\infty(0,T;H^m(\Omega)), \quad m = max\{2, k+1\},$$
$$v_t, w_t \in L^\infty(0,T;H^{k+1}(\Omega)), \quad v_{tt}, w_{tt} \in L^\infty(0,T;L^2(\Omega)).$$

Then the finite dimensional solution (v_h, w_h) *to Algorithm (3.2.1) converges to the true solution: for any* $\Delta t > 0$,

$$\begin{aligned}\|v(T) - v_h^M\| + \|w(T) - w_h^M\| + \frac{\nu\nu_m}{2(\nu+\nu_m)}\Bigg\{\Delta t\sum_{n=1}^{M}\big(\|\nabla(v(t^n) - v_h^n)\|^2 \\ + \|\nabla(w(t^n) - w_h^n)\|^2\big)\Bigg\}^{\frac{1}{2}} \leq C(h^k + \Delta t). \qquad (3.9)\end{aligned}$$

Proof. We begin by obtaining the error equations. Continuous variational formulation

of (1.5)-(1.8) at the time level t^{n+1} is given

$$\begin{aligned}
&\left(\frac{v(t^{n+1})-v(t^n)}{\Delta t},\chi_h\right)+(w(t^{n+1})\cdot\nabla v(t^{n+1}),\chi_h)\\
&-(\tilde{B}_0(t^{n+1})\cdot\nabla v(t^{n+1}),\chi_h)+\frac{\nu+\nu_m}{2}(\nabla v(t^{n+1}),\nabla\chi_h)\\
&+\frac{\nu-\nu_m}{2}(\nabla(w(t^{n+1})-w(t^n)),\nabla\chi_h)+\frac{\nu-\nu_m}{2}(\nabla w(t^n),\nabla\chi_h)\\
&=-\left(v_t(t^{n+1})-\frac{v(t^{n+1})-v(t^n)}{\Delta t},\chi_h\right)+(f_1(t^{n+1}),\chi_h)
\end{aligned}\tag{3.10}$$

and

$$\begin{aligned}
&\left(\frac{w(t^{n+1})-w(t^n)}{\Delta t},l_h\right)+(v(t^{n+1})\cdot\nabla w(t^{n+1}),l_h)\\
&+(\tilde{B}_0(t^{n+1})\cdot\nabla w(t^{n+1}),l_h)+\frac{\nu+\nu_m}{2}(\nabla w(t^{n+1}),\nabla l_h)\\
&+\frac{\nu-\nu_m}{2}(\nabla(v(t^{n+1})-v(t^n)),\nabla l_h)+\frac{\nu-\nu_m}{2}(\nabla v(t^n),\nabla l_h)\\
&=-\left(w_t(t^{n+1})-\frac{w(t^{n+1})-w(t^n)}{\Delta t},l_h\right)+(f_2(t^{n+1}),l_h)
\end{aligned}\tag{3.11}$$

for all $\chi_h, l_h \in V_h$. Denote the errors by $e_v^{n+1} := v(t^{n+1}) - v_h^{n+1}$ and $e_w^{n+1} := w(t^{n+1}) - w_h^{n+1}$ for all $n = 0, 1, ..., M-1$. Subtracting (3.10) and (3.11) from (3.1) and (3.2), respectively, produces

$$\begin{aligned}
&\left(\frac{e_v^{n+1}-e_v^n}{\Delta t},\chi_h\right)+\frac{\nu+\nu_m}{2}(\nabla e_v^{n+1},\nabla\chi_h)+\frac{\nu-\nu_m}{2}(\nabla e_w^n,\nabla\chi_h)\\
&\qquad-(\tilde{B}_0(t^{n+1})\cdot\nabla e_v^{n+1},\chi_h)+(e_w^n\cdot\nabla v(t^{n+1}),\chi_h)\\
&\qquad+(w_h^n\cdot\nabla e_v^{n+1},\chi_h)=-G_1(t,v,w,\chi_h)
\end{aligned}\tag{3.12}$$

and

$$\left(\frac{e_w^{n+1}-e_w^n}{\Delta t},l_h\right)+\frac{\nu+\nu_m}{2}(\nabla e_w^{n+1},\nabla l_h)+\frac{\nu-\nu_m}{2}(\nabla e_v^n,\nabla l_h)+(\tilde{B}_0(t^{n+1})\cdot\nabla e_w^{n+1},l_h)$$
$$+(e_v^n\cdot\nabla w(t^{n+1}),l_h)+(v_h^n\cdot\nabla e_w^{n+1},l_h)=-G_2(t,v,w,l_h), \tag{3.13}$$

here

$$G_1(t,v,w,\chi_h):=\left(v_t(t^{n+1})-\frac{v(t^{n+1})+v(t^n)}{\Delta t},\chi_h\right)$$
$$+((w(t^{n+1})-w(t^n))\cdot\nabla v(t^{n+1}),\chi_h)+\frac{\nu-\nu_m}{2}(\nabla(w(t^{n+1})-w(t^n)),\nabla\chi_h),$$

and

$$G_2(t,v,w,\chi_h):=\left(w_t(t^{n+1})-\frac{w(t^{n+1})-w(t^n)}{\Delta t},\chi_h\right)+$$
$$((v(t^{n+1})-v(t^n))\cdot\nabla w(t^{n+1}),\chi_h)+\frac{\nu-\nu_m}{2}(\nabla(v(t^{n+1})-v(t^n)),\nabla\chi_h).$$

Decompose the errors into the interpolation errors and approximations terms:

$$e_v^{n+1}:=v(t^{n+1})-v_h^{n+1}=(v(t^{n+1})-\tilde{v}^{n+1})-(v_h^{n+1}-\tilde{v}^{n+1}):=\eta_v^{n+1}-\phi_h^{n+1},$$
$$e_w^{n+1}:=w(t^{n+1})-w_h^{n+1}=(w(t^{n+1})-\tilde{w}^{n+1})-(w_h^{n+1}-\tilde{w}^{n+1}):=\eta_w^{n+1}-\psi_h^{n+1},$$

take $\chi_h=\phi_h^{n+1}$ and $\chi_h=\psi_h^{n+1}$, use the polarization identity $2(a-b,a)=\|a\|^2-\|b\|^2+\|a-b\|^2$, and noting that

$$(\tilde{B}_0(t^{n+1})\cdot\nabla\phi_h^{n+1},\phi_h^{n+1})=(\tilde{B}_0(t^{n+1})\cdot\nabla\psi_h^{n+1},\psi_h^{n+1})=0,$$
$$(w_h^n\cdot\nabla\phi_h^{n+1},\phi_h^{n+1})=(v_h^n\cdot\nabla\psi_h^{n+1},\psi_h^{n+1})=0,$$

we then have

$$\begin{aligned}
&\frac{1}{2\Delta t}\left(\|\phi_h^{n+1}\|^2-\|\phi_h^n\|^2+\|\phi_h^{n+1}-\phi_h^n\|^2\right)+\frac{\nu+\nu_m}{2}\|\nabla\phi_h^{n+1}\|^2\\
&\le\left|\frac{1}{\Delta t}(\eta_v^{n+1}-\eta_v^n,\phi_h^{n+1})\right|+\frac{\nu+\nu_m}{2}|(\nabla\eta_v^{n+1},\nabla\phi_h^{n+1})|+\frac{|\nu-\nu_m|}{2}|(\nabla\eta_w^n,\nabla\phi_h^{n+1})|\\
&+\frac{|\nu-\nu_m|}{2}|(\nabla\psi_h^n,\nabla\phi_h^{n+1})|+|(\tilde{B}_0(t^{n+1})\cdot\nabla\eta_v^{n+1},\phi_h^{n+1})|+|(w_h^n\cdot\nabla\eta_v^{n+1},\phi_h^{n+1})|\\
&+|(\eta_w^n\cdot\nabla v(t^{n+1}),\phi_h^{n+1})|+|(\psi_h^n\cdot\nabla v(t^{n+1}),\phi_h^{n+1})|+|G_1(t,v,w,\phi_h^{n+1})| \qquad (3.14)
\end{aligned}$$

and

$$\begin{aligned}
&\frac{1}{2\Delta t}\left(\|\psi_h^{n+1}\|^2-\|\psi_h^n\|^2+\|\psi_h^{n+1}-\psi_h^n\|^2\right)+\frac{\nu+\nu_m}{2}\|\nabla\psi_h^{n+1}\|^2\\
&\le\frac{1}{\Delta t}\left|(\eta_w^{n+1}-\eta_w^n,\psi_h^{n+1})\right|+\frac{\nu+\nu_m}{2}|(\nabla\eta_w^{n+1},\nabla\psi_h^{n+1})|+\frac{|\nu-\nu_m|}{2}|(\nabla\eta_v^n,\nabla\psi_h^{n+1})|\\
&+\frac{|\nu-\nu_m|}{2}|(\nabla\phi_h^n,\nabla\psi_h^{n+1})|+|(\tilde{B}_0(t^{n+1})\cdot\nabla\eta_w^{n+1},\psi_h^{n+1})|+|(v_h^n\cdot\nabla\eta_w^{n+1},\psi_h^{n+1})|\\
&+|(\eta_v^n\cdot\nabla w(t^{n+1}),\psi_h^{n+1})|+|(\phi_h^n\cdot\nabla w(t^{n+1}),\psi_h^{n+1})|+|G_2(t,v,w,\psi_h^{n+1})|. \qquad (3.15)
\end{aligned}$$

We now find bounds on the right hand side terms of (3.14) only, since the estimates are similar for (3.15). Applying Cauchy-Schwarz and Young inequalities on the first four terms results in

$$\begin{aligned}
\frac{1}{\Delta t}\left|(\eta_v^{n+1}-\eta_v^n,\phi_h^{n+1})\right| &\le \frac{\nu\nu_m}{16(\nu+\nu_m)}\|\nabla\phi_h^{n+1}\|^2+\frac{C(\nu+\nu_m)}{\nu\nu_m(\Delta t)}\int_{t^n}^{t^{n+1}}\|\partial_t\eta_v\|^2d\tau,\\
\frac{\nu+\nu_m}{2}|(\nabla\eta_v^{n+1},\nabla\phi_h^{n+1})| &\le \frac{\nu\nu_m}{16(\nu+\nu_m)}\|\nabla\phi_h^{n+1}\|^2+\frac{(\nu+\nu_m)^3}{\nu\nu_m}\|\nabla\eta_v^{n+1}\|^2,\\
\frac{|\nu-\nu_m|}{2}|(\nabla\eta_w^n,\nabla\phi_h^{n+1})| &\le \frac{\nu\nu_m}{16(\nu+\nu_m)}\|\nabla\phi_h^{n+1}\|^2+\frac{(\nu-\nu_m)^2(\nu+\nu_m)}{\nu\nu_m}\|\nabla\eta_w^n\|^2,\\
\frac{|\nu-\nu_m|}{2}|(\nabla\psi_h^n,\nabla\phi_h^{n+1})| &\le \frac{\nu+\nu_m}{4}\|\nabla\phi_h^{n+1}\|^2+\frac{(\nu-\nu_m)^2}{4(\nu+\nu_m)}\|\nabla\psi_h^n\|^2.
\end{aligned}$$

Applying Hölder and Young's inequalities with (2.1) on the first three nonlinear terms

yields

$$
\begin{aligned}
|(\tilde{B}_0(t^{n+1})\cdot\nabla\eta_v^{n+1},\phi_h^{n+1})| &\le C\|\tilde{B}_0(t^{n+1})\|_\infty\|\nabla\eta_v^{n+1}\|\|\nabla\phi_h^{n+1}\| \\
&\le \frac{\nu\nu_m}{16(\nu+\nu_m)}\|\nabla\phi_h^{n+1}\|^2+\frac{C(\nu+\nu_m)}{\nu\nu_m}\|\tilde{B}_0(t^{n+1})\|_\infty^2\|\nabla\eta_v^{n+1}\|^2, \\
|(w_h^n\cdot\nabla\eta_v^{n+1},\phi_h^{n+1})| &\le C\|\nabla w_h^n\|\|\nabla\eta_v^{n+1}\|\|\nabla\phi_h^{n+1}\| \\
&\le \frac{\nu\nu_m}{16(\nu+\nu_m)}\|\nabla\phi_h^{n+1}\|^2+\frac{C(\nu+\nu_m)}{\nu\nu_m}\|\nabla w_h^n\|^2\|\nabla\eta_v^{n+1}\|^2, \\
|(\eta_w^n\cdot\nabla v(t^{n+1}),\phi_h^{n+1})| &\le C\|\nabla\eta_w^n\|\|\nabla v(t^{n+1})\|\|\nabla\phi_h^{n+1}\| \\
&\le \frac{\nu\nu_m}{16(\nu+\nu_m)}\|\nabla\phi_h^{n+1}\|^2+\frac{C(\nu+\nu_m)}{\nu\nu_m}\|\nabla v(t^{n+1})\|^2\|\nabla\eta_w^n\|^2.
\end{aligned}
$$

For the last nonlinear term, we use Hölder's inequality, Sobolev embedding theorems, Poincare's and Young's inequalities to reveal

$$
\begin{aligned}
|(\psi_h^n\cdot\nabla v(t^{n+1}),\phi_h^{n+1})| &\le C\|\psi_h^n\|\nabla v(t^{n+1})\|_{L^6}\|\phi_h^{n+1}\|_{L^3} \\
&\le C\|\psi_h^n\|\|v(t^{n+1})\|_{H^2}\|\phi_h^n\|^{1/2}\|\nabla\phi_h^{n+1}\|^{1/2} \\
&\le C\|\psi_h^n\|\|v(t^{n+1})\|_{H^2}\|\nabla\phi_h^{n+1}\| \\
&\le \frac{\nu\nu_m}{16(\nu+\nu_m)}\|\nabla\phi_h^{n+1}\|^2+\frac{C(\nu+\nu_m)}{\nu\nu_m}\|v(t^{n+1})\|_{H^2}^2\|\psi_h^n\|^2.
\end{aligned}
$$

The last term is evaluated as in [59]:

$$
\begin{aligned}
|G_1(t,v,w,\phi_h^{n+1})| \le \frac{(\Delta t)^2(\nu+\nu_m)}{\nu\nu_m}\Big(&C\|v_{tt}(t^{**})\|^2+\frac{(\nu-\nu_m)^2}{4}\|\nabla w_t(s^*)\|^2 \\
&+C\|\nabla w_t(s^*)\|^2\|\nabla v(t^{n+1})\|^2\Big)+\frac{\nu\nu_m}{16(\nu+\nu_m)}\|\nabla\phi_h^{n+1}\|^2,
\end{aligned}
$$

with $t^{**},s^*\in[t^n,t^{n+1}]$. Putting these estimates into (3.14) and dropping non-negative

term on the left hand side produces

$$\frac{1}{2\Delta t}\bigg(\|\phi_h^{n+1}\|^2-\|\phi_h^n\|^2\bigg)+\frac{\nu^2+\nu_m^2}{4(\nu+\nu_m)}\|\nabla\phi_h^{n+1}\|^2\le\frac{(\nu-\nu_m)^2}{4(\nu+\nu_m)}\|\nabla\psi_h^n\|^2$$
$$+\frac{C(\nu+\nu_m)}{\nu\nu_m}\|v(t^{n+1})\|_{H^2}^2\|\psi_h^n\|^2+\frac{C(\nu+\nu_m)}{\nu\nu_m(\Delta t)}\int_{t^n}^{t^{n+1}}\|\partial_t\eta_v\|^2d\tau+\frac{(\nu+\nu_m)^3}{\nu\nu_m}\|\nabla\eta_v^{n+1}\|^2$$
$$+\frac{(\nu-\nu_m)^2(\nu+\nu_m)}{\nu\nu_m}\|\nabla\eta_w^n\|^2+\frac{C(\nu+\nu_m)}{\nu\nu_m}\bigg[\bigg(\|\tilde{B}_0(t^{n+1})\|_\infty^2+\|\nabla w_h^n\|^2\bigg)\|\nabla\eta_v^{n+1}\|^2$$
$$+\|\nabla v(t^{n+1})\|^2\|\nabla\eta_w^n\|^2\bigg]+\frac{(\Delta t)^2(\nu+\nu_m)}{\nu\nu_m}\bigg(C\|v_{tt}(t^{**})\|^2$$
$$+\frac{(\nu-\nu_m)^2}{4}\|\nabla w_t(s^*)\|^2+C\|\nabla w_t(s^*)\|^2\|\nabla v(t^{n+1})\|^2\bigg).\tag{3.16}$$

Applying similar techniques to (3.15), we get

$$\frac{1}{2\Delta t}\bigg(\|\psi_h^{n+1}\|^2-\|\psi_h^n\|^2\bigg)+\frac{\nu^2+\nu_m^2}{4(\nu+\nu_m)}\|\nabla\psi_h^{n+1}\|^2\le\frac{(\nu-\nu_m)^2}{4(\nu+\nu_m)}\|\nabla\phi_h^n\|^2$$
$$+\frac{C(\nu+\nu_m)}{\nu\nu_m}\|w(t^{n+1})\|_{H^2}^2\|\phi_h^n\|^2+\frac{C(\nu+\nu_m)}{\nu\nu_m(\Delta t)}\int_{t^n}^{t^{n+1}}\|\partial_t\eta_w\|^2d\tau+\frac{(\nu+\nu_m)^3}{\nu\nu_m}\|\nabla\eta_w^{n+1}\|^2$$
$$+\frac{(\nu-\nu_m)^2(\nu+\nu_m)}{\nu\nu_m}\|\nabla\eta_v^n\|^2+\frac{C(\nu+\nu_m)}{\nu\nu_m}\bigg[\bigg(\|\tilde{B}_0(t^{n+1})\|_\infty^2+\|\nabla v_h^n\|^2\bigg)\|\nabla\eta_w^{n+1}\|^2$$
$$+\|\nabla w(t^{n+1})\|^2\|\nabla\eta_v^n\|^2\bigg]+\frac{(\Delta t)^2(\nu+\nu_m)}{\nu\nu_m}\bigg(C\|w_{tt}(s^{**})\|^2$$
$$+\frac{(\nu-\nu_m)^2}{4}\|\nabla v_t(t^*)\|^2+C\|\nabla v_t(t^*)\|^2\|\nabla w(t^{n+1})\|^2\bigg),\tag{3.17}$$

with $s^{**},t^*\in[t^n,t^{n+1}]$. Now add equations (3.16) and (3.17), multiply by $2\Delta t$ and sum over the time steps. Using interpolation properties (2.3)-(2.4) with noting that

$\|\psi_h^0\| = \|\phi_h^0\| = 0$ and $\Delta t M = T$ yields

$$\begin{aligned}
&\left(\|\phi_h^M\|^2 + \|\psi_h^M\|^2\right) + \frac{\nu^2+\nu_m^2}{4(\nu+\nu_m)}(\|\nabla\phi_h^M\|^2 + \|\nabla\psi_h^M\|^2) \\
&\quad + \frac{\nu\nu_m}{2(\nu+\nu_m)}\Delta t\sum_{n=0}^{M-2}(\|\nabla\phi_h^{n+1}\|^2 + \|\nabla\psi_h^{n+1}\|^2) \\
&\quad \le \Delta t\sum_{n=0}^{M-1} C\frac{(\nu+\nu_m)}{\nu\nu_m}\left(\|w\|^2_{L^\infty(0,T;H^2(\Omega))}\|\phi_h^n\|^2 + \|v\|^2_{L^\infty(0,T;H^2(\Omega))}\|\psi_h^n\|^2\right) \\
&\quad + \frac{C(\nu+\nu_m)}{\nu\nu_m}\int_0^T\left(\|\partial_t\eta_v\|^2 + \|\partial_t\eta_w\|^2\right)d\tau \\
&\quad + C^*h^{2k}\Delta t\sum_{n=0}^{M-1}\left(|v(t^{n+1})|^2_{k+1} + |w(t^{n+1})|^2_{k+1}\right) \\
&\quad + C^*h^{2k}\Delta t\sum_{n=0}^{M-1}\left(|v(t^{n})|^2_{k+1} + |w(t^{n})|^2_{k+1}\right) + C^*(\Delta t)^2 \\
&\quad + C^*h^{2k}\Delta t\sum_{n=0}^{M-1}\left(\|\nabla v_h^n\|^2|w(t^{n+1})|^2_{k+1} + \|\nabla w_h^n\|^2|v(t^{n+1})|^2_{k+1}\right) \qquad (3.18)
\end{aligned}$$

here $C^* := C^*(C, T, \nu, \nu_m, v, w, \tilde{B}_0(t))$ and it is independent of the time step Δt and h. Using smoothness assumptions, approximation properties (2.3)-(2.4), and the stability bounds on the discrete solutions in (3.18) gives

$$\begin{aligned}
&\left(\|\phi_h^M\|^2 + \|\psi_h^M\|^2\right) + \frac{\nu^2+\nu_m^2}{4(\nu+\nu_m)}(\|\nabla\phi_h^M\|^2 + \|\nabla\psi_h^M\|^2) \\
&\qquad + \frac{\nu\nu_m}{2(\nu+\nu_m)}\Delta t\sum_{n=0}^{M-2}(\|\nabla\phi_h^{n+1}\|^2 + \|\nabla\psi_h^{n+1}\|^2) \\
&\qquad \le \Delta t\sum_{n=0}^{M-1} C^*\left(\|\phi_h^n\|^2 + \|\psi_h^n\|^2\right) + C^*(\Delta t)^2 + C^*(h^{2k} + h^{2k+2}).
\end{aligned}$$

The result follows from application of the discrete Gronwall lemma and the triangle inequality. We note that since there is no $\|\phi_h^M\|^2$ or $\|\psi_h^M\|^2$ on the right hand side (the sum ends at M-1) there is no timestep restriction for the application of the Gronwall

lemma.

□

3.3 Penalty-projection method for MHD in Elsässer Variables

The algorithm studied in the previous section decouples into 2 sub-problems at each timestep, each of which takes the form of an Oseen problem. It is known that splitting methods such as the penalty-projection method can more efficiently give solutions to such problems, with often very little sacrifice in accuracy [12, 53, 65]. We therefore propose in this section a scheme that uses penalty-projection methods for the 2 sub-problems. Because of the splitting, it is necessary to define an additional velocity space: $Y_h = (P_k)^d \cap H_0^{div}(\Omega)^d$. The only difference between Y_h and X_h is simply that the boundary condition of Y_h is only enforced in the normal direction, while for X_h it is enforced in all directions.

The proposed scheme takes the following form.

Algorithm 3.3.1. *(Grad-div stabilized projection scheme): Let* $f_1, f_2 \in L^\infty(0,T; H^{-1}(\Omega))$, *stabilization parameter* $\gamma > 0$ *and time step* $\Delta t > 0$ *and end time* $T > 0$ *be given. Set* $M = T/\Delta t$ *and start with* $\tilde{v}^0 = v(0), \tilde{w}^0 = w(0) \in H^2 \cup V$. *For all* $n = 0, 1, ..., M-1$, *compute* $\hat{v}_h^{n+1}, \hat{w}_h^{n+1}, \hat{p}_h^{n+1}, \hat{q}_h^{n+1}$ *via:*
Step 1: Find $\hat{v}^{n+1} \in X_h$ *satisfying for all* $\chi_h \in X_h$,

$$\left(\frac{\hat{v}_h^{n+1} - \tilde{v}_h^n}{\Delta t}, \chi_h\right) + b^*(\hat{w}_h^n, \hat{v}_h^{n+1}, \chi_h) - (\tilde{B}_0(t^{n+1}) \cdot \nabla \hat{v}_h^{n+1}, \chi_h) + \frac{\nu + \nu_m}{2}(\nabla \hat{v}_h^{n+1}, \nabla \chi_h) + \frac{\nu - \nu_m}{2}(\nabla \hat{w}_h^n, \nabla \chi_h) + \gamma(\nabla \cdot \hat{v}_h^{n+1}, \nabla \cdot \chi_h) = (f_1(t^{n+1}), \chi_h). \tag{3.19}$$

Step 2: Find $(\tilde{v}_h^{n+1}, \hat{q}_h^{n+1}) \in (Y_h \times Q_h)$ *satisfying for all* $(v_h, q_h) \in (Y_h \times Q_h)$,

$$\left(\frac{\tilde{v}_h^{n+1} - \hat{v}_h^{n+1}}{\Delta t}, v_h\right) - (\hat{q}_h^{n+1}, \nabla \cdot v_h) = 0, \tag{3.20}$$

$$(\nabla \cdot \tilde{v}^{n+1}, q_h) = 0. \tag{3.21}$$

Step 3: Compute $\hat{w}_h^{n+1} \in X_h$ *for all* $l_h \in X_h$,

$$\left(\frac{\hat{w}_h^{n+1} - \tilde{w}_h^n}{\Delta t}, l_h\right) + b^*(\hat{v}_h^n, \hat{w}_h^{n+1}, l_h) + (\tilde{B}_0(t^{n+1}) \cdot \nabla \hat{w}_h^{n+1}, l_h) + \frac{\nu + \nu_m}{2}(\nabla \hat{w}_h^{n+1}, \nabla l_h) + \frac{\nu - \nu_m}{2}(\nabla \hat{v}_h^n, \nabla l_h) + \gamma(\nabla \cdot \hat{w}_h^{n+1}, \nabla \cdot l_h) = (f_2(t^{n+1}), l_h). \tag{3.22}$$

Step 4: Find $(\tilde{w}_h^{n+1}, \hat{\lambda}_h^{n+1}) \in (Y_h \times Q_h)$ *satisfying for all* $(s_h, r_h) \in (Y_h \times Q_h)$,

$$\left(\frac{\tilde{w}_h^{n+1} - \hat{w}_h^{n+1}}{\Delta t}, s_h\right) - (\hat{\lambda}_h^{n+1}, \nabla \cdot s_h) = 0, \tag{3.23}$$

$$(\nabla \cdot \tilde{w}_h^{n+1}, r_h) = 0. \tag{3.24}$$

Since $X_h \subset Y_h$, we can choose $v_h = \chi_h$ in (3.20), $s_h = l_h$ in (3.23) and combine these with equations (3.19) and (3.22), respectively, to get

$$\left(\frac{\hat{v}_h^{n+1} - \hat{v}_h^n}{\Delta t}, \chi_h\right) + b^*(\hat{w}_h^n, \hat{v}_h^{n+1}, \chi_h) - (\tilde{B}_0(t^{n+1}) \cdot \nabla \hat{v}_h^{n+1}, \chi_h) + \frac{\nu + \nu_m}{2}(\nabla \hat{v}_h^{n+1}, \nabla \chi_h) + \frac{\nu - \nu_m}{2}(\nabla \hat{w}_h^n, \nabla \chi_h) + \gamma(\nabla \cdot \hat{v}_h^{n+1}, \nabla \cdot \chi_h) - (\hat{q}_h^n, \nabla \cdot \chi_h) = (f_1(t^{n+1}), \chi_h). \tag{3.25}$$

and

$$\left(\frac{\hat{w}_h^{n+1} - \hat{w}_h^n}{\Delta t}, l_h\right) + b^*(\hat{v}_h^n, \hat{w}_h^{n+1}, l_h) + (\tilde{B}_0(t^{n+1}) \cdot \nabla \hat{w}_h^{n+1}, l_h) + \frac{\nu + \nu_m}{2}(\nabla \hat{w}_h^{n+1}, \nabla l_h) + \frac{\nu - \nu_m}{2}(\nabla \hat{v}_h^n, \nabla l_h) + \gamma(\nabla \cdot \hat{w}_h^{n+1}, \nabla \cdot l_h) - (\hat{\lambda}_h^n, \nabla \cdot l_h) = (f_2(t^{n+1}), l_h). \tag{3.26}$$

We first prove unconditional stability of the penalty-projection scheme.

Lemma 3.3.1. *(Unconditional Stability) Let* $(\hat{v}_h^{n+1}, \hat{w}_h^{n+1}, \hat{q}_h^{n+1}, \hat{\lambda}_h^{n+1})$ *be the solution of Algorithm 3.3.1 and* $f_1, f_2 \in L^\infty(0,T;H^{-1}(\Omega))$*. Then for all* $\Delta t > 0$*, we have the following unconditional stability bound:*

$$\begin{aligned}
&\|\hat{v}_h^M\|^2 + \|\hat{w}_h^M\|^2 + \frac{(\nu-\nu_m)^2}{2(\nu+\nu_m)}\Delta t(\|\nabla\hat{v}_h^M\|^2 + \|\nabla\hat{w}_h^M\|^2) \\
&\quad + \frac{\nu\nu_m}{\nu+\nu_m}\Delta t\sum_{n=0}^{M-1}\left(\|\nabla\hat{v}_h^{n+1}\|^2 + \|\nabla\hat{w}_h^{n+1}\|^2\right) \\
&\quad + \Delta t\sum_{n=0}^{M-1}\gamma(\|\nabla\cdot\hat{v}_h^{n+1}\|^2 + \|\nabla\cdot\hat{w}_h^{n+1}\|^2) \\
&\quad \le \|\hat{v}_h^0\|^2 + \|\hat{w}_h^0\|^2 + \frac{(\nu-\nu_m)^2}{2(\nu+\nu_m)}\Delta t(\|\nabla\hat{v}_h^0\|^2 + \|\nabla\hat{w}_h^0\|^2) \\
&\quad + \frac{\nu+\nu_m}{\nu\nu_m}\Delta t\sum_{n=0}^{M-1}(\|f_1(t^{n+1})\|_{-1}^2 + \|f_2(t^{n+1})\|_{-1}^2)
\end{aligned} \tag{3.27}$$

Proof. Taking $\chi_h = \hat{v}_h^{n+1}$ in (3.19) and $l_h = \hat{w}_h^{n+1}$ in (3.22) with the polarization identity produces

$$\begin{aligned}
&\frac{1}{2\Delta t}(\|\hat{v}_h^{n+1}\|^2 - \|\tilde{v}_h^n\|^2 + \|\hat{v}_h^{n+1} - \tilde{v}_h^n\|^2) + \frac{\nu+\nu_m}{2}\|\nabla\hat{v}_h^{n+1}\|^2 + \gamma\|\nabla\cdot\hat{v}_h^{n+1}\|^2 \\
&\qquad = -\frac{\nu-\nu_m}{2}(\nabla\hat{w}_h^n, \nabla\hat{v}_h^{n+1}) + (f_1(t^{n+1}), \hat{v}_h^{n+1})
\end{aligned} \tag{3.28}$$

and

$$\begin{aligned}
&\frac{1}{2\Delta t}(\|\hat{w}_h^{n+1}\|^2 - \|\tilde{w}_h^n\|^2 + \|\hat{w}_h^{n+1} - \tilde{w}_h^n\|^2) + \frac{\nu+\nu_m}{2}\|\nabla\hat{w}_h^{n+1}\|^2 + \gamma\|\nabla\cdot\hat{w}_h^{n+1}\|^2 \\
&\qquad = -\frac{\nu-\nu_m}{2}(\nabla\hat{v}_h^n, \nabla\hat{w}_h^{n+1}) + (f_2(t^{n+1}), \hat{w}_h^{n+1}).
\end{aligned} \tag{3.29}$$

Applying Cauchy-Schwarz and Young's inequalities on the right hand sides terms of

(3.28) and (3.29) gives

$$\frac{|\nu-\nu_m|}{2}|(\nabla\hat{w}_h^n,\nabla\hat{v}_h^{n+1})| \le \frac{\nu+\nu_m}{4}\|\nabla\hat{v}_h^{n+1}\|^2 + \frac{(\nu-\nu_m)^2}{4(\nu+\nu_m)}\|\nabla\hat{w}_h^n\|^2,$$
$$|(f_1(t^{n+1}),\hat{v}_h^{n+1})| \le \frac{\nu\nu_m}{2(\nu+\nu_m)}\|\nabla\hat{v}_h^{n+1}\|^2 + \frac{(\nu+\nu_m)}{2(\nu\nu_m)}\|f_1(t^{n+1})\|_{-1}^2,$$
$$\frac{|\nu-\nu_m|}{2}|(\nabla\hat{v}_h^n,\nabla\hat{w}_h^{n+1})| \le \frac{\nu+\nu_m}{4}\|\nabla\hat{w}_h^{n+1}\|^2 + \frac{(\nu-\nu_m)^2}{4(\nu+\nu_m)}\|\nabla\hat{v}_h^n\|^2,$$
$$|(f_2(t^{n+1}),\hat{w}_h^{n+1})| \le \frac{\nu\nu_m}{2(\nu+\nu_m)}\|\nabla\hat{w}_h^{n+1}\|^2 + \frac{(\nu+\nu_m)}{2(\nu\nu_m)}\|f_2(t^{n+1})\|_{-1}^2.$$

Now choose $v_h = \tilde{v}_h^{n+1}$ in (3.20), $q_h = \hat{q}_h^{n+1}$ in (3.21) and $s_h = \tilde{w}_h^{n+1}$ in (3.23), $r_h = \hat{\lambda}_h^{n+1}$ in (3.24). Then apply Cauchy-Schwarz and Young's inequalities to obtain

$$\|\tilde{v}_h^{n+1}\|^2 \le \|\hat{v}_h^{n+1}\|^2,$$
$$\|\tilde{w}_h^{n+1}\|^2 \le \|\hat{w}_h^{n+1}\|^2.$$

for all $n = 0, 1, 2, ..., M-1$. Plugging these estimates into (3.28) and (3.29), dropping the non-negative terms results in

$$\frac{1}{2\Delta t}(\|\hat{v}_h^{n+1}\|^2 - \|\hat{v}_h^n\|^2) + \frac{(\nu-\nu_m)^2}{4(\nu+\nu_m)}\|\nabla\hat{v}_h^{n+1}\|^2 + \frac{\nu\nu_m}{2(\nu+\nu_m)}\|\nabla\hat{v}_h^{n+1}\|^2 + \gamma\|\nabla\cdot\hat{v}_h^{n+1}\|^2 \le \frac{(\nu-\nu_m)^2}{4(\nu+\nu_m)}\|\nabla\hat{w}_h^n\|^2 + \frac{\nu+\nu_m}{2\nu\nu_m}\|f_1(t^{n+1})\|_{-1}^2 \quad (3.30)$$

and

$$\frac{1}{2\Delta t}(\|\hat{w}_h^{n+1}\|^2 - \|\hat{w}_h^n\|^2) + \frac{(\nu-\nu_m)^2}{4(\nu+\nu_m)}\|\nabla\hat{w}_h^{n+1}\|^2 + \frac{\nu\nu_m}{2(\nu+\nu_m)}\|\nabla\hat{w}_h^{n+1}\|^2 + \gamma\|\nabla\cdot\hat{w}_h^{n+1}\|^2 \le \frac{(\nu-\nu_m)^2}{4(\nu+\nu_m)}\|\nabla\hat{v}_h^n\|^2 + \frac{\nu+\nu_m}{2\nu\nu_m}\|f_2(t^{n+1})\|_{-1}^2. \quad (3.31)$$

Adding these two equations, multiplying by $2\Delta t$ and summing over time steps finishes

the proof. □

We now prove convergence of Algorithm 3.3.1 to Algorithm 3.2.1 as $\gamma \to \infty$. To do so, we will need to define the space $R_h := V_h^{\perp} \subset X_h$ to be the orthogonal complement of V_h with respect to the norm $H^1(\Omega)$. The following lemma gives the equivalence of the divergence and gradient norms in the space R_h, which is proven in [34] in a very general setting, and a simpler proof for the case of Scott-Vogelius elements is given in [65].

Lemma 3.3.2. *Let $(X_h, Q_h) \subset (X, Q)$ be finite element pairs satisfying the inf-sup condition* (2.2) *and the divergence-free property, i.e., $\nabla \cdot X_h \subset Q_h$. Then there exists a constant C_R independent of h such that*

$$\|\nabla v_h\| \leq C_R \|\nabla \cdot v_h\|, \quad \forall v_h \in R_h.$$

Assumption 3.3.1. *Let's assume that there exists a constant C_* which is independent of $h, \Delta t$ and γ, such that for sufficiently small h and Δt, the solutions of Algorithm 3.2.1 and Algorithm 3.3.1 satisfy*

$$\max_{1\leq n\leq M}(\|\nabla v_h^n\|_{L^3} + \|\nabla w_h^n\|_{L^3} + \|v_h^n\|_\infty + \|w_h^n\|_\infty) \leq C_*,$$

$$\max_{1\leq n\leq M}(\|\nabla \hat{v}_h^n\| + \|\nabla \hat{w}_h^n\|) \leq C_*.$$

Theorem 2. *Let $(v_h^{n+1}, w_h^{n+1}, q_h^{n+1})$ and $(\hat{v}_h^{n+1}, \hat{w}_h^{n+1}, \hat{q}_h^{n+1})$ be solutions of the Algorithm 3.2.1 and Algorithm 3.3.1, respectively, for $n = 0, 1, 2, ..., M-1$. We then have*

the following:

$$\left(\Delta t \sum_{=0}^{M-1} \left(\|\nabla(v_h^{n+1} - \hat{v}_h^{n+1})\|^2 + \|\nabla(w_h^{n+1} - \hat{w}_h^{n+1})\|^2\right)\right)^{1/2} \leq$$
$$\gamma^{-1} C \max\left\{C_*(\frac{\nu+\nu_m}{\nu\nu_m})^{1/2}, (\Delta t)^{-1/2}\right\}\left(\Delta t \sum_{n=0}^{M-1}\left(\|q_h^{n+1} - \hat{q}_h^n\|^2 + \|\lambda_h^{n+1} - \hat{\lambda}_h^n\|^2\right)\right)^{1/2}.$$

Remark 3.3.1. *The theorem shows that on a fixed mesh and timestep, penalty-projection solutions have first order convergence to the Algorithm 3.2.1 solution as* $\gamma \to \infty$. *This shows that for large penalty parameters, we can use the penalty-projection method and get the same accuracy as Algorithm 3.2.1.*

Proof. Denote $e^{n+1} := v_h^{n+1} - \hat{v}_h^{n+1}$ and $\epsilon^{n+1} := w_h^{n+1} - \hat{w}_h^{n+1}$ and decompose the errors orthogonally as follows:

$$e^{n+1} := e_0^{n+1} + e_R^{n+1},\ \epsilon^{n+1} := \epsilon_0^{n+1} + \epsilon_R^{n+1}$$

with $e_0^{n+1}, \epsilon_0^{n+1} \in V_h$ and $e_R^{n+1}, \epsilon_R^{n+1} \in R_h$, $n = 0, 1, ..., M-1$.

Step 1: *Estimate of* $e_R^{n+1}, \epsilon_R^{n+1}$*:*

Subtracting the equation (3.1) from (3.25) and (3.2) from (3.26) produces

$$\begin{aligned}\frac{1}{\Delta t}\Big(e^{n+1} - e^n, \chi_h\Big) &+ \frac{\nu+\nu_m}{2}(\nabla e^{n+1}, \nabla\chi_h) + \gamma(\nabla\cdot e_R^{n+1}, \nabla\cdot\chi_h)\\ &+ \frac{\nu-\nu_m}{2}(\nabla\epsilon^n, \nabla\chi_h) - (\tilde{B}_0(t^{n+1})\cdot\nabla e^{n+1}, \chi_h) + b^*(\epsilon^n, v_h^{n+1}, \chi_h)\\ &+ b^*(\hat{w}_h^n, e^{n+1}, \chi_h) - (q_h^{n+1} - \hat{q}_h^n, \nabla\cdot\chi_h) = 0, \end{aligned} \tag{3.32}$$

and

$$\frac{1}{\Delta t}\left(\epsilon^{n+1}-\epsilon^n, l_h\right) + \frac{\nu+\nu_m}{2}(\nabla\epsilon^{n+1}, \nabla l_h) + \gamma(\nabla\cdot\epsilon_R^{n+1}, \nabla\cdot l_h) + \frac{\nu-\nu_m}{2}(\nabla e^n, \nabla l_h) + (\tilde{B}_0(t^{n+1})\cdot\nabla\epsilon^{n+1}, l_h) + b^*(e^n, w_h^{n+1}, l_h) + b^*(\hat{v}_h^n, \epsilon^{n+1}, l_h) - (\lambda_h^{n+1} - \hat{\lambda}_h^n, \nabla\cdot l_h) = 0. \tag{3.33}$$

Take $\chi_h = e^{n+1}$ in (3.32), $l_h = \epsilon^{n+1}$ in (3.33), which yield

$$b^*(\hat{w}_h^n, e^{n+1}, e^{n+1}) = (\tilde{B}_0(t^{n+1})\cdot\nabla e^{n+1}, e^{n+1}) = 0$$
$$b^*(\hat{v}_h^n, \epsilon^{n+1}, \epsilon^{n+1}) = (\tilde{B}_0(t^{n+1})\cdot\nabla\epsilon^{n+1}, \epsilon^{n+1}) = 0$$

and use polarization identity $2(a-b,a) = \|a\|^2 - \|b\|^2 + \|a-b\|^2$ to get

$$\frac{1}{2\Delta t}\left(\|e^{n+1}\|^2 - \|e^n\|^2 + \|e^{n+1}-e^n\|^2\right) + \frac{\nu+\nu_m}{2}\|\nabla e^{n+1}\|^2 + \gamma\|\nabla\cdot e_R^{n+1}\|^2 = -\frac{\nu-\nu_m}{2}(\nabla\epsilon^n, \nabla e^{n+1}) + (q_h^{n+1} - \hat{q}_h^n, \nabla\cdot e_R^{n+1}) - b^*(\epsilon^n, v_h^{n+1}, e^{n+1}) \tag{3.34}$$

and

$$\frac{1}{2\Delta t}\left(\|\epsilon^{n+1}\|^2 - \|\epsilon^n\|^2 + \|\epsilon^{n+1}-\epsilon^n\|^2\right) + \frac{\nu+\nu_m}{2}\|\nabla\epsilon^{n+1}\|^2 + \gamma\|\nabla\cdot\epsilon_R^{n+1}\|^2 = -\frac{\nu-\nu_m}{2}(\nabla e^n, \nabla\epsilon^{n+1}) + (\lambda_h^{n+1} - \hat{\lambda}_h^n, \nabla\cdot\epsilon_R^{n+1}) - b^*(e^n, w_h^{n+1}, \epsilon^{n+1}). \tag{3.35}$$

Applying Cauchy-Schwarz and Young's inequalities to the first two terms of (3.34)

provides

$$\frac{|\nu-\nu_m|}{2}|(\nabla\epsilon^n,\nabla e^{n+1})| \le \frac{(\nu-\nu_m)^2}{4(\nu+\nu_m)}\|\nabla\epsilon^n\|^2 + \frac{\nu+\nu_m}{4}\|\nabla e^{n+1}\|^2,$$
$$(q_h^{n+1}-\hat{q}_h^n,\nabla\cdot e_R^{n+1}) \le \frac{\gamma^{-1}}{2}\|q_h^{n+1}-\hat{q}_h^n\|^2 + \frac{\gamma}{2}\|\nabla\cdot e_R^{n+1}\|^2.$$

and using Hölder's and Young's inequalities with Sobolev embedding theorem along with Assumption 3.3.1 on the non-linear term yields:

$$\begin{aligned}|b^*(\epsilon^n,v_h^{n+1},e^{n+1})| &\le C\bigg(\|\epsilon^n\|\|\nabla v_h^{n+1}\|_{L^3}\|\nabla e^{n+1}\| + \|\epsilon^n\|\|v_h^{n+1}\|_{L^\infty}\|\nabla e^{n+1}\|\bigg)\\ &\le CC_*\|\epsilon^n\|\|\nabla e^{n+1}\|\\ &\le \frac{\nu\nu_m}{2(\nu+\nu_m)}\|\nabla e^{n+1}\|^2 + \frac{CC_*^2(\nu+\nu_m)}{\nu\nu_m}\|\epsilon^n\|^2.\end{aligned}$$

Substituting these estimates in (3.34), adding and subtracting the term $\frac{\nu\nu_m}{2(\nu+\nu_m)}\|\nabla e^{n+1}\|^2$ with dropping the non-negative term $\|e^{n+1}-e^n\|^2$ gives us

$$\begin{aligned}\frac{1}{2\Delta t}(\|e^{n+1}\|^2-\|e^n\|^2) + \frac{(\nu-\nu_m)^2}{4(\nu+\nu_m)}\|\nabla e^{n+1}\|^2 + \frac{\nu\nu_m}{2(\nu+\nu_m)}\|\nabla e^{n+1}\|^2 + \frac{\gamma}{2}\|\nabla\cdot e_R^{n+1}\|^2\\ \le \frac{(\nu-\nu_m)^2}{4(\nu+\nu_m)}\|\nabla\epsilon^n\|^2 + \frac{CC_*^2(\nu+\nu_m)}{\nu\nu_m}\|\epsilon^n\|^2 + \frac{\gamma^{-1}}{2}\|q_h^{n+1}-\hat{q}_h^n\|^2. \quad (3.36)\end{aligned}$$

Now apply similar estimates to the right hand side terms of (3.35) to produce

$$\begin{aligned}\frac{1}{2\Delta t}(\|\epsilon^{n+1}\|^2-\|\epsilon^n\|^2) + \frac{(\nu-\nu_m)^2}{4(\nu+\nu_m)}\|\nabla\epsilon^{n+1}\|^2 + \frac{\nu\nu_m}{2(\nu+\nu_m)}\|\nabla\epsilon^{n+1}\|^2 + \frac{\gamma}{2}\|\nabla\cdot\epsilon_R^{n+1}\|^2\\ \le \frac{(\nu-\nu_m)^2}{4(\nu+\nu_m)}\|\nabla e^n\|^2 + \frac{CC_*^2(\nu+\nu_m)}{\nu\nu_m}\|e^n\|^2 + \frac{\gamma^{-1}}{2}\|\lambda_h^{n+1}-\hat{\lambda}_h^n\|^2. \quad (3.37)\end{aligned}$$

Then add the equations (3.36) and (3.37), multiply by $2\Delta t$ and sum over time steps

to obtain

$$\begin{aligned}\|e^M\|^2+\|\epsilon^M\|^2 + \frac{(\nu-\nu_m)^2}{2(\nu+\nu_m)}\Delta t\Big(\|\nabla e^M\|^2+\|\nabla\epsilon^M\|^2\Big)\\ + \frac{\nu\nu_m}{\nu+\nu_m}\Delta t\sum_{n=0}^{M-1}\left(\|\nabla e^{n+1}\|^2+\|\nabla\epsilon^{n+1}\|^2\right)\\ + \Delta t\sum_{n=0}^{M-1}\gamma\left(\|\nabla\cdot e_R^{n+1}\|^2+\|\nabla\cdot\epsilon_R^{n+1}\|^2\right)\\ \le \Delta t\sum_{n=0}^{M-1}\frac{CC_*^2(\nu+\nu_m)}{\nu\nu_m}\left(\|e^n\|^2+\|\epsilon^n\|^2\right)\\ + \Delta t\sum_{n=0}^{M-1}\gamma^{-1}\left(\|q_h^{n+1}-\hat{q}_h^n\|^2+\|\lambda_h^{n+1}-\hat{\lambda}_h^n\|^2\right).\end{aligned}$$

and apply discrete Gronwall Lemma to get

$$LHS \le \gamma^{-1}exp\left(CC_*^2\frac{(\nu+\nu_m)}{\nu\nu_m}\right)\left(\Delta t\sum_{n=0}^{M-1}(\|q_h^{n+1}-\hat{q}_h^n\|^2+\|\lambda_h^{n+1}-\hat{\lambda}_h^n\|^2)\right). \quad (3.38)$$

Using Lemma 3.3.2 with (3.38) yields the following desired bound:

$$\begin{aligned}\Delta t\sum_{n=0}^{M-1}(\|\nabla e_R^{n+1}\|^2+\|\nabla\epsilon_R^{n+1}\|^2) \le C_R^2\left(\Delta t\sum_{n=0}^{M-1}\left(\|\nabla\cdot e_R^{n+1}\|^2+\|\nabla\cdot\epsilon_R^{n+1}\|^2\right)\right)\\ \le \gamma^{-2}C_R^2exp\left(CC_*^2\frac{(\nu+\nu_m)}{\nu\nu_m}\right)\left(\Delta t\sum_{n=0}^{M-1}(\|q_h^{n+1}-\hat{q}_h^n\|^2+\|\lambda_h^{n+1}-\hat{\lambda}_h^n\|^2)\right). \quad (3.39)\end{aligned}$$

Step 2: *Estimates of* $e_0^{n+1}, \epsilon_0^{n+1}$ *:*
To find a bound on $\left(\Delta t\sum_{n=0}^{M-1}\left(\|\nabla e_0^{n+1}\|^2+\|\nabla\epsilon_0^{n+1}\|^2\right)\right)$, choose $\chi_h = e_0^{n+1}$ in (3.32)

and $l_h = \epsilon_0^{n+1}$ in (3.33) to get

$$\frac{1}{\Delta t}(e^{n+1} - e^n, e_0^{n+1}) + \frac{\nu + \nu_m}{2}\|\nabla e_0^{n+1}\|^2 = -\frac{\nu - \nu_m}{2}(\nabla \epsilon_0^n, \nabla e_0^{n+1}) + (\tilde{B}_0(t^{n+1}) \cdot \nabla e_R^{n+1}, e_0^{n+1}) - b^*(\epsilon^n, v_h^{n+1}, e_0^{n+1}) - b^*(\hat{w}_h^n, e_R^{n+1}, e_0^{n+1}), \quad (3.40)$$

and

$$\frac{1}{\Delta t}(\epsilon^{n+1} - \epsilon^n, \epsilon_0^{n+1}) + \frac{\nu + \nu_m}{2}\|\nabla \epsilon_0^{n+1}\|^2 = -\frac{\nu - \nu_m}{2}(\nabla e_0^n, \nabla \epsilon_0^{n+1}) + (\tilde{B}_0(t^{n+1}) \cdot \nabla \epsilon_R^{n+1}, \epsilon_0^{n+1}) - b^*(e^n, w_h^{n+1}, \epsilon_0^{n+1}) - b^*(\hat{v}_h^n, \epsilon_R^{n+1}, \epsilon_0^{n+1}). \quad (3.41)$$

Applying Cauchy-Schwarz and Hölder's inequalities with (2.1) on the right hand side terms of (3.40) and (3.41) yields

$$\begin{aligned}\frac{1}{\Delta t}(e^{n+1} - e^n, e_0^{n+1}) + \frac{\nu + \nu_m}{2}\|\nabla e_0^{n+1}\|^2 &\leq \frac{|\nu - \nu_m|}{2}\|\nabla \epsilon_0^n\|\|\nabla e_0^{n+1}\| + C\|\tilde{B}_0(t^{n+1})\|_\infty\|\nabla e_R^{n+1}\|\|e_0^{n+1}\| \\ &+ C\bigg(\|\epsilon^n\|\|\nabla v_h^{n+1}\|_{L^3}\|\nabla e_0^{n+1}\| + \|\epsilon^n\|\|v_h^{n+1}\|_\infty\|\nabla e_0^{n+1}\|\bigg) \\ &+ C\|\nabla \hat{w}_h^n\|\|\nabla e_R^{n+1}\|\|\nabla e_0^{n+1}\| \quad (3.42)\end{aligned}$$

and

$$\begin{aligned}\frac{1}{\Delta t}(\epsilon^{n+1} - \epsilon^n, \epsilon_0^{n+1}) + \frac{\nu + \nu_m}{2}\|\nabla \epsilon_0^{n+1}\|^2 &\leq \frac{|\nu - \nu_m|}{2}\|\nabla e_0^n\|\|\nabla \epsilon_0^{n+1}\| + C\|\tilde{B}_0(t^{n+1})\|_\infty\|\nabla \epsilon_R^{n+1}\|\|\epsilon_0^{n+1}\| \\ &+ C\bigg(\|e^n\|\|\nabla w_h^{n+1}\|_{L^3}\|\nabla \epsilon_0^{n+1}\| + \|e^n\|\|w_h^{n+1}\|_\infty\|\nabla \epsilon_0^{n+1}\|\bigg) \\ &+ C\|\nabla \hat{v}_h^n\|\|\nabla \epsilon_R^{n+1}\|\|\nabla \epsilon_0^{n+1}\|. \quad (3.43)\end{aligned}$$

First use Poincare's inequality with the Assumption 3.3.1 on the second and third right hand side terms of (3.42) and (3.43), respectively. Next, apply Young's inequality with appropriate ϵ to produce:

$$\begin{aligned}
&\frac{1}{\Delta t}(e^{n+1}-e^n, e_0^{n+1}) + \frac{\nu+\nu_m}{2}\|\nabla e_0^{n+1}\|^2 \\
&\leq \frac{(\nu-\nu_m)^2}{4(\nu+\nu_m)}\|\nabla \epsilon_0^n\|^2 + \frac{\nu+\nu_m}{4}\|\nabla e_0^{n+1}\|^2 + \frac{\nu\nu_m}{2(\nu+\nu_m)}\|\nabla e_0^{n+1}\|^2 \\
&+ CC_*^2\frac{\nu+\nu_m}{\nu\nu_m}(\|\epsilon^n\|^2 + \|\nabla e_R^{n+1}\|^2)
\end{aligned} \tag{3.44}$$

and

$$\begin{aligned}
&\frac{1}{\Delta t}(\epsilon^{n+1}-\epsilon^n, \epsilon_0^{n+1}) + \frac{\nu+\nu_m}{2}\|\nabla \epsilon_0^{n+1}\|^2 \\
&\leq \frac{(\nu-\nu_m)^2}{4(\nu+\nu_m)}\|\nabla e_0^n\|^2 + \frac{\nu+\nu_m}{4}\|\nabla \epsilon_0^{n+1}\|^2 + \frac{\nu\nu_m}{2(\nu+\nu_m)}\|\nabla \epsilon_0^{n+1}\|^2 \\
&+ CC_*^2\frac{\nu+\nu_m}{\nu\nu_m}(\|e^n\|^2 + \|\nabla \epsilon_R^{n+1}\|^2).
\end{aligned} \tag{3.45}$$

To evaluate the time derivative above, add and subtract the term e_R^{n+1}, and use the polarization identity. Then applying Cauchy-Schwarz, Young's and Poincare's inequalities gives us the following bound :

$$\begin{aligned}
\frac{1}{\Delta t}(e^{n+1}-e^n, e_0^{n+1}) &= \frac{1}{\Delta t}(e^{n+1}-e^n, e^{n+1}) - \frac{1}{\Delta t}(e^{n+1}-e^n, e_R^{n+1}) \\
&\geq \frac{1}{2\Delta t}(\|e^{n+1}\|^2 - \|e^n\|^2) + \frac{1}{2\Delta t}\|e^{n+1}-e^n\|^2 - \frac{1}{\Delta t}(e^{n+1}-e^n, e_R^{n+1}) \\
&\geq \frac{1}{2\Delta t}(\|e^{n+1}\|^2 - \|e^n\|^2) - \frac{1}{2\Delta t}\|e_R^{n+1}\|^2 \\
&\geq \frac{1}{2\Delta t}(\|e^{n+1}\|^2 - \|e^n\|^2) - \frac{C}{2\Delta t}\|\nabla e_R^{n+1}\|^2.
\end{aligned}$$

Plugging these estimates into (3.44) with adding and subtracting the term $\frac{\nu\nu_m}{2(\nu+\nu_m)}\|\nabla e_0^{n+1}\|^2$

results in

$$\frac{1}{2\Delta t}(\|e^{n+1}\|^2-\|e^n\|^2)+\frac{(\nu-\nu_m)^2}{4(\nu+\nu_m)}\|\nabla e_0^{n+1}\|^2 + \frac{\nu\nu_m}{2(\nu+\nu_m)}\|\nabla e_0^{n+1}\|^2 \le \frac{(\nu-\nu_m)^2}{4(\nu+\nu_m)}\|\nabla \epsilon_0^n\|^2 + CC_*^2\frac{\nu+\nu_m}{\nu\nu_m}\|\epsilon^n\|^2 + C\left(C_*^2\frac{\nu+\nu_m}{\nu\nu_m}+(\Delta t)^{-1}\right)\|\nabla e_R^{n+1}\|^2. \tag{3.46}$$

Using similar estimates on the right hand side terms of (3.45), we get

$$\frac{1}{2\Delta t}(\|\epsilon^{n+1}\|^2-\|\epsilon^n\|^2)+\frac{(\nu-\nu_m)^2}{4(\nu+\nu_m)}\|\nabla \epsilon_0^{n+1}\|^2 + \frac{\nu\nu_m}{2(\nu+\nu_m)}\|\nabla \epsilon_0^{n+1}\|^2 \le \frac{(\nu-\nu_m)^2}{4(\nu+\nu_m)}\|\nabla e_0^n\|^2 + CC_*^2\frac{\nu+\nu_m}{\nu\nu_m}\|e^n\|^2 + C\left(C_*^2\frac{\nu+\nu_m}{\nu\nu_m}+(\Delta t)^{-1}\right)\|\nabla \epsilon_R^{n+1}\|^2. \tag{3.47}$$

Adding the equations (3.46) and (3.47), multiplying by $2\Delta t$ on both sides and summing over time steps and rearranging the terms results in

$$\begin{aligned}&\|e^M\|^2+\|\epsilon^M\|^2+\frac{(\nu-\nu_m)^2}{2(\nu+\nu_m)}\Delta t(\|\nabla e_0^M\|^2+\|\nabla \epsilon_0^M\|^2)\\ &+\frac{\nu\nu_m}{(\nu+\nu_m)}\Delta t\sum_{n=0}^{M-1}(\|\nabla e_0^{n+1}\|^2+\|\nabla \epsilon_0^{n+1}\|^2)\\ &\le \Delta t\sum_{n=0}^{M-1}CC_*^2\frac{(\nu+\nu_m)}{\nu\nu_m}\left(\|e^n\|^2+\|\epsilon^n\|^2\right)\\ &+\Delta t\sum_{n=0}^{M-1}C\left(C_*^2\frac{(\nu+\nu_m)}{\nu\nu_m}+(\Delta t)^{-1}\right)\left(\|\nabla e_R^{n+1}\|^2+\|\nabla \epsilon_R^{n+1}\|^2\right).\end{aligned} \tag{3.48}$$

Now drop the non-negative terms on the left hand side, apply Lemma 3.3.2 along

with Gronwall Lemma to get

$$\begin{aligned}\|e^M\|^2+\|\epsilon^M\|^2 + \frac{\nu\nu_m}{(\nu+\nu_m)}\Delta t\sum_{n=0}^{M-1}(\|\nabla e_0^{n+1}\|^2+\|\nabla\epsilon_0^{n+1}\|^2)\\ \leq exp\left(CC_*^2\frac{\nu+\nu_m}{\nu\nu_m}\right)CC_R^2\left(C_*^2\frac{\nu+\nu_m}{\nu\nu_m}+(\Delta t)^{-1}\right)\\ \left(\Delta t\sum_{n=0}^{M-1}(\|\nabla\cdot e_R^{n+1}\|^2+\|\nabla\cdot\epsilon_R^{n+1}\|^2)\right).\end{aligned} \tag{3.49}$$

and then use (3.39) in (3.49), which produces

$$\begin{aligned}&\Delta t\sum_{n=0}^{M-1}\left(\|\nabla e_0^{n+1}\|^2+\|\nabla\epsilon_0^{n+1}\|^2\right)\\ &\leq\gamma^{-2}C\left(C_*^2\frac{\nu+\nu_m}{\nu\nu_m}+(\Delta t)^{-1}\right)\left(\Delta t\sum_{n=0}^{M-1}(\|q_h^{n+1}-\hat{q}_h^n\|^2+\|\lambda_h^{n+1}-\hat{\lambda}_h^n\|^2)\right)\end{aligned} \tag{3.50}$$

Finally, applying the triangle inequality to $(\|\nabla(v_h^{n+1}-\hat{v}_h^{n+1})\|+\|\nabla(w_h^{n+1}-\hat{w}_h^{n+1})\|)$ with

$$(a+b)^2\leq 2(a^2+b^2),\ \ \forall a,b\geq 0$$

and combining the results (3.39) and (3.50) finishes the proof. □

3.4 Numerical experiments

In this section, we describe the numerical experiments used to test the proposed scheme and theory above. We first verify predicted convergence rates as h and Δt goes to 0 for an analytical test problem. We then compare computed solutions from the proposed scheme to those of a typical simulation using primitive variables for a channel flow problem. Finally, we test the proposed scheme on a test problem of channel flow over step. For all of our simulations, we choose (P_2, P_1^{disc})

Scott-Vogelius elements, which are known to be stable on barycenter refined regular triangular meshes [13]. These elements remove the effect of the (often large in MHD) pressure discretization error on the velocity/magnetic field errors. All the tests hereafter are performed using FreeFEM++ [42].

3.4.1 Numerical experiment 1: Convergence as $h, \Delta t \to 0$

We now test the predicted convergence rates of our analysis, for the mesh width h and timestep Δt tending to 0. We picked the analytical solution

$$v = \begin{pmatrix} \cos y + (1+e^t)\sin y \\ \sin x + (1+e^t)\cos x \end{pmatrix}, \; w = \begin{pmatrix} \cos y - (1+e^t)\sin y \\ \sin x - (1+e^t)\cos x \end{pmatrix},$$

$$p = -\lambda = (1+e^t)\sin(x+y),$$

domain $\Omega = (0,1)^2$, $\nu = \nu_m = 1$, and compute f_1 and f_2 from this. We then computed with Algorithm 3.2.1, and compared our computed solution with this known analytical solution. Recall our analysis predicts that

$$\|v - v_h\|_{2,1} + \|w - w_h\|_{2,1} \leq C(\Delta t + h^2)$$

for this element choice, with $\|\phi\|_{2,1} := \|\phi\|_{L^2(0,T;H^1(\Omega)^d)}$.

To test the spatial convergence rate, we select a small end time $T = 0.001$, timestep $\Delta t = T/8$, and compute on successively refined meshes. Errors and rates are shown in table 3.1, and we observe second order spatial convergence, which is in agreement with our analysis. To test the temporal convergence rate, we use a mesh width of $h = 1/64$, end time $T = 1$, and compute with varying timestep

sizes. Errors and rates are shown in Table 3.2, and the expected first order temporal convergence is observed. We want to mention here that, we also implemented our code in Dealii [14] using (Q_2, Q_1) Taylor-Hood element and got the expected spatial and temporal convergence rates.

h	$dim(X_h)$	$\|v - v_h\|_{2,1}$	Rate	$\|w - w_h\|_{2,1}$	Rate
1/4	324	1.0769e-4		2.0638e-4	
1/8	1156	2.7072e-5	1.9921	5.1557e-5	2.0011
1/16	4356	6.7771e-6	1.9980	1.2887e-5	2.0003
1/32	16900	1.6949e-6	1.9995	3.2216e-6	2.0001
1/64	66564	4.2380e-7	1.9997	8.0541e-7	2.0000

Table 3.1: This table gives errors and convergence rates for analytical test problem with very small end time and varying meshwidths.

Δt	$\|v - v_h\|_{2,1}$	Rate	$\|w - w_h\|_{2,1}$	Rate
$T/1$	4.1088e-2		4.0721e-2	
$T/2$	2.0206e-2	1.0239	1.9987e-2	1.0267
$T/4$	9.9334e-3	1.0244	9.8156e-3	1.0259
$T/8$	4.9141e-3	1.0154	4.8534e-3	1.0161
$T/16$	2.4430e-3	1.0083	2.4123e-3	1.0086
$T/32$	1.2181e-3	1.0040	1.2029e-3	1.0040

Table 3.2: This table gives errors and convergence rates for analytical test problem with a fine mesh, large end time and varying timestep size.

3.4.2 Numerical experiment 2: Comparison of proposed Elsässer variable scheme to primitive variable scheme

Next, we compare the proposed scheme against a typical scheme for primitive variable MHD, which is given in the case of homogeneous Dirichlet boundary

conditions by: Find $(u_h^n, p_h^n, B_h^n, \lambda_h^n) \in X_h \times Q_h \times X_h \times Q_h$ such that

$$\frac{1}{\Delta t}(u_h^{n+1} - u_h^n, v_h) + b^*(u_h^n, u_h^{n+1}, v_h) - (p_h^{n+1}, \nabla \cdot v_h)$$
$$+\nu(\nabla u_h^{n+1}, \nabla v_h) - sb^*(B_h^n, B_h^{n+1}, v_h) = (f(t^{n+1}), v_h), \quad (3.51)$$
$$(\nabla \cdot u_h^{n+1}, r_h) = 0, \quad (3.52)$$
$$\frac{1}{\Delta t}(B_h^{n+1} - B_h^n, \chi_h) + b^*(u_h^n, B_h^{n+1}, \chi_h) - b^*(B_h^n, u_h^{n+1}, \chi_h)$$
$$-(\lambda_h^{n+1}, \nabla \cdot \chi_h) + \nu_m(\nabla B_h^{n+1}, \nabla \chi_h) = (\nabla \times g(t^{n+1}), \chi_h), \quad (3.53)$$
$$(\nabla \cdot B_h^{n+1}, \rho_h) = 0, \quad (3.54)$$

for every $(v_h, r_h, \chi_h, \rho_h) \in X_h \times Q_h \times X_h \times Q_h$. In the case of non homogeneous Dirichlet boundary conditions, the usual change to the solution spaces is made. We believe this is a fair comparison to make, since this scheme is an unconditionally stable linearized backward Euler scheme, just as the proposed Elsässer variable scheme in Algorithm 3.2.1 is. Of course, the proposed Elsässer variable is much more efficient, since it decouples the problem. It is an open problem how to decouple a primitive variable MHD system in an unconditionally stable way.

For this comparison of schemes, we consider channel flow on a 10×40 rectangle, with initial condition $B = 0$ and $u =< (1 - y^2)/2, 0 >$. These initial conditions also define the inflow/outflow conditions for all $t > 0$. On the upper and lower walls, no slip conditions are enforced for velocity, and a magnetic field $B =< 0, 1 >$ is enforced. The magnetic diffusivity constant is selected as $\nu_m = 1$. The coupling number s and the kinematic viscosity ν are varied in the tests. For all tests, a steady state was reached by $T = 40$ (using timesteps of $\Delta t = 0.05$, and shown in Figure 3.1 are velocity and magnetic field steady state profiles at $x = 20$ for both schemes. A

barycenter refined mesh that provided a total of 41652 degrees of freedom was used.

From the plots, we observe excellent agreement in the solutions of the primitive and Elsässer variable schemes for each choice of s and ν, as the plots of the profiles lie on top of each other. We note that several other variations of $\nu,\ \nu_m,\ s$ were made, and in all cases the profile plots of solutions of primitive and Elsässer variable schemes had excellent agreement.

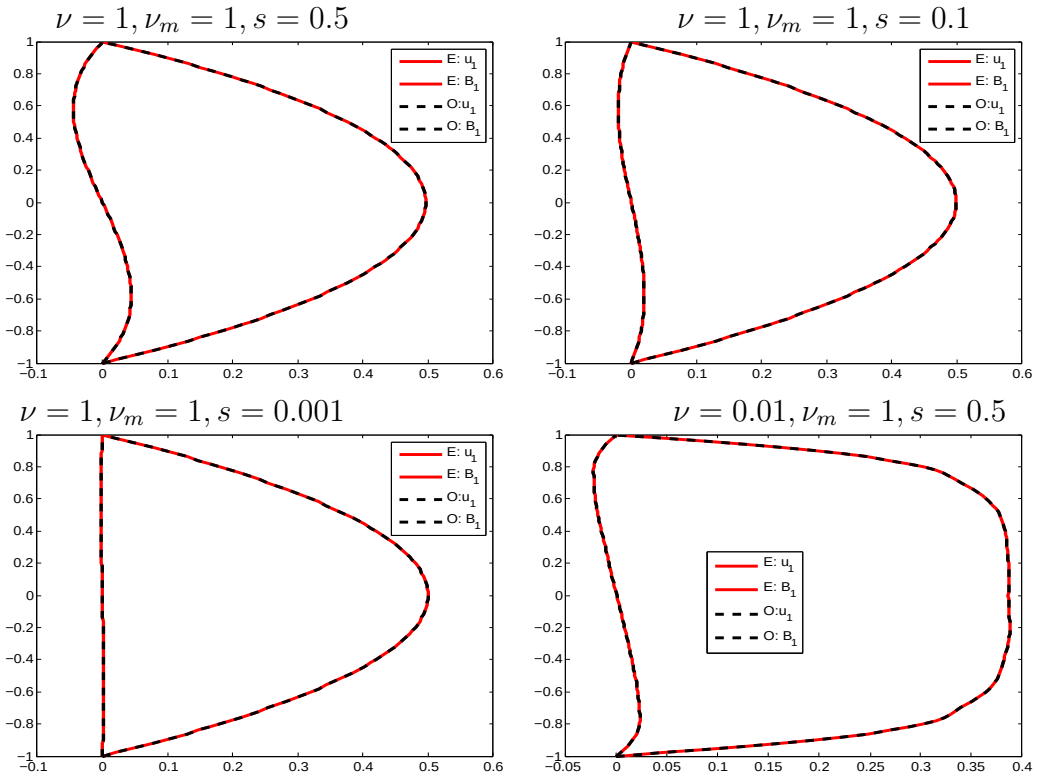

Figure 3.1: Steady state velocity and magnetic field profiles from Elsässer (E) and primitive (O) variable schemes, for various ν and s.

3.4.3 Numerical experiment 3: MHD channel flow over a step

For our final numerical experiment, we test Algorithm 3.2.1 on two dimensional channel flow over a forward and backward facing step [39], in presence of a magnetic field, with $\nu = 0.001$ and $\nu_m = 1$. It is expected that as the strength of the magnetic field grows, transient behavior will be damped, and the velocity flow profile will change from parabolic to nearly plug-like (away from the step), similar to the previous example.

We choose a domain that is a 30×10 rectangle with a 1×1 step five units into the channel at the bottom. We enforce boundary conditions for v and w that correspond to no slip velocity and $B = \langle 0, 1 \rangle^T$ on the walls and step, and $u = \langle y(10-y)/25, 0 \rangle^T$ at the inflow, $B = 0$ at the inflow and outflow, and with outflow conditions for u. The initial conditions are $\tilde{B}_0 = 0$ and $u_0 = \langle y(10-y)/25, 0 \rangle^T$. A diagram of the flow domain is shown in Figure 3.2. Computations are run to $T = 40$, using a timestep of $\Delta t = 0.025$ and a mesh that provided $568,535$ total degrees of freedom. Plots for the solutions with $s = 0,\ 0.01$ and $s = 0.05$ are shown at T=40 in Figure 3.3. We observe as s increases, the shedding of eddies behind the step is inhibited, and the change in velocity profile is clearly altered away from a parabolic shape. The magnetic field plots show a clear interaction between the flow and induced magnetic field which changes the magnetic field.

3.5 Conclusion

We have proposed, analyzed and tested an efficient, fully discrete numerical scheme for MHD. By formulating with Elsässer variables, unconditionally stability is

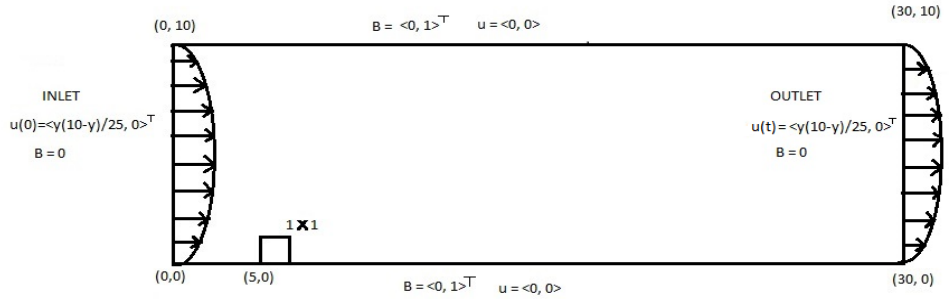

Figure 3.2: Shown above is domain for the 2D channel over a step probelm.

proven in a decoupled algorithm (decoupling of the 4-equation, 4-unknown system into 2-equation, 2-unknown systems). Unconditional stability with respect to meshwidth and timestep size are also proven. Moreover, a more efficient penalty-projection method for each 2-equation system, and this method is proven to be equivalent to the 2-equation, 2-unknown scheme for large penalty parameters.

Results of several successful numerical experiments were presented. Convergence rates to a chosen analytical solution were found to be optimal, which is in agreement with our analysis. Convergence of the penalty-projection scheme to the 2-equation, 2-unknown scheme was found to be first order as $\gamma \to \infty$, which agrees with our theory. Two channel flow problems were also studied. The first was a comparison of the Elsässer scheme solution to that of primitive variable MHD, for a variety of viscosities and coupling numbers, and in each case excellent agreement between the solutions was found. Finally, we tested MHD channel flow over a step, and observed the changing of physical behavior as the coupling number increased.

For future work, we believe that more testing of the scheme needs performed. If it can be established that this scheme gives solutions very similar to primitive variable schemes with the same mesh and timestep on a wide variety of problems, then the proposed schemes (or perhaps variants of them) could be an enabling tool to

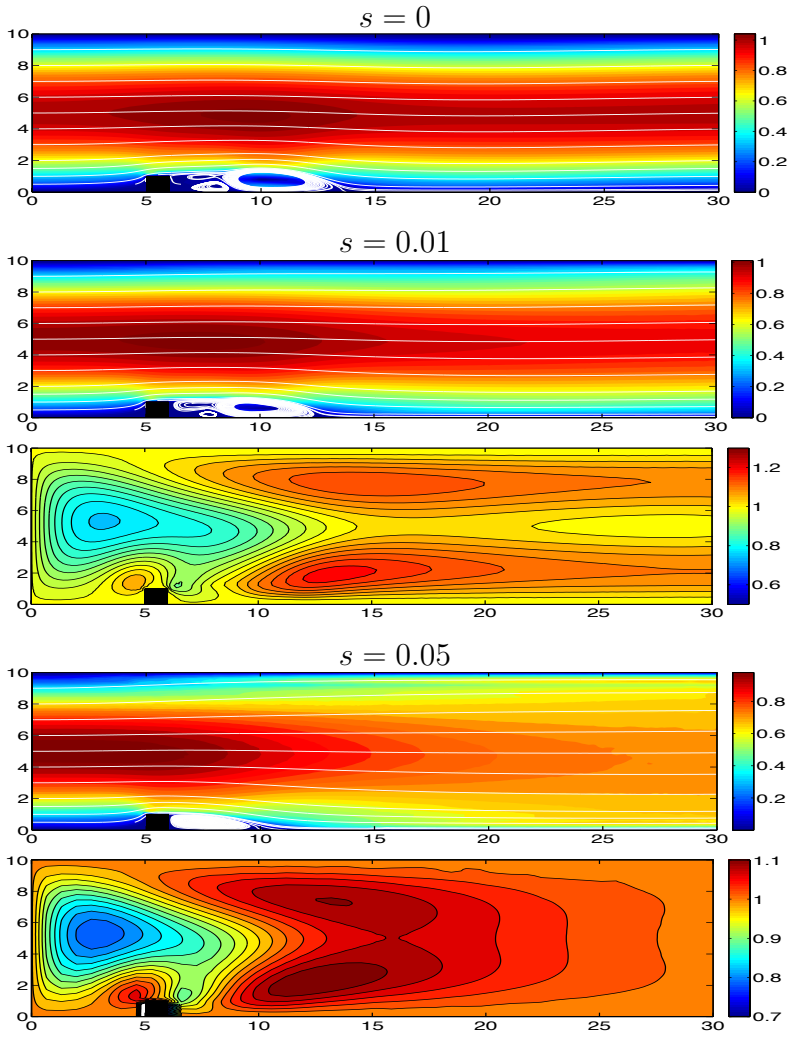

Figure 3.3: Shown above are $T = 40$ velocity solutions (shown as streamlines over speed contours) for MHD Channel flow over a step with varying s, and associated magnetic field magnitudes.

simulate larger scale 3D problems than is currently possible. Also, for MHD problems with higher Reynolds number, reduced order modeling with large eddy simulation, in the context of the scheme proposed herein, should be explored.

Even though the unconditional stability and decouple features of the scheme are huge advantages in computation of MHD flows, the limitation is it provides only first order convergence in time. In the next chapter, we propose, analyze, and test

a practically second order accurate in time and unconditionally stable timestepping algorithm for MHD simulation.

Chapter 4

Extension to a higher order timestepping scheme

4.1 Introduction

In the previous chapter, we studied first order timestepping methods in Elsässer variables. Although it was a successful idea, a drawback to the scheme is that it is limited to first order temporal accuracy. An extension to second order timestepping is a natural next step, however the analogous BDF2 scheme turns out not to be effective, as we will show. As we split the magnetic field as $B = B_0 + b$, where B_0 is mean and b is fluctuation, for simplicity of our analysis, we will assume $B_0 = 0$, since adding this term would not change the main ideas or results. Li and Trenchea [63] studied the following second order scheme for MHD in Elsässer variables.

Second order decoupled method of Li and Trenchea [63]:

$$\begin{aligned}
\frac{1}{\Delta t}(3v^{n+1}-4v^n+v^{n-1})+(2w^n-w^{n-1})\cdot\nabla v^{n+1}+\nabla q^{n+1} & \\
-\frac{\nu+\nu_m}{2}\Delta v^{n+1}-\frac{\nu-\nu_m}{2}\Delta(2w^n-w^{n-1}) &= f_1^{n+1}, \\
\nabla\cdot v^{n+1} &= 0, \\
\frac{1}{\Delta t}(3w^{n+1}-4w^n+w^{n-1})+(2v^n-v^{n-1})\cdot\nabla w^{n+1}+\nabla r^{n+1} & \\
-\frac{\nu+\nu_m}{2}\Delta w^{n+1}-\frac{\nu-\nu_m}{2}\Delta(2v^n-v^{n-1}) &= f_2^{n+1}, \\
\nabla\cdot w^{n+1} &= 0,
\end{aligned}$$

which is the case when $\theta = 1$ in our proposed θ-scheme and found it was unconditionally stable only under the restriction $\frac{1}{2} < \frac{\nu}{\nu_m} < 2$. In [9] this bound was shown to be sharp, and thus there is a serious restriction on its applicability in practice for many problems. For example current estimates suggest $Pr_m \sim 10^{-5}$ in the Earth's core ($Re \sim 10^8$, $Re_m \sim 10^3$, see [55,77]) proved stability of the BDF2 scheme for magnetic Prandtl number $Pr_m := \frac{\nu}{\nu_m} \in (1/2, 2)$. Belenli, Kaya and Rebholz [7] showed this BDF2 scheme became unstable when $Pr_m = 2.1$.

This chapter is organized as follows: in Section 2 we state the usual BDF2 scheme, prove its conditional stability and propose a scheme with slight modification in usual BDF2, we call it θ-scheme. In Section 3, we prove the unconditional stability and convergence theorems for the θ-scheme. Section 4 represents the convergence rate verification and some numerical experiments of the BDF2 and θ-scheme on a benchmark channel flow problem over a step. Finally, we draw conclusion and future direction in section 5.

4.2 BDF2 Scheme and stability analysis

Algorithm 4.2.1. *(BDF2 Scheme): Let $f_1, f_2 \in L^\infty(0,T;H^{-1}(\Omega))$ and time step $\Delta t > 0$ and end time $T > 0$ be given. Set $M = T/\Delta t$ and start with $v^0, w^0, v^1, w^1 \in H^2 \cup V$. For all $n = 1, \cdots, M-1$, compute $(v_h^{n+1}, w_h^{n+1}) \in V_h \times V_h$ satisfying for all $(\chi_h, l_h) \in V_h \times V_h$,*

$$\left(\frac{3v_h^{n+1} - 4v_h^n + v_h^{n-1}}{2\Delta t}, \chi_h\right) + ((2w_h^n - w_h^{n-1}) \cdot \nabla v_h^{n+1}, \chi_h) + \frac{\nu + \nu_m}{2}\left(\nabla v_h^{n+1}, \nabla \chi_h\right)$$
$$+ \frac{\nu - \nu_m}{2}\left(\nabla(2w_h^n - w_h^{n-1}), \nabla \chi_h\right) = (f_1(t^{n+1}), \chi_h), \ \ \forall \chi_h \in V_h \tag{4.1}$$

and

$$\left(\frac{3w_h^{n+1} - 4w_h^n + w_h^{n-1}}{2\Delta t}, l_h\right) + ((2v_h^n - v_h^{n-1}) \cdot \nabla w_h^{n+1}, l_h) + \frac{\nu + \nu_m}{2}\left(\nabla w_h^{n+1}, \nabla l_h\right)$$
$$+ \frac{\nu - \nu_m}{2}\left(\nabla(2v_h^n - v_h^{n-1}), \nabla l_h\right) = (f_2(t^{n+1}), l_h), \ \ \forall l_h \in V_h. \tag{4.2}$$

Lemma 4.2.1. *If the mesh is sufficiently regular so that the inverse inequality holds (with constant C_i) and the time step is chosen to satisfy*

$$\Delta t \leq \frac{h^2(\nu + \nu_m - |\nu - \nu_m|)}{C_i(\nu - \nu_m)^2},$$

where $f_1,\ f_2 \in L^2(0,T;H^{-1}(\Omega))$, and $v_h^0,\ w_h^0,\ v_h^1,\ w_h^1 \in L^2(\Omega)$ then the Algorithm (4.2.1) is stable and solutions satisfy

$$\|v_h^M\|^2 + \|w_h^M\|^2 + \frac{(\nu + \nu_m - |\nu - \nu_m|)\Delta t}{2} \sum_{n=1}^{M-1} \left(\|\nabla v_h^{n+1}\|^2 + \|\nabla w_h^{n+1}\|^2\right)$$
$$\leq C(\nu, \nu_m, v_h^0, v_h^1, w_h^0, w_h^1, f_1, f_2) \tag{4.3}$$

Proof. Choose $\chi_h = v_h^{n+1} \in V_h$ and $l_h = w_h^{n+1} \in V_h$ in Algorithm (4.2.1), (4.1)-(4.2). This vanishes the nonlinear and pressure terms, and leaves

$$\begin{aligned}\frac{1}{2\Delta t}\big(3v_h^{n+1} - 4v_h^n + v_h^{n-1}, v_h^{n+1}\big) + \frac{\nu+\nu_m}{2}\|\nabla v_h^{n+1}\|^2 \\ + \frac{\nu-\nu_m}{2}\big(\nabla(2w_h^n - w_h^{n-1}), \nabla v_h^{n+1}\big) = (f_1^{n+1}, v_h^{n+1}),\end{aligned} \tag{4.4}$$

and

$$\begin{aligned}\frac{1}{2\Delta t}(3w_h^{n+1} - 4w_h^n + w_h^{n-1}, w_h^{n+1}) + \frac{\nu+\nu_m}{2}\|\nabla w_h^{n+1}\|^2 \\ + \frac{\nu-\nu_m}{2}(\nabla(2v_h^n - v_h^{n-1}), \nabla w_h^{n+1}) = (f_2^{n+1}, w_h^{n+1}).\end{aligned} \tag{4.5}$$

Using the following BDF2 identity

$$(3a - 4b + c, a) = \frac{a^2 + (2a-b)^2}{2} - \frac{b^2 + (2b-c)^2}{2} + \frac{(a-2b+c)^2}{2}, \tag{4.6}$$

on the time derivative terms and adding (4.4) and (4.5) yields

$$\begin{aligned}\frac{1}{4\Delta t}\Big(&\|v_h^{n+1}\|^2 - \|v_h^n\|^2 + \|2v_h^{n+1} - v_h^n\|^2 - \|2v_h^n - v_h^{n-1}\|^2 \\ &+ \|v_h^{n+1} - 2v_h^n + v_h^{n-1}\|^2 + \|w_h^{n+1}\|^2 - \|w_h^n\|^2 \\ &+ \|2w_h^{n+1} - w_h^n\|^2 - \|2w_h^n - w_h^{n-1}\|^2 + \|w_h^{n+1} - 2w_h^n + w_h^{n-1}\|^2\Big) \\ &+ \frac{\nu+\nu_m}{2}\big(\|\nabla v_h^{n+1}\|^2 + \|\nabla w_h^{n+1}\|^2\big) + \frac{\nu-\nu_m}{2}(\nabla(2w_h^n - w_h^{n-1}), \nabla v_h^{n+1}) \\ &+ \frac{\nu-\nu_m}{2}(\nabla(2v_h^n - v_h^{n-1}), \nabla w_h^{n+1}) = (f_1^{n+1}, v_h^{n+1}) + (f_2^{n+1}, w_h^{n+1}).\end{aligned} \tag{4.7}$$

Adding and subtracting the term $\frac{\nu-\nu_m}{2}\left(\nabla v_h^{n+1}, \nabla w_h^{n+1}\right)$ twice

$$\begin{aligned}
&\frac{1}{4\Delta t}\Big(\|v_h^{n+1}\|^2 - \|v_h^n\|^2 + \|2v_h^{n+1} - v_h^n\|^2 - \|2v_h^n - v_h^{n-1}\|^2 \\
&\quad + \|v_h^{n+1} - 2v_h^n + v_h^{n-1}\|^2 + \|w_h^{n+1}\|^2 - \|w_h^n\|^2 + \|2w_h^{n+1} - w_h^n\|^2 \\
&\quad - \|2w_h^n - w_h^{n-1}\|^2 + \|w_h^{n+1} - 2w_h^n + w_h^{n-1}\|^2\Big) \\
&\quad + \frac{\nu+\nu_m}{2}\big(\|\nabla v_h^{n+1}\|^2 + \|\nabla w_h^{n+1}\|^2\big) - \frac{\nu-\nu_m}{2}(\nabla(v_h^{n+1} - 2v_h^n + v_h^{n-1}), \nabla w_h^{n+1}) \\
&\quad - \frac{\nu-\nu_m}{2}(\nabla(w_h^{n+1} - 2w_h^n + w_h^{n-1}), \nabla v_h^{n+1}) + \frac{\nu-\nu_m}{2}(\nabla w_h^{n+1}, \nabla v_h^{n+1}) \\
&\quad + \frac{\nu-\nu_m}{2}(\nabla v_h^{n+1}, \nabla w_h^{n+1}) = (f_1^{n+1}, v_h^{n+1}) + (f_2^{n+1}, w_h^{n+1}). \qquad (4.8)
\end{aligned}$$

Using the Cauchy-Schwarz inequality,

$$\begin{aligned}
&\frac{1}{4\Delta t}\Big(\|v_h^{n+1}\|^2 - \|v_h^n\|^2 + \|2v_h^{n+1} - v_h^n\|^2 - \|2v_h^n - v_h^{n-1}\|^2 \\
&+ \|v_h^{n+1} - 2v_h^n + v_h^{n-1}\|^2 + \|w_h^{n+1}\|^2 - \|w_h^n\|^2 + \|2w_h^{n+1} - w_h^n\|^2 \\
&- \|2w_h^n - w_h^{n-1}\|^2 + \|w_h^{n+1} - 2w_h^n + w_h^{n-1}\|^2\Big) \\
&+ \frac{\nu+\nu_m}{2}\big(\|\nabla v_h^{n+1}\|^2 + \|\nabla w_h^{n+1}\|^2\big) \le \frac{|\nu-\nu_m|}{2}\|\nabla(w_h^{n+1} - 2w_h^n + w_h^{n-1})\|\|\nabla v_h^{n+1}\| \\
&+ \frac{|\nu-\nu_m|}{2}|\|\nabla(v_h^{n+1} - 2v_h^n + v_h^{n-1})\|\|\nabla w_h^{n+1}\| + |\nu-\nu_m|\|\nabla w_h^{n+1}\|\|\nabla v_h^{n+1}\| \\
&+ \|f_1^{n+1}\|_{-1}\|\nabla v_h^{n+1}\| + \|f_2^{n+1}\|_{-1}\|\nabla w_h^{n+1}\|. \qquad (4.9)
\end{aligned}$$

We now focus on finding bounds on the right side terms of (4.9). Applying the following version of Young's inequality $ab \le \frac{\epsilon}{2}a^2 + \frac{1}{2\epsilon}b^2$ for $\epsilon = \frac{\nu+\nu_m-|\nu-\nu_m|}{2}$, we get from first and second terms,

$$\begin{aligned}
\frac{|\nu-\nu_m|}{2}|\|\nabla(w_h^{n+1} - 2w_h^n + w_h^{n-1})\|\|\nabla v_h^{n+1}\| &\le \frac{\nu+\nu_m-|\nu-\nu_m|}{4}\|\nabla v_h^{n+1}\|^2 \\
&+ \frac{(\nu-\nu_m)^2}{4(\nu+\nu_m-|\nu-\nu_m|)}\|\nabla(w_h^{n+1} - 2w_h^n + w_h^{n-1})\|^2,
\end{aligned}$$

and

$$\frac{|\nu-\nu_m|}{2}\|\nabla(v_h^{n+1}-2v_h^n+v_h^{n-1})\|\|\nabla w_h^{n+1}\| \le \frac{\nu+\nu_m-|\nu-\nu_m|}{4}\|\nabla w_h^{n+1}\|^2 + \frac{(\nu-\nu_m)^2}{4(\nu+\nu_m-|\nu-\nu_m|)}\|\nabla(v_h^{n+1}-2v_h^n+v_h^{n-1})\|^2.$$

For $\epsilon = 1$, the third term yields

$$|\nu-\nu_m|\|\nabla v_h^{n+1}\|\|\nabla w_h^{n+1}\| \le \frac{|\nu-\nu_m|}{2}\|\nabla v_h^{n+1}\|^2 + \frac{|\nu-\nu_m|}{2}\|\nabla w_h^{n+1}\|^2.$$

For $\epsilon = \frac{\nu+\nu_m-|\nu-\nu_m|}{4}$, we can write the last two terms as

$$\|f_1^{n+1}\|_{-1}\|\nabla v_h^{n+1}\| \le \frac{\nu+\nu_m-|\nu-\nu_m|}{8}\|\nabla v_h^{n+1}\|^2 + \frac{2}{\nu+\nu_m-|\nu-\nu_m|}\|f_1^{n+1}\|_{-1}^2,$$

$$\|f_2^{n+1}\|_{-1}\|\nabla w_h^{n+1}\| \le \frac{\nu+\nu_m-|\nu-\nu_m|}{8}\|\nabla w_h^{n+1}\|^2 + \frac{2}{\nu+\nu_m-|\nu-\nu_m|}\|f_2^{n+1}\|_{-1}^2.$$

Using these estimates in (4.9) produces

$$\begin{aligned}
&\frac{1}{4\Delta t}\Big(\|v_h^{n+1}\|^2-\|v_h^n\|^2+\|2v_h^{n+1}-v_h^n\|^2-\|2v_h^n-v_h^{n-1}\|^2+\|v_h^{n+1}-2v_h^n+v_h^{n-1}\|^2\\
&+\|w_h^{n+1}\|^2-\|w_h^n\|^2+\|2w_h^{n+1}-w_h^n\|^2-\|2w_h^n-w_h^{n-1}\|^2+\|w_h^{n+1}-2w_h^n+w_h^{n-1}\|^2\Big)\\
&+\frac{\nu+\nu_m-|\nu-\nu_m|}{8}\big(\|\nabla v_h^{n+1}\|^2+\|\nabla w_h^{n+1}\|^2\big)\\
&\le \frac{(\nu-\nu_m)^2}{4(\nu+\nu_m-|\nu-\nu_m|)}\big(\|\nabla(v_h^{n+1}-2v_h^n+v_h^{n-1})\|^2+\|\nabla(w_h^{n+1}-2w_h^n+w_h^{n-1})\|^2\big)\\
&+\frac{2}{\nu+\nu_m-|\nu-\nu_m|}\big(\|f_1^{n+1}\|_{-1}^2+\|f_2^{n+1}\|_{-1}^2\big). \qquad (4.10)
\end{aligned}$$

Using the inverse inequality

$$\|\nabla(z_h^{n+1} - 2z_h^n + z_h^{n-1})\|^2 \leq C_i h^{-2} \|z_h^{n+1} - 2z_h^n + z_h^{n-1}\|^2,$$

and so equation (4.10) can be written as

$$\begin{aligned}
&\frac{1}{4\Delta t}\Big(\|v_h^{n+1}\|^2 - \|v_h^n\|^2 + \|2v_h^{n+1} - v_h^n\|^2 - \|2v_h^n - v_h^{n-1}\|^2 \\
&+ \|w_h^{n+1}\|^2 - \|w_h^n\|^2 + \|2w_h^{n+1} - w_h^n\|^2 - \|2w_h^n - w_h^{n-1}\|^2 \Big) \\
&+ \left[\frac{1}{4\Delta t} - \frac{(\nu - \nu_m)^2 C_i h^{-2}}{4(\nu + \nu_m - |\nu - \nu_m|)} \right] \|w_h^{n+1} - 2w_h^n + w_h^{n-1}\|^2 \\
&+ \left[\frac{1}{4\Delta t} - \frac{(\nu - \nu_m)^2 C_i h^{-2}}{4(\nu + \nu_m - |\nu - \nu_m|)} \right] \|v_h^{n+1} - 2v_h^n + v_h^{n-1}\|^2 \\
&+ \frac{\nu + \nu_m - |\nu - \nu_m|}{8} \big(\|\nabla v_h^{n+1}\|^2 + \|\nabla w_h^{n+1}\|^2 \big) \\
&\leq \frac{2}{\nu + \nu_m - |\nu - \nu_m|} \left(\|f_1^{n+1}\|_{-1}^2 + \|f_2^{n+1}\|_{-1}^2 \right). \qquad (4.11)
\end{aligned}$$

Now using the assumption $\Delta t \leq \frac{h^2(\nu + \nu_m - |\nu - \nu_m|)}{C_i(\nu - \nu_m)^2}$, we can remove non-negative terms from the left hand side to get

$$\begin{aligned}
&\frac{1}{4\Delta t}\Big(\|v_h^{n+1}\|^2 - \|v_h^n\|^2 + \|2v_h^{n+1} - v_h^n\|^2 - \|2v_h^n - v_h^{n-1}\|^2 \\
&\qquad + \|w_h^{n+1}\|^2 - \|w_h^n\|^2 + \|2w_h^{n+1} - w_h^n\|^2 - \|2w_h^n - w_h^{n-1}\|^2 \Big) \\
&\qquad + \frac{\nu + \nu_m - |\nu - \nu_m|}{8} \big(\|\nabla v_h^{n+1}\|^2 + \|\nabla w_h^{n+1}\|^2 \big) \\
&\qquad \leq \frac{2}{\nu + \nu_m - |\nu - \nu_m|} \big(\|f_1^{n+1}\|_{-1}^2 + \|f_2^{n+1}\|_{-1}^2 \big). \qquad (4.12)
\end{aligned}$$

Multiplying both sides by $4\Delta t$, using summing over timesteps and dropping non-negative terms from left, we get

$$\|v_h^M\|^2+\|w_h^M\|^2 + \frac{(\nu+\nu_m-|\nu-\nu_m|)\Delta t}{2}\sum_{n=1}^{M-1}\left(\|\nabla v_h^{n+1}\|^2+\|\nabla w_h^{n+1}\|^2\right)$$
$$\leq \|v_h^1\|^2+\|2v_h^1-v_h^0\|^2+\|w_h^1\|^2+\|2w_h^1-w_h^0\|^2$$
$$+\frac{8\Delta t}{\nu+\nu_m-|\nu-\nu_m|}\sum_{n=1}^{M-1}\left(\|f_1^{n+1}\|_{-1}^2+\|f_2^{n+1}\|_{-1}^2\right). \tag{4.13}$$

□

That is, the above second order method can be stable without restriction on $Pr_m = \frac{\nu}{\nu_m}$, if a timestep restriction of $\Delta t < O(h^2)$ is satisfied. Note that this condition is also often not practical.

Due to the conditional stability of the BDF2 scheme and from some numerical experiments (shown later), we found that simulation with BDF2 scheme is not effective. We thus propose and study a decoupled, unconditionally stable and higher order accurate scheme that has no restriction on ν and ν_m. By careful consideration of the analysis in [63, 94], we identify the 'Problem terms' that lead to the restriction are the $(\nu-\nu_m)$ terms. In the first order case, these can be handled, but in the second order case, a restriction on the data becomes necessary. Thus we propose a method that treats the $(\nu-\nu_m)$ terms as a linear combination (i.e. a θ-method) of the first and second order schemes above, which takes the form:

Proposed decoupled θ-method:

$$\begin{aligned}
\frac{1}{2\Delta t}(3v^{n+1}-4v^n+v^{n-1})+(2w^n-w^{n-1})\cdot\nabla v^{n+1}+\nabla q^{n+1}& \\
-\frac{\nu+\nu_m}{2}\Delta v^{n+1}-\theta\frac{\nu-\nu_m}{2}\Delta(2w^n-w^{n-1})-(1-\theta)\frac{\nu-\nu_m}{2}\Delta w^n &= f_1^{n+1},\\
\nabla\cdot v^{n+1} &= 0,\\
\frac{1}{2\Delta t}(3w^{n+1}-4w^n+w^{n-1})+(2v^n-v^{n-1})\cdot\nabla w^{n+1}+\nabla r^{n+1}& \\
-\frac{\nu+\nu_m}{2}\Delta w^{n+1}-\theta\frac{\nu-\nu_m}{2}\Delta(2v^n-v^{n-1})-(1-\theta)\frac{\nu-\nu_m}{2}\Delta v^n &= f_2^{n+1},\\
\nabla\cdot w^{n+1} &= 0,
\end{aligned}$$

For this method, we prove unconditional stability of the method for any ν and ν_m, provided θ is chosen to satisfy $\frac{\theta}{1+\theta} < \frac{\nu}{\nu_m} < \frac{1+\theta}{\theta}$, $0 \le \theta \le 1$. This can be achieved for any $\frac{\nu}{\nu_m}$, because the bounds tend towards negative and positive infinity for θ going to zero. We also prove this scheme has temporal accuracy $O(\Delta t^2 + (1-\theta)|\nu-\nu_m|\Delta t)$. Even though the method is not second order unless $\theta = 1$ (the case where the BDF2 scheme is stable), in practice ν and ν_m are typically small, and thus the method will typically behave like a second order method. To return to the example of Earth's core, there $|\nu-\nu_m|$ is in the order of 10^{-3}. We also note that the two decoupled Oseen problems can be solved independently, allowing for a parallel solution approach if desired.

We study the new decoupled θ-method in a fully discrete setting, using a finite element spatial discretization. We prove the proposed scheme is unconditionally stable (with correct choice of θ), well-posed, optimally accurate in space, and with temporal accuracy $O(\Delta t^2 + (1-\theta)|\nu-\nu_m|\Delta t)$, *without any restrictions on* ν *and* ν_m (see Section 4.3). The proposed method is the only unconditionally stable, decoupled method for MHD with general ν and ν_m that is better than first order accurate in

time, and thus could represent a potentially significant step forward for MHD flow simulations. In Section 4.4 we perform several numerical experiments that both validate the theory and show the method is very effective on some benchmark problems where the full second order method of [63] is unstable.

4.3 An efficient and stable θ-scheme for MHD

We now present and analyze an efficient decoupled scheme for MHD. After defining the scheme, we analyze its stability and convergence. The scheme is a generalization of a linearized BDF2 scheme applied to the Elsässer MHD system, and differs in the treatment of the $\frac{\nu-\nu_m}{2}$ terms. As is common with BDF2 schemes, we need two initial conditions; if only one is known, then a linearized backward Euler method (i.e. the first order method of Trenchea [94]) can be used on the first step without affecting stability or accuracy.

Algorithm 4.3.1. *Given ν and ν_m, choose θ sufficiently small so that $\frac{\theta}{1+\theta} < \frac{\nu}{\nu_m} < \frac{1+\theta}{\theta}$, $0 \leq \theta \leq 1$. Let $f_1, f_2 \in L^\infty(0,T;H^{-1}(\Omega)^d)$, initial conditions $v^0, w^0, v^1, w^1 \in V_h$, time step $\Delta t > 0$ and end time $T > 0$ be given. Set $M = T/\Delta t$ and for $n = 1, \cdots, M-1$, compute:*

Find $v_h^{n+1} \in V_h$ satisfying, for all $\chi_h \in V_h$:

$$\left(\frac{3v_h^{n+1} - 4v_h^n + v_h^{n-1}}{2\Delta t}, \chi_h\right) + b^*(2w_h^n - w_h^{n-1}, v_h^{n+1}, \chi_h) + \frac{\nu+\nu_m}{2}\left(\nabla v_h^{n+1}, \nabla\chi_h\right) + \frac{\nu-\nu_m}{2}\left((1-\theta)\nabla w_h^n + \theta\nabla(2w_h^n - w_h^{n-1}), \nabla\chi_h\right) = (f_1(t^{n+1}), \chi_h), \quad (4.14)$$

Find $w_h^{n+1} \in V_h$ satisfying, for all $l_h \in V_h$:

$$\left(\frac{3w_h^{n+1} - 4w_h^n + w_h^{n-1}}{2\Delta t}, l_h\right) + b^*(2v_h^n - v_h^{n-1}, w_h^{n+1}, l_h) + \frac{\nu + \nu_m}{2}\left(\nabla w_h^{n+1}, \nabla l_h\right) + \frac{\nu - \nu_m}{2}\left((1-\theta)\nabla v_h^n + \theta\nabla(2v_h^n - v_h^{n-1}), \nabla l_h\right) = (f_2(t^{n+1}), l_h). \quad (4.15)$$

Remark 4.3.1. *The key to the efficiency of the scheme is that the equations* (4.14) *and* (4.15) *are decoupled; in fact, they could be solved simultaneously if the computational resources are available. We prove below the scheme maintains stability despite this decoupling, provided θ is chosen so that $\frac{\theta}{1+\theta} < \frac{\nu}{\nu_m} < \frac{1+\theta}{\theta}$, $0 \le \theta \le 1$.*

Remark 4.3.2. *if $|\nu - \nu_m|$ is small, we should have convergence of $O(h^k + \Delta t^2)$.*

Remark 4.3.3. *Note that when $\theta = 1$, the above scheme reduces to usual linearized BDF2 scheme*

$$\left(\frac{3v_h^{n+1} - 4v_h^n + v_h^{n-1}}{2\Delta t}, \chi_h\right) + ((2w_h^n - w_h^{n-1}) \cdot \nabla v_h^{n+1}, \chi_h) + \frac{\nu + \nu_m}{2}\left(\nabla v_h^{n+1}, \nabla \chi_h\right) + \frac{\nu - \nu_m}{2}\left(\nabla(2w_h^n - w_h^{n-1}), \nabla \chi_h\right) = (f_1(t^{n+1}), \chi_h), \ \ \forall \chi_h \in V_h$$

and

$$\left(\frac{3w_h^{n+1} - 4w_h^n + w_h^{n-1}}{2\Delta t}, l_h\right) + ((2v_h^n - v_h^{n-1}) \cdot \nabla w_h^{n+1}, l_h) + \frac{\nu + \nu_m}{2}\left(\nabla w_h^{n+1}, \nabla l_h\right) + \frac{\nu - \nu_m}{2}\left(\nabla(2v_h^n - v_h^{n-1}), \nabla l_h\right) = (f_2(t^{n+1}), l_h), \ \ \forall l_h \in V_h$$

studied by Li and Trenchea in [63]. However, in [63] it was proven that this case is unconditionally stable when $\frac{1}{2} < \frac{\nu}{\nu_m} < 2$, and it was later verified in [9] that this bound is sharp. This lack of stability is the motivation for the θ-scheme we propose above, since one cannot expect such a restriction on ν and ν_m in general.

4.3.1 Stability analysis

We now prove unconditional stability and well-posedness for the Algorithm 4.3.1. To simplify notation, denote $\alpha := \nu + \nu_m - |\nu - \nu_m|(1+2\theta)$, and note that by the choice of θ, it holds that $\alpha > 0$.

Lemma 4.3.1. *Solutions to Algorithm (4.3.1) are unconditionally stable: for any* $\Delta t > 0$,

$$\begin{aligned}\|v_h^M\|^2 + \|2v_h^M - v_h^{M-1}\|^2 + \|w_h^M\|^2 + \|2w_h^M - w_h^{M-1}\|^2 + \alpha\Delta t\sum_{n=2}^{M}\big(\|\nabla v_h^n\|^2 + \|\nabla w_h^n\|^2\big)\\ \leq\ \|v_h^0\|^2 + \|w_h^0\|^2 + \|2v_h^1 - v_h^0\|^2 + \|2w_h^1 - w_h^0\|^2\\ + (\nu+\nu_m)\Delta t\big(\|\nabla v_h^1\|^2 + \|\nabla w_h^1\|^2 + 2\|\nabla v_h^0\|^2 + 2\|\nabla w_h^0\|^2\big)\\ + \frac{4\Delta t}{\alpha}\sum_{n=1}^{M}\big(\|f_1(t^n)\|_{-1}^2 + \|f_2(t^n)\|_{-1}^2\big).\end{aligned}$$

Remark 4.3.4. *Since Algorithm 4.3.1 is linear at each timestep and finite dimensional, the stability bound above is sufficient to provide well-posedness of the scheme. Uniqueness follows due to linearity, since the bounds on the difference between two solutions follow exactly as for the stability bound, but with a zero right hand side. Since the scheme is finite dimensional and linear at each time step, uniqueness implies existence, and thus solutions to Algorithm 4.3.1 must exist uniquely. That the unique solutions are bounded continuously by the data is given in the stability bound above.*

Proof. Choose $\chi_h = v_h^{n+1} \in V_h$ and $l_h = w_h^{n+1} \in V_h$ in (4.14)-(4.15). Then the trilinear

terms vanish, leaving

$$\frac{1}{2\Delta t}(3v_h^{n+1} - 4v_h^n + v_h^{n-1}, v_h^{n+1}) + \frac{\nu + \nu_m}{2}\|\nabla v_h^{n+1}\|^2 + \frac{\nu - \nu_m}{2}((1+\theta)\nabla w_h^n - \theta\nabla w_h^{n-1}, \nabla v_h^{n+1}) = ({f_1}^{n+1}, v_h^{n+1})$$

and

$$\frac{1}{2\Delta t}(3w_h^{n+1} - 4w_h^n + w_h^{n-1}, w_h^{n+1}) + \frac{\nu + \nu_m}{2}\|\nabla w_h^{n+1}\|^2 + \frac{\nu - \nu_m}{2}((1+\theta)\nabla v_h^n - \theta\nabla v_h^{n-1}, \nabla w_h^{n+1}) = (f_2^{n+1}, w_h^{n+1}).$$

Adding these equations and using the identity

$$(3a - 4b + c, a) = \frac{a^2 + (2a-b)^2}{2} - \frac{b^2 + (2b-c)^2}{2} + \frac{(a-2b+c)^2}{2}, \tag{4.16}$$

we obtain

$$\begin{aligned}
&\frac{1}{4\Delta t}\Big(\|v_h^{n+1}\|^2 - \|v_h^n\|^2 + \|2v_h^{n+1} - v_h^n\|^2 - \|2v_h^n - v_h^{n-1}\|^2 + \|w_h^{n+1}\|^2 - \|w_h^n\|^2 \\
&+ \|2w_h^{n+1} - w_h^n\|^2 - \|2w_h^n - w_h^{n-1}\|^2 + \|v_h^{n+1} - 2v_h^n + v_h^{n-1}\|^2 \\
&+ \|w_h^{n+1} - 2w_h^n + w_h^{n-1}\|^2\Big) + \frac{\nu + \nu_m}{2}\big(\|\nabla v_h^{n+1}\|^2 + \|\nabla w_h^{n+1}\|^2\big) \\
&+ \frac{\nu - \nu_m}{2}((1+\theta)\nabla w_h^n - \theta\nabla w_h^{n-1}, \nabla v_h^{n+1}) + \frac{\nu - \nu_m}{2}((1+\theta)\nabla v_h^n - \theta\nabla v_h^{n-1}, \nabla w_h^{n+1}) \\
&= (f_1^{n+1}, v_h^{n+1}) + (f_2^{n+1}, w_h^{n+1}).
\end{aligned} \tag{4.17}$$

Applying Cauchy-Schwarz, Young's inequalities to the $(\nu - \nu_m)$ terms and dropping

non-negative terms provides the bound

$$\begin{aligned}
&\frac{1}{4\Delta t}\Big(\|v_h^{n+1}\|^2 - \|v_h^n\|^2 + \|2v_h^{n+1} - v_h^n\|^2 - \|2v_h^n - v_h^{n-1}\|^2 + \|w_h^{n+1}\|^2 - \|w_h^n\|^2 \\
&\qquad + \|2w_h^{n+1} - w_h^n\|^2 - \|2w_h^n - w_h^{n-1}\|^2\Big) + \frac{\nu+\nu_m}{2}\big(\|\nabla v_h^{n+1}\|^2 + \|\nabla w_h^{n+1}\|^2\big) \\
&\qquad \le \frac{|\nu-\nu_m|}{4}(1+\theta)\Big(\|\nabla w_h^n\|^2 + \|\nabla v_h^{n+1}\|^2 + \|\nabla v_h^n\|^2 + \|\nabla w_h^{n+1}\|^2\Big) \\
&\qquad + \frac{|\nu-\nu_m|}{4}\theta\Big(\|\nabla w_h^{n-1}\|^2 + \|\nabla v_h^{n+1}\|^2 + \|\nabla v_h^{n-1}\|^2 + \|\nabla w_h^{n+1}\|^2\Big) \\
&\qquad + \|f_1^{n+1}\|_{-1}\|\nabla v_h^{n+1}\| + \|f_2^{n+1}\|_{-1}\|\nabla w_h^{n+1}\|. \qquad (4.18)
\end{aligned}$$

Next, we apply Young's inequality using α with the forcing terms, rearrange, and noting that $\alpha > 0$ by the assumed choice of θ,

$$\begin{aligned}
&\frac{1}{4\Delta t}\Big(\|v_h^{n+1}\|^2 - \|v_h^n\|^2 + \|2v_h^{n+1} - v_h^n\|^2 - \|2v_h^n - v_h^{n-1}\|^2 + \|w_h^{n+1}\|^2 - \|w_h^n\|^2 \\
&\qquad + \|2w_h^{n+1} - w_h^n\|^2 - \|2w_h^n - w_h^{n-1}\|^2\Big) + \frac{\nu+\nu_m}{2}\big(\|\nabla v_h^{n+1}\|^2 + \|\nabla w_h^{n+1}\|^2\big) \\
&\qquad \le \frac{|\nu-\nu_m|}{4}(1+\theta)\big(\|\nabla w_h^n\|^2 + \|\nabla v_h^n\|^2\big) + \frac{|\nu-\nu_m|}{4}\theta\big(\|\nabla w_h^{n-1}\|^2 + \|\nabla v_h^{n-1}\|^2\big) \\
&\qquad + \frac{\alpha + |\nu-\nu_m|(1+2\theta)}{4}\left(\|\nabla v_h^{n+1}\|^2 + \|\nabla w_h^{n+1}\|^2\right) \\
&\qquad + \frac{1}{\alpha}\left(\|f_1(t^{n+1})\|_{-1} + \|f_2(t^{n+1})\|_{-1}\right).
\end{aligned}$$

Hiding terms on the left hand side, and adding and subtracting terms appropriately,

we obtain

$$\begin{aligned}
&\frac{1}{4\Delta t}\Big(\|v_h^{n+1}\|^2 - \|v_h^n\|^2 + \|2v_h^{n+1} - v_h^n\|^2 - \|2v_h^n - v_h^{n-1}\|^2 \\
&\qquad + \|w_h^{n+1}\|^2 - \|w_h^n\|^2 + \|2w_h^{n+1} - w_h^n\|^2 - \|2w_h^n - w_h^{n-1}\|^2\Big) \\
&\qquad + \frac{\nu+\nu_m}{4}\Big(\|\nabla v_h^{n+1}\|^2 - \|\nabla v_h^n\|^2 + \|\nabla w_h^{n+1}\|^2 - \|\nabla w_h^n\|^2\Big) \\
&\qquad + \frac{\nu+\nu_m - |\nu-\nu_m|(1+\theta)}{4}\Big(\|\nabla v_h^n\|^2 - \|\nabla v_h^{n-1}\|^2 + \|\nabla w_h^n\|^2 - \|\nabla w_h^{n-1}\|^2\Big) \\
&\qquad + \frac{\nu+\nu_m - |\nu-\nu_m|(1+2\theta)}{4}(\|\nabla v_h^{n-1}\|^2 + \|\nabla w_h^{n-1}\|^2) \\
&\qquad \le \frac{1}{\alpha}\left(\|f_1(t^{n+1})\|_{-1}^2 + \|f_2(t^{n+1})\|_{-1}^2\right). \qquad (4.19)
\end{aligned}$$

Now multiplying both sides by $4\Delta t$ and summing over time steps $n = 1, \cdots, M-1$, we get

$$\begin{aligned}
&\|v_h^M\|^2 + \|2v_h^M - v_h^{M-1}\|^2 + \|w_h^M\|^2 + \|2w_h^M - w_h^{M-1}\|^2 \\
&\qquad + \alpha\Delta t\sum_{n=2}^{M}\Big(\|\nabla v_h^n\|^2 + \|\nabla w_h^n\|^2\Big) \le \|v_h^0\|^2 + \|w_h^0\|^2 + \|2v_h^1 - v_h^0\|^2 \\
&\qquad + \|2w_h^1 - w_h^0\|^2 + (\nu+\nu_m)\Delta t\Big(\|\nabla v_h^1\|^2 + \|\nabla w_h^1\|^2 + 2\|\nabla v_h^0\|^2 + 2\|\nabla w_h^0\|^2\Big) \\
&\qquad + \frac{4\Delta t}{\alpha}\sum_{n=1}^{M}(\|f_1(t^n)\|_{-1}^2 + \|f_2(t^n)\|_{-1}^2), \qquad (4.20)
\end{aligned}$$

which finishes the proof. □

4.3.2 Convergence

We now consider convergence of the proposed decoupled, unconditionally stable scheme. Since the method departs from a second order framework when $\theta > 1$, we do not expect a second order in time result. However, we are able to prove the method is nearly second order in practice; that is, in the typical case that ν and ν_m are small,

the second order temporal error will be the dominant source of temporal error. Spatial convergence is found to be optimal.

Theorem 3. *For (v, w, p) satisfying (1.5)-(1.8) with regularity assumptions $v, w \in L^\infty(0,T;\, H^{k+1}(\Omega))$, $v_t, w_t, v_{tt}, w_{tt} \in L^\infty(0,T; H^1(\Omega))$, $v_{ttt}, w_{ttt} \in L^\infty(0,T; L^2(\Omega))$ and $q, r \in L^\infty(0,T;\, H^k(\Omega))$, then the solution (v_h, w_h) to the Algorithm (4.3.1) converges unconditionally to the true solution: for any $\Delta t > 0$,*

$$\|v(T) - v_h^M\| + \|w(T) - w_h^M\| + \alpha\Delta t \sum_{n=2}^{M} \left(\|\nabla(v(t^n) - v_h^n)\|^2 + \|\nabla(w(t^n) - w_h^n)\|^2\right)^{\frac{1}{2}}$$
$$\leq C\left(h^k + (\Delta t)^2 + (1-\theta)|\nu - \nu_m|\Delta t\right)$$

Proof. We start our proof by obtaining the error equations. At time level t^{n+1}, the continuous variational formulations of (1.5) and (1.8) can be written as

$$\begin{aligned}
&\Big(\frac{3v(t^{n+1}) - 4v(t^n) + v(t^{n-1})}{2\Delta t},\ \chi_h\Big) + \frac{\nu + \nu_m}{2}\left(\nabla v(t^{n+1}),\ \nabla\chi_h\right) \\
&+ b^*\left(w(t^{n+1}) - 2w(t^n) + w(t^{n-1}),\ v(t^{n+1}),\ \chi_h\right) \\
&+ b^*\left(2w(t^n) - w(t^{n-1}),\ v(t^{n+1}),\ \chi_h\right) - \left(q(t^{n+1}) - \rho_h,\ \nabla\cdot\chi_h\right) \\
&+ \frac{\nu - \nu_m}{2}\left(\nabla\big(w(t^{n+1}) - (1+\theta)w(t^n) + \theta w(t^{n-1})\big),\ \nabla\chi_h\right) \\
&+ \frac{\nu - \nu_m}{2}\left((1+\theta)\nabla w(t^n) - \theta\nabla w(t^{n-1}),\ \nabla\chi_h\right) \\
&= \left(f_1(t^{n+1}),\ \chi_h\right) - \left(v_t(t^{n+1}) - \frac{3v(t^{n+1}) - 4v(t^n) + v(t^{n-1})}{2\Delta t},\ \chi_h\right), \qquad (4.21)
\end{aligned}$$

and

$$\begin{aligned}
&\Big(\frac{3w(t^{n+1})-4w(t^n)+w(t^{n-1})}{2\Delta t},\ l_h\Big)+\frac{\nu+\nu_m}{2}\left(\nabla w(t^{n+1}),\ \nabla l_h\right)\\
&+b^*\left(v(t^{n+1})-2v(t^n)+v(t^{n-1}),\ w(t^{n+1}),\ l_h\right)\\
&+b^*\left(2v(t^n)-v(t^{n-1}),\ w(t^{n+1}),\ l_h\right)-\left(r(t^{n+1})-\zeta_h,\ \nabla\cdot l_h\right)\\
&+\frac{\nu-\nu_m}{2}\left(\nabla\big(v(t^{n+1})-(1+\theta)v(t^n)+\theta v(t^{n-1})\big),\ \nabla l_h\right)\\
&+\frac{\nu-\nu_m}{2}\left((1+\theta)\nabla v(t^n)-\theta\nabla v(t^{n-1}),\ \nabla l_h\right)\\
&=\left(f_2(t^{n+1}),\ l_h\right)-\left(w_t(t^{n+1})-\frac{3w(t^{n+1})-4w(t^n)+w(t^{n-1})}{2\Delta t},\ l_h\right),
\end{aligned}\tag{4.22}$$

for all $\chi_h, l_h \in V_h$. Denote the errors by $e_v^n := v(t^n) - v_h^n$ and $e_w^n := w(t^n) - w_h^n$. Subtracting (4.14) and (4.15) from (4.21) and (4.22) respectively, provides

$$\begin{aligned}
&\Big(\frac{3e_v^{n+1}-4e_v^n+e_v^{n-1}}{2\Delta t},\ \chi_h\Big)+\frac{\nu+\nu_m}{2}\left(\nabla e_v^{n+1},\ \nabla\chi_h\right)\\
&+\frac{\nu-\nu_m}{2}\left((1+\theta)\nabla e_w^n-\theta\nabla e_w^{n-1},\ \nabla\chi_h\right)\\
&-\left(q(t^{n+1})-\rho_h,\ \nabla\cdot\chi_h\right)+b^*(2e_w^n-e_w^{n-1},\ v(t^{n+1}),\ \chi_h)\\
&+b^*(2w_h^n-w_h^{n-1},\ e_v^{n+1},\ \chi_h)=-G_1(t,v,w,\chi_h),
\end{aligned}\tag{4.23}$$

and

$$\begin{aligned}
&\Big(\frac{3e_w^{n+1}-4e_w^n+e_w^{n-1}}{2\Delta t},\ l_h\Big)+\frac{\nu+\nu_m}{2}\left(\nabla e_w^{n+1},\ \nabla l_h\right)\\
&+\frac{\nu-\nu_m}{2}\left((1+\theta)\nabla e_v^n-\theta\nabla e_v^{n-1},\ \nabla l_h\right)\\
&-\left(r(t^{n+1})-\zeta_h,\ \nabla\cdot l_h\right)+b^*(2e_v^n-e_v^{n-1},\ w(t^{n+1}),\ l_h)\\
&+b^*(2v_h^n-v_h^{n-1},\ e_w^{n+1},\ l_h)=-G_2(t,v,w,l_h),
\end{aligned}\tag{4.24}$$

where ρ_h and ζ_h are arbitrary in Q_h, and

$$\begin{aligned} G_1(t,v,w,\chi_h) := & \frac{\nu-\nu_m}{2}\big(\nabla(w(t^{n+1})-(1+\theta)w(t^n)+\theta w(t^{n-1})),\ \nabla\chi_h\big) \\ & + b^*\left(w(t^{n+1})-2w(t^n)+w(t^{n-1}),\ v(t^{n+1}),\ \chi_h\right) \\ & + \left(v_t(t^{n+1})-\frac{3v(t^{n+1})-4v(t^n)+v(t^{n-1})}{2\Delta t},\ \chi_h\right), \end{aligned}$$

and

$$\begin{aligned} G_2(t,v,w,l_h) := & \frac{\nu-\nu_m}{2}\big(\nabla(v(t^{n+1})-(1+\theta)v(t^n)+\theta v(t^{n-1})),\ \nabla l_h\big) \\ & + b^*\big(v(t^{n+1})-2v(t^n)+v(t^{n-1}),\ w(t^{n+1}),\ l_h\big) \\ & + \left(w_t(t^{n+1})-\frac{3w(t^{n+1})-4w(t^n)+w(t^{n-1})}{2\Delta t},\ l_h\right). \end{aligned}$$

Now we decompose the errors as

$$\begin{aligned} e_v^n := v(t^n)-v_h^n = (v(t^n)-\tilde{v}^n)-(v_h^n-\tilde{v}^n) := \eta_v^n-\phi_h^n, \\ e_w^n := w(t^n)-w_h^n = (w(t^n)-\tilde{w}^n)-(w_h^n-\tilde{w}^n) := \eta_w^n-\psi_h^n, \end{aligned}$$

where $\tilde{v}^n = P_{V_h}^{L^2}(v(t^n)) \in V_h$ and $\tilde{w}^n = P_{V_h}^{L^2}(w(t^n)) \in V_h$ are the L^2 projections of $v(t^n)$ and $w(t^n)$ into V_h respectively. Note that $(\eta_v^n, v_h) = (\eta_w^n, v_h) = 0\ \forall v_h \in V_h$.

Rewriting, we have for χ_h, $l_h \in V_h$

$$\begin{aligned}
&\Big(\frac{3\phi_h^{n+1}-4\phi_h^n+\phi_h^{n-1}}{2\Delta t},\ \chi_h\Big)+\frac{\nu+\nu_m}{2}\left(\nabla\phi_h^{n+1},\ \nabla\chi_h\right)\\
&+\frac{\nu-\nu_m}{2}\left((1+\theta)\nabla\psi_h^n-\theta\nabla\psi_h^{n-1},\ \nabla\chi_h\right)+b^*\left(2\psi_h^n-\psi_h^{n-1},\ v(t^{n+1}),\ \chi_h\right)\\
&+b^*(2w_h^n-w_h^{n-1},\ \phi_h^{n+1},\ \chi_h)-(q(t^{n+1})-\rho_h,\ \nabla\cdot\chi_h)=\frac{\nu+\nu_m}{2}\left(\nabla\eta_v^{n+1},\ \nabla\chi_h\right)\\
&+\frac{\nu-\nu_m}{2}\left((1+\theta)\nabla\eta_w^n-\theta\nabla\eta_w^{n-1},\ \nabla\chi_h\right)+b^*\left(2\eta_w^n-\eta_w^{n-1},\ v(t^{n+1}),\ \chi_h\right)\\
&+b^*\left(2w_h^n-w_h^{n-1},\ \eta_v^{n+1},\ \chi_h\right)+G_1(t,v,w,\chi_h),
\end{aligned}\tag{4.25}$$

and

$$\begin{aligned}
&\Big(\frac{3\psi_h^{n+1}-4\psi_h^n+\psi_h^{n-1}}{2\Delta t},\ l_h\Big)+\frac{\nu+\nu_m}{2}\left(\nabla\psi_h^{n+1},\ \nabla l_h\right)\\
&+\frac{\nu-\nu_m}{2}\left((1+\theta)\nabla\phi_h^n-\theta\nabla\phi_h^{n-1},\ \nabla l_h\right)+b^*(2\phi_h^n-\phi_h^{n-1},\ w(t^{n+1}),\ l_h)\\
&+b^*(2v_h^n-v_h^{n-1},\ \psi_h^{n+1},\ l_h)-(r(t^{n+1})-\zeta_h,\ \nabla\cdot l_h)\\
&=\frac{\nu+\nu_m}{2}\left(\nabla\eta_w^{n+1},\ \nabla l_h\right)+\frac{\nu-\nu_m}{2}\left((1+\theta)\nabla\eta_v^n-\theta\nabla\eta_v^{n-1},\ \nabla l_h\right)\\
&+b^*(2\eta_v^n-\eta_v^{n-1},\ w(t^{n+1}),\ l_h)+b^*(2v_h^n-v_h^{n-1},\ \eta_w^{n+1},\ l_h)+G_2(t,v,w,l_h).
\end{aligned}\tag{4.26}$$

Choose $\chi_h=\phi_h^{n+1}$, $l_h=\psi_h^{n+1}$ and use the identity (4.16) in (5.29) and (5.30), to

obtain

$$\begin{aligned}
&\frac{1}{4\Delta t}\Big(\|\phi_h^{n+1}\|^2-\|\phi_h^n\|^2+\|2\phi_h^{n+1}-\phi_h^n\|^2-\|2\phi_h^n-\phi_h^{n-1}\|^2+\|\phi_h^{n+1}-2\phi_h^n+\phi_h^{n-1}\|^2\Big)\\
&\quad+\frac{\nu+\nu_m}{2}\|\nabla\phi_h^{n+1}\|^2\le(1+\theta)\frac{|\nu-\nu_m|}{2}\Big\{|\left(\nabla\eta_w^n,\ \nabla\phi_h^{n+1}\right)|+|(\nabla\psi_h^n,\ \nabla\phi_h^{n+1})|\Big\}\\
&\quad+\theta\frac{|\nu-\nu_m|}{2}\Big\{|\left(\nabla\eta_w^{n-1},\ \nabla\phi_h^{n+1}\right)|+|(\nabla\psi_h^{n-1},\ \nabla\phi_h^{n+1})|\Big\}\\
&\quad+\frac{\nu+\nu_m}{2}|\left(\nabla\eta_v^{n+1},\ \nabla\phi_h^{n+1}\right)|+C\|q(t^{n+1})-\rho_h\|\|\nabla\phi_h^{n+1}\|\\
&\quad+|b^*\left(2\eta_w^n-\eta_w^{n-1},\ v(t^{n+1}),\ \phi_h^{n+1}\right)|+|b^*\left(2w_h^n-w_h^{n-1},\ \eta_v^{n+1},\ \phi_h^{n+1}\right)|\\
&\quad+|b^*\left(2\psi_h^n-\psi_h^{n-1},\ v(t^{n+1}),\ \phi_h^{n+1}\right)|+|G_1(t,v,w,\phi_h^{n+1})|,
\end{aligned}\tag{4.27}$$

and

$$\begin{aligned}
&\frac{1}{4\Delta t}\Big(\|\psi_h^{n+1}\|^2-\|\psi_h^n\|^2+\|2\psi_h^{n+1}-\psi_h^n\|^2-\|2\psi_h^n-\psi_h^{n-1}\|^2+\|\psi_h^{n+1}-2\psi_h^n+\psi_h^{n-1}\|^2\Big)\\
&\quad+\frac{\nu+\nu_m}{2}\|\nabla\psi_h^{n+1}\|^2\le(1+\theta)\frac{|\nu-\nu_m|}{2}\Big\{|\left(\nabla\eta_v^n,\ \nabla\psi_h^{n+1}\right)|+|(\nabla\phi_h^n,\ \nabla\psi_h^{n+1})|\Big\}\\
&\quad+\theta\frac{|\nu-\nu_m|}{2}\Big\{|\left(\nabla\eta_v^{n-1},\ \nabla\psi_h^{n+1}\right)|+|(\nabla\phi_h^{n-1},\ \nabla\psi_h^{n+1})|\Big\}\\
&\quad+\frac{\nu+\nu_m}{2}|\left(\nabla\eta_w^{n+1},\ \nabla\psi_h^{n+1}\right)|+C\|r(t^{n+1})-\zeta_h\|\|\nabla\psi_h^{n+1}\|\\
&\quad+|b^*\left(2\eta_v^n-\eta_v^{n-1},\ w(t^{n+1}),\ \psi_h^{n+1}\right)|+|b^*\left(2v_h^n-v_h^{n-1},\ \eta_w^{n+1},\ \psi_h^{n+1}\right)|\\
&\quad+|b^*\left(2\phi_h^n-\phi_h^{n-1},\ w(t^{n+1}),\ \psi_h^{n+1}\right)|+|G_2(t,v,w,\psi_h^{n+1})|
\end{aligned}\tag{4.28}$$

We now turn our attention to finding bounds on the right side terms of(4.27) (the estimates for (4.28) are similar). Applying Cauchy-Schwarz and Young's inequalities

on the first six terms results in

$$
\begin{aligned}
(1+\theta)\frac{|\nu-\nu_m|}{2}|(\nabla\psi_h^n,\nabla\phi_h^{n+1})| &\le (1+\theta)\frac{|\nu-\nu_m|}{4}\left(\|\nabla\psi_h^n\|^2+\|\nabla\phi_h^{n+1}\|^2\right),\\
\theta\frac{|\nu-\nu_m|}{2}|(\nabla\psi_h^{n-1},\nabla\phi_h^{n+1})| &\le \theta\frac{|\nu-\nu_m|}{4}\left(\|\nabla\phi_h^{n+1}\|^2+\|\nabla\psi_h^{n-1}\|^2\right),\\
(1+\theta)\frac{|\nu-\nu_m|}{2}|\left(\nabla\eta_w^n,\nabla\phi_h^{n+1}\right)| &\le \frac{\alpha}{32}\|\nabla\phi_h^{n+1}\|^2+\frac{2(1+\theta)^2(\nu-\nu_m)^2}{\alpha}\|\nabla\eta_w^n\|^2,\\
\theta\frac{|\nu-\nu_m|}{2}|\left(\nabla\eta_w^{n-1},\nabla\phi_h^{n+1}\right)| &\le \frac{\alpha}{32}\|\nabla\phi_h^{n+1}\|^2+\frac{2\theta^2(\nu-\nu_m)^2}{\alpha}\|\nabla\eta_w^{n-1}\|^2,\\
\frac{\nu+\nu_m}{2}|\left(\nabla\eta_v^{n+1},\nabla\phi_h^{n+1}\right)| &\le \frac{\alpha}{32}\|\nabla\phi_h^{n+1}\|^2+\frac{2(\nu+\nu_m)^2}{\alpha}\|\nabla\eta_v^{n+1}\|^2,\\
C\|q(t^{n+1})-\rho_h\|\|\nabla\phi_h^{n+1}\| &\le \frac{\alpha}{32}\|\nabla\phi_h^{n+1}\|^2+\frac{8C^2}{\alpha}\|q(t^{n+1})-\rho_h\|^2
\end{aligned}
$$

Applying Hölder and Young's inequalities with (2.1) on the first two nonlinear terms yields

$$
\begin{aligned}
|b^*\left(2\eta_w^n-\eta_w^{n-1},v(t^{n+1}),\phi_h^{n+1}\right)| &\le C\|\nabla(2\eta_w^n-\eta_w^{n-1})\|\|\nabla v(t^{n+1})\|\|\nabla\phi_h^{n+1}\|\\
&\le \frac{\alpha}{32}\|\nabla\phi_h^{n+1}\|^2+\frac{8C}{\alpha}\|\nabla v(t^{n+1})\|^2\|\nabla(2\eta_w^n-\eta_w^{n-1})\|^2,\\
|b^*\left(2w_h^n-w_h^{n-1},\eta_v^{n+1},\phi_h^{n+1}\right)| &\le C\|\nabla(2w_h^n-w_h^{n-1})\|\|\nabla\eta_v^{n+1}\|\|\nabla\phi_h^{n+1}\|\\
&\le \frac{\alpha}{32}\|\nabla\phi_h^{n+1}\|^2+\frac{8C}{\alpha}\|\nabla(2w_h^n-w_h^{n-1})\|^2\|\nabla\eta_v^{n+1}\|^2.
\end{aligned}
$$

For the third nonlinear term, we use Hölder's inequality, Sobolev embedding theorems, Poincare's and Young's inequalities to reveal

$$
\begin{aligned}
|\left((2\psi_h^n-\psi_h^{n-1})\cdot\nabla v(t^{n+1}),\phi_h^{n+1}\right)| &\le C\|2\psi_h^n-\psi_h^{n-1}\|\|\nabla v(t^{n+1})\|_{L^6}\|\phi_h^{n+1}\|_{L^3}\\
&\le C\|2\psi_h^n-\psi_h^{n-1}\|\|v(t^{n+1})\|_{H^2}\|\phi_h^n\|^{1/2}\|\nabla\phi_h^{n+1}\|^{1/2}\\
&\le C\|2\psi_h^n-\psi_h^{n-1}\|\|v(t^{n+1})\|_{H^2}\|\nabla\phi_h^{n+1}\|\\
&\le \frac{\alpha}{32}\|\nabla\phi_h^{n+1}\|^2+\frac{8C}{\alpha}\|v(t^{n+1})\|_{H^2}^2\|2\psi_h^n-\psi_h^{n-1}\|^2.
\end{aligned}
$$

Using Taylor's series, Cauchy-Schwarz and Young's inequalities the last term is evaluated as

$$|G_1(t,v,w,\chi_h)| \leq C(\Delta t)^4\big(\|v_{ttt}(t^*)\|^2 + \|\nabla w_{tt}(t^{**})\|^2\|\nabla v(t^{n+1})\|^2\big) + \frac{2(\nu-\nu_m)^2(1-\theta)^2(\Delta t)^2}{\alpha}\|\nabla w_t(t^{***})\|^2 + \frac{\alpha}{32}\|\nabla\phi_h^{n+1}\|^2,$$

with $t^*, t^{**}, t^{***} \in [t^{n-1}, t^{n+1}]$. Using these estimates in (4.27) and reducing produces

$$\begin{aligned}
&\frac{1}{4\Delta t}\Big(\|\phi_h^{n+1}\|^2 - \|\phi_h^n\|^2 + \|2\phi_h^{n+1} - \phi_h^n\|^2 - \|2\phi_h^n - \phi_h^{n-1}\|^2\Big) \\
&\quad + \frac{\nu+\nu_m}{4}\|\nabla\phi_h^{n+1}\|^2 \leq \theta\frac{|\nu-\nu_m|}{4}\|\nabla\psi_h^{n-1}\|^2 + (1+\theta)\frac{|\nu-\nu_m|}{4}\|\nabla\psi_h^n\|^2 \\
&\quad + \frac{2(1+\theta)^2(\nu-\nu_m)^2}{\alpha}\|\nabla\eta_w^n\|^2 + \frac{2\theta^2(\nu-\nu_m)^2}{\alpha}\|\nabla\eta_w^{n-1}\|^2 \\
&\quad + \frac{2(\nu+\nu_m)^2}{\alpha}\|\nabla\eta_v^{n+1}\|^2 + \frac{8C}{\alpha}\|\nabla v(t^{n+1})\|^2\|\nabla(2\eta_w^n - \eta_w^{n-1})\|^2 \\
&\quad + \frac{8C}{\alpha}\|\nabla(2w_h^n - w_h^{n-1})\|^2\|\nabla\eta_v^{n+1}\|^2 + \frac{8C}{\alpha}\|v(t^{n+1})\|_{H^2}^2\|2\psi_h^n - \psi_h^{n-1}\|^2 \\
&\quad + C(\Delta t)^4\left(\|v_{ttt}(t^*)\|^2 + \|\nabla w_{tt}(t^{**})\|^2\|\nabla v(t^{n+1})\|^2\right) \\
&\quad + \frac{2(\nu-\nu_m)^2(1-\theta)^2(\Delta t)^2}{\alpha}\|\nabla w_t(t^{***})\|^2 + \frac{8C^2}{\alpha}\|q(t^{n+1}) - \rho_h\|^2. \quad (4.29)
\end{aligned}$$

Apply similar techniques to (4.28), we get

$$\begin{aligned}
&\frac{1}{4\Delta t}\Big(\|\psi_h^{n+1}|^2 - \|\psi_h^n\|^2 + \|2\psi_h^{n+1} - \psi_h^n\|^2 - \|2\psi_h^n - \psi_h^{n-1}\|^2\Big) \\
&\qquad + \frac{\nu+\nu_m}{4}\|\nabla\psi_h^{n+1}\|^2 \le \theta\frac{|\nu-\nu_m|}{4}\|\nabla\phi_h^{n-1}\|^2 + (1+\theta)\frac{|\nu-\nu_m|}{4}\|\nabla\phi_h^n\|^2 \\
&\qquad + \frac{2(1+\theta)^2(\nu-\nu_m)^2}{\alpha}\|\nabla\eta_v^n\|^2 + \frac{2\theta^2(\nu-\nu_m)^2}{\alpha}\|\nabla\eta_v^{n-1}\|^2 \\
&\qquad + \frac{2(\nu+\nu_m)^2}{\alpha}\|\nabla\eta_w^{n+1}\|^2 + \frac{8C}{\alpha}\|\nabla w(t^{n+1})\|^2\|\nabla(2\eta_v^n - \eta_v^{n-1})\|^2 \\
&\qquad + \frac{8C}{\alpha}\|\nabla(2v_h^n - v_h^{n-1})\|^2\|\nabla\eta_w^{n+1}\|^2 + \frac{8C}{\alpha}\|w(t^{n+1})\|_{H^2}^2\|2\phi_h^n - \phi_h^{n-1}\|^2 \\
&\qquad + C(\Delta t)^4\left(\|w_{ttt}(s^*)\|^2 + \|\nabla v_{tt}(s^{**})\|^2\|\nabla w(t^{n+1})\|^2\right) \\
&\qquad + \frac{2(\nu-\nu_m)^2(1-\theta)^2(\Delta t)^2}{\alpha}\|\nabla v_t(s^{***})\|^2 + \frac{8C^2}{\alpha}\|r(t^{n+1}) - \zeta_h\|^2, \quad (4.30)
\end{aligned}$$

with $s^*, s^{**}, s^{***} \in [t^{n-1}, t^{n+1}]$. Now add equations (4.29) and (4.30), multiply by $4\Delta t$, use regularity assumptions, $\|\phi_h^0\| = \|\psi_h^0\| = \|\phi_h^1\| = \|\psi_h^1\| = 0$, $\Delta t M = T$, and sum over the time steps to find

$$\begin{aligned}
&\|\phi_h^M\|^2 + \|2\phi_h^M - \phi_h^{M-1}\|^2 + \|\psi_h^M\|^2 + \|2\psi_h^M - \psi_h^{M-1}\|^2 \\
&\quad + \alpha\Delta t\sum_{n=2}^{M}\left(\|\nabla\phi_h^n\|^2 + \|\nabla\psi_h^n\|^2\right) \le C\Delta t\sum_{n=0}^{M}\left(\|\nabla\eta_v^n\|^2 + \|\nabla\eta_w^n\|^2\right) \\
&\quad + C\left((\Delta t)^4 + (\nu-\nu_m)^2(1-\theta)^2(\Delta t)^2\right) \\
&\quad + C\Delta t\sum_{n=1}^{M-1}\left(\|\nabla\left(2w_h^n - w_h^{n-1}\right)\|^2\|\nabla\eta_v^{n+1}\|^2 + \|\nabla\left(2v_h^n - v_h^{n-1}\right)\|^2\|\nabla\eta_w^{n+1}\|^2\right) \\
&\quad + C\Delta t\sum_{n=1}^{M-1}\Big(\|w(t^{n+1})\|_{L^\infty(0,T;H^2(\Omega))}^2\|2\phi_h^n - \phi_h^{n-1}\|^2 \\
&\quad + \|v(t^{n+1})\|_{L^\infty(0,T;H^2(\Omega))}^2\|2\psi_h^n - \psi_h^{n-1}\|^2\Big) \\
&\quad + \frac{32C^2}{\alpha}\Delta t\sum_{n=1}^{M-1}\left(\|q(t^{n+1}) - \rho_h\|^2 + \|r(t^{n+1}) - \zeta_h\|^2\right). \quad (4.31)
\end{aligned}$$

Applying the discrete Gronwall lemma and interpolation estimates for v, w, q, and r we have for any $\Delta t > 0$ that

$$\|\phi_h^M\|^2 + \|\psi_h^M\|^2 + \alpha\Delta t \sum_{n=2}^{M} \left(\|\nabla\phi_h^n\|^2 + \|\nabla\psi_h^n\|^2\right) \leq C\left(h^{2k} + (\Delta t)^4 + (\nu - \nu_m)^2(1-\theta)^2(\Delta t)^2\right).$$

Now using the triangle inequality we can write,

$$\begin{aligned}
&\|v(T) - v_h^M\|^2 + \|w(T) - w_h^M\|^2 \\
&\qquad + 2\alpha\Delta t \sum_{n=2}^{M} \left(\|\nabla(v(t^n) - v_h^n)\|^2 + \|\nabla(w(t^n) - w_h^n)\|^2\right) \\
&\qquad \leq 2\Big(\|\eta_v^M\|^2 + \|\phi_h^M\|^2 + \|\eta_w^M\|^2 + \|\psi_h^M\|^2 \\
&\qquad + 2\alpha\Delta t \sum_{n=2}^{M} \left(\|\nabla\eta_v^n\|^2 + \|\nabla\eta_w^n\|^2 + \|\nabla\phi_h^n\|^2 + \|\nabla\psi_h^n\|^2\right)\Big) \\
&\qquad \leq 2C^*(h^{2k+2} + h^{2k}) + C\left(h^{2k} + (\Delta t)^4 + (\nu - \nu_m)^2(1-\theta)^2(\Delta t)^2\right) \\
&\qquad \leq C\left(h^{2k} + (\Delta t)^4 + (\nu - \nu_m)^2(1-\theta)^2(\Delta t)^2\right) \qquad (4.32)
\end{aligned}$$

Which implies

$$\begin{aligned}
\|v(T) - v_h^M\| + \|w(T) - w_h^M\| + 2\alpha\Delta t \sum_{n=2}^{M} \left(\|\nabla(v(t^n) - v_h^n)\|^2 + \|\nabla(w(t^n) - w_h^n)\|^2\right)^{\frac{1}{2}} \\
\leq C\left(h^k + (\Delta t)^2 + (1-\theta)|\nu - \nu_m|\Delta t\right) \qquad (4.33)
\end{aligned}$$

□

4.4 Numerical Experiments

In this section, we perform three numerical experiments: a test of stability with varying θ, a verification of convergence rates, and simulation of MHD channel flow past a step. For the first two tests, we use the test problem with analytical solution

$$v = \begin{pmatrix} \cos y + (1+e^t)\sin y \\ \sin x + (1+e^t)\cos x \end{pmatrix}, w = \begin{pmatrix} \cos y - (1+e^t)\sin y \\ \sin x - (1+e^t)\cos x \end{pmatrix},$$

$$p = -\lambda = \sin(x+y)(1+e^t),$$

on the domain $\Omega = (0,1)^2$. The forcings f_1 and f_2 are calculated from the true solution, the values of ν and ν_m, and the initial conditions and boundary conditions use the analytical solution. All simulations were run using the software Freefem++ [42], and on barycenter refined triangular meshes.

4.4.1 Numerical experiment 1: Testing stability versus θ

For our first numerical test, we consider stability of the proposed algorithm for varying θ, using the test problem described above with $\nu = 1$ and $\nu_m = 0.1$. We simulate until $T = 1$ using Algorithm 4.3.1 with $h = 1/64$, $\Delta t = 1/256$, and three choices of θ: $\theta = 1$ (the BDF2 case), $\theta = 0.167$ and $\theta = \theta_{critical} = 0.111$. Our theoretical results prove that the scheme is stable for $\theta < \theta_{critical}$, and suggest the scheme is unstable for larger θ.

Figure 4.1-4.2 shows plots of $\frac{1}{2}\|\nabla v_h^n\|^2$ and $\frac{1}{2}\|\nabla w_h^n\|^2$ with time, for each of the θ values. The solution norms remain stable for $\theta = \theta_{critical} = 0.111$. However, for both cases of $\theta > \theta_{critical}$, we observe solution blowup/instability. In particular, for the BDF2 case ($\theta = 1$), the blowup occurs very quickly.

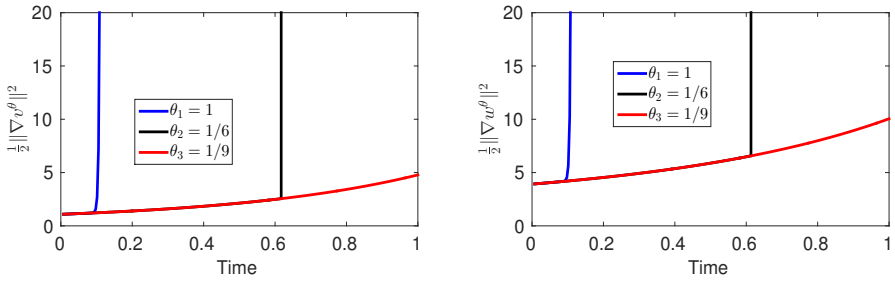

Figure 4.1: Plots of $\frac{1}{2}\|\nabla v_h\|^2$ and $\frac{1}{2}\|\nabla w_h\|^2$ versus time, for numerical experiment 1 using (P_2, P_1^{disc}) Scott-Vogelius elements. Only the case of $\theta = \theta_{critical}$ remains stable.

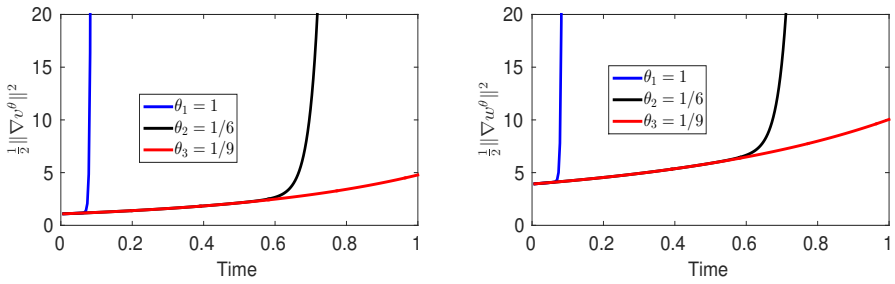

Figure 4.2: Plots of $\frac{1}{2}\|\nabla v_h\|^2$ and $\frac{1}{2}\|\nabla w_h\|^2$ versus time, for numerical experiment 1 using (P_2, P_1) Taylor Hood elements. Only the case of $\theta = \theta_{critical}$ remains stable.

4.4.2 Numerical experiment 2: Convergence rate verification

Next, we test the theoretical convergence rates predicted by the theory. Here, we use the same analytical test problem as the first numerical example, but now with $\nu = 0.001$ and $\nu_m = 0.01$, $\theta = \theta_{critical} = \frac{1}{9}$, and (P_2, P_1^{disc}) Scott-Vogelius elements on barycenter refined triangular meshes. Spatial and temporal convergence rates are calculated, and from the theory we expect $O(h^2+\Delta t^2+(1-\theta)|\nu-\nu_m|\Delta t)$ convergence. For spatial convergence testing, we select a very small endtime $T = 0.001$, fix $\Delta t = \frac{T}{8}$, and then compute on successively refined uniform meshes. For temporal convergence, we fix $h = 1/64$, $T = 1$, and compute with successively refined time step sizes.

Errors and rates are shown in table 4.1 for v, and we omit the w results since

they are very similar. From the tables, we observe second order spatial convergence as expected. For temporal convergence, we also observe a rate near 2. We also compute errors and rates for usual BDF2 ($\theta = 1$) as Δt is refined, and we observe from the tables that BDF2 error blows up as $\Delta t \to 0$; these terrible BDF2 results are expected since $1 \gg \theta_{critical}$. For (P_2, P_1) Taylor-Hood element, we found almost similar convergence table.

Temporal convergence (fixed h=1/64)				
	$\theta = 1$(BDF2)		$\theta = 1/9$	
Δt	$\|v - v_h\|_{2,1}$	rate	$\|v - v_h\|_{2,1}$	rate
$\frac{T}{4}$	9.006e-2		7.410e-2	
$\frac{T}{8}$	3.625e-2	1.31	2.574e-2	1.53
$\frac{T}{16}$	9.298e-2	–	7.668e-3	1.75
$\frac{T}{32}$	4.995e+2	–	1.962e-3	1.97
$\frac{T}{64}$	5.217e+4	–	4.178e-4	2.23

Spatial convergence (fixed T=0.001, $\Delta t = \frac{T}{8}$)		
	$\theta = 1/9$	
h	$\|v - v_h\|_{2,1}$	rate
$\frac{1}{4}$	1.009e-4	
$\frac{1}{8}$	2.538e-5	1.99
$\frac{1}{16}$	6.363e-6	2.00
$\frac{1}{32}$	1.598e-6	1.99
$\frac{1}{64}$	4.014e-7	1.99

Table 4.1: Spatial and temporal convergence rates for $\nu = 0.01$, $\nu_m = 0.001$, using the critical $\theta = \frac{1}{9}$ and (P_2, P_1^{disc}) Scott-Vogelius elements. Also shown is the blowup of error as $\Delta t \to 0$ when $\theta = 1$ (the usual BDF2 case).

4.4.3 Numerical experiment 3: MHD Channel Flow over a step

Our final experiment is to test the proposed method for MHD channel flow past a step. The problem setup follows the classical NSE benchmark [39], using $\Omega = (0, 30) \times (0, 10)$ with a 1×1 step placed five units into the channel on the bottom. We take $T = 40$, $\Delta t = 0.025$, and full Dirichlet boundary conditions corresponding to no slip velocity on the walls, $u =< y(10 - y)/25, 0 >^T$ on the inlet and outlet, and $B =< 0, 1 >^T$ on all boundaries. The initial conditions corresponds to no magnetic field and a parabolic velocity profile $u_0 =< y(10 - y)/25, 0 >^T$. A coupling number of $s = 0.01$ is used in all the simulations, as is a Delaunay generated triangulation which provides 1,778,630 total degrees of freedom when used with (P_2, P_1^{disc}) Scott-Vogelius

elements.

We show results for two cases below, the case $\nu = 0.001$ and $\nu_m = 1$ in figure 4.3, and $\nu = 0.001$ and $\nu_m = 0.1$ in figure 4.4. For each case, we ran simulations with $\theta = \theta_{critical}$, a somewhat larger θ, and also $\theta = 1$ (BDF2). The figures show plots of streamlines over speed contours, and magnetic field contours at $T = 40$. Only the simulations with $\theta = \theta_{critical}$ remained stable and accurate to $T = 40$. The simulations with larger θ are clearly very inaccurate, and exhibit spurious oscillations and instability. We also run for (P_2, P_1) Taylor-Hood element. The plots are indistinguishable.

4.5 Conclusion

We proposed, analyzed, and tested a new, efficient scheme for MHD, and rigorously proved its unconditional stability, well-posedness, and convergence, under an appropriate choice of θ (which is made a priori, based on ν and ν_m). The proposed method may be an enabling tool for MHD simulations, since it stably decouples the MHD system into two Oseen problems at each timestep that can be solved simultaneously, converges optimally in space, and behaves like second order in time when ν and ν_m are small, all without any restriction on the time step size or on data ν and ν_m (which the full BDF2 method does require). The decoupling allows for the solving of potentially much bigger problems than primitive variable MHD algorithms can solve, since schemes in primitive variables require solving very large coupled linear systems (or excessively small time step sizes) for stable computations.

In addition to the possibility of more easily solving bigger MHD problems with the proposed method compared to fully coupled methods based on primitive variable formulations, it is worth exploring if the proposed scheme can likely be combined with

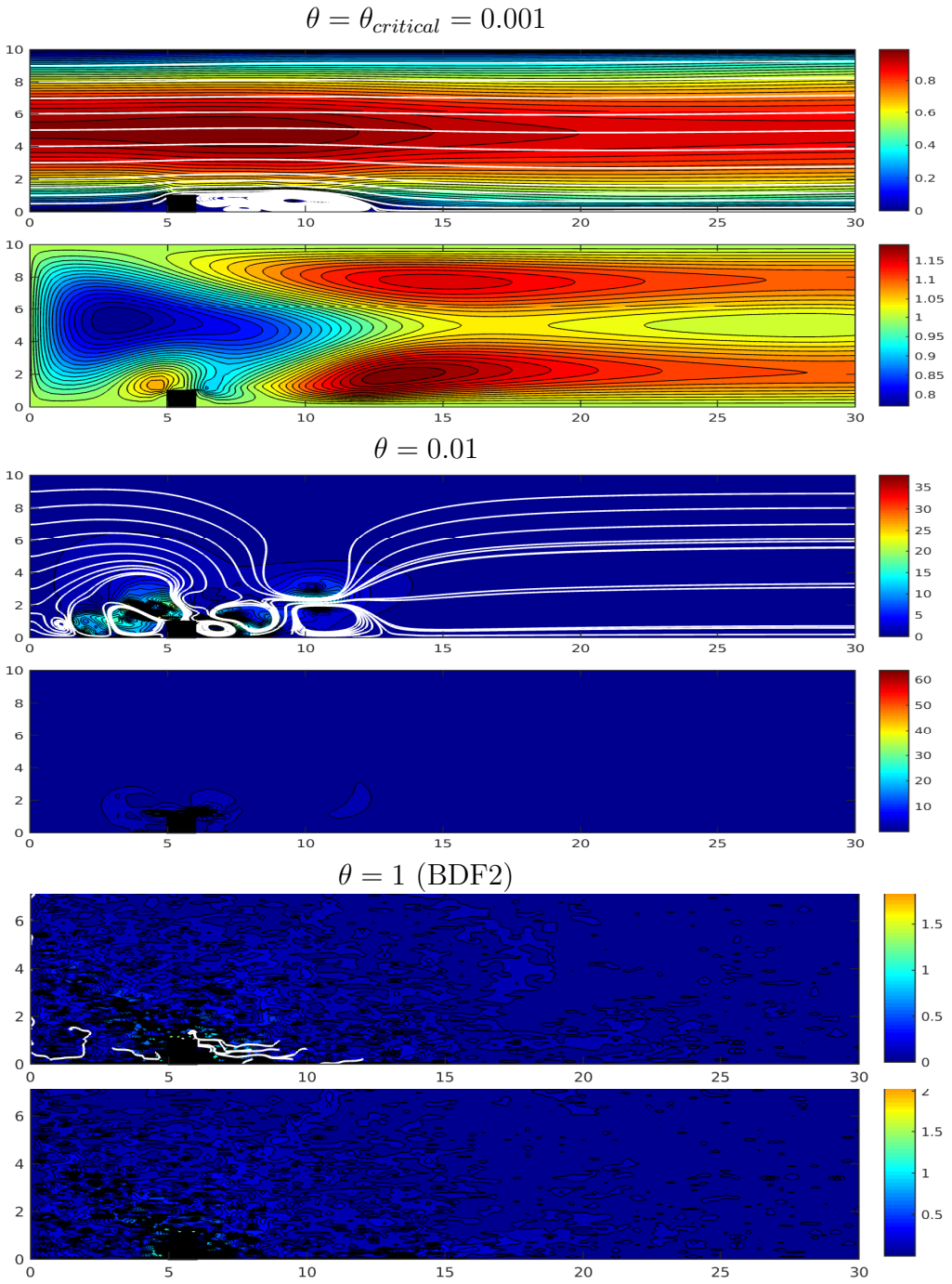

Figure 4.3: Velocity and magnetic field solutions at $T = 40$, for $s = 0.01$, $\nu = 0.001$ and $\nu_m = 1.0$, for varying θ. For $\theta = \theta_{critical}$, a stable and accurate solution is found, and unstable solutions are found for larger θ.

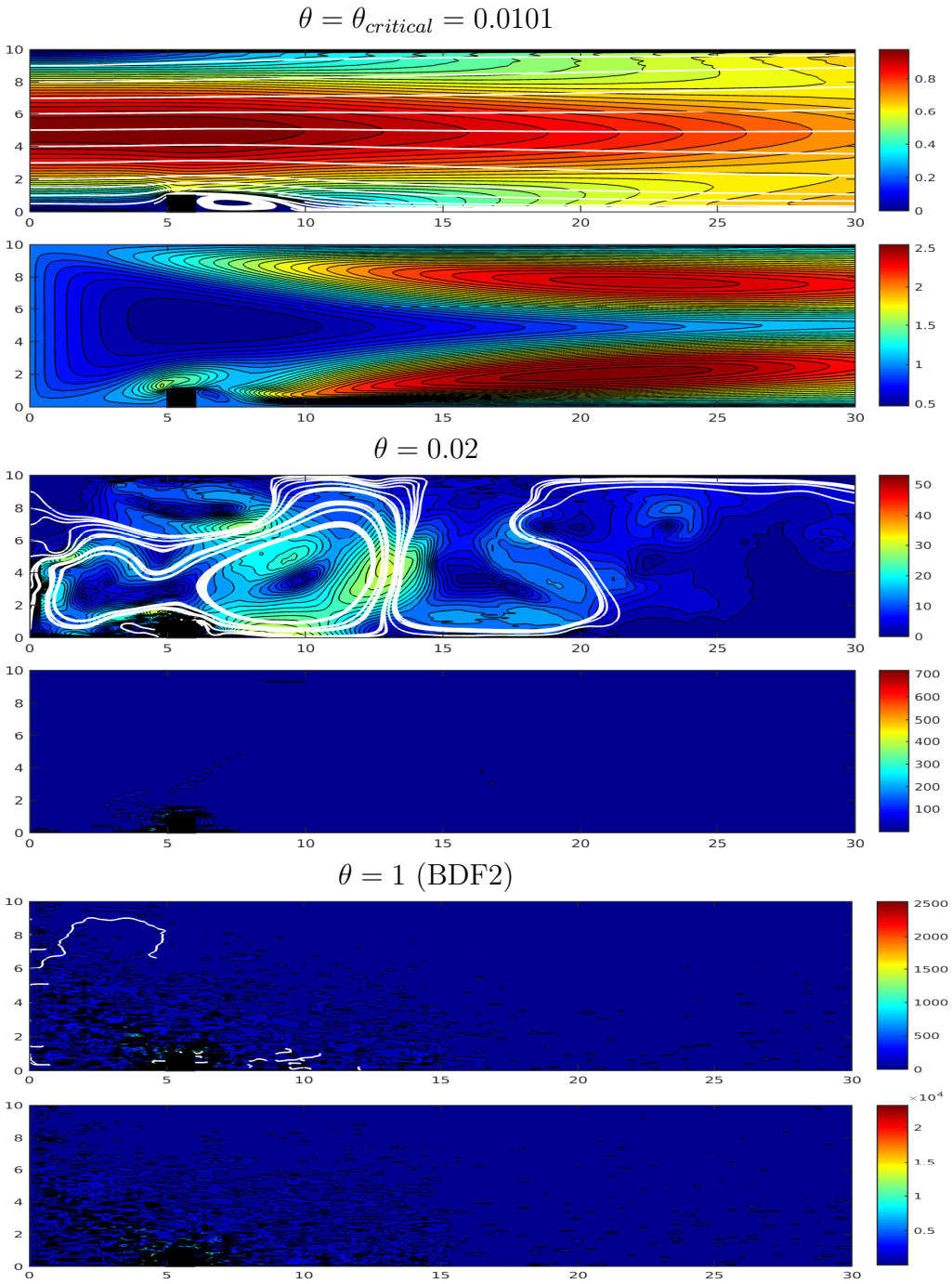

Figure 4.4: Velocity and magnetic field solutions at $T = 40$, for $s = 0.01$, $\nu = 0.001$ and $\nu_m = 0.1$, for varying θ. For $\theta = \theta_{critical}$, a stable and accurate solution is found, and unstable solutions are found for larger θ.

recent stabilization ideas such as that in [98], for more accurate large scale simulations that don't have sufficient resolution to fully resolve all active scales.

In numerical simulation uncertainties arise due to lack of data and inherent irregularity of the physical process involved. Uncertainties may be in initial and boundary conditions. We are interested to know the impact of uncertainties on the solutions. In the next chapter, we propose an efficient algorithm for computation of MHD flow ensembles. We prove its unconditional stability and convergence theorems, and tested it with benchmark problems.

Chapter 5

An Efficient Algorithm for Computation of MHD Flow Ensembles

5.1 Introduction

In the numerical simulation of MHD flows, uncertainties arise due to both the lack of data, and the inherent irregularity of the physical process involved [29, 33]. Uncertainty quantification (UQ) is the process of characterizing the impacts of uncertainty on the final quantities of interest, and in MHD flow simulations with incomplete data, UQ plays an important role in the validation of simulation methodologies and aims at developing rigorous methods to characterize the effect of the variability. A typical approach involves computing flow ensembles [22, 61, 62, 67, 71, 78], where J separate realizations of the problem are solved, and are then used to calculate means and sensitivities. This leads to J separate MHD systems needing solved, and denoting

solutions of realization j with u_j, B_j and p_j, the systems take the form, for j=1,2,...,J:

$$u_{j,t} + u_j \cdot \nabla u_j - sB_j \cdot \nabla B_j - \nu \Delta u_j + \nabla p_j = f_j(x,t), \text{ in } \Omega \times (0,T), \tag{5.1}$$

$$\nabla \cdot u_j = 0 \text{ in } \Omega, \tag{5.2}$$

$$u_j(x,0) = u_j^0(x) \text{ in } \Omega, \tag{5.3}$$

$$B_{j,t} + u_j \cdot \nabla B_j - B_j \cdot \nabla u_j - \nu_m \Delta B_j + \nabla \lambda_j = \nabla \times g_j(x,t) \text{ in } \Omega \times (0,T), \tag{5.4}$$

$$\nabla \cdot B_j = 0, \quad \text{in } \Omega, \tag{5.5}$$

$$B_j(x,0) = B_j^0(x) \text{ in } \Omega, \tag{5.6}$$

$$u_j = 0 \text{ on } \partial\Omega, \tag{5.7}$$

$$B_j = 0 \text{ on } \partial\Omega. \tag{5.8}$$

and for simplicity we equip both velocity and magnetic fields with homogeneous Dirichlet boundary conditions (our analysis and results will still hold, although with minor modifications, in the case of periodic boundary conditions or inhomogeneous Dirichlet boundary conditions).

In the recent works [6, 44, 73, 94], it was shown that algorithms based on the Elsässer variable formulation of MHD lead to more efficient algorithms, as they can be decoupled in a stable way so that two Oseen-type problems need solved at each time step, instead of a fully coupled linear system. Defining

$$v_j := u_j + \sqrt{s}B_j, \quad w_j := u_j - \sqrt{s}B_j,$$

$$f_{1,j} := f_j + \sqrt{s}\nabla \times g, \quad f_{2,j} := f_j - \sqrt{s}\nabla \times g,$$

$$q_j := p_j + \sqrt{s}\lambda_j; \quad r_j := p_j - \sqrt{s}\lambda_j$$

produces the Elsässer variable formulation of the J realizations:

$$v_{j,t} + w_j \cdot \nabla v_j + \nabla q_j - \frac{\nu + \nu_m}{2}\Delta v_j - \frac{\nu - \nu_m}{2}\Delta w_j = f_{1,j}, \tag{5.9}$$

$$w_{j,t} + v_j \cdot \nabla w_j + \nabla r_j - \frac{\nu + \nu_m}{2}\Delta w_j - \frac{\nu - \nu_m}{2}\Delta v_j = f_{2,j}, \tag{5.10}$$

$$\nabla \cdot v_j = \nabla \cdot w_j = 0, \tag{5.11}$$

together with initial and boundary conditions.

It is the purpose of this paper to develop and study efficient algorithms for computing (5.9)-(5.11), in particular for the purpose of efficiently computing ensemble averages of the J solutions. The key ideas we use follow in the same spirit as those used for Navier-Stokes simulations in [49,50,52,75], in particular we will create an algorithm which solves for all J solutions together, where the matrices that arise at each time step are the same for all J simulations. Thus, preconditioners need developed only once, and one may also take advantage of block solvers. This leads to a simulation far more efficient than computing J solutions independently, which takes the form (suppressing the spatial discretization):

Step 1: for j=1,...,J,

$$\frac{v_j^{n+1} - v_j^n}{\Delta t} + \nabla q_j^{n+1} - \frac{\nu + \nu_m}{2}\Delta v_j^{n+1} - \frac{\nu - \nu_m}{2}\Delta w_j^n + < w >^n \cdot \nabla v_j^{n+1}$$
$$+ (w_j^n - < w >^n) \cdot \nabla v_j^n - \nabla \cdot (2\nu_T(w', t^n)\nabla v_j^{n+1}) = f_{1,j}(t^{n+1}), \tag{5.12}$$

Step 2: for j=1,...,J,

$$\frac{w_j^{n+1} - w_j^n}{\Delta t} + \nabla r_j^{n+1} - \frac{\nu + \nu_m}{2}\Delta w_j^{n+1} - \frac{\nu - \nu_m}{2}\Delta v_j^n + < v >^n \cdot \nabla w_j^{n+1}$$
$$+ (v_j^n - < v >^n) \cdot \nabla w_j^n - \nabla \cdot (2\nu_T(v', t^n)\nabla w_j^{n+1}) = f_{2,j}(t^{n+1}). \tag{5.13}$$

Here the ensemble mean, fluctuation and its magnitude are denoted by $< v >$, $v_j^{'}$ and $|v^{'}|$, respectively, and defined as follows:
mean $< v >:= \frac{1}{J}\sum_{j=1}^{J} v_j$, fluctuation $v_j^{'} := v_j - < v >$ and magnitude $|v^{'}| := \sqrt{\sum_{j=1}^{J} |v_j^{'}|^2}$. The ν_T terms represent $O(\Delta t)$ eddy viscosity terms based on mixing lengths, and are included to provide stability for flows that are not resolvable on particular meshes, following ideas in [52]. The precise definitions for these terms are given in section 3. With these stabilization terms, we are able to prove unconditional (with respect to the time step size) stability of the algorithm, but without them, stability requires a time step restriction.

A key feature of the method above is that the MHD systems decouple into two Oseen problems, and further the matrices that arise at each time step are identical; only the right hand sides change at each time step. We will prove that the ensemble of the J computed solutions converges (as the spatial and temporal mesh width tend to zero) to the ensemble solution of the J MHD solutions. Numerical tests will be given that verify our theoretical results.

This chapter is arranged as follows. Section 2 presents and analyzes a fully discrete algorithm corresponding to (5.12)-(5.13), and proves it is stable and convergent. Numerical tests are presented in section 3, and finally conclusions are drawn in section 4.

5.2 Fully Discrete Scheme and Analysis of Ensemble Eddy Viscosity

We are now ready to present the fully discrete scheme for efficient MHD ensemble calculations. It equips (5.9)-(5.11) with a finite element spatial discretization. The

eddy viscosity term is defined using mixing length phenomenology, following [52], and is given by

$$\nu_T(u_h^{'}, t^n) := \mu \Delta t |u_h^{'n}|^2, \text{ where } |u_h^{'n}| = \max_j |u_{j,h}^{'n}| = \max_j |(u_{j,h}^n)^{'}|,$$

and μ is a tuning parameter. There are different ways to define the mixing length, and multiple definitions are studied in [52]. We chose this one due to its simplicity, and the fact that it leads to a stable and optimally convergent algorithm. The scheme is defined as follows.

Algorithm 5.2.1. *Given time step $\Delta t > 0$, end time $T > 0$, initial conditions $v_{j,h}^0,\ w_{j,h}^0 \in V_h$ and forcing terms $f_{1,j},\ f_{2,j} \in L^\infty(0,T;H^{-1}(\Omega)^d)$ for $j = 1, 2, \cdots, J$. Set $M = T/\Delta t$ and for $n = 1, \cdots, M-1$, compute:*

Find $v_{j,h}^{n+1} \in V_h$ satisfying, for all $\chi_h \in V_h$:

$$\begin{aligned}\Big(\frac{v_{j,h}^{n+1} - v_{j,h}^n}{\Delta t},\ \chi_h\Big) + \frac{\nu+\nu_m}{2}(\nabla v_{j,h}^{n+1}, \nabla \chi_h) + \frac{\nu-\nu_m}{2}(\nabla w_{j,h}^n, \nabla \chi_h) \\ + (< w_h >^n \cdot \nabla v_{j,h}^{n+1}, \chi_h) + ((w_{j,h}^n - < w_h >^n) \cdot \nabla v_{j,h}^n,\ \chi_h) \\ + (2\nu_T(w_h^{'}, t^n)\nabla v_{j,h}^{n+1},\ \nabla \chi_h) = (f_{1,j}(t^{n+1}),\ \chi_h),\end{aligned} \tag{5.14}$$

Find $w_{j,h}^{n+1} \in V_h$ satisfying, for all $l_h \in V_h$:

$$\begin{aligned}\Big(\frac{w_{j,h}^{n+1} - w_{j,h}^n}{\Delta t},\ l_h\Big) + \frac{\nu+\nu_m}{2}(\nabla w_{j,h}^{n+1}, \nabla l_h) + \frac{\nu-\nu_m}{2}(\nabla v_{j,h}^n, \nabla l_h) \\ + (< v_h >^n \cdot \nabla w_{j,h}^{n+1},\ l_h) + ((v_{j,h}^n - < v_h >^n) \cdot \nabla w_{j,h}^n,\ l_h) \\ + (2\nu_T(v_h^{'}, t^n)\nabla w_{j,h}^{n+1},\ \nabla l_h) = (f_{2,j}(t^{n+1}),\ l_h).\end{aligned} \tag{5.15}$$

Remark 5.2.1. *At each time step, all J realizations for step 1 will have the same matrix for the linear systems that arise, and similarly for step 2. Thus, block solvers can be taken advantage of, and matrices and preconditioners need built just once instead of J times. The key idea is a particular explicit treatment of part of the nonlinear term for each realization, and the stabilization term is used to stabilize this explicit treatment.*

Remark 5.2.2. *For simplicity of notation, the algorithm is presented in a V_h-formulation. While this is equivalent to an (X_h, Q_h) formulation and is more convenient for analysis (see e.g. [59]), implementation should be performed using the (X_h, Q_h) formulation since it is unknown how to efficiently construct a basis for V_h.*

We now prove that Algorithm 5.2.1 is unconditionally stable with respect to the time step size, provided $\mu \geq \frac{1}{2}$.

Theorem 4. *(Unconditional Stability) Suppose $f_{1,j}, f_{2,j} \in L^\infty(0,T;H^{-1}(\Omega))$, $v_{j,h}^0, w_{j,h}^0 \in H^1(\Omega)$, then for any $\Delta t > 0$ and $\mu \geq \frac{1}{2}$, solutions to (5.12)-(5.13) satisfy*

$$\begin{aligned}
&\|v_{j,h}^M\|^2 + \|w_{j,h}^M\|^2 + \frac{(\nu-\nu_m)^2}{2(\nu+\nu_m)}\Delta t\left(\|\nabla v_{j,h}^M\|^2 + \|\nabla w_{j,h}^M\|^2\right) \\
&\quad \leq \|v_{j,h}^0\|^2 + \|w_{j,h}^0\|^2 + \frac{(\nu-\nu_m)^2}{2(\nu+\nu_m)}\Delta t\left(\|\nabla v_{j,h}^0\|^2 + \|\nabla w_{j,h}^0\|^2\right) \\
&\quad + \frac{\nu+\nu_m}{2\nu\nu_m}\Delta t\sum_{n=0}^{M-1}\left(\|f_{1,j}(t^{n+1})\|_{-1}^2 + \|f_{2,j}(t^{n+1})\|_{-1}^2\right).
\end{aligned}$$

Proof. Choose $\chi_h = v_{j,h}^{n+1}$ in (5.14), the first nonlinear term vanishes and we obtain

$$\begin{aligned}
&\frac{1}{\Delta t}(v_{j,h}^{n+1} - v_{j,h}^n, v_{j,h}^{n+1}) + \frac{\nu+\nu_m}{2}\left(\nabla v_{j,h}^{n+1}, \nabla v_{j,h}^{n+1}\right) \\
&\quad + \frac{\nu-\nu_m}{2}\left(\nabla w_{j,h}^n, \nabla v_{j,h}^{n+1}\right) + \left((w_{j,h}^n - < w_h >^n)\cdot\nabla v_{j,h}^n, v_{j,h}^{n+1}\right) \\
&\quad + \left(2\nu_T(w_h', t^n)\nabla v_{j,h}^{n+1}, \nabla v_{j,h}^{n+1}\right) = \left(f_{1,j}(t^{n+1}), v_{j,h}^{n+1}\right). \qquad (5.16)
\end{aligned}$$

Using the polarization identity and that

$$\left(2\nu_T(w_h^{'}, t^n)\nabla v_{j,h}^{n+1}, \nabla v_{j,h}^{n+1}\right) = 2\mu\Delta t\| \, |w_h^{'n}| \, |\nabla v_{j,h}^{n+1}| \, \|^2,$$

we get

$$\begin{aligned}\frac{1}{2\Delta t}\left(\|v_{j,h}^{n+1} - v_{j,h}^n\|^2 + \|v_{j,h}^{n+1}\|^2 - \|v_{j,h}^n\|^2\right) + \frac{\nu+\nu_m}{2}\|\nabla v_{j,h}^{n+1}\|^2 \\ + \frac{\nu-\nu_m}{2}\left(\nabla w_{j,h}^n, \nabla v_{j,h}^{n+1}\right) + \left((w_{j,h}^n - < w_h >^n)\cdot\nabla v_{j,h}^n, v_{j,h}^{n+1}\right) \\ + 2\mu\Delta t\|\,|w_h^{'n}| \, |\nabla v_{j,h}^{n+1}|\,\|^2 = \left(f_{1,j}(t^{n+1}), v_{j,h}^{n+1}\right). \end{aligned} \tag{5.17}$$

Similarly, choose $l_h = w_{j,h}^{n+1}$ in (5.15), we have

$$\begin{aligned}\frac{1}{2\Delta t}\left(\|w_{j,h}^{n+1} - w_{j,h}^n\|^2 + \|w_{j,h}^{n+1}\|^2 - \|w_{j,h}^n\|^2\right) + \frac{\nu+\nu_m}{2}\|\nabla w_{j,h}^{n+1}\|^2 \\ + \frac{\nu-\nu_m}{2}\left(\nabla v_{j,h}^n, \nabla w_{j,h}^{n+1}\right) + \left((v_{j,h}^n - < v_h >^n)\cdot\nabla w_{j,h}^n, w_{j,h}^{n+1}\right) \\ + 2\mu\Delta t\|\,|v_h^{'n}| \, |\nabla w_{j,h}^{n+1}|\,\|^2 = \left(f_{2,j}(t^{n+1}), w_{j,h}^{n+1}\right). \end{aligned} \tag{5.18}$$

Adding equations (5.17) and (5.18) yields

$$\begin{aligned}\frac{1}{2\Delta t}\Big(\|v_{j,h}^{n+1} - v_{j,h}^n\|^2 + \|v_{j,h}^{n+1}\|^2 - \|v_{j,h}^n\|^2 + \|w_{j,h}^{n+1} - w_{j,h}^n\|^2 \\ + \|w_{j,h}^{n+1}\|^2 - \|w_{j,h}^n\|^2\Big) + \frac{\nu+\nu_m}{2}\left(\|\nabla v_{j,h}^{n+1}\|^2 + \|\nabla w_{j,h}^{n+1}\|^2\right) \\ + \frac{\nu-\nu_m}{2}\left\{\left(\nabla w_{j,h}^n, \nabla v_{j,h}^{n+1}\right) + \left(\nabla v_{j,h}^n, \nabla w_{j,h}^{n+1}\right)\right\} \\ + \left((w_{j,h}^n - < w_h >^n)\cdot\nabla v_{j,h}^n, v_{j,h}^{n+1}\right) + \left((v_{j,h}^n - < v_h >^n)\cdot\nabla w_{j,h}^n, w_{j,h}^{n+1}\right) \\ + 2\mu\Delta t\|\,|w_h^{'n}| \, |\nabla v_{j,h}^{n+1}|\,\|^2 + 2\mu\Delta t\|\,|v_h^{'n}| \, |\nabla w_{j,h}^{n+1}|\,\|^2 \\ = \left(f_{1,j}(t^{n+1}), v_{j,h}^{n+1}\right) + \left(f_{2,j}(t^{n+1}), w_{j,h}^{n+1}\right). \end{aligned} \tag{5.19}$$

Next, using

$$\begin{aligned}\Big((w_{j,h}^n - < w_h >^n)\cdot\nabla v_{j,h}^n, v_{j,h}^{n+1}\Big) &= -\big((w_{j,h}^n - < w_h >^n)\cdot\nabla v_{j,h}^{n+1}, v_{j,h}^n\big)\\ &= \big((w_{j,h}^n - < w_h >^n)\cdot\nabla v_{j,h}^{n+1}, v_{j,h}^{n+1} - v_{j,h}^n\big)\\ &\le \|(w_{j,h}^n - < w_h >^n)\cdot\nabla v_{j,h}^{n+1}\|\,\|v_{j,h}^{n+1} - v_{j,h}^n\|\\ &\le \|\,|w_{j,h}^{'n}|\,|\nabla v_{j,h}^{n+1}|\|\,\|v_{j,h}^{n+1} - v_{j,h}^n\|\\ &\le \|\,|w_h^{'n}|\,|\nabla v_{j,h}^{n+1}|\|\,\|v_{j,h}^{n+1} - v_{j,h}^n\|\end{aligned}$$

with Cauchy-Schwarz and Young's, we reduce (5.19) to

$$\begin{aligned}\frac{1}{2\Delta t}\Big(&\|v_{j,h}^{n+1} - v_{j,h}^n\|^2 + \|v_{j,h}^{n+1}\|^2 - \|v_{j,h}^n\|^2 + \|w_{j,h}^{n+1} - w_{j,h}^n\|^2\\ &+ \|w_{j,h}^{n+1}\|^2 - \|w_{j,h}^n\|^2\Big) + \frac{\nu+\nu_m}{2}\left(\|\nabla v_{j,h}^{n+1}\|^2 + \|\nabla w_{j,h}^{n+1}\|^2\right)\\ &+ 2\mu\Delta t\||w_h^{'n}|\,|\nabla v_{j,h}^{n+1}|\|^2 + 2\mu\Delta t\||v_h^{'n}|\,|\nabla w_{j,h}^{n+1}|\|^2\\ &\le \frac{\nu+\nu_m}{4}\left(\|\nabla w_{j,h}^{n+1}\|^2 + \|\nabla v_{j,h}^{n+1}\|^2\right) + \frac{(\nu-\nu_m)^2}{4(\nu+\nu_m)}\left(\|\nabla v_{j,h}^n\|^2 + \|\nabla w_{j,h}^n\|^2\right)\\ &+ \|f_{1,j}(t^{n+1})\|_{-1}\|\nabla v_{j,h}^{n+1}\| + \|f_{2,j}(t^{n+1})\|_{-1}\|\nabla w_{j,h}^{n+1}\|\\ &+ \||w_h^{'n}|\,|\nabla v_{j,h}^{n+1}|\,\|\|v_{j,h}^{n+1} - v_{j,h}^n\| + \||v_h^{'n}|\,|\nabla w_{j,h}^{n+1}|\,\|\|w_{j,h}^{n+1} - w_{j,h}^n\|.\end{aligned}$$

After using Young's inequality again on the last two terms, we are able to hide these terms that arise from the explicit treatment of part of the nonlinearity in the positive

stabilization terms on the left hand side:

$$\begin{aligned}
&\frac{1}{4\Delta t}\left(\|v_{j,h}^{n+1}-v_{j,h}^{n}\|^2+\|w_{j,h}^{n+1}-w_{j,h}^{n}\|^2\right)\\
&\quad+\frac{1}{2\Delta t}\left(\|v_{j,h}^{n+1}\|^2-\|v_{j,h}^{n}\|^2+\|w_{j,h}^{n+1}\|^2-\|w_{j,h}^{n}\|^2\right)\\
&\quad+\frac{\nu+\nu_m}{4}\left(\|\nabla v_{j,h}^{n+1}\|^2+\|\nabla w_{j,h}^{n+1}\|^2\right)\\
&\quad+(2\mu-1)\Delta t\left(\||w_h^{'n}|\,|\nabla v_h^{n+1}|\|^2+\||v_{j,h}^{'n}|\,|\nabla w_{j,h}^{n+1}|\|^2\right)\\
&\quad\le\frac{(\nu-\nu_m)^2}{4(\nu+\nu_m)}\left(\|\nabla v_{j,h}^{n}\|^2+\|\nabla w_{j,h}^{n}\|^2\right)\\
&\quad+\|f_{1,j}(t^{n+1})\|_{-1}\|\nabla v_{j,h}^{n+1}\|+\|f_{2,j}(t^{n+1})\|_{-1}\|\nabla w_{j,h}^{n+1}\|.
\end{aligned}$$

Dropping the non-negative terms $\|v_{j,h}^{n+1}-v_{j,h}^{n}\|^2$ and $\|w_{j,h}^{n+1}-w_{j,h}^{n}\|^2$, and using Young's inequality, we get

$$\begin{aligned}
&\frac{1}{2\Delta t}\left(\|v_{j,h}^{n+1}\|^2-\|v_{j,h}^{n}\|^2+\|w_{j,h}^{n+1}\|^2-\|w_{j,h}^{n}\|^2\right)\\
&\quad+(2\mu-1)\Delta t\left(\||w_h^{'n}|\,|\nabla v_{j,h}^{n+1}|\|^2+\||v_h^{'n}|\,|\nabla w_{j,h}^{n+1}|\|^2\right)\\
&\quad+\frac{(\nu-\nu_m)^2}{4(\nu+\nu_m)}\left(\|\nabla v_{j,h}^{n+1}\|^2-\|\nabla v_{j,h}^{n}\|^2+\|\nabla w_{j,h}^{n+1}\|^2-\|\nabla w_{j,h}^{n}\|^2\right)\\
&\quad\le\frac{\nu+\nu_m}{4\nu\nu_m}\left(\|f_{1,j}(t^{n+1})\|_{-1}^2+\|f_{2,j}(t^{n+1})\|_{-1}^2\right). \qquad (5.20)
\end{aligned}$$

The term $(2\mu-1)\Delta t\left(\||w_h^{'n}|\,|\nabla v_j^{n+1}|\|^2+\||v_h^{'n}|\,|\nabla w_j^{n+1}|\|^2\right)$ can have two signs. To make it non-negative, we choose $\mu\ge\frac{1}{2}$, and then drop term it. Next, multiply the

both sides by $2\Delta t$ and sum over time steps:

$$\begin{aligned}\|v_{j,h}^M\|^2 + \|w_{j,h}^M\|^2 + \frac{(\nu-\nu_m)^2}{2(\nu+\nu_m)}\Delta t\left(\|\nabla v_{j,h}^M\|^2 + \|\nabla w_{j,h}^M\|^2\right)\\ \leq \|v_{j,h}^0\|^2 + \|w_{j,h}^0\|^2 + \frac{(\nu-\nu_m)^2}{2(\nu+\nu_m)}\Delta t\left(\|\nabla v_{j,h}^0\|^2 + \|\nabla w_{j,h}^0\|^2\right)\\ + \frac{\nu+\nu_m}{2\nu\nu_m}\Delta t\sum_{n=0}^{M-1}\left(\|f_{1,j}(t^{n+1})\|_{-1}^2 + \|f_{2,j}(t^{n+1})\|_{-1}^2\right). \qquad (5.21)\end{aligned}$$

This finishes the proof. □

Corollary 1. *Let* $F_1 = \max_j \|f_{1,j}\|_{L^\infty(0,\infty,H^{-1}(\Omega))}$, $F_2 = \max_j \|f_{2,j}\|_{L^\infty(0,\infty,H^{-1}(\Omega))}$ *and suppose* $F_1, F_2 \leq K$. *Then if* $\mu \geq \frac{1}{2}$, *solution of Algorithm* (5.2.1) *are long-time stable:* $\exists C < \infty \ni \forall n \in \mathbb{Z}^+,\ 1 \leq j \leq J$,

$$\|v_j^n\| + \|w_j^n\| \leq C,$$

independent of Δt.

Another eddy viscosity term is defined in the appendix and we proved the conditional stability for the solution of Algorithm (5.2.1) with respect to the time step size. We will now give a full error analysis of the proposed algorithm which converges in space and in time, provided sufficient smoothness of the true solutions.

Theorem 5. *For* (v_j, w_j, q_j, r_j) *satisfying* (5.9)-(5.11) *and regularity assumptions for* $m = \max\{3, k+1\}$, $v_j, w_j \in L^\infty(0,T;H^m(\Omega)^d)$, $v_{j,t}, w_{j,t} \in L^\infty(0,T;H^2(\Omega)^d)$, *and* $v_{j,tt}, w_{j,tt} \in L^\infty(0,T;L^2(\Omega)^d)$, *the ensemble solution* $(< v_h >, < w_h >)$ *to the Algorithm* (5.2.1) *unconditionally converges to the true ensemble solution : for any* $\Delta t > 0$

and $\mu > \frac{1}{2}$*:*

$$\begin{aligned}
&\| < v > (T) - < v_h >^M \|^2 + \| < w > (T) - < w_h >^M \|^2 \\
&\quad + \frac{3\alpha}{4}\Delta t \sum_{j=1}^{J}\sum_{n=1}^{M} \left(\|\nabla(< v > (t^n) - < v_h >^n)\|^2 + \|\nabla(< w > (t^n) - < w_h >^n)\|^2 \right) \\
&\qquad\qquad \leq C e^{\frac{CT(1+\Delta t^2)}{\alpha}} (h^{2k} + h^{2k-1}\Delta t + \Delta t^2(1 + h^{2-d}) + h^{2k}\Delta t^2). \quad (5.22)
\end{aligned}$$

where $\alpha := \nu + \nu_m - |\nu - \nu_m|$.

Remark 5.2.3. *In 3D, this result predicts the temporal convergence rate could be reduced to* $O((\Delta t(1 + h^{-1/2}))$*, which is less than the optimal rate of* $O(\Delta t)$*. This reduction in error comes from the use of the inverse inequality in the analysis of the stabilization term. This can be improved to* $O(\Delta t)$ *by removing the stabilization term, but that will in turn cause a time step restriction for stability and convergence results.*

Proof. We begin by obtaining error equations. Testing (5.9) and (5.10) with $\chi_h, l_h \in V_h$ at $t = t^{n+1}$ yields

$$\begin{aligned}
&\frac{1}{\Delta t}\big(v_j(t^{n+1}) - v_j(t^n), \chi_h\big) + \big(w_j(t^{n+1}) \cdot \nabla v_j(t^{n+1}), \chi_h\big) + \frac{\nu + \nu_m}{2}\left(\nabla v_j(t^{n+1}), \nabla \chi_h\right) \\
&\quad + \frac{\nu - \nu_m}{2}(\nabla w_j(t^n), \nabla \chi_h) = -\left(v_{j,t}(t^{n+1}) - \frac{v_j(t^{n+1}) - v_j(t^n)}{\Delta t}, \chi_h\right) \\
&\quad - \frac{\nu - \nu_m}{2}\big(\nabla w_j(t^{n+1}) - \nabla w_j(t^n), \nabla \chi_h\big) + (f_{1,j}(t^{n+1}), \chi_h), \qquad (5.23)
\end{aligned}$$

and

$$\begin{aligned}
&\frac{1}{\Delta t}(w_j(t^{n+1}) - w_j(t^n), l_h) + (v_j(t^{n+1}) \cdot \nabla w_j(t^{n+1}), l_h) + \frac{\nu + \nu_m}{2}\left(\nabla w_j(t^{n+1}), \nabla l_h\right) \\
&\quad + \frac{\nu - \nu_m}{2}(\nabla v_j(t^n), \nabla l_h) = -\left(w_{j,t}(t^{n+1}) - \frac{w_j(t^{n+1}) - w_j(t^n)}{\Delta t}, l_h\right) \\
&\quad - \frac{\nu - \nu_m}{2}(\nabla v_j(t^{n+1}) - \nabla v_j(t^n), \nabla l_h) + (f_{2,j}(t^{n+1}), l_h). \qquad (5.24)
\end{aligned}$$

Denote $e^n_{j,v} := v_j(t^n) - v^n_{h,j}$, $e^n_{j,w} := w_j(t^n) - w^n_{h,j}$, $< e_v >^n := \frac{1}{J}\sum_{j=1}^{J} e^n_{j,v}$ and $< e_w >^n := \frac{1}{J}\sum_{j=1}^{J} e^n_{j,w}$. Subtracting (5.14) and (5.15) from (5.23) and (5.24), respectively, produces

$$\begin{aligned}
&\frac{1}{\Delta t}(e^{n+1}_{v,j} - e^n_{v,j}, \chi_h) + (< e_w >^n \cdot\nabla(v_j(t^{n+1}) - v_j(t^n)), \chi_h) \\
&\quad + (< w_h >^n \cdot\nabla e^{n+1}_{v,j}, \chi_h) + \frac{\nu+\nu_m}{2}(\nabla e^{n+1}_{v,j}, \nabla\chi_h) + \frac{\nu-\nu_m}{2}(\nabla e^n_{w,j}, \nabla\chi_h) \\
&\quad + \left(w'^n_{j,h} \cdot \nabla e^n_{v,j}, \chi_h\right) + 2\mu\Delta t\left(|w'^n_h|^2\nabla e^{n+1}_{v,j}, \nabla\chi_h\right) + \left(e^n_{w,j} \cdot \nabla v_j(t^n), \chi_h\right) \\
&\quad - 2\mu\Delta t\left(|w'^n_h|^2\nabla v_j(t^{n+1}), \nabla\chi_h\right) = -G_1(t, v_j, w_j, \chi_h), \qquad (5.25)
\end{aligned}$$

and

$$\begin{aligned}
&\frac{1}{\Delta t}(e^{n+1}_{w,j} - e^n_{w,j}, l_h) + (< e_v >^n \cdot\nabla(w_j(t^{n+1}) - w_j(t^n)), l_h) \\
&\quad + (< v_h >^n \cdot\nabla e^{n+1}_{w,j}, l_h) + \frac{\nu+\nu_m}{2}(\nabla e^{n+1}_{w,j}, \nabla l_h) + \frac{\nu-\nu_m}{2}(\nabla e^n_{v,j}, \nabla l_h) \\
&\quad + \left(v'^n_{j,h} \cdot \nabla e^n_{w,j}, l_h\right) + 2\mu\Delta t\left(|v'^n_h|^2\nabla e^{n+1}_{w,j}, \nabla l_h\right) + \left(e^n_{v,j} \cdot \nabla w_j(t^n), l_h\right) \\
&\quad - 2\mu\Delta t\left(|v'^n_h|^2\nabla w_j(t^{n+1}), \nabla l_h\right) = -G_2(t, v_j, w_j, l_h), \qquad (5.26)
\end{aligned}$$

where

$$\begin{aligned}
G_1(t, v_j, w_j, \chi_h) &= \left(v_{j,t}(t^{n+1}) - \frac{v_j(t^{n+1}) - v_j(t^n)}{\Delta t}, \chi_h\right) \\
&+ \frac{\nu-\nu_m}{2}(\nabla w_j(t^{n+1}) - \nabla w_j(t^n), \nabla\chi_h) + \left((w_j(t^{n+1}) - w_j(t^n)) \cdot \nabla v_j(t^{n+1}), \chi_h\right) \\
&\quad + \left((w_j(t^n) - < w(t^n) >) \cdot \nabla(v_j(t^{n+1}) - v_j(t^n)), \chi_h\right) \qquad (5.27)
\end{aligned}$$

and

$$G_2(t, v_j, w_j, l_h) = \left(w_{j,t}(t^{n+1}) - \frac{w_j(t^{n+1}) - w_j(t^n)}{\Delta t}, l_h\right)$$
$$+ \frac{\nu - \nu_m}{2}\big(\nabla v_j(t^{n+1}) - \nabla v_j(t^n), \nabla l_h\big) + \left((v_j(t^{n+1}) - v_j(t^n)) \cdot \nabla w_j(t^{n+1}), l_h\right)$$
$$+ \big((v_j(t^n) - < v(t^n) >) \cdot \nabla (w_j(t^{n+1}) - w_j(t^n)), l_h\big). \quad (5.28)$$

Now we decompose the errors as

$$e^n_{v,j} := v_j(t^n) - v^n_{j,h} = (v_j(t^n) - \tilde{v_j}^n) - (v^n_{j,h} - \tilde{v_j}^n) := \eta^n_{v,j} - \phi^n_{j,h},$$
$$e^n_{w,j} := w_j(t^n) - w^n_{j,h} = (w_j(t^n) - \tilde{w_j}^n) - (w^n_{j,h} - \tilde{w_j}^n) := \eta^n_{w,j} - \psi^n_{j,h},$$

where $\tilde{v_j}^n = P^{L^2}_{V_h}(v_j(t^n)) \in V_h$ and $\tilde{w_j}^n = P^{L^2}_{V_h}(w_j(t^n)) \in V_h$ are the L^2 projections of $v_j(t^n)$ and $w_j(t^n)$ into V_h respectively. Note that $(\eta^n_{v,j}, v_h) = 0 \ \forall v_h \in V_h$ and $(\eta^n_{w_j}, v_h) = 0 \ \forall v_h \in V_h$. Rewriting, we have for χ_h, $l_h \in V_h$,

$$\frac{1}{\Delta t}\big(\phi^{n+1}_{j,h} - \phi^n_{j,h}, \chi_h\big) + \big(< \psi_h >^n \cdot \nabla (v_j(t^{n+1}) - v_j(t^n)), \chi_h\big)$$
$$+ \big(< w_h >^n \cdot \nabla \phi^{n+1}_{j,h}, \chi_h\big) + \frac{\nu + \nu_m}{2}\left(\nabla \phi^{n+1}_{j,h}, \nabla \chi_h\right) + \frac{\nu - \nu_m}{2}\left(\nabla \psi^n_{j,h}, \nabla \chi_h\right)$$
$$+ \left(w'^n_{j,h} \cdot \nabla \phi^n_{j,h}, \chi_h\right) + \big(\psi^n_{j,h} \cdot \nabla v_j(t^n), \chi_h\big) + 2\mu \Delta t \left(|w'^n_h|^2 \nabla \phi^{n+1}_{j,h}, \nabla \chi_h\right)$$
$$= \frac{\nu - \nu_m}{2}\left(\nabla \eta^n_{w,j}, \nabla \chi_h\right) + \big(< w_h >^n \cdot \nabla \eta^{n+1}_{v,j}, \chi_h\big) + \frac{\nu + \nu_m}{2}\left(\nabla \eta^{n+1}_{v,j}, \nabla \chi_h\right)$$
$$+ \left(w'^n_{j,h} \cdot \nabla \eta^n_{v,j}, \chi_h\right) + \big(< \eta_w >^n \cdot \nabla (v_j(t^{n+1}) - v_j(t^n)), \chi_h\big)$$
$$+ \big(\eta^n_{w,j} \cdot \nabla v_j(t^n), \chi_h\big) + 2\mu \Delta t \left(|w'^n_h|^2 \nabla \eta^{n+1}_{v,j}, \nabla \chi_h\right)$$
$$+ 2\mu \Delta t | \left(|w'^n_h|^2 \nabla v_j(t^{n+1}), \nabla \chi_h\right) | + |G_1(t, v_j, w_j, \chi_h)|, \quad (5.29)$$

and

$$\begin{aligned}
&\frac{1}{\Delta t}\big(\psi_{j,h}^{n+1}-\psi_{j,h}^{n},l_h\big)+\big(<\phi_h>^n\cdot\nabla(w_j(t^{n+1})-w_j(t^n)),l_h\big)\\
&+\big(<v_h>^n\cdot\nabla\psi_{j,h}^{n+1},l_h\big)+\frac{\nu+\nu_m}{2}\left(\nabla\psi_{j,h}^{n+1},\nabla l_h\right)+\frac{\nu-\nu_m}{2}\left(\nabla\phi_{j,h}^{n},\nabla l_h\right)\\
&+\left(v_{j,h}^{'n}\cdot\nabla\psi_{j,h}^{n},l_h\right)+\big((\phi_{j,h}^{n}-<\phi_h>^n)\cdot\nabla w_j(t^n),l_h\big)+2\mu\Delta t\left(|v_h^{'n}|^2\nabla\psi_{j,h}^{n+1},\nabla l_h\right)\\
&=\big(<\eta_v>^n\cdot\nabla(w_j(t^{n+1})-w_j(t^n)),l_h\big)+\big(<v_h>^n\cdot\nabla\eta_{w,j}^{n+1},l_h\big)\\
&+\frac{\nu+\nu_m}{2}\left(\nabla\eta_{w,j}^{n+1},\nabla l_h\right)+\frac{\nu-\nu_m}{2}\left(\nabla\eta_{v,j}^{n},\nabla l_h\right)+\left(v_{j,h}^{'n}\cdot\nabla\eta_{w,j}^{n},l_h\right)\\
&+\big(\eta_{v,j}^{n}\cdot\nabla w_j(t^n),l_h\big)+2\mu\Delta t\left(|v_h^{'n}|^2\nabla\eta_{w,j}^{n+1},\nabla l_h\right)\\
&+2\mu\Delta t|\left(|v_h^{'n}|^2\nabla w_j(t^{n+1}),\nabla l_h\right)|+|G_2(t,v_j,w_j,l_h)|. \qquad (5.30)
\end{aligned}$$

Choose $\chi_h=\phi_{j,h}^{n+1}$, $l_h=\psi_{j,h}^{n+1}$ and use the polarization identity in (5.29) and (5.30), to obtain

$$\begin{aligned}
&\frac{1}{2\Delta t}\big(\|\phi_{j,h}^{n+1}\|^2-\|\phi_{j,h}^{n}\|^2+\|\phi_{j,h}^{n+1}-\phi_{j,h}^{n}\|^2\big)+\frac{\nu+\nu_m}{2}\|\nabla\phi_{j,h}^{n+1}\|^2\\
&+2\mu\Delta t\|\,|w_h^{'n}|\,|\nabla\phi_{j,h}^{n+1}|\,\|^2\le\frac{|\nu-\nu_m|}{2}|\left(\nabla\psi_{j,h}^{n},\nabla\phi_{j,h}^{n+1}\right)|\\
&+\frac{\nu+\nu_m}{2}|\left(\nabla\eta_{v,j}^{n+1},\nabla\phi_{j,h}^{n+1}\right)|+\frac{|\nu-\nu_m|}{2}|\left(\nabla\eta_{w,j}^{n},\nabla\phi_{j,h}^{n+1}\right)|\\
&+2\mu\Delta t|\left(|w_h^{'n}|^2\nabla\eta_{v,j}^{n+1},\nabla\phi_{j,h}^{n+1}\right)|+2\mu\Delta t|\left(|w_h^{'n}|^2\nabla v_j(t^{n+1}),\nabla\phi_{j,h}^{n+1}\right)|\\
&+|\left(<\psi_h>^n\cdot\nabla(v_j(t^{n+1})-v_j(t^n)),\phi_{j,h}^{n+1}\right)|+|\left(\psi_{j,h}^{n}\cdot\nabla v_j(t^n),\phi_{j,h}^{n+1}\right)|\\
&+|\left(w_{j,h}^{'n}\cdot\nabla\phi_{j,h}^{n},\phi_{j,h}^{n+1}\right)|+|\left(<\eta_w>^n\cdot\nabla(v_j(t^{n+1})-v_j(t^n)),\phi_{j,h}^{n+1}\right)|\\
&+|\left(<w_h>^n\cdot\nabla\eta_{v,j}^{n+1},\phi_{j,h}^{n+1}\right)|+|\left(w_{j,h}^{'n}\cdot\nabla\eta_{v,j}^{n},\phi_{j,h}^{n+1}\right)|\\
&+|\left(\eta_{w,j}^{n}\cdot\nabla v_j(t^n),\phi_{j,h}^{n+1}\right)|+|G_1(t,v_j,w_j,\phi_{j,h}^{n+1})|, \qquad (5.31)
\end{aligned}$$

and

$$\frac{1}{2\Delta t}\left(\|\psi_{j,h}^{n+1}\|^2-\|\psi_{j,h}^{n}\|^2+\|\psi_{j,h}^{n+1}-\psi_{j,h}^{n}\|^2\right)+\frac{\nu+\nu_m}{2}\|\nabla\psi_{j,h}^{n+1}\|^2$$
$$+2\mu\Delta t\|\,|v_h^{'n}|\,|\nabla\psi_{j,h}^{n+1}|\,\|^2\le\frac{|\nu-\nu_m|}{2}|\left(\nabla\phi_{j,h}^{n},\nabla\psi_{j,h}^{n+1}\right)|+\frac{\nu+\nu_m}{2}|\left(\nabla\eta_{w,j}^{n+1},\nabla\psi_{j,h}^{n+1}\right)|$$
$$+\frac{|\nu-\nu_m|}{2}|\left(\nabla\eta_{v,j}^{n},\nabla\psi_{j,h}^{n+1}\right)|+2\mu\Delta t|\left(|v_h^{'n}|^2\nabla\eta_{w,j}^{n+1},\nabla\psi_{j,h}^{n+1}\right)|$$
$$+2\mu\Delta t|\left(|v_h^{'n}|^2\nabla w_j(t^{n+1}),\nabla\psi_{j,h}^{n+1}\right)|+|\left(<\phi_h>^n\cdot\nabla(w_j(t^{n+1})-w_j(t^n)),\psi_{j,h}^{n+1}\right)|$$
$$+|\left(\phi_{j,h}^{n}\cdot\nabla w_j(t^n),\psi_{j,h}^{n+1}\right)|+|\left(v_{j,h}^{'n}\cdot\nabla\psi_{j,h}^{n},\psi_{j,h}^{n+1}\right)|+|\left(<v_h>^n\cdot\nabla\eta_{w,j}^{n+1},\psi_{j,h}^{n+1}\right)|$$
$$+|\left(<\eta_v>^n\cdot\nabla(w_j(t^{n+1})-w_j(t^n)),\psi_{j,h}^{n+1}\right)|+|\left(v_{j,h}^{'n}\cdot\nabla\eta_{w,j}^{n},\psi_{j,h}^{n+1}\right)|$$
$$+|\left(\eta_{v,j}^{n}\cdot\nabla w_j(t^n),\psi_{j,h}^{n+1}\right)|+|G_2(t,v_j,w_j,\psi_{j,h}^{n+1})|. \tag{5.32}$$

Define $\alpha:=\nu+\nu_m-|\nu-\nu_m|>0$, assume $\mu>\frac{1}{2}$ and turn our attention to finding bounds on the right side terms of(5.31) (the estimates for (5.32) are similar). Applying Cauchy-Schwarz and Young's inequalities on the first three terms results in

$$\frac{|\nu-\nu_m|}{2}|\left(\nabla\psi_{j,h}^{n},\nabla\phi_{j,h}^{n+1}\right)|\le\frac{|\nu-\nu_m|}{4}\|\nabla\phi_{j,h}^{n+1}\|^2+\frac{|\nu-\nu_m|}{4}\|\nabla\psi_{j,h}^{n}\|^2$$
$$\frac{\nu+\nu_m}{2}|\left(\nabla\eta_{v,j}^{n+1},\nabla\phi_{j,h}^{n+1}\right)|\le\frac{\alpha}{32}\|\nabla\phi_{j,h}^{n+1}\|^2+\frac{6(\nu+\nu_m)^2}{\alpha}\|\nabla\eta_{v,j}^{n+1}\|^2$$
$$\frac{|\nu-\nu_m|}{2}|\left(\nabla\eta_{w,j}^{n},\nabla\phi_{j,h}^{n+1}\right)|\le\frac{\alpha}{32}\|\nabla\phi_{j,h}^{n+1}\|^2+\frac{6(\nu-\nu_m)^2}{\alpha}\|\nabla\eta_{w,j}^{n}\|^2.$$

The fourth and fifth right hand side terms of (5.31) are less standard. For the fourth term, we apply Cauchy-Schwarz and Young's inequalities to obtain

$$2\mu\Delta t|\left(|w_h^{'n}|^2\nabla\eta_{v,j}^{n+1},\nabla\phi_{j,h}^{n+1}\right)|=2\mu\Delta t\left(|w_h^{'n}|\nabla\eta_{v,j}^{n+1},|w_h^{'n}|\nabla\phi_{j,h}^{n+1}\right)$$
$$\le\frac{2\mu-1}{4}\Delta t\|\,|w_h^{'n}|\,|\nabla\phi_{j,h}^{n+1}|\|^2+\frac{4\mu^2\Delta t}{2\mu-1}\|\,|w_h^{'n}|\nabla\eta_{v,j}^{n+1}\|^2.$$

For the fifth term, we use with Hölder's inequality, and the regularity assumptions of

the true solution to get

$$2\mu\Delta t|\left(|w_h^{'n}|^2\nabla v_j(t^{n+1}),\nabla\phi_{j,h}^{n+1}\right)| \le C\mu\Delta t\|\nabla v_j(t^{n+1})\|_{L^\infty}\|w_h^{'n}\|_{L^4}^2\|\nabla\phi_{j,h}^{n+1}\| \le \frac{\alpha}{32}\|\nabla\phi_{j,h}^{n+1}\|^2 + C\frac{\mu^2\Delta t^2}{\alpha}\|w_h^{'n}\|_{L^4}^4.$$

For the first and second nonlinear terms, we use Hölder's inequality, Sobolev embedding theorems, Poincare's and Young's inequalities to reveal

$$\begin{aligned}|\big(<\psi_h>^n\cdot\nabla(v_j(t^{n+1})-v_j(t^n)),\phi_{j,h}^{n+1}\big)| &\le C\|<\psi_h>^n\|\,\|\nabla(v_j(t^{n+1})-v_j(t^n))\|_{L^6}\|\phi_{j,h}^{n+1}\|_{L^3}\\ &\le C\|<\psi_h>^n\|\,\|v_j(t^{n+1})-v_j(t^n)\|_2\|\phi_{j,h}^{n+1}\|^{1/2}\|\nabla\phi_{j,h}^{n+1}\|^{1/2}\\ &\le C\|<\psi_h>^n\|\,\|v_j(t^{n+1})-v_j(t^n)\|_2\|\nabla\phi_{j,h}^{n+1}\|\\ &\le \frac{\alpha}{32}\|\nabla\phi_{j,h}^{n+1}\|^2+\frac{C\Delta t^2}{\alpha}\|<\psi_h>^n\|^2\|v_{j,t}(t^*)\|_2^2,\end{aligned}$$

$$|\left(\psi_{j,h}^n\cdot\nabla v_j(t^n),\phi_{j,h}^{n+1}\right)| \le \frac{\alpha}{32}\|\nabla\phi_{j,h}^{n+1}\|^2+\frac{C}{\alpha}\|\psi_{j,h}^n\|^2\|v_j(t^n)\|_2^2.$$

For the third nonlinear term, rearranging and applying Cauchy-Schwarz and Young's inequalities yields

$$\begin{aligned}|\left(w_{j,h}^{'n}\cdot\nabla\phi_{j,h}^n,\phi_{j,h}^{n+1}\right)| &= |-\left(w_{j,h}^{'n}\cdot\nabla\phi_{j,h}^{n+1},\phi_{j,h}^n\right)|\\ &= |\left(w_{j,h}^{'n}\cdot\nabla\phi_{j,h}^{n+1},\phi_{j,h}^{n+1}-\phi_{j,h}^n\right)|\\ &\le \|\,|w_{j,h}^{'n}|\,|\nabla\phi_{j,h}^{n+1}|\,\|\,\|\phi_{j,h}^{n+1}-\phi_{j,h}^n\|\\ &\le \frac{1}{4\Delta t}\|\phi_{j,h}^{n+1}-\phi_{j,h}^n\|^2+\Delta t\|\,|w_h^{'n}|\,|\nabla\phi_{j,h}^{n+1}|\,\|^2.\end{aligned}$$

For the fourth, fifth, sixth and seventh nonlinear terms, apply Hölder and Young's

inequalities with (2.1) to obtain

$$
\begin{aligned}
|\big(< \eta_w >^n \cdot\nabla(v_j(t^{n+1})-v_j(t^n)), \phi_{j,h}^{n+1}\big)| & \\
&\le C\|\nabla < \eta_{w,j} >^n \|\|\nabla(v_j(t^{n+1}) - v_j(t^n))\|\|\nabla\phi_{j,h}^{n+1}\| \\
&\le \frac{\alpha}{32}\|\nabla\phi_{j,h}^{n+1}\|^2 + \frac{C\Delta t^2}{\alpha}\|\nabla < \eta_w >^n \|^2\|\nabla v_{j,t}(t^{**})\|^2 \\
|\left(< w_h >^n \cdot\nabla\eta_{v,j}^{n+1}, \phi_{j,h}^{n+1}\right)| &\le C\|\nabla < w_h >^n \|\|\nabla\eta_{v,j}^{n+1}\|\|\nabla\phi_{j,h}^{n+1}\| \\
&\le \frac{\alpha}{32}\|\nabla\phi_{j,h}^{n+1}\|^2 + \frac{C}{\alpha}\|\nabla < w_h >^n \|^2\|\nabla\eta_{v,j}^{n+1}\|^2 \\
|\left(w_{j,h}^{'n} \cdot \nabla\eta_{v,j}^n, \phi_{j,h}^{n+1}\right)| &\le C\|\nabla w_{j,h}^{'n}\|\|\nabla\eta_{v,j}^n\|\|\nabla\phi_{j,h}^{n+1}\| \\
&\le \frac{\alpha}{32}\|\nabla\phi_{j,h}^{n+1}\|^2 + \frac{C}{\alpha}\|\nabla w_{j,h}^{'n}\|^2\|\nabla\eta_{v,j}^n\|^2 \\
|\left(\eta_{w,j}^n \cdot \nabla v_j(t^n), \phi_{j,h}^{n+1}\right)| &\le C\|\nabla\eta_{w,j}^n\|\|\nabla v_j(t^n)\|\|\nabla\phi_{j,h}^{n+1}\| \\
&\le \frac{\alpha}{32}\|\nabla\phi_{j,h}^{n+1}\|^2 + \frac{C}{\alpha}\|\nabla\eta_{w,j}^n\|^2\|\|\nabla v_j(t^n)\|^2.
\end{aligned}
$$

Using Taylor's series, Cauchy-Schwarz and Young inequalities, the last term is evaluated as

$$
\begin{aligned}
|G_1(t, v_j, w_j, \phi_{j,h}^{n+1})| \le \frac{\alpha}{24}\|\nabla\phi_{j,h}^{n+1}\|^2 + \frac{\Delta t^2 C}{\alpha}\Big(&\|v_{j,tt}(t^*)\|^2 + \|\nabla w_{j,t}(s^*)\|^2 \\
&+ \|\nabla w_{j,t}(s^*)\|^2\|\nabla v_j(t^{n+1})\|^2 + \|\nabla(w_j(t^n) - < w(t^n) >)\|^2\|\nabla v_{j,t}(t^*)\|^2\Big),
\end{aligned}
$$

with $s^*, t^* \in [t^{n-1}, t^{n+1}]$. Using these estimates in (5.31) and reducing produces

$$\begin{aligned}
&\frac{1}{2\Delta t}\big(\|\phi_{j,h}^{n+1}\|^2 - \|\phi_{j,h}^{n}\|^2\big) + \frac{1}{4\Delta t}\|\phi_{j,h}^{n+1} - \phi_{j,h}^{n}\|^2 + \frac{\alpha + 2(\nu+\nu_m)}{8}\|\nabla\phi_{j,h}^{n+1}\|^2 + \\
&\quad \frac{3(2\mu-1)\Delta t}{4}\| \, |w_h^{'n}| \, |\nabla\phi_{j,h}^{n+1}| \, \|^2 \le \frac{|\nu-\nu_m|}{4}\|\nabla\psi_{j,h}^{n}\|^2 + \frac{6(\nu-\nu_m)^2}{\alpha}\|\nabla\eta_{w,j}^{n}\|^2 \\
&\quad + \frac{6(\nu+\nu_m)^2}{\alpha}\|\nabla\eta_{v,j}^{n+1}\|^2 + \frac{C}{\alpha}\|\psi_{j,h}^{n}\|^2\|v_j(t^n)\|_2^2 + \frac{4\mu^2\Delta t}{2\mu-1}\| \, |w_h^{'n}|\nabla\eta_{v,j}^{n+1}\|^2 \\
&\quad + \frac{C\Delta t^2}{\alpha}\| < \psi_h >^n \|^2\|v_{j,t}(t^*)\|_2^2 + \frac{C\Delta t^2}{\alpha}\|\nabla < \eta_w >^n \|^2\|\nabla v_{j,t}(t^*)\|^2 \\
&\quad + C\frac{\mu^2\Delta t^2}{\alpha}\|w_h^{'n}\|_{L^4}^4 + \frac{C}{\alpha}\|\nabla < w_h >^n \|^2\|\nabla\eta_{v,j}^{n+1}\|^2 + \frac{C}{\alpha}\|\nabla w_{j,h}^{'n}\|^2\|\nabla\eta_{v,j}^{n}\|^2 \\
&\quad + \frac{C}{\alpha}\|\nabla\eta_{w,j}^{n}\|^2\|\nabla v_j(t^n)\|^2 + \frac{C\Delta t^2}{\alpha}\Big(\|v_{j,tt}(t^*)\|^2 + \|\nabla w_{j,t}(s^*)\|^2 \\
&\quad + \|\nabla w_{j,t}(s^*)\|^2\|\nabla v_j(t^{n+1})\|^2 + \|\nabla(w_j(t^n) - < w(t^n) >)\|^2\|\nabla v_{j,t}(t^*)\|^2\Big). \quad (5.33)
\end{aligned}$$

Apply similar techniques to (5.32), we get

$$\begin{aligned}
&\frac{1}{2\Delta t}\big(\|\psi_{j,h}^{n+1}\|^2 - \|\psi_{j,h}^{n}\|^2\big) + \frac{1}{4\Delta t}\|\psi_{j,h}^{n+1} - \psi_{j,h}^{n}\|^2 + \frac{\alpha + 2(\nu+\nu_m)}{8}\|\nabla\psi_{j,h}^{n+1}\|^2 \\
&\quad + \frac{3(2\mu-1)\Delta t}{4}\| \, |v_h^{'n}| \, |\nabla\psi_{j,h}^{n+1}| \, \|^2 \le \frac{|\nu-\nu_m|}{4}\|\nabla\phi_{j,h}^{n}\|^2 + \frac{6(\nu-\nu_m)^2}{\alpha}\|\nabla\eta_{v,j}^{n}\|^2 \\
&\quad + \frac{6(\nu+\nu_m)^2}{\alpha}\|\nabla\eta_{w,j}^{n+1}\|^2 + \frac{C}{\alpha}\|\phi_{j,h}^{n}\|^2\|w_j(t^n)\|_2^2 + \frac{4\mu^2\Delta t}{2\mu-1}\| \, |v_h^{'n}|\nabla\eta_{w,j}^{n+1}\|^2 \\
&\quad + C\frac{\mu^2\Delta t^2}{\alpha}\|v_h^{'n}\|_{L^4}^4 + \frac{C\Delta t^2}{\alpha}\| < \phi_h >^n \|^2\|w_{j,t}(s^{**})\|_2^2 + \frac{C}{\alpha}\|\nabla v_{j,h}^{'n}\|^2\|\nabla\eta_{w,j}^{n}\|^2 \\
&\quad + \frac{C\Delta t^2}{\alpha}\|\nabla < \eta_v >^n \|^2\|\nabla w_{j,t}(s^{**})\|^2 + \frac{C}{\alpha}\|\nabla < v_h >^n \|^2\|\nabla\eta_{w,j}^{n+1}\|^2 \\
&\quad + \frac{C}{\alpha}\|\nabla\eta_{v,j}^{n}\|^2\|\nabla w_j(t^n)\|^2 + \frac{C\Delta t^2}{\alpha}\Big(\|w_{j,tt}(s^{**})\|^2 + \|\nabla v_{j,t}(t^{**})\|^2 \\
&\quad + \|\nabla v_{j,t}(t^{**})\|^2\|\nabla w_j(t^{n+1})\|^2 + \|\nabla(v_j(t^n) - < v(t^n) >)\|^2\|\nabla w_{j,t}(s^{**})\|^2\Big) \quad (5.34)
\end{aligned}$$

with $s^{**}, t^{**} \in [t^{n-1}, t^{n+1}]$. Dropping non-negative terms on the left hand side and adding equations (5.33) and (5.34), multiplying by $2\Delta t$, using regularity assumptions, $\|\phi_{j,h}^0\| = \|\psi_{j,h}^0\| = \|\nabla\phi_{j,h}^0\| = \|\nabla\psi_{j,h}^0\| = 0$, $\Delta t M = T$, and summing over the time

steps yields

$$
\begin{aligned}
&\|\phi_{j,h}^M\|^2 + \|\psi_{j,h}^M\|^2 + \frac{3\alpha}{4}\Delta t \sum_{n=1}^{M} \left(\|\nabla\phi_{j,h}^n\|^2 + \|\nabla\psi_{j,h}^n\|^2\right) \\
&\leq \frac{12\Delta t(\nu-\nu_m)^2}{\alpha} \sum_{n=0}^{M-1} \left(\|\nabla\eta_{v,j}^n\|^2 + \|\nabla\eta_{w,j}^n\|^2\right) \\
&+ \frac{8\mu^2\Delta t^2}{2\mu-1} \sum_{n=0}^{M-1} \Big(\| \, |v_h'^n|\nabla\eta_{w,j}^{n+1}\|^2 + \| \, |w_h'^n|\nabla\eta_{v,j}^{n+1}\|^2\Big) \\
&+ \frac{C\Delta t}{\alpha} \sum_{n=0}^{M-1} \Big(\|\phi_{j,h}^n\|^2 \|w_j(t)\|_{L^\infty(0,T;H^2)} + \|\psi_{j,h}^n\|^2 \|v_j(t)\|_{L^\infty(0,T;H^2)}\Big) \\
&+ \frac{C\Delta t^2}{\alpha} \sum_{n=0}^{M-1} \Delta t\Big(\| < \phi_h >^n \|^2 \|w_{j,t}(t)\|_{L^\infty(0,T;H^2)}^2 + \| < \psi_h >^n \|^2 \|v_{j,t}(t)\|_{L^\infty(0,T;H^2)}^2\Big) \\
&+ \frac{12\Delta t(\nu+\nu_m)^2}{\alpha} \sum_{n=0}^{M-1} \left(\|\nabla\eta_{v,j}^{n+1}\|^2 + \|\nabla\eta_{w,j}^{n+1}\|^2\right) + C\Delta t\frac{\mu^2\Delta t^2}{\alpha} \sum_{n=0}^{M-1} \Big(\|w_h'^n\|_{L^4}^4 + \|v_h'^n\|_{L^4}^4\Big) \\
&+ \frac{C\Delta t^2}{\alpha} \sum_{n=0}^{M-1} \Delta t\Big(\|\nabla < \eta_v >^n \|^2 \|w_{j,t}(t)\|_{L^\infty(0,T;H^1)}^2 + \|\nabla < \eta_w >^n \|^2 \|v_{j,t}(t)\|_{L^\infty(0,T;H^1)}^2\Big) \\
&+ \frac{C\Delta t}{\alpha} \sum_{n=0}^{M-1} \Big(\|\nabla < v_h >^n \|^2 \|\nabla\eta_{w,j}^{n+1}\|^2 + \|\nabla < w_h >^n \|^2 \|\nabla\eta_{v,j}^{n+1}\|^2\Big) \\
&+ \frac{C\Delta t}{\alpha} \sum_{n=0}^{M-1} \Big(\|\nabla v_{j,h}'^n\|^2 \|\nabla\eta_{w,j}^n\|^2 + \|\nabla w_{j,h}'^n\|^2 \|\nabla\eta_{v,j}^n\|^2\Big) + C(h^{2k} + \Delta t^2). \qquad (5.35)
\end{aligned}
$$

The second sum on the right hand side term is nonstandard. For the first part of it (the second follows analogously), we begin with Hölder's inequality and the

generalized inverse inequality [21]:

$$\begin{aligned}
\Delta t^2 \sum_{n=0}^{M-1} \| \, |v_h^{'n}| \nabla \eta_{w,j}^{n+1} \|^2 &\leq \Delta t^2 \sum_{n=0}^{M-1} \|v_h^{'n}\|_\infty^2 \|\nabla \eta_{w,j}^{n+1}\|^2 \\
&\leq Ch^{-1} \Delta t^2 \sum_{n=0}^{M-1} \|\nabla v_h^{'n}\|^2 \|\nabla \eta_{w,j}^{n+1}\|^2 \\
&\leq Ch^{2k-1} \Delta t^2 \sum_{n=0}^{M-1} \|\nabla v_h^{'n}\|^2 |w_j^{n+1}|_{k+1}^2 \\
&\leq Ch^{2k-1} \Delta t,
\end{aligned}$$

with the last two steps following from standard estimates of the L^2 projection error in the H^1 norm for finite element functions, and the stability estimate.

For the sixth sum on the right hand side, we get different bounds for 2D and 3D due to different Sobolev embeddings:

$$\begin{aligned}
2D: \ \|w_h^{'n}\|_{L^4}^4 &\leq C\|w_h^{'n}\|^2 \|\nabla w_h^{'n}\|^2 \leq C\|\nabla w_h^{'n}\|^2, \\
3D: \ \|w_h^{'n}\|_{L^4}^4 &\leq C\|w_h^{'n}\| \|\nabla w_h^{'n}\|^3 \leq C\|\nabla w_h^{'n}\|^3,
\end{aligned}$$

and similarly for $v_h^{'n}$, with the second upper bound in each inequality from the stability theorem 4. With the inverse inequality and the stability bound (used on the L^2 norm), we obtain the bound

$$\|\nabla w_h^{'n}\| \leq Ch^{-1},$$

and thus we obtain the bounds for both 2D or 3D:

$$\begin{aligned}
\|w_h^{'n}\|_{L^4}^4 &\leq Ch^{2-d} \|\nabla w_h^{'n}\|^2, \\
\|v_h^{'n}\|_{L^4}^4 &\leq Ch^{2-d} \|\nabla v_h^{'n}\|^2.
\end{aligned}$$

Using these bounds and the stability bound, the sixth sum on the right is bounded as

$$\begin{aligned} C\Delta t\frac{\mu^2\Delta t^2}{\alpha}\sum_{n=0}^{M-1}\left(\|w_h'^n\|_{L^4}^4+\|v_h'^n\|_{L^4}^4\right) &\leq Ch^{2-d}\Delta t\frac{\mu^2\Delta t^2}{\alpha}\sum_{n=0}^{M-1}\left(\|\nabla w_h'^n\|^2+\|\nabla v_h'^n\|^2\right) \\ &\leq Ch^{2-d}\frac{\mu^2\Delta t^2}{\alpha}. \end{aligned}$$

Now, summing over j and using the standard bounds for $\|\nabla\eta_v\|$ and $\|\nabla\eta_w\|$, we obtain

$$\begin{aligned} &\sum_{j=1}^{J}\|\phi_{j,h}^M\|^2+\sum_{j=1}^{J}\|\psi_{j,h}^M\|^2+\frac{3\alpha}{4}\Delta t\sum_{j=1}^{J}\sum_{n=1}^{M}\left(\|\nabla\phi_{j,h}^n\|^2+\|\nabla\psi_{j,h}^n\|^2\right) \\ &\qquad\leq C(h^{2k}+h^{2k-1}\Delta t+\Delta t^2(1+h^{2-d})+h^{2k}\Delta t^2) \\ &\qquad+\sum_{n=0}^{M-1}\frac{C}{\alpha}\left(\Delta t+\Delta t^3\right)\left(\sum_{j=1}^{J}\|\phi_{j,h}^n\|^2+\sum_{j=1}^{J}\|\psi_{j,h}^n\|^2\right). \quad (5.36) \end{aligned}$$

Applying the discrete Gronwall lemma, we have

$$\begin{aligned} &\sum_{j=1}^{J}\|\phi_{j,h}^M\|^2+\sum_{j=1}^{J}\|\psi_{j,h}^M\|^2+\frac{3\alpha}{4}\Delta t\sum_{j=1}^{J}\sum_{n=1}^{M}\left(\|\nabla\phi_{j,h}^n\|^2+\|\nabla\psi_{j,h}^n\|^2\right) \\ &\qquad\leq Ce^{\frac{CT(1+\Delta t^2)}{\alpha}}(h^{2k}+h^{2k-1}\Delta t+\Delta t^2(1+h^{2-d})+h^{2k}\Delta t^2). \quad (5.37) \end{aligned}$$

Using the triangle inequality allows us to write

$$\sum_{j=1}^{J}\|e_{v,j}^{M}\|^2+\sum_{j=1}^{J}\|e_{w,j}^{M}\|^2+\frac{3\alpha}{4}\Delta t\sum_{j=1}^{J}\sum_{n=1}^{M}\left(\|\nabla e_{v,j}^{n}\|^2+\|\nabla e_{w,j}^{n}\|^2\right)$$
$$\leq 2\Bigg(\sum_{j=1}^{J}\|\eta_{v,j}^{M}\|^2+\sum_{j=1}^{J}\|\phi_{j,h}^{M}\|^2+\sum_{j=1}^{J}\|\psi_{j,h}^{M}\|^2+\sum_{j=1}^{J}\|\eta_{w,j}^{M}\|^2$$
$$+\frac{3\alpha}{4}\Delta t\sum_{j=1}^{J}\sum_{n=1}^{M}\left(\|\nabla\eta_{v,j}^{n}\|^2+\|\nabla\phi_{j,h}^{n}\|^2+\|\nabla\psi_{j,h}^{n}\|^2+\|\nabla\eta_{w,j}^{n}\|^2\right)\Bigg)\leq 2C^{*}(h^{2k+2}+h^{2k})$$
$$+2Ce^{\frac{CT(1+\Delta t^2)}{\alpha}}\left(h^{2k}+h^{2k}\frac{\Delta t}{h}+\Delta t^2(1+h^{2-d})+h^{2k}\Delta t^2\right), \tag{5.38}$$

which implies

$$\sum_{j=1}^{J}\|e_{v,j}^{M}\|^2+\sum_{j=1}^{J}\|e_{w,j}^{M}\|^2+\frac{3\alpha}{4}\Delta t\sum_{j=1}^{J}\sum_{n=1}^{M}\left(\|\nabla e_{v,j}^{n}\|^2+\|\nabla e_{w,j}^{n}\|^2\right)$$
$$\leq Ce^{\frac{CT(1+\Delta t^2)}{\alpha}}\left(h^{2k}+h^{2k-1}\Delta t+\Delta t^2(1+h^{2-d})+h^{2k}\Delta t^2\right). \tag{5.39}$$

Now using the triangle inequality again,

$$\|<e_v>^T\|^2+\|<e_w>^T\|^2+\frac{3\alpha}{4}\Delta t\sum_{j=1}^{J}\sum_{n=1}^{M}\left(\|\nabla<e_v>^n\|^2+\|\nabla<e_w>^n\|^2\right)$$
$$\leq Ce^{\frac{CT(1+\Delta t^2)}{\alpha}}\left(h^{2k}+h^{2k-1}\Delta t+\Delta t^2(1+h^{2-d})+h^{2k}\Delta t^2\right), \tag{5.40}$$

which completes the proof. □

5.3 Numerical experiments

This section presents results of numerical experiments used to test the proposed scheme and theory. In all tests, we used (P_2, P_1^{disc}) Scott-Vogelius elements on barycenter refined, regular triangular meshes. The tuning parameter $\mu = 1$ in all

tests. The choice of $J = 4$ is made in all of our simulations; although in practice we expect much larger J, our intent here is for a first proof of concept. The codes were written in FreeFem++ [42], and since the experiments are essentially proof of concept tests in 2D, we used the UMFPACK direct solver built into FreeFem++ for the individual systems. In practice, for larger problems and especially in 3D, it is critical to make the solvers more efficient, by using block solver algorithms to simultaneously solve $Ax = b$ with multiple right-hand sides, or to reuse efficient preconditioners; see [38, 50, 51] for more discussion of this important step.

5.3.1 Convergence rate verification

Our first experiment tests the convergence rates predicted by the theory in section 5.2, which proved the $L^2(0,T;H^1(\Omega))$ error to be $O(\Delta t + h^2 + h^{3/2}\Delta t^{1/2})$ in two dimensions, due to our choice of elements. Provided $\Delta t < O(h)$ or $h < \Delta t^{1/3}$, the predicted error becomes $O(\Delta t + h^2)$; in our tests, we ensure these criteria are met.

We begin this test by selecting an analytical function with $s = 1$,

$$v = \begin{pmatrix} \cos y + (1+t)\sin y \\ \sin x + (1+t)\cos x \end{pmatrix}, \; w = \begin{pmatrix} \cos y - (1+t)\sin y \\ \sin x - (1+t)\cos x \end{pmatrix},$$

$$p = (x-y)(1+t), \; \lambda = 0.$$

on the domain $\Omega = (0,\ 1)^2$ and then compute the right side function $f =< f_1, f_2 >^T$,

we have

$$f = \begin{pmatrix} (1+\nu_m+\nu_m t)\sin y + (1+t)\sin(x+y) - \sin x \sin y \\ -(1+t)^2 \cos x \cos y + \nu \cos y + t + 1 \\ \\ (1+\nu_m+\nu_m t)\cos x - (1+t)\sin(x+y) + \cos x \cos y \\ +(1+t)^2 \sin x \sin y + \nu \sin x - t - 1 \\ \\ -(1+\nu_m+\nu_m t)\sin y - (1+t)\sin(x+y) - \sin x \sin y \\ -(1+t)^2 \cos x \cos y + \nu \cos y + t + 1 \\ \\ -(1+\nu_m+\nu_m t)\cos x + (1+t)\sin(x+y) + \cos x \cos y \\ +(1+t)^2 \sin x \sin y + \nu \sin x - t - 1 \end{pmatrix}$$

Next, we choose four perturbed solutions, which are defined by $v_j = (1 \pm \epsilon)v$, $w_j = (1 \pm \epsilon)w$, for $j = 1, 2$, and $v_j = (1 \pm 2\epsilon)v$, $w_j = (1 \pm 2\epsilon)w$, for $j = 3, 4$. From these perturbed solutions and the choices $\nu = 0.01$, $\nu_m = 0.1$, initial conditions, Dirichlet boundary conditions and right hand side forcing terms are calculated. The ensemble scheme will be used to calculate $< w_h^n >$ and $< v_h^n >$, and we will compare that to the true average $< w(t^n) >$ and $< v(t^n) >$. The error is defined as $< e_v > := \| < v > - < v_h > \|_{2,1}$. Note that errors and rates for w are very similar to those of v, and are omitted.

We first test the temporal convergence. To do so, we fix $h = 1/64$ and end time $T = 1$, and compute solutions with varying Δt. For several choices of ϵ, we show errors and convergence rates in Table 5.1, and observe first order temporal convergence.

	$\epsilon = 0.1$		$\epsilon = 0.01$		$\epsilon = 0.001$	
Δt	$\| < e_v > \|_{2,1}$	rate	$\| < e_v > \|_{2,1}$	rate	$\| < e_v > \|_{2,1}$	rate
$T/4$	3.241e-2		2.201e-2		2.292e-2	
$T/8$	2.340e-2	0.47	1.774e-2	0.31	1.781e-2	0.36
$T/16$	1.582e-2	0.56	9.447e-3	0.91	9.488e-3	0.91
$T/32$	9.968e-3	0.67	4.923e-3	0.94	4.944e-3	0.94
$T/64$	5.852e-3	0.77	2.517e-3	0.97	2.527e-3	0.97
$T/128$	3.238e-3	0.85	1.273e-3	0.98	1.277e-3	0.98
$T/256$	1.718e-3	0.91	6.403e-4	0.99	6.426e-4	0.99

Table 5.1: Temporal convergence rates for $\nu = 0.01$, $\nu_m = 0.1$, $T = 1.0$, and fixed $h = \frac{1}{64}$.

To test spatial convergence, we fix $T = 0.001$ and $\Delta t = \frac{T}{8}$, and compute on varying mesh widths. Errors and rates are shown in Table 5.2 for several choices of ϵ, and in all cases we observe second order convergence.

	$\epsilon = 0.1$		$\epsilon = 0.01$		$\epsilon = 0.001$	
h	$\| < e_v > \|_{2,1}$	rate	$\| < e_v > \|_{2,1}$	rate	$\| < e_v > \|_{2,1}$	rate
$\frac{1}{4}$	1.363e-4		1.363e-4		1.363e-4	
$\frac{1}{8}$	3.405e-5	2.00	3.408e-5	2.00	3.408e-5	2.00
$\frac{1}{16}$	8.512e-6	2.00	8.531e-6	2.00	8.531e-6	2.00
$\frac{1}{32}$	2.128e-6	2.00	2.136e-6	2.00	2.135e-6	2.00
$\frac{1}{64}$	5.320e-7	2.00	5.345e-7	2.00	5.334e-7	2.00

Table 5.2: Spatial convergence rates for $\nu = 0.01$, $\nu_m = 0.1$, and fixed $T = 0.001$, $\Delta t = T/8$.

5.3.2 Perturbation in the initial condition

In this subsection, our objective is to test the ensemble eddy viscosity terms as the numerical regularizations. To do so we examine how the norm of fluctuations, v_j' and w_j' behave over time introducing a perturbation parameter ϵ into the initial conditions. The domain under consideration is the $\Omega = (0,\ 1)^2$. We considered the end time $T = 10$, time step $\Delta t = 0.025$, $\mu = 1$ and a mesh width of $h = 1/64$

and then computed with the Algorithm 5.2.1. An inhomogeneous Dirichlet boundary conditions $v_j = v$ and $w_j = w$ on $\partial\Omega$ were taken on this problem.

In this test, we consider an ensemble of four members v_j, w_j, for $j = 1, 2, 3, 4$, which are the solutions corresponding to the four different initial conditions which are defined by $v_j^0 = (1\pm\epsilon)v$, $w_j^0 = (1\pm\epsilon)w$, for $j = 1, 2$, and $v_j^0 = (1\pm 2\epsilon)v$, $w_j^0 = (1\pm 2\epsilon)w$, for $j = 3, 4$, where the perturbation parameter $\epsilon = 10^{-3}, 10^{-2}, 10^{-1}$ and 1. The ensemble averages $< v_h >= \frac{\sum_{j=1}^{4} v_{j,h}}{4}$ and $< w_h >= \frac{\sum_{j=1}^{4} w_{j,h}}{4}$ are computed at each time step. In Figure 5.1, we plotted norms of $v_j^{'}$ and $w_j^{'}$ versus time for the above specified values of ϵ. In each case, we observe that, as time increase the fluctuation norms vanish.

5.3.3 Perturbation in the right hand side functions

In this case, we perturb the right side functions as $f_j = (1 \pm \epsilon)f$, for $j = 1, 2$ and $f_j = (1 \pm 2\epsilon)f$ for $j = 3, 4$ where $\epsilon = 10^{-3},\ 10^{-2},\ 10^{-1}$ and 1. An inhomogeneous Dirichlet boundary conditions $v_j = v$ and $w_j = w$ on $\partial\Omega$ were taken on this problem too. Same initial conditions $v_j = v$ and $w_j = w$ are chosen for all j. The domain is $\Omega = (0,\ 1)^2$. Fluctuation norms are calculated against time and are shown in Figures 5.2-5.3. In each case, we see that the values of the computed norms are significantly small.

5.3.4 MHD Channel flow over a step

For our fourth test, we consider channel flow in a 30×10 rectangular domain with a 1×1 step five units into the channel, in the presence of a magnetic field. No slip boundary conditions are enforced for velocity components and $B =< 0, 1 >^T$ is used on the walls and step, $u =< y(10 - y)/25, 0 >^T$ and $B =< 0, 1 >^T$ at the

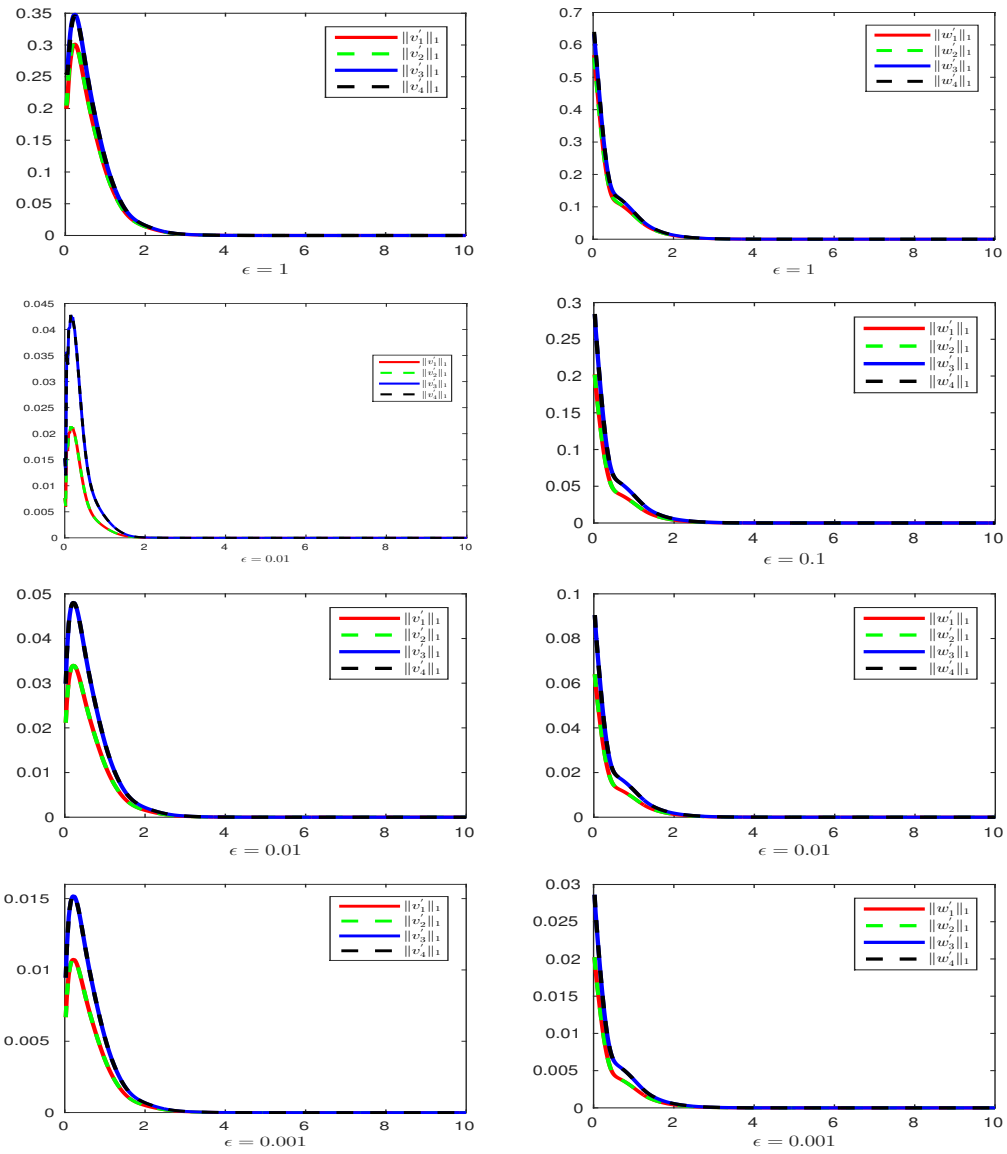

Figure 5.1: Perturbation in the initial condition when $\nu = 0.01$ and $\nu_m = 0.1$.

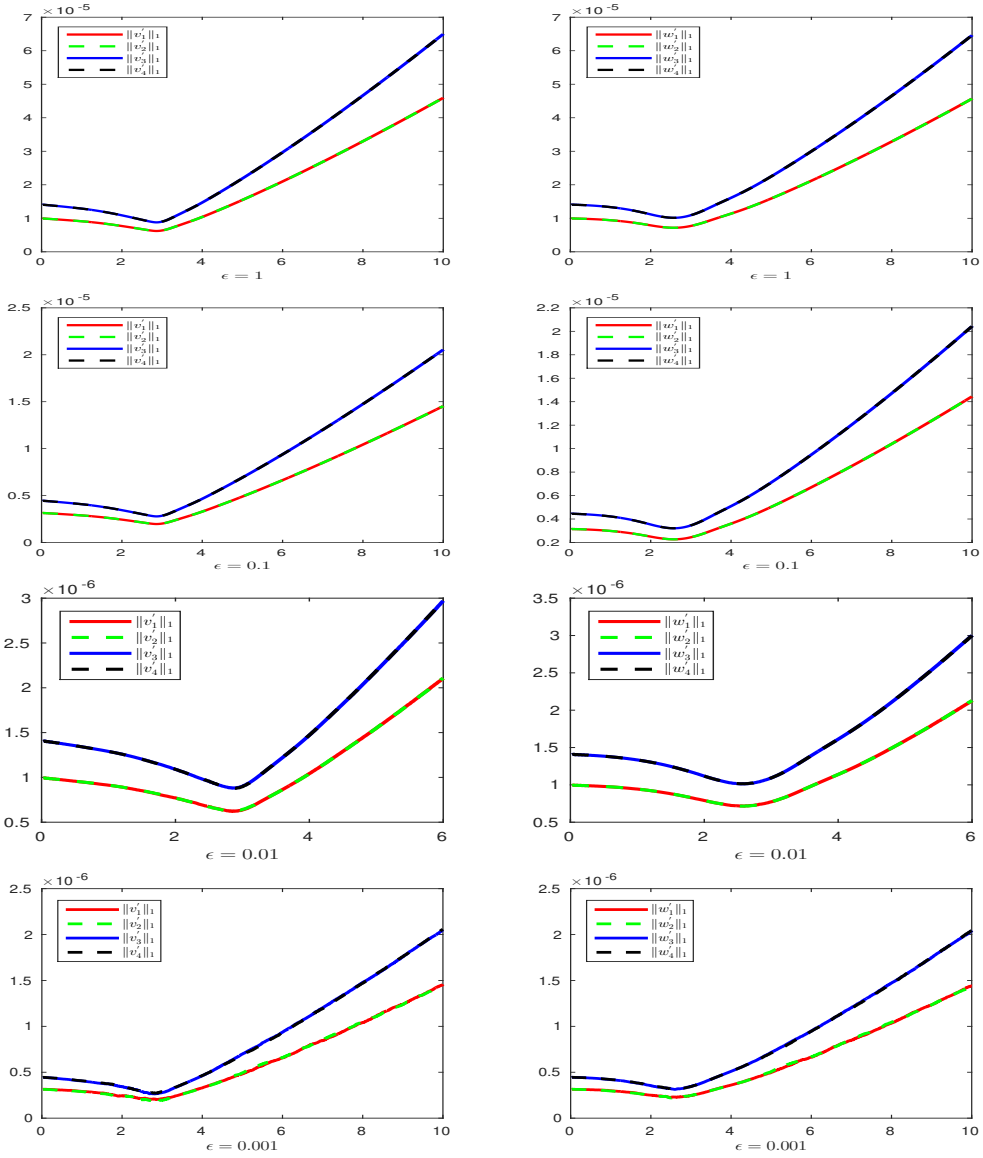

Figure 5.2: Perturbation in the forcing terms with $\nu = 10, \nu_m = 0.1$.

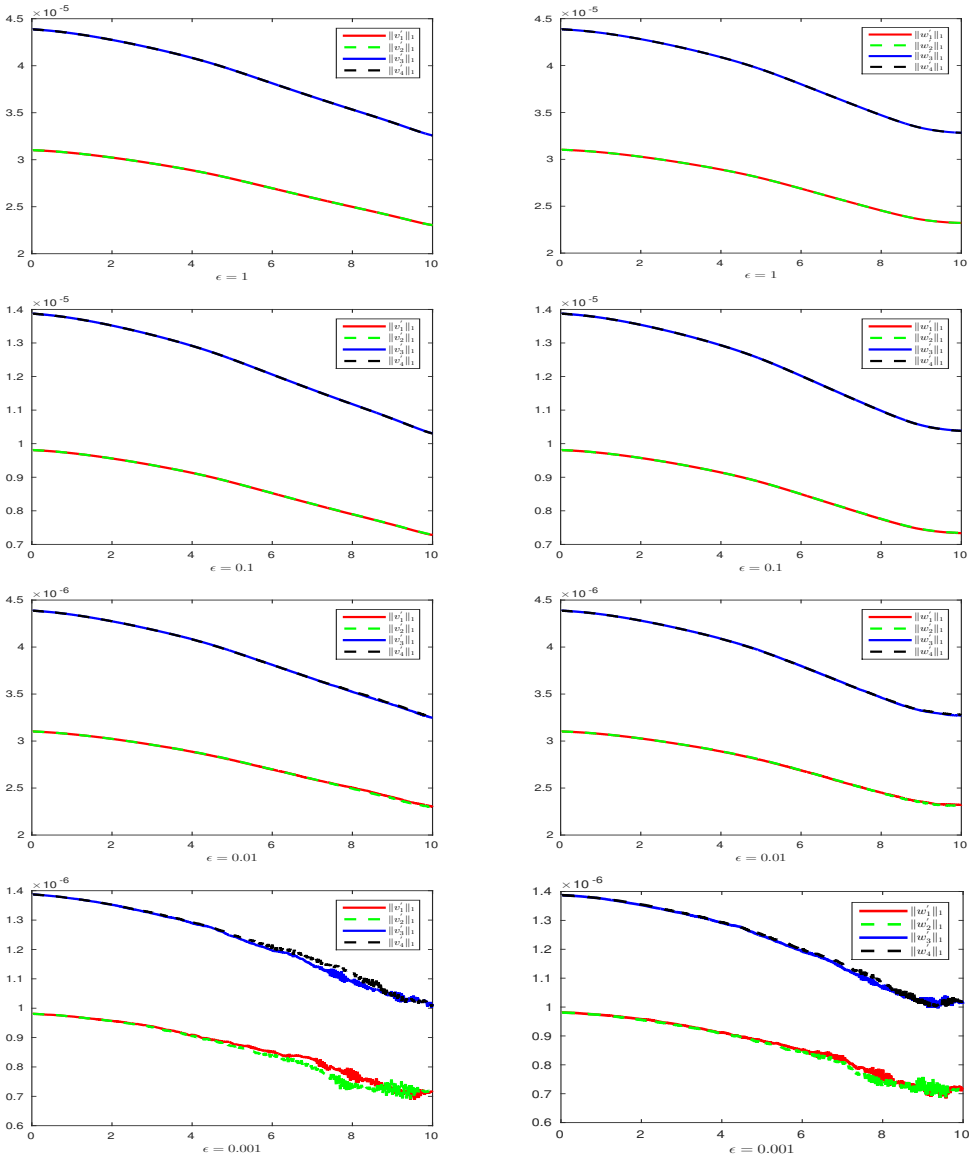

Figure 5.3: Perturbation in the forcing terms with $\nu = 0.01$ and $\nu_m = 0.1$.

inflow, and the outflow condition uses a channel extension of 10 units, and at the end of the extension we set the outflow velocity and magnetic field equal to the inflow. The coupling number $s = 0.01$, $\nu = 1/1000$ and $\nu_m = 0.1$. The initial conditions are $u_0 =< y(10-y)/25, 0 >^T$ and $B_0 =< 0, 1 >^T$.

We consider an ensemble of four different solutions with the initial and boundary conditions perturbed by multiplicative factors of $(1 \pm \epsilon)$, and $(1 \pm 2\epsilon)$. The simulations are carried out for various choices of ϵ using Algorithm 5.2.1 until $T = 40$, with a time step of $\Delta t = 0.05$, and a mesh that provided 75,222 degrees of freedom. We plot the H^1-norm of ensemble averages, $\| < u > \|_1$ and $\| < B > \|_1$ versus time until $T = 10$ in Figure 5.4. Plots of ensemble velocity solutions for varying ϵ are shown in figure 5.5, and magnetic field solutions in figure 5.6. For comparison, we also give results of a single run with $\epsilon = 0$ (single solution with no perturbation). As expected, we observe that as $\epsilon \to 0$, ensemble solutions solutions appear to converge to the unperturbed solution. We also observe that the ensemble solution for all choices of ϵ match the unperturbed solution well.

5.4 Conclusion

This chapter represents an extension of the breakthrough idea for efficient flow ensemble calculation of Jiang and Layton [51], originally performed for Navier-Stokes, to MHD. We have developed herein an efficient algorithm for calculating ensemble averages of MHD flows. The keys to the efficiency are i) at each time step, each of the J realizations solves linear systems with the same matrices - this means assembly needs done once instead of J times, block linear solvers can potentially be used, and preconditioners can be reused; and ii) due to use of the Elsässer variable formulation, the linear systems at each time step are not fully coupled, but instead split into two

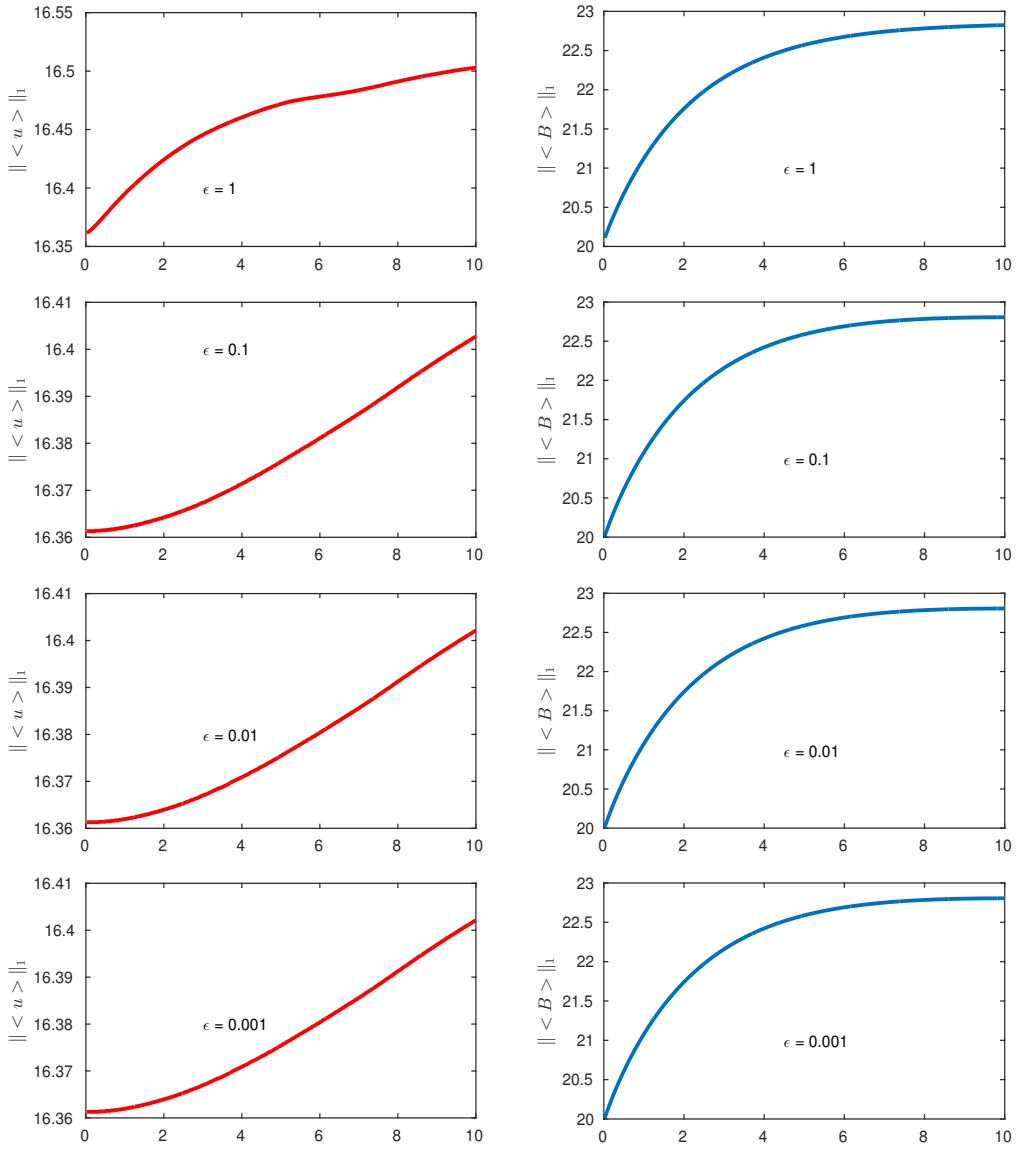

Figure 5.4: $\| < u > \|_1$ and $\| < B > \|_1$ with $\nu = 0.001$ and $\nu_m = 1$.

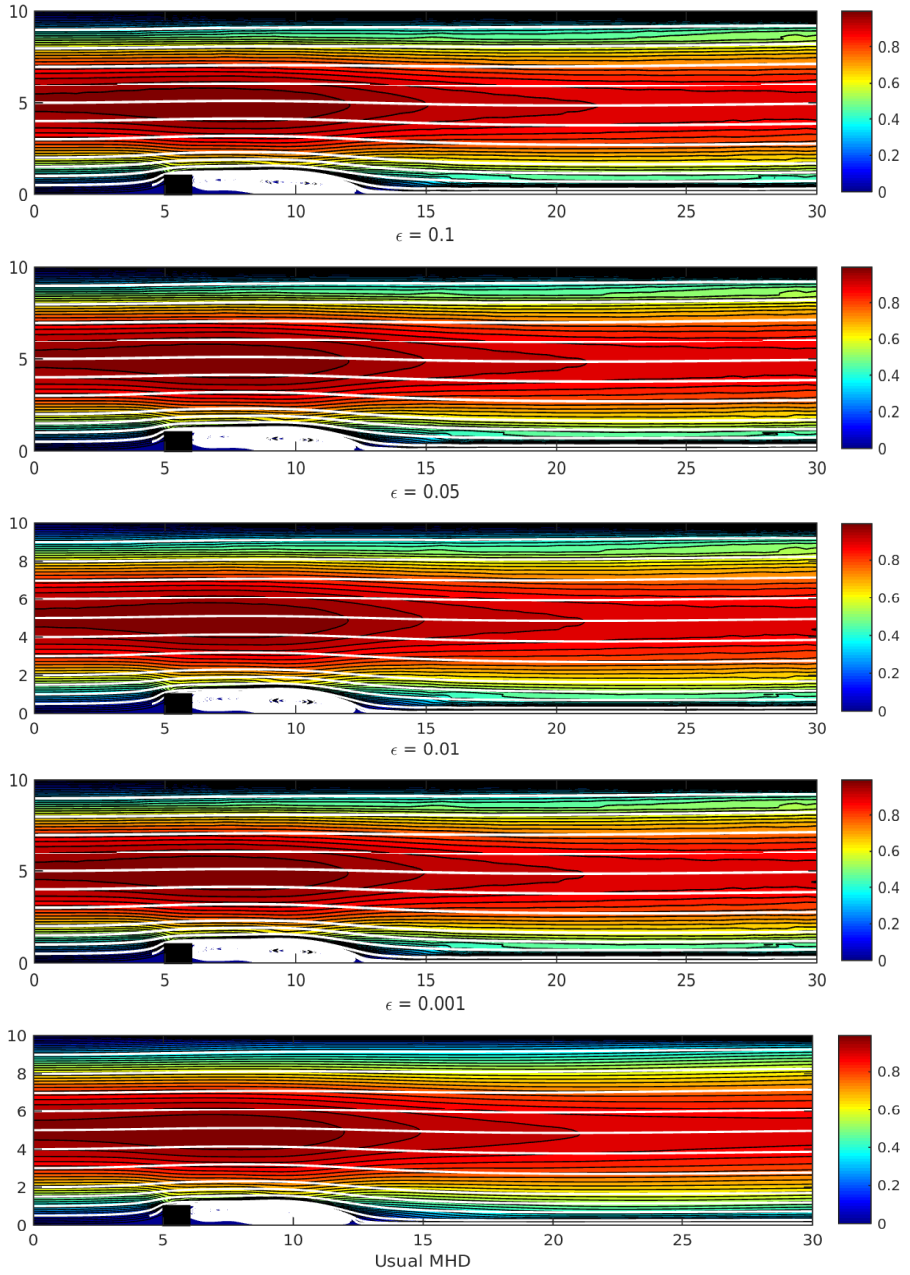

Figure 5.5: Shown above are $T = 40$, velocity ensemble solutions (shown as streamlines over speed contours) for MHD channel flow over a step with $dt = 0.05$, $s = 0.01$ and $dof = 75222$.

Oseen problems, which are much easier to solve.

The algorithm is proven to be unconditionally stable with respect to the time

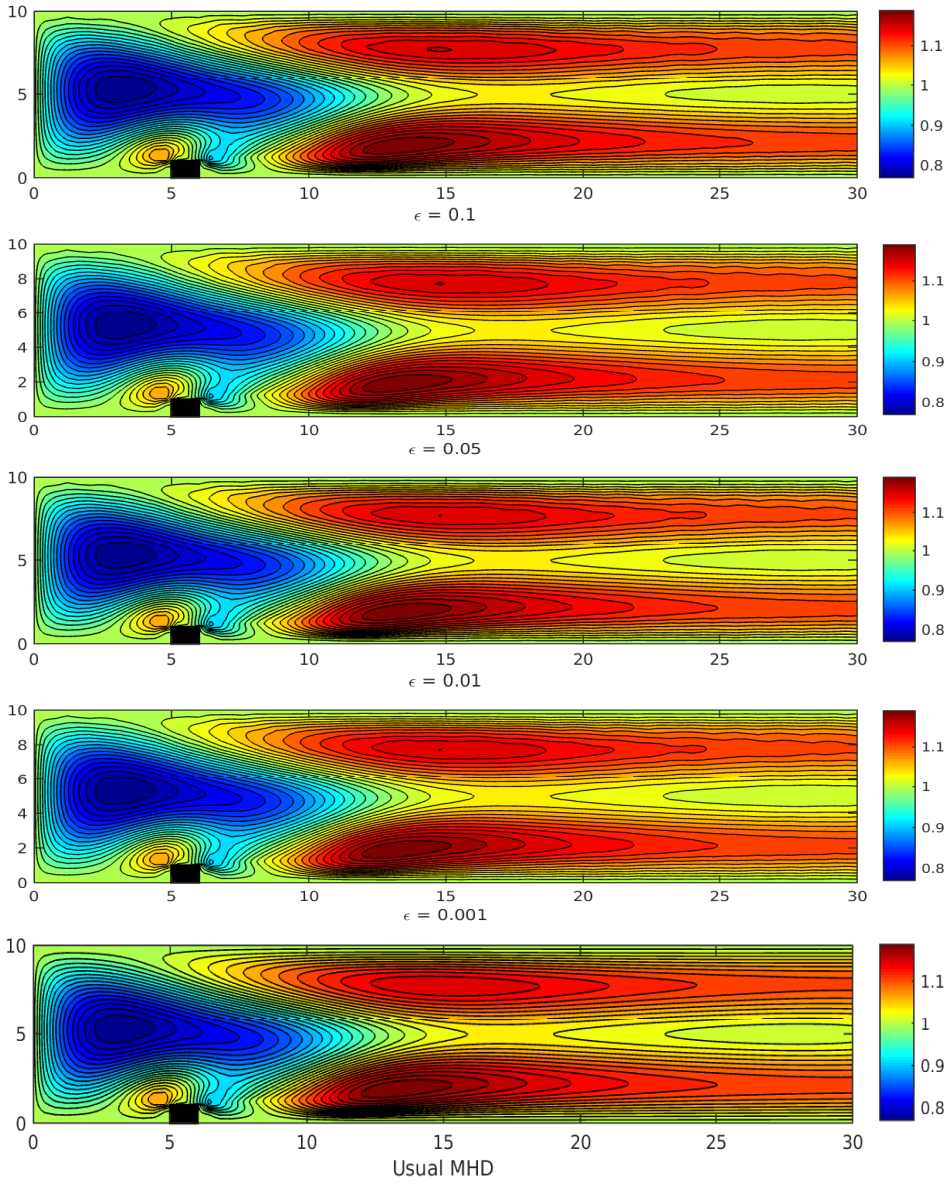

Figure 5.6: Shown above are $T = 40$, magnitudes of ensemble magnetic field solutions (magnitude) for MHD channel flow over a step with $dt = 0.05$, $s = 0.01$ and $dof = 75222$.

step size, which is somewhat remarkable since the systems are split into two Oseen problems at each timestep, and the schemes are such that some of the nonlinearity is treated explicitly at each time step. We also prove the method is convergent; in

2D, the convergence is optimal under very mild criteria, but in 3D the convergence is proven to be possibly suboptimal due to a $\frac{\Delta t}{h^{1/2}}$ term that arises (instead of Δt, which would be optimal) due to a worse 3D Sobolev embedding used in the analysis. Numerical tests were performed that verified the predicted convergence rates, and also showed the method performed well on a more physically relevant test problem.

An important next step would be to apply the ideas herein to a the higher order decoupled MHD scheme proposed in [44], which would present significantly more challenges in the analysis.

Chapter 6

High order algebraic splitting methods

6.1 Introduction

Even though Elsässer formulation of MHD provides efficient algorithm, in some cases, it remains an open question about the boundary conditions on Elsässer variables. We also believe that it is necessary to perform more testing on these schemes to verify that they give solutions very similar to primitive variables schemes with the same mesh and timestep on a wide range of problems. At this point we want to propose, analyze and test some schemes of MHD simulations in primitive variables. As the simulation of MHD flows is known to be quite difficult, and one major reason for this is the difficulties that arise because of the large, nonsymmetric, ill-conditioned block saddle point linear systems that arise at each time step. It is the purpose of this chapter to propose, analyze and test an accurate and efficient linear solver for these systems, by extending some recent work of the authors on saddle point linear systems for Navier-Stokes (NS) [86] to the block saddle point systems that arise in MHD. The key ideas are combining the Yosida algebraic splitting with a particular incremental formulation of the MHD system at each time step, which leads

to a Schur complement (the main difficulty of the linear solve) that decouples into two Stokes-type Schur complements, each of which are symmetric positive definite, and are also the same at each time step. We will fully analyze the splitting error and show it is third order (fourth order if block pressure-correction is applied), and to our knowledge, this is the first higher order algebraic splitting method studied for the block saddle point systems in MHD.

Applying a temporal discretization to the MHD system in primitive variables, we obtain the problem at each time step [8]: find a velocity u, a magnetic field B and Lagrange multipliers P, λ satisfying

$$\frac{\alpha}{\Delta t}u - \nu\Delta u + \mathcal{U}\cdot\nabla u - \mathcal{B}\cdot\nabla B + \nabla P = \tilde{f}, \tag{6.1}$$

$$\nabla\cdot u = 0, \tag{6.2}$$

$$\frac{\alpha}{\Delta t}B - \nu_m\Delta B + \mathcal{U}\cdot\nabla B - \mathcal{B}\cdot\nabla u - \nabla\lambda = \tilde{g}, \tag{6.3}$$

$$\nabla\cdot B = 0, \tag{6.4}$$

where Δt is a time-step size, $\mathcal{U}$ and $\mathcal{B}$ are given solenoidal velocity and magnetic fields (e.g. extrapolated from previous time steps), and $\tilde{f}$ and $\tilde{g}$ are the forcing terms combined with left hand side terms that are known from previous time steps. For a BDF2 time-stepping scheme, for example, $\alpha = \frac{3}{2}$, $\mathcal{U} = 2u^n - u^{n-1}$, $\mathcal{B} = 2B^n - B^{n-1}$, $\tilde{f} = f + \frac{2}{\Delta t}u^n - \frac{1}{\Delta t}u^{n-1}$, and $\tilde{g} = \nabla\times g + \frac{2}{\Delta t}B^n - \frac{1}{\Delta t}B^{n-1}$.

Applying a finite element discretization to (6.1)-(6.4), where we search for $\bar{u}, \bar{B} \in X_h$ and $\bar{P}, \bar{\lambda} \in Q_h$, with (X_h, Q_h) satisfying the LBB stability property [21] (details of the finite element discretization are given in section 3), a block linear

system arises of the form

$$\begin{pmatrix} A_1 & N_1 & C_1 & 0 \\ N_2 & A_2 & 0 & C_1 \\ C_1^T & 0 & 0 & 0 \\ 0 & C_1^T & 0 & 0 \end{pmatrix} \begin{pmatrix} \bar{u} \\ \bar{B} \\ \bar{P} \\ \bar{\lambda} \end{pmatrix} = \begin{pmatrix} \bar{F}_1 \\ \bar{F}_2 \\ 0 \\ 0 \end{pmatrix}, \tag{6.5}$$

where $A_1 := \frac{\alpha}{\Delta t} M + \nu S + \tilde{N}_1$, $A_2 := \frac{\alpha}{\Delta t} M + \nu_m S + \tilde{N}_2$, with M denoting the X_h mass matrix, S the X_h stiffness matrix, C_1 the rectangular matrix representing the gradient operator acting on Q_h and tested with X_h, $\tilde{N}_1$ the nonlinear contributions from the momentum equation, and $\tilde{N}_2$ the nonlinear contributions from Maxwell's equation. Denoting

$$A = \begin{pmatrix} A_1 & N_1 \\ N_2 & A_2 \end{pmatrix}, C = \begin{pmatrix} C_1 & 0 \\ 0 & C_1 \end{pmatrix}, \bar{X} = \begin{pmatrix} \bar{u} \\ \bar{B} \end{pmatrix}, \bar{Y} = \begin{pmatrix} \bar{P} \\ \bar{\lambda} \end{pmatrix}, \bar{F} = \begin{pmatrix} \bar{F}_1 \\ \bar{F}_2 \end{pmatrix},$$

the equation (6.5) can now be written as a block saddle point linear system:

$$\begin{pmatrix} A & C \\ C^T & 0 \end{pmatrix} \begin{pmatrix} \bar{X} \\ \bar{Y} \end{pmatrix} = \begin{pmatrix} \bar{F} \\ 0 \end{pmatrix}. \tag{6.6}$$

A common approach to solving saddle point systems that arise in Navier-Stokes saddle point systems is to apply algebraic splitting methods, which reduces the difficulty of the solves, but introduces error due to the approximations that are made. Yosida-type splitting methods work by making an approximation of the Schur

complement. Setting

$$\tilde{A} = \begin{pmatrix} \frac{\alpha}{\Delta t} M + \nu S & 0 \\ 0 & \frac{\alpha}{\Delta t} M + \nu_m S \end{pmatrix},$$

or possibly without viscous contributions, the following approximation of the block LU decomposition is made:

$$\begin{aligned} \begin{pmatrix} A & C \\ C^T & 0 \end{pmatrix} &\approx \begin{pmatrix} A & 0 \\ C^T & -C^T \tilde{A}^{-1} C \end{pmatrix} \begin{pmatrix} I & A^{-1}C \\ 0 & Q \end{pmatrix} \\ &= \begin{pmatrix} A & C \\ C^T & C^T A^{-1} C - C^T \tilde{A}^{-1} C Q \end{pmatrix}, \end{aligned} \tag{6.7}$$

where $Q = (C^T \tilde{A}^{-1} A \tilde{A}^{-1} C)^{-1} \left(C^T \tilde{A}^{-1} C \right)$ yields the pressure corrected Yosida method developed by Veneziani et. al [32, 87], and $Q = I$ yields the classical Yosida method. We note that this clever choice of Q increases the accuracy of the Yosida splitting from $O(\Delta t^2)$ to $O(\Delta t^3)$, and requires two more solves with SPD matrix $\tilde{A}$, and one more SPD Schur complement solve. Additionally, this approach has the advantage of easily allowing for adaptive time stepping. One potential disadvantage was shown in [86] with both analysis and numerical tests, which is that the pressure correction step can have error that scales negatively with respect to the spatial mesh width, and thus seems best suited for problems where the temporal scales are smaller than the spatial scales (e.g. for blood flow problems Veneziani et. al has shown it works very well).

Taking $Q = I$ for simplicity, the Yosida approximation requires solving

$$\begin{pmatrix} A & 0 \\ C^T & -C^T\tilde{A}^{-1}C \end{pmatrix} \begin{pmatrix} I & A^{-1}C \\ 0 & I \end{pmatrix} \begin{pmatrix} \hat{X} \\ \hat{Y} \end{pmatrix} = \begin{pmatrix} F \\ 0 \end{pmatrix},$$

which is equivalent to the following three steps:

1. Solve $A\hat{z} = \hat{F}$ for $\hat{z}$.

2. Solve $C^T\widetilde{A}^{-1}C\hat{Y} = C^T\hat{z}$ for $\hat{Y}$.

3. Solve $A\hat{X} = A\hat{z} - C\hat{Y}$ for $\hat{X}$.

The only difference between the linear systems arising from the Yosida method and unaltered linear system is that the Yosida method uses the matrix $\tilde{A}$ instead of A in step 2, but this small change leads to a dramatic reduction of complexity. Since $\tilde{A}$ is block diagonal, the Schur complement $C^T\widetilde{A}^{-1}C$ reduces to

$$C^T\widetilde{A}^{-1}C = \begin{pmatrix} C_1^T\left(\frac{\alpha}{\Delta t}M + \nu S\right)^{-1}C_1 & 0 \\ 0 & C_1^T\left(\frac{\alpha}{\Delta t}M + \nu_m S\right)^{-1}C_1, \end{pmatrix}$$

and thus is decoupled into two smaller SPD time-dependent-Stokes-type Schur complements. It is well known how to solve such systems (see [86] and references therein). Hence the Yosida splitting creates linear systems that are much easier to solve.

Of course, with approximations comes error, and from (6.7) we observe the error created is in the 2,2 block of the recombined matrix, as the term $C^T(A^{-1}-\tilde{A}^{-1})C$ appears instead of 0. An expansion of $A^{-1} - \tilde{A}^{-1}$ from [87] reveals that

$$A^{-1} - \tilde{A}^{-1} = -\tilde{A}^{-1}N\tilde{A}^{-1} + (\tilde{A}^{-1}N)^2\tilde{A}^{-1} + ...,$$

which implies a splitting error of $\mathcal{O}(\Delta t^2)$, since $N = O(1)$ and $\tilde{A} = O(\Delta t^{-1})$. We note that if pressure correction is used, the first term of the expansion is cancelled, producing $\mathcal{O}(\Delta t^3)$ error.

Our goal in this chapter is to apply ideas of [86] for NSE saddle point linear systems to the block MHD systems. In particular, before applying the Yosida approximation, we will rewrite the system (6.1)-(6.4) in terms of increments of the pressure variables $\delta_P = P - P^n$, $\delta_\lambda = \lambda - \lambda^n$, where we seek $(u, \delta_P, B, \delta_\lambda)$ satisfying

$$\frac{\alpha}{\Delta t}u - \nu\Delta u + \mathcal{U}\cdot\nabla u - \mathcal{B}\cdot\nabla B + \nabla\delta_P = \tilde{\tilde{f}}, \tag{6.8}$$

$$\nabla\cdot u = 0, \tag{6.9}$$

$$\frac{\alpha}{\Delta t}B - \nu_m\Delta B + \mathcal{U}\cdot\nabla B - \mathcal{B}\cdot\nabla u - \nabla\delta_\lambda = \tilde{\tilde{g}}, \tag{6.10}$$

$$\nabla\cdot B = 0, \tag{6.11}$$

with appropriately defined right hand sides. Since the problem is linearized at each time step, this change of variables produces the exact same matrix, but with an altered right hand side. The general idea is that the Yosida appproximation creates $O(\Delta t^2)$ error in the primitive variables, so if approximation is made to $O(\Delta t)$ increments instead of the $O(1)$ original variables, then the total error will be reduced to $O(\Delta t^3)$ (and if pressure correction is used, then accuracy will be $O(\Delta t^4)$). Analysis and testing of this idea showed that it works quite well, and these higher order rates were found to hold. Interestingly, our finite element analysis in the NS-case revealed that the same asymptotic rates could be found if only the pressure increment was used [86], and velocity was solved for as usual; this leads back to a method proposed for the NSE in [45]. Since using only pressure increments is a simpler approach, we will apply this approach herein. Another nice feature of using only the pressure

increments is that grad-div stabilization can be immediately applied, which is well known to provide for reduction in divergence errors, improvements in overall accuracy, improvements in accuracy in Yosida methods, and aids in effectively preconditioning Schur complement solvers [19, 54, 60, 76, 85].

The purpose of this chapter will be to analyze and test the Yosida method for the system (6.8)-(6.11), and we call this method the 'Yosida-updates' (YU) method for MHD. The linear algebraic splitting analysis is identical to the NSE case, and is discussed above. However, such analysis is not attractive mathematically, since the linear algebra vector norms are not in the natural spaces of the variables, and any negative scaling of the error with respect to the spatial mesh width would be neglected. Hence, we apply a finite element-type error analysis to quantify the difference between solutions found by solving the linear system using an exact linear solver and the YU splitting approximation by casting the algebraic systems back into finite element problems. Our analysis considers the basic YU case, with no grad-div stabilization and without pressure correction. However, the ideas of [85, 86] can be applied to the block systems herein to extend our results further. In our computational tests, however, both grad-div stabilization and pressure correction are used. The chapter is organized as follows. Section 2 performs the analysis for YU applied to MHD while Section 3 the analysis for YUPC applied to MHD, in Section 4 we give numerical experiments to illustrate the theory and show the effectiveness of the method on a benchmark test problem, and finally in Section 5, we provide a brief summary, draw conclusion and future research directions.

6.2 Analysis of the Yosida updates method

The linear algebra analysis of the splitting methods is in terms of the vector norms of the coefficients of the variables, and not in terms of the natural norms of the finite element spaces. Thus, important constants and potential negative scalings with respect to the mesh width could be left out of the linear algebra results. We begin by presenting the numerical method related to the usual finite element discretization of the MHD equations. For simplicity of analysis, we only consider one step time discretization, and take the coupling number $s = 1$.

The exact (unapproximated) single step discrete MHD scheme is defined by: find $(\hat{u}_h, \hat{P}_h, \hat{B}_h, \hat{\lambda}_h) \in (X_h, Q_h, X_h, Q_h)$ satisfying, $\forall (v_h, q_h, \psi_h, r_h) \in (X_h, Q_h, X_h, Q_h)$,

$$\frac{\alpha}{\Delta t}(\hat{u}_h, v_h) + \nu(\nabla \hat{u}_h, \nabla v_h) + (\mathcal{U} \cdot \nabla \hat{u}_h, v_h) - (\mathcal{B} \cdot \nabla \hat{B}_h, v_h)$$
$$-(\hat{P}_h, \nabla \cdot v_h) = (\widetilde{f}, v_h), \quad (6.12)$$
$$(\nabla \cdot \hat{u}_h, q_h) = 0, \quad (6.13)$$
$$\frac{\alpha}{\Delta t}\left(\hat{B}_h, \psi_h\right) + \nu_m(\nabla \hat{B}_h, \nabla \psi_h) + (\mathcal{U} \cdot \nabla \hat{B}_h, \psi_h) - (\mathcal{B} \cdot \nabla \hat{u}_h, \psi_h)$$
$$+(\hat{\lambda}_h, \nabla \cdot \psi_h) = (\widetilde{g}, \psi_h), \quad (6.14)$$
$$(\nabla \cdot \hat{B}_h, r_h) = 0. \quad (6.15)$$

Given $(P^n, \lambda^n) \in (Q_h, Q_h)$, which are the solutions from the previous step, denote $\hat{\delta}_P := \hat{P}_h - P^n$, $\hat{\delta}_\lambda := \hat{\lambda}_h - \lambda^n$. Then the scheme (6.12)-(6.15) is equivalently written in terms of velocity, magnetic field, and updates of the Lagrange multipliers: find

$(\hat{u}_h, \hat{\delta_P}, \hat{B}_h, \hat{\delta}_\lambda) \in (X_h, Q_h, X_h, Q_h)$ such that $\forall (v_h, q_h, \psi_h, r_h) \in (X_h, Q_h, X_h, Q_h)$,

$$\frac{\alpha}{\Delta t}(\hat{u}_h, v_h) + \nu(\nabla \hat{u}_h, \nabla v_h) + (\mathcal{U} \cdot \nabla \hat{u}_h, v_h) - (\mathcal{B} \cdot \nabla \hat{B}_h, v_h)$$
$$-(\hat{\delta}_P, \nabla \cdot v_h) = (\tilde{\tilde{f}}, v_h), \quad (6.16)$$
$$(\nabla \cdot \hat{u}_h, q_h) = 0, \quad (6.17)$$
$$\frac{\alpha}{\Delta t}\left(\hat{B}_h, \psi_h\right) + \nu_m(\nabla \hat{B}_h, \nabla \psi_h) + (\mathcal{U} \cdot \nabla \hat{B}_h, \psi_h) - (\mathcal{B} \cdot \nabla \hat{u}_h, \psi_h)$$
$$+(\hat{\delta}_\lambda, \nabla \cdot \psi_h) = (\tilde{\tilde{g}}, \psi_h), \quad (6.18)$$
$$(\nabla \cdot \hat{B}_h, r_h) = 0, \quad (6.19)$$

where $\tilde{\tilde{f}} := \tilde{f} - \nabla P^n$, $\tilde{\tilde{g}} := \tilde{g} + \nabla \lambda^n$. To recover $\hat{P}_h$ and $\hat{\lambda}_h$, add the increments to the previous time step solutions: $\hat{P}_h = \hat{\delta}_P + P^n$, $\hat{\lambda}_h = \hat{\delta}_\lambda + \lambda^n$. The system (6.16)-(6.19) produces the block saddle point linear system:

$$\begin{pmatrix} A & C \\ C^T & 0 \end{pmatrix} \begin{pmatrix} \hat{X} \\ \hat{\delta}_Y \end{pmatrix} = \begin{pmatrix} F \\ 0 \end{pmatrix}, \quad (6.20)$$

where $\hat{X} = \begin{pmatrix} \hat{u} \\ \hat{B} \end{pmatrix}$, $\hat{\delta}_Y = \begin{pmatrix} \hat{\delta}_P \\ \hat{\delta}_\lambda \end{pmatrix}$, $F = \begin{pmatrix} F_1 \\ F_2 \end{pmatrix}$. Applying the Yosida splitting to the updates formulation algebraic system (6.16)-(6.19): first write the matrix A as

$$A = \begin{pmatrix} \tilde{A}_1 & 0 \\ 0 & \tilde{A}_2 \end{pmatrix} + \begin{pmatrix} \tilde{N}_1 & N_1 \\ N_2 & \tilde{N}_2 \end{pmatrix} =: \tilde{A} + \tilde{N}, \quad (6.21)$$

where $\tilde{A}$ is SPD. Now use the approximation $C^T \tilde{A}^{-1} C$ for the Schur complement

matrix $C^T A^{-1} C$, which leads to the approximation:

$$\begin{pmatrix} A & C \\ C^T & 0 \end{pmatrix} \approx \begin{pmatrix} A & 0 \\ C^T & -C^T \tilde{A}^{-1} C \end{pmatrix} \begin{pmatrix} I & A^{-1}C \\ 0 & I \end{pmatrix}. \tag{6.22}$$

With this approximation, we solve the linear system

$$\begin{pmatrix} A & 0 \\ C^T & -C^T \tilde{A}^{-1} C \end{pmatrix} \begin{pmatrix} I & A^{-1}C \\ 0 & I \end{pmatrix} \begin{pmatrix} X \\ \delta_Y \end{pmatrix} = \begin{pmatrix} F \\ 0 \end{pmatrix}, \tag{6.23}$$

with $X = \begin{pmatrix} u \\ B \end{pmatrix}$, $\delta_Y = \begin{pmatrix} \delta_P \\ \delta_\lambda \end{pmatrix}$. Solving the linear system (6.23) is equivalent to the three steps:

1. Solve $\begin{pmatrix} A_1 & N_1 \\ N_2 & A_2 \end{pmatrix} \begin{pmatrix} z_1 \\ z_2 \end{pmatrix} = \begin{pmatrix} F_1 \\ F_2 \end{pmatrix}$ for $\begin{pmatrix} z_1 \\ z_2 \end{pmatrix}$,

2a. Solve $(C_1^T \tilde{A}_1^{-1} C_1)\delta_P = C_1^T z_1$ for δ_P,

2b. Solve $(C_1^T \tilde{A}_2^{-1} C_1)\delta_\lambda = C_1^T z_2$ for δ_λ,

3. Solve $\begin{pmatrix} A_1 & N_1 \\ N_2 & A_2 \end{pmatrix} \begin{pmatrix} u \\ B \end{pmatrix} = \begin{pmatrix} A_1 & N_1 \\ N_2 & A_2 \end{pmatrix} \begin{pmatrix} z_1 \\ z_2 \end{pmatrix} - \begin{pmatrix} C_1^T & 0 \\ 0 & C_1^T \end{pmatrix} \begin{pmatrix} \delta_P \\ \delta_\lambda \end{pmatrix}$ for $\begin{pmatrix} u \\ B \end{pmatrix}$.

Finally, set $P_h = \delta_P + P^n$ and $\lambda_h = \delta_\lambda + \lambda^n$.

For analysis purposes, we define a finite element formulation that is equivalent to 3-step YU linear algebraic system above. We note that YU implementation should not be computed in this way, but as the simple linear algebraic implementation presented in the introduction.

Algorithm 6.2.1 (YU finite element formulation)**.** *Given* $(P^n, \lambda^n) \in (Q_h, Q_h)$*, we want to find* $(u_h, P_h, B_h, \lambda_h) \in (X_h, Q_h, X_h, Q_h)$ *via the following steps:*

1. *Find* $(z_h, \omega_h) \in (X_h, X_h)$ *satisfying,* $\forall (v_h, \psi_h) \in (X_h, X_h)$,

$$\frac{\alpha}{\Delta t}(z_h, v_h) + \nu(\nabla z_h, \nabla v_h) + (\mathcal{U} \cdot \nabla z_h, v_h) - (\mathcal{B} \cdot \nabla \omega_h, v_h) = (\tilde{\tilde{f}}, v_h), \quad (6.24)$$

$$\frac{\alpha}{\Delta t}(\omega_h, \psi_h) + \nu_m(\nabla \omega_h, \nabla \psi_h) + (\mathcal{U} \cdot \nabla \omega_h, \psi_h) - (\mathcal{B} \cdot \nabla z_h, \psi_h) = (\tilde{\tilde{g}}, \psi_h). \quad (6.25)$$

2. *Find* $(\chi_h, \delta_P, \mu_h, \delta_\lambda) \in (X_h, Q_h, X_h, Q_h)$ *satisfying,*
$\forall (v_h, q_h, \psi_h, r_h) \in (X_h, Q_h, X_h, Q_h)$,

$$\frac{\alpha}{\Delta t}(\chi_h, v_h) + \nu(\nabla \chi_h, \nabla v_h) - (\delta_P, \nabla \cdot v_h) = 0, \quad (6.26)$$

$$(\nabla \cdot \chi_h, q_h) = -(\nabla \cdot z_h, q_h), \quad (6.27)$$

$$\frac{\alpha}{\Delta t}(\mu_h, \psi_h) + \nu_m(\nabla \mu_h, \nabla \psi_h) + (\delta_\lambda, \nabla \cdot \psi_h) = 0, \quad (6.28)$$

$$(\nabla \cdot \mu_h, r_h) = -(\nabla \cdot \omega_h, r_h). \quad (6.29)$$

3. *Find* $(u_h, B_h) \in (X_h, X_h)$ *satisfying,* $\forall (v_h, \psi_h) \in (X_h, X_h)$,

$$\frac{\alpha}{\Delta t}(u_h, v_h) + \nu(\nabla u_h, \nabla v_h) + (\mathcal{U} \cdot \nabla u_h, v_h) - (\mathcal{B} \cdot \nabla B_h, v_h) = \frac{\alpha}{\Delta t}(z_h, v_h)$$
$$+ \nu(\nabla z_h, \nabla v_h) + (\mathcal{U} \cdot \nabla z_h, v_h) - (\mathcal{B} \cdot \nabla \omega_h, v_h) + (\delta_P, \nabla \cdot v_h), \quad (6.30)$$

$$\frac{\alpha}{\Delta t}(B_h, \psi_h) + \nu_m(\nabla B_h, \nabla \psi_h) + (\mathcal{U} \cdot \nabla B_h, \psi_h) - (\mathcal{B} \cdot \nabla u_h, \psi_h) = \frac{\alpha}{\Delta t}(\omega_h, \psi_h)$$
$$+ \nu_m(\nabla \omega_h, \nabla \psi_h) + (\mathcal{U} \cdot \nabla \omega_h, \psi_h) - (\mathcal{B} \cdot \nabla z_h, \psi_h) - (\delta_\lambda, \nabla \cdot \psi_h). \quad (6.31)$$

4. *Recover* P_h, λ_h *by setting* $P_h = \delta_P + P^n$ *and* $\lambda_h = \delta_\lambda + \lambda^n$.

Remark 6.2.1. *Combining Step 1 and Step 3 of Algorithm 6.2.1 produces*

$$\frac{\alpha}{\Delta t}(u_h, v_h) + \nu(\nabla u_h, \nabla v_h) + (\mathcal{U} \cdot \nabla u_h, v_h) - (\mathcal{B} \cdot \nabla B_h, v_h) \\ -(\delta_P, \nabla \cdot v_h,) = (\tilde{\tilde{f}}, v_h), \tag{6.32}$$

$$\frac{\alpha}{\Delta t}(B_h, \psi_h) + \nu_m(\nabla B_h, \nabla \psi_h) + (\mathcal{U} \cdot \nabla B_h, \psi_h) - (\mathcal{B} \cdot \nabla u_h, \psi_h) \\ +(\delta_\lambda, \nabla \cdot \psi_h) = (\tilde{\tilde{g}}, \psi_h). \tag{6.33}$$

Replacing $\tilde{\tilde{f}}$, $\tilde{\tilde{g}}$, δ_P and δ_λ by their definitions and recombining gives, for any v_h or $\psi_h \in X_h$,

$$\frac{\alpha}{\Delta t}(u_h, v_h) + \nu(\nabla u_h, \nabla v_h) + (\mathcal{U} \cdot \nabla u_h, v_h) - (\mathcal{B} \cdot \nabla B_h, v_h) \\ -(P_h, \nabla \cdot v_h) = (\tilde{f}, v_h), \tag{6.34}$$

$$\frac{\alpha}{\Delta t}(B_h, \psi_h) + \nu_m(\nabla B_h, \nabla \psi_h) + (\mathcal{U} \cdot \nabla B_h, \psi_h) - (\mathcal{B} \cdot \nabla u_h, \psi_h) \\ +(\lambda_h, \nabla \cdot \psi_h) = (\tilde{g}, \psi_h), \tag{6.35}$$

which shows that the YU method preserves the momentum and magnetic field evolution equations.

We now prove that the solutions of the Yosida updates method converge to the solutions of the unaltered discrete scheme (6.16)-(6.19). For simplicity of the analysis, we assume that $\alpha = 1$ and the convective velocity $\mathcal{U}$ from (6.1) and the magnetic field $\mathcal{B}$ from (6.3) satisfy $\nabla \cdot \mathcal{U} = 0$ with $\|\mathcal{U}\|_{L^\infty(\Omega)} \leq C_U < \infty$ and $\nabla \cdot \mathcal{B} = 0$ with $\|\mathcal{B}\|_{L^\infty(\Omega)} \leq C_B < \infty$. Extension to the case of only weakly divergence-free $\mathcal{U}$ and $\mathcal{B}$ can be done by skew-symmetrizing the nonlinear terms, and if these variables

have only $H^1(\Omega)$ regularity then different Hölder and Sobolev bounds could be used. Neither of these changes would affect convergence rates in Δt, but could affect the scaling with the mesh width h.

Theorem 6. *Let $\hat{u}_h, \hat{P}_h, \hat{B}_h$ and $\hat{\lambda}_h$ be the solution of* (6.12)-(6.15) *(the unapproximated linear system solution), and u_h, P_h, B_h, λ_h the solutions to Algorithm 6.2.1 (the YU solution). Further, assume that the pressure solutions of the unapproximated solution satisfy $\|\hat{P}_h - P^n\| \leq C_P \Delta t$, $\|\hat{\lambda}_h - \lambda^n\| \leq C_\lambda \Delta t$. Then the error in YU satisfies*

$$\begin{aligned}\|\hat{u}_h - u_h\| + \|\hat{B}_h - B_h\| \\ \leq \frac{2C_i^3 \Delta t^3}{\beta h^3}\left(C_U + C_B\right)\left(C_P + C_\lambda\right)\left(2C_{PF} + \frac{C_* C_i \Delta t}{h}\right) = O(\Delta t^3),\end{aligned}$$

where $C_* := \min\{\nu, \nu_m\}$.

Remark 6.2.2. *The negative scaling with respect to h arises due to use of the inverse inequality, as to find the $O(\Delta t^3)$, it was necessary to bound H^1 terms from the right hand side, in L^2 terms on the left hand side. The negative dependence on h could be reduced or even eliminated in the analysis, but this would in turn lower the order of convergence with respect to Δt. However, it was observed for the YU applied to the NSE that the negative scaling of h on several test problems was much milder, $O(h^{-1/2})$, instead of $O(h^{-3})$. In our convergence rate tests, we observed no negative scaling with h, although we did observe some slight deterioration of the third order convergence with respect to Δt.*

Proof. The proof is rather long, and we split it up into three major steps. Denote

$e_u := \hat{u}_h - u_h$, $e_B := \hat{B}_h - B_h$, and note that

$$\hat{P}_h - P_h = (\hat{P}_h - P^n) - (P_h - P^n) =: \hat{\delta}_P - \delta_P,$$
$$\hat{\lambda}_h - \lambda_h = (\hat{\lambda}_h - \lambda^n) - (\lambda_h - \lambda^n) =: \hat{\delta}_\lambda - \delta_\lambda.$$

Step 1: Claim:

$$\|e_u\| + \|e_B\| \leq \frac{\sqrt{2}C_i\Delta t}{h}\left(\|\hat{\delta}_P - \delta_P\| + \|\hat{\delta}_\lambda - \delta_\lambda\|\right). \tag{6.36}$$

Begin by subtracting (6.32) from (6.16) and (6.33) from (6.18), which gives

$$\frac{1}{\Delta t}(e_u, v_h) + \nu(\nabla e_u, \nabla v_h) + (\mathcal{U}\cdot\nabla e_u, v_h) - (\mathcal{B}\cdot\nabla e_B, v_h) - (\hat{\delta}_P - \delta_P, \nabla\cdot v_h) = 0,$$
$$\frac{1}{\Delta t}(e_B, \psi_h) + \nu_m(\nabla e_B, \nabla\psi_h) + (\mathcal{U}\cdot\nabla e_B, \psi_h) - (\mathcal{B}\cdot\nabla e_u, \psi_h) + (\hat{\delta}_\lambda - \delta_\lambda, \nabla\cdot\psi_h) = 0.$$

Setting $v_h = e_u$ and $\psi_h = e_B$ yields $(\mathcal{U}\cdot\nabla e_u, e_u) = 0$, $(\mathcal{U}\cdot\nabla e_B, e_B) = 0$ since $\nabla\cdot\mathcal{U} = 0$ [59]. Then using Cauchy-Schwarz and Young's inequalities along with the inverse inequality provides

$$\begin{aligned}
\frac{1}{\Delta t}\|e_u\|^2 + \nu\|\nabla e_u\|^2 &\leq (\mathcal{B}\cdot\nabla e_B, e_u) + \|\hat{\delta}_P - \delta_P\|\|\nabla\cdot e_u\| \\
&\leq (\mathcal{B}\cdot\nabla e_B, e_u) + \|\hat{\delta}_P - \delta_P\|\|\nabla e_u\| \\
&\leq (\mathcal{B}\cdot\nabla e_B, e_u) + \frac{C_i}{h}\|\hat{\delta}_P - \delta_P\|\|e_u\| \\
&\leq (\mathcal{B}\cdot\nabla e_B, e_u) + \frac{1}{2\Delta t}\|e_u\|^2 + \frac{C_i^2\Delta t}{2h^2}\|\hat{\delta}_P - \delta_P\|^2, \qquad (6.37) \\
\frac{1}{\Delta t}\|e_B\|^2 + \nu_m\|\nabla e_B\|^2 &\leq (\mathcal{B}\cdot\nabla e_u, e_B) + \|\hat{\delta}_\lambda - \delta_\lambda\|\|\nabla\cdot e_B\| \\
&\leq (\mathcal{B}\cdot\nabla e_u, e_B) + \frac{C_i}{h}\|\hat{\delta}_\lambda - \delta_\lambda\|\|e_B\| \\
&\leq (\mathcal{B}\cdot\nabla e_u, e_B) + \frac{1}{2\Delta t}\|e_B\|^2 + \frac{C_i^2\Delta t}{2h^2}\|\hat{\delta}_\lambda - \delta_\lambda\|^2. \qquad (6.38)
\end{aligned}$$

Next, sum (6.37) and (6.38). Notice that $(\mathcal{B}\cdot\nabla e_B, e_u) = -(\mathcal{B}\cdot\nabla e_u, e_B)$, and after dropping the viscous terms on the left hand side, we find that

$$\|e_u\|^2 + \|e_B\|^2 \leq \frac{C_i^2\Delta t^2}{h^2}\left(\|\hat{\delta}_P - \delta_P\|^2 + \|\hat{\delta}_\lambda - \delta_\lambda\|^2\right),$$

and taking square root of both sides gives the claimed bound.

Step 2: Claim:

$$\begin{aligned}
&\|\hat{\delta}_P - \delta_P\| + \|\hat{\delta}_\lambda - \delta_\lambda\| \\
&\quad\leq \beta^{-1}\left(C_U + C_B\right)\left(2C_{PF} + \frac{C_* C_i \Delta t}{h}\right)\left(\|\nabla(\hat{u}_h - z_h)\| + \|\nabla(\hat{B}_h - \omega_h)\|\right) \\
&\quad\leq \frac{C_i}{\beta h}\left(C_U + C_B\right)\left(2C_{PF} + \frac{C_* C_i \Delta t}{h}\right)\left(\|\hat{u}_h - z_h\| + \|\hat{B}_h - \omega_h\|\right). \quad (6.39)
\end{aligned}$$

For this step of the proof, begin by adding Step 1 and Step 2 from the Yosida updates algorithm to obtain

$$\begin{aligned}
\frac{1}{\Delta t}(\chi_h + z_h, v_h) + \nu(\nabla(\chi_h + z_h), \nabla v_h) + (\mathcal{U}\cdot\nabla z_h, v_h) \\
-(\mathcal{B}\cdot\nabla\omega_h, v_h) - (\delta_P, \nabla\cdot v_h) = (\tilde{\tilde{f}}, v_h), \\
(\nabla\cdot(\chi_h + z_h), q_h) = 0, \\
\frac{1}{\Delta t}(\mu_h + \omega_h, \psi_h) + \nu_m(\nabla(\mu_h + \omega_h), \nabla\psi_h) + (\mathcal{U}\cdot\nabla\omega_h, \psi_h) \\
-(\mathcal{B}\cdot\nabla z_h, \psi_h) + (\delta_\lambda, \nabla\cdot\psi_h) = (\tilde{\tilde{g}}, \psi_h), \\
(\nabla\cdot(\mu_h + \omega_h), r_h) = 0.
\end{aligned}$$

Subtracting this system from the unapproximated MHD system (6.16)-(6.19) yields

$$\frac{1}{\Delta t}(\hat{u}_h - (\chi_h + z_h), v_h) + \nu(\nabla(\hat{u}_h - (\chi_h + z_h)), \nabla v_h) + (\mathcal{U} \cdot \nabla(\hat{u}_h - z_h), v_h) - (\mathcal{B} \cdot \nabla(\hat{B}_h - \omega_h), v_h) - (\hat{\delta}_P - \delta_P, \nabla \cdot v_h) = 0, \quad (6.40)$$

$$(\nabla \cdot (\hat{u}_h - (\chi_h + z_h)), q_h) = 0, \quad (6.41)$$

$$\frac{1}{\Delta t}(\hat{B}_h - (\mu_h + \omega_h), \psi_h) + \nu_m(\nabla(\hat{B}_h - (\mu_h + \omega_h)), \nabla \psi_h) + (\mathcal{U} \cdot \nabla(\hat{B}_h - \omega_h), \psi_h) - (\mathcal{B} \cdot \nabla(\hat{u}_h - z_h), \psi_h) + (\hat{\delta}_\lambda - \delta_\lambda, \nabla \cdot \psi_h) = 0, \quad (6.42)$$

$$(\nabla \cdot (\hat{B}_h - (\mu_h + \omega_h)), r_h) = 0. \quad (6.43)$$

Now isolate the pressure error in (6.40), and divide both sides by $\|\nabla v_h\|$. Then using the Cauchy-Schwarz and Hölder's inequalities produces

$$\frac{\left(\hat{\delta}_P - \delta_P, \nabla \cdot v_h\right)}{\|\nabla v_h\|} \leq \frac{1}{\Delta t} \frac{\|\hat{u}_h - (\chi_h + z_h)\| \|v_h\|}{\|\nabla v_h\|} + \frac{\nu \|\nabla(\hat{u}_h - (\chi_h + z_h))\| \|\nabla v_h\|}{\|\nabla v_h\|} + \frac{\|\mathcal{U}\|_{L^\infty} \|\nabla(\hat{u}_h - z_h)\| \|v_h\|}{\|\nabla v_h\|} + \frac{\|\mathcal{B}\|_{L^\infty} \|\nabla(\hat{B}_h - \omega_h)\| \|v_h\|}{\|\nabla v_h\|}. \quad (6.44)$$

Similarly, we can get the following from (6.42):

$$\frac{\left(\hat{\delta}_\lambda - \delta_\lambda, \nabla \cdot \psi_h\right)}{\|\nabla \psi_h\|} \leq \frac{1}{\Delta t} \frac{\|\hat{B}_h - (\mu_h + \omega_h)\| \|\psi_h\|}{\|\nabla \psi_h\|} + \frac{\nu_m \|\nabla(\hat{B}_h - (\mu_h + \omega_h))\| \|\nabla \psi_h\|}{\|\nabla \psi_h\|} + \frac{\|\mathcal{U}\|_{L^\infty} \|\nabla(\hat{B}_h - \omega_h)\| \|\psi_h\|}{\|\nabla \psi_h\|} + \frac{\|\mathcal{B}\|_{L^\infty} \|\nabla(\hat{u}_h - z_h)\| \|\psi_h\|}{\|\nabla \psi_h\|}. \quad (6.45)$$

Using the LBB condition together with the Poincaré-Friedrich's inequality and reducing gives the estimates

$$\beta\|\hat{\delta}_P - \delta_P\| \leq \frac{C_{PF}}{\Delta t}\|\hat{u}_h - (\chi_h + z_h)\| + \nu\|\nabla(\hat{u}_h - (\chi_h + z_h))\| + C_{PF}C_U\|\nabla(\hat{u}_h - z_h)\| + C_{PF}C_B\|\nabla(\hat{B}_h - \omega_h)\|, \quad (6.46)$$

and

$$\beta\|\hat{\delta}_\lambda - \delta_\lambda\| \leq \frac{C_{PF}}{\Delta t}\|\hat{B}_h - (\mu_h + \omega_h)\| + \nu_m\|\nabla(\hat{B}_h - (\mu_h + \omega_h))\| + C_{PF}C_U\|\nabla(\hat{B}_h - \omega_h)\| + C_{PF}C_B\|\nabla(\hat{u}_h - z_h)\|. \quad (6.47)$$

After applying the inverse inequality to the second right hand side terms of (6.46)-(6.47), sum them to get

$$\begin{aligned}\|\hat{\delta}_P - \delta_P\| + \|\hat{\delta}_\lambda - \delta_\lambda\| &\leq \beta^{-1}\Bigg[\left(\frac{C_{PF}}{\Delta t} + \frac{C_* C_i}{h}\right)\Big(\|\hat{u}_h - (\chi_h + z_h)\| + \|\hat{B}_h - (\mu_h + \omega_h)\|\Big) \\ &\quad + C_{PF}(C_U + C_B)\Big(\|\nabla(\hat{u}_h - z_h)\| + \|\nabla(\hat{B}_h - \omega_h)\|\Big)\Bigg], \quad (6.48)\end{aligned}$$

where $C_* = \min\{\nu, \nu_m\}$.

Next, set $v_h = \hat{u}_h - (\chi_h + z_h)$ in (6.40), $q_h = \hat{\delta}_P - \delta_P$ in (6.41), $\psi_h = \hat{B}_h - (\mu_h + \omega_h)$

in (6.42), and $r_h = \hat{\delta}_\lambda - \delta_\lambda$ in (6.43). Apply Hölder's inequality to produce

$$\begin{aligned}
&\frac{1}{\Delta t}\|\hat{u}_h - (\chi_h + z_h)\|^2 + \nu\|\nabla(\hat{u}_h - (\chi_h + z_h))\|^2 \\
&\leq \|\mathcal{U}\|_{L^\infty}\|\nabla(\hat{u}_h - z_h)\|\|\hat{u}_h - (\chi_h + z_h)\| + \|\mathcal{B}\|_{L^\infty}\|\nabla(\hat{B}_h - \omega_h)\|\|\hat{u}_h - (\chi_h + z_h)\| \\
&\qquad = \Big(C_U\|\nabla(\hat{u}_h - z_h)\| + C_B\|\nabla(\hat{B}_h - \omega_h)\|\Big)\,\|\hat{u}_h - (\chi_h + z_h)\|,
\end{aligned}$$

and

$$\begin{aligned}
&\frac{1}{\Delta t}\|\hat{B}_h - (\mu_h + \omega_h)\|^2 + \nu_m\|\nabla(\hat{B}_h - (\mu_h + \omega_h))\|^2 \\
&\leq \|\mathcal{U}\|_{L^\infty}\|\nabla(\hat{B}_h - \omega_h)\|\|\hat{B}_h - (\mu_h + \omega_h)\| + \|\mathcal{B}\|_{L^\infty}\|\nabla(\hat{u}_h - z_h)\|\|\hat{B}_h - (\mu_h + \omega_h)\| \\
&\qquad = \Big(C_U\|\nabla(\hat{B}_h - \omega_h)\| + C_B\|\nabla(\hat{u}_h - z_h)\|\Big)\,\|\hat{B}_h - (\mu_h + \omega_h)\|.
\end{aligned}$$

Reducing the terms produces

$$\|\hat{u}_h - (\chi_h + z_h)\| \leq \Delta t\left(C_U\|\nabla(\hat{u}_h - z_h)\| + C_B\|\nabla(\hat{B}_h - \omega_h)\|\right), \tag{6.49}$$

and

$$\|\hat{B}_h - (\mu_h + \omega_h)\| \leq \Delta t\left(C_U\|\nabla(\hat{B}_h - \omega_h)\| + C_B\|\nabla(\hat{u}_h - z_h)\|\right). \tag{6.50}$$

Now sum (6.49) and (6.50) to get the estimate

$$\begin{aligned}
&\|\hat{u}_h - (\chi_h + z_h)\| + \|\hat{B}_h - (\mu_h + \omega_h)\| \\
&\qquad \leq \Delta t(C_U + C_B)\Big(\|\nabla(\hat{u}_h - z_h)\| + \|\nabla(\hat{B}_h - \omega_h)\|\Big).
\end{aligned} \tag{6.51}$$

Finally, using (6.51) in (6.48) together with the inverse inequality yields

$$\begin{aligned}
&\|\hat{\delta}_P - \delta_P\| + \|\hat{\delta}_\lambda - \delta_\lambda\| \\
&\quad \leq \beta^{-1}\Bigg[\left(C_{PF} + \frac{C_* C_i \Delta t}{h}\right)(C_U + C_B)\Big(\|\nabla(\hat{u}_h - z_h)\| + \|\nabla(\hat{B}_h - \omega_h)\|\Big) \\
&\qquad\qquad + C_{PF}(C_U + C_B)\Big(\|\nabla(\hat{u}_h - z_h)\| + \|\nabla(\hat{B}_h - \omega_h)\|\Big)\Bigg] \\
&\quad = \beta^{-1}\Big(C_U + C_B\Big)\left(2C_{PF} + \frac{C_* C_i \Delta t}{h}\right)\Big(\|\nabla(\hat{u}_h - z_h)\| + \|\nabla(\hat{B}_h - \omega_h)\|\Big) \\
&\qquad \leq \frac{C_i}{\beta h}\Big(C_U + C_B\Big)\left(2C_{PF} + \frac{C_* C_i \Delta t}{h}\right)\Big(\|\hat{u}_h - z_h\| + \|\hat{B}_h - \omega_h\|\Big), \quad (6.52)
\end{aligned}$$

which proves the stated second claim.

Step 3: Completion of the proof

It remains to bound the terms $\|\hat{u}_h - z_h\|$ and $\|\hat{B}_h - \omega_h\|$ to get our stated result in the theorem. Subtract (6.24) from (6.16), and (6.25) from (6.18) to obtain

$$\begin{aligned}
&\frac{1}{\Delta t}(\hat{u}_h - z_h, v_h) + \nu(\nabla(\hat{u}_h - z_h), \nabla v_h) \\
&+(\mathcal{U}\cdot\nabla(\hat{u}_h - z_h), v_h) = (\mathcal{B}\cdot\nabla(\hat{B}_h - \omega_h), v_h) + (\hat{\delta}_P, \nabla\cdot v_h), \quad (6.53)
\end{aligned}$$

$$\begin{aligned}
&\frac{1}{\Delta t}(\hat{B}_h - \omega_h, \psi_h) + \nu_m(\nabla(\hat{B}_h - \omega_h), \nabla\psi_h) \\
&+(\mathcal{U}\cdot\nabla(\hat{B}_h - \omega_h), \psi_h) = (\mathcal{B}\cdot\nabla(\hat{u}_h - z_h), \psi_h) - (\hat{\delta}_\lambda, \nabla\cdot\psi_h). \quad (6.54)
\end{aligned}$$

Setting $v_h = \hat{u}_h - z_h$ in (6.53) and $\psi_h = \hat{B}_h - \omega_h$ (6.54) vanishes the nonlinear terms $(\mathcal{U}\cdot\nabla(\hat{u}_h - z_h), \hat{u}_h - z_h)$ and $(\mathcal{U}\cdot\nabla(\hat{B}_h - \omega_h), \hat{B}_h - \omega_h)$ since $\nabla\cdot\mathcal{U} = 0$. The equations

(6.53) and (6.54) are then reduced to

$$\frac{1}{\Delta t}\|\hat{u}_h - z_h\|^2 + \nu\|\nabla(\hat{u}_h - z_h)\|^2 \\ = (\mathcal{B}\cdot\nabla(\hat{u}_h - \omega_h), \hat{u}_h - z_h) + (\hat{\delta}_P, \nabla\cdot(\hat{u}_h - z_h)), \tag{6.55}$$

$$\frac{1}{\Delta t}\|\hat{B}_h - \omega_h\|^2 + \nu_m\|\nabla(\hat{B}_h - \omega_h)\|^2 \\ = (\mathcal{B}\cdot\nabla(\hat{u}_h - z_h), \hat{B}_h - \omega_h) - (\hat{\delta}_\lambda, \nabla\cdot(\hat{B}_h - \omega_h)). \tag{6.56}$$

Now apply the Cauchy-Schwarz, Young's and the inverse inequalities on the second right hand side term of (6.55) and (6.56) to get

$$\frac{1}{\Delta t}\|\hat{u}_h - z_h\|^2 + \nu\|\nabla(\hat{u}_h - z_h)\|^2 \leq (\mathcal{B}\cdot\nabla(\hat{B}_h - \omega_h), \hat{u}_h - z_h) \\ + \frac{1}{2\Delta t}\|\hat{u}_h - z_h\|^2 + \frac{C_i^2\Delta t}{2h^2}\|\hat{\delta}_P\|^2,$$

$$\frac{1}{\Delta t}\|\hat{B}_h - \omega_h\|^2 + \nu_m\|\nabla(\hat{B}_h - \omega_h)\|^2 \leq (\mathcal{B}\cdot\nabla(\hat{u}_h - z_h), \hat{B}_h - \omega_h) \\ + \frac{1}{2\Delta t}\|\hat{B}_h - \omega_h\|^2 + \frac{C_i^2\Delta t}{2h^2}\|\hat{\delta}_\lambda\|^2.$$

Rearranging terms now yields

$$\|\hat{u}_h - z_h\|^2 + 2\nu\Delta t\|\nabla(\hat{u}_h - z_h)\|^2 \\ \leq 2\Delta t(\mathcal{B}\cdot\nabla(\hat{B}_h - \omega_h), \hat{u}_h - z_h) + \frac{C_i^2\Delta t^2}{h^2}\|\hat{\delta}_P\|^2, \tag{6.57}$$

$$\|\hat{B}_h - \omega_h\|^2 + 2\nu_m \Delta t \|\nabla(\hat{B}_h - \omega_h)\|^2 \\ \leq 2\Delta t(\mathcal{B}\cdot\nabla(\hat{u}_h - z_h), \hat{B}_h - \omega_h) + \frac{C_i^2 \Delta t^2}{h^2}\|\hat{\delta}_\lambda\|^2. \tag{6.58}$$

Notice that $(\mathcal{B}\cdot\nabla(\hat{B}_h - \omega_h), \hat{u}_h - z_h) = -(\mathcal{B}\cdot\nabla(\hat{u}_h - z_h), \hat{B}_h - \omega_h)$ since $\nabla\cdot\mathcal{B} = 0$, so by summing (6.57), (6.58), and using the assumptions $\|\hat{\delta}_P\| \leq C_P\Delta t, \|\hat{\delta}_\lambda\| \leq C_\lambda \Delta t$, we find that

$$\|\hat{u}_h - z_h\|^2 + \|\hat{B}_h - \omega_h\|^2 \leq \frac{C_i^2\Delta t^2}{h^2}\bigg(\|\hat{\delta}_P\|^2 + \|\hat{\delta}_\lambda\|^2\bigg) \leq \frac{C_i^2\Delta t^4}{h^2}\bigg(C_P^2 + C_\lambda^2\bigg),$$

which after taking square root of both sides produces

$$\|\hat{u}_h - z_h\| + \|\hat{B}_h - \omega_h\| \leq \frac{\sqrt{2}C_i\Delta t^2}{h}\bigg(C_P + C_\lambda\bigg). \tag{6.59}$$

To finish the proof, use (6.59) in (6.52), which gives the bound

$$\|\hat{\delta}_P - \delta_P\| + \|\hat{\delta}_\lambda - \delta_\lambda\| \\ \leq \frac{\sqrt{2}C_i^2\Delta t^2}{\beta h^2}\bigg(C_U + C_B\bigg)\bigg(C_P + C_\lambda\bigg)\bigg(2C_{PF} + \frac{C_* C_i \Delta t}{h}\bigg), \tag{6.60}$$

and finally use (6.60) in (6.36). □

Lemma 6.2.1 (Stability of YU)**.** *Assume $\tilde{f} = f + \frac{1}{\Delta t}u^n$ and $\tilde{g} = g + \frac{1}{\Delta t}B^n$ (i.e. the backward Euler case). Then if $\Delta t \leq O(h^{4/3}) \leq O(h)$, the Yosida updates method is stable, and solutions satisfies*

$$\frac{1}{\Delta t}\left(\|u_h\|^2 - \|u^n\|^2 + \|u_h - u^n\|^2\right) + \frac{1}{\Delta t}\left(\|B_h\|^2 - \|B^n\|^2 + \|B_h - B^n\|^2\right) \\ + \nu\|\nabla u_h\|^2 + \nu_m\|\nabla B_h\|^2 \leq C(data).$$

Proof. Setting $v_h = u_h$ in (6.34), $\psi_h = B_h$ in (6.35) and using the definition of $\tilde{f}$ and $\tilde{g}$ gives the following:

$$\frac{1}{2\Delta t}\left(\|u_h\|^2 - \|u^n\|^2 + \|u_h - u^n\|^2\right) + \nu\|\nabla u_h\|^2 = (\mathcal{B}\cdot\nabla B_h, u_h) + (P_h, \nabla\cdot u_h) + (f, u_h), \tag{6.61}$$

$$\frac{1}{2\Delta t}\left(\|B_h\|^2 - \|B^n\|^2 + \|B_h - B^n\|^2\right) + \nu_m\|\nabla B_h\|^2 = (\mathcal{B}\cdot\nabla u_h, B_h) - (\lambda_h, \nabla\cdot B_h) + (\nabla\times g, B_h). \tag{6.62}$$

Notice that $(P_h, \nabla\cdot\hat{u}_h) = 0$ and $(\lambda_h, \nabla\cdot\hat{B}_h) = 0$ since $\hat{u}_h, \hat{B}_h \in V_h$. Now add these terms to the right hand side of (6.61) and (6.62), respectively. Then apply the Cauchy-Schwarz, Young's inequalities on the forcing terms and Cauchy-Schwarz, Young's inequality together with the inverse inequality to the second right hand side terms, which produces

$$\begin{aligned}
&\frac{1}{2\Delta t}(\|u_h\|^2 - \|u^n\|^2 + \|u_h - u^n\|^2) + \nu\|\nabla u_h\|^2 \\
&\qquad = (\mathcal{B}\cdot\nabla B_h, u_h) - (P_h, \nabla\cdot(\hat{u}_h - u_h)) + (f, u_h) \\
&\qquad \le (\mathcal{B}\cdot\nabla B_h, u_h) + \|P_h\|\|\nabla\cdot(\hat{u}_h - u_h)\| + \|f\|_{-1}\|\nabla u_h\| \\
&\qquad \le (\mathcal{B}\cdot\nabla B_h, u_h) + \frac{C_i}{h}\|P_h\|\|\hat{u}_h - u_h\| + \frac{\nu^{-1}}{2}\|f\|_{-1}^2 + \frac{\nu}{2}\|\nabla u_h\|^2 \\
&\qquad \le (\mathcal{B}\cdot\nabla B_h, u_h) + \frac{C\Delta t^3}{h^4}\|P_h\| + \frac{\nu^{-1}}{2}\|f\|_{-1}^2 + \frac{\nu}{2}\|\nabla u_h\|^2,
\end{aligned} \tag{6.63}$$

and similarly

$$\begin{aligned}
&\frac{1}{2\Delta t}(\|B_h\|^2 - \|B^n\|^2 + \|B_h - B^n\|^2) + \nu_m\|\nabla B_h\|^2 \\
&\qquad \le (\mathcal{B}\cdot\nabla u_h, B_h) + \frac{C\Delta t^3}{h^4}\|\lambda_h\| + \frac{\nu_m^{-1}}{2}\|\nabla\times g\|_{-1}^2 + \frac{\nu_m}{2}\|\nabla B_h\|^2,
\end{aligned} \tag{6.64}$$

where C is a constant independent of h and Δt. Sum (6.63) and (6.64) and notice that $(\mathcal{B}\cdot\nabla u_h, B_h) = -(\mathcal{B}\cdot\nabla B_h, u_h)$, Then multiplying by 2 produces

$$\frac{1}{\Delta t}(\|u_h\|^2 - \|u^n\|^2 + \|u_h - u^n\|^2) + \frac{1}{\Delta t}\left(\|B_h\|^2 - \|B^n\|^2 + \|B_h - B^n\|^2\right) + \nu\|\nabla u_h\|^2 + \nu_m\|\nabla B_h\|^2 \leq \frac{C\Delta t^3}{h^4}\left(\|P_h\| + \|\lambda_h\|\right) + \nu^{-1}\|f\|_{-1}^2 + \nu_m^{-1}\|\nabla\times g\|_{-1}^2.$$

We now bound the term $(\|P_h\| + \|\lambda_h\|)$. Adding $\pm\hat{P}^n$, $\pm\hat{\lambda}^n$, and applying the triangle inequality along with (6.52) provides

$$\begin{aligned}\|P_h\| + \|\lambda_h\| &= \|\hat{P}_h + P_h - \hat{P}_h\| + \|\hat{\lambda}_h + \lambda_h - \hat{\lambda}_h\| \\ &\leq \|\hat{P}_h\| + \|\hat{\lambda}_h\| + \|\hat{\delta}_P - \delta_P\| + \|\hat{\delta}_\lambda - \delta_\lambda\| \leq C\left(1 + \frac{\Delta t^2}{h^2}\right), \qquad (6.65)\end{aligned}$$

where C is a constant independent of Δt and h. Then using the assumption $\Delta t \leq O(h^{4/3}) \leq O(h)$ in (6.65) gives the desired stability bound. □

6.3 The Yosida updates pressure correction (YUPC) method

The addition of pressure correction to Yosida algorithms has been shown by Veneziani et. al [32, 87] to increase the order of accuracy of the solver. We now consider pressure correction applied to the YU method, which we call the Yosida-updates pressure correction (YUPC) method, and show it is $O(\Delta t^4)$ accurate.

YUPC is defined by applying the pressure-corrected Yosida method to (6.16)-

(6.19): Find approximations $u_h, \delta_P, B_h, \delta_\lambda$ satisfying

$$\begin{pmatrix} A & 0 \\ C^T & -C^T\tilde{A}^{-1}C \end{pmatrix} \begin{pmatrix} I & A^{-1}C \\ 0 & Q \end{pmatrix} \begin{pmatrix} X \\ \delta_Y \end{pmatrix} = \begin{pmatrix} F \\ 0 \end{pmatrix}, \tag{6.66}$$

where $X = \begin{pmatrix} u \\ B \end{pmatrix}$, $\delta_Y = \begin{pmatrix} \delta_P \\ \delta_\lambda \end{pmatrix}$, with $Q := (C^T\tilde{A}^{-1}A\tilde{A}^{-1}C)^{-1}(C^T\tilde{A}^{-1}C)$. Finding approximations for $u, \delta_P, B, \delta_\lambda$ is equivalent to 6-steps:

1. Solve $\begin{pmatrix} A_1 & N_1 \\ N_2 & A_2 \end{pmatrix} \begin{pmatrix} z_1 \\ z_2 \end{pmatrix} = \begin{pmatrix} F_1 \\ F_2 \end{pmatrix}$ for $\begin{pmatrix} z_1 \\ z_2 \end{pmatrix}$,

2. Solve $\begin{pmatrix} C_1^T\tilde{A}_1^{-1}C_1 & 0 \\ 0 & C_1^T\tilde{A}_2^{-1}C_1 \end{pmatrix} \begin{pmatrix} q_1 \\ q_2 \end{pmatrix} = \begin{pmatrix} C_1^T & 0 \\ 0 & C_1^T \end{pmatrix} \begin{pmatrix} z_1 \\ z_2 \end{pmatrix}$ for $\begin{pmatrix} q_1 \\ q_2 \end{pmatrix}$,

3. Solve $\begin{pmatrix} \tilde{A}_1 & 0 \\ 0 & \tilde{A}_2 \end{pmatrix} \begin{pmatrix} \phi_1 \\ \phi_2 \end{pmatrix} = \begin{pmatrix} C_1 & 0 \\ 0 & C_2 \end{pmatrix} \begin{pmatrix} q_1 \\ q_2 \end{pmatrix}$ for $\begin{pmatrix} \phi_1 \\ \phi_2 \end{pmatrix}$.

4. Solve $\begin{pmatrix} \tilde{A}_1 & 0 \\ 0 & \tilde{A}_2 \end{pmatrix} \begin{pmatrix} \psi_1 \\ \psi_2 \end{pmatrix} = \begin{pmatrix} A_1 & N_1 \\ N_2 & A_2 \end{pmatrix} \begin{pmatrix} \phi_1 \\ \phi_2 \end{pmatrix}$ for $\begin{pmatrix} \psi_1 \\ \psi_2 \end{pmatrix}$.

5. Solve $\begin{pmatrix} C_1^T\tilde{A}_1^{-1}C_1 & 0 \\ 0 & C_1^T\tilde{A}_2^{-1}C_1 \end{pmatrix} \begin{pmatrix} \delta_P \\ \delta_\lambda \end{pmatrix} = \begin{pmatrix} C_1^T & 0 \\ 0 & C_1^T \end{pmatrix} \begin{pmatrix} z_1 \\ z_2 \end{pmatrix}$ for $\begin{pmatrix} \delta_P \\ \delta_\lambda \end{pmatrix}$,

6. Solve $\begin{pmatrix} A_1 & N_1 \\ N_2 & A_2 \end{pmatrix} \begin{pmatrix} u \\ B \end{pmatrix} = \begin{pmatrix} A_1 & N_1 \\ N_2 & A_2 \end{pmatrix} \begin{pmatrix} z_1 \\ z_2 \end{pmatrix} - \begin{pmatrix} C_1 & 0 \\ 0 & C_1 \end{pmatrix} \begin{pmatrix} \delta_P \\ \delta_\lambda \end{pmatrix}$ for $\begin{pmatrix} u \\ B \end{pmatrix}$.

Then set $P_h = \delta_P + P^n$ and $\lambda_h = \delta_\lambda + \lambda^n$.

Remark 6.3.1. *The additional work resulting form the YUPC method is to solve a second pressure-update solution with Q. This produces three additional steps: one step is solved with the SPD Yosida Schur complement and the other two steps with $\tilde{A}$. Thus it is not a major expense to apply pressure correction.*

In order to analyze the method, we now cast it into a finite element framework. We note that this is for analysis purposed only, and implementation of YUPC should only be considered from a linear algebraic viewpoint.

Algorithm 6.3.1 (YUPC)**.** .

Given $(P^n, \lambda^n) \in (Q_h, Q_h)$, find $(u_h, P_h, B_h, \lambda_h) \in (X_h, Q_h, X_h, Q_h)$ via the following steps:

1. *Find $(z_h, \omega_h) \in (X_h, X_h)$ satisfying, $\forall (v_h, \psi_h) \in (X_h, X_h)$,*

$$\frac{\alpha}{\Delta t}(z_h, v_h) + \nu(\nabla z_h, \nabla v_h) + (\mathcal{U} \cdot \nabla z_h, v_h) - (\mathcal{B} \cdot \nabla \omega_h, v_h) = (\tilde{\tilde{f}}, v_h), \quad (6.67)$$

$$\frac{\alpha}{\Delta t}(\omega_h, \psi_h) + \nu_m(\nabla \omega_h, \nabla \psi_h) + (\mathcal{U} \cdot \nabla \omega_h, \psi_h) - (\mathcal{B} \cdot \nabla z_h, \psi_h) = (\tilde{\tilde{g}}, \psi_h). \quad (6.68)$$

2. *Find $(\chi_h, p_h, \mu_h, \pi_h) \in (X_h, Q_h, X_h, Q_h)$ satisfying,*
   $\forall (v_h, q_h, \psi_h, r_h) \in (X_h, Q_h, X_h, Q_h)$,

$$\frac{\alpha}{\Delta t}(\chi_h, v_h) + \nu(\nabla \chi_h, \nabla v_h) - (p_h, \nabla \cdot v_h) = 0, \quad (6.69)$$

$$(\nabla \cdot \chi_h, q_h) = -(\nabla \cdot z_h, q_h), \quad (6.70)$$

$$\frac{\alpha}{\Delta t}(\mu_h, \psi_h) + \nu_m(\nabla \mu_h, \nabla \psi_h) + (\pi_h, \nabla \cdot \psi_h) = 0, \quad (6.71)$$

$$(\nabla \cdot \mu_h, r_h) = -(\nabla \cdot \omega_h, r_h). \quad (6.72)$$

3. Find $(\varphi_h, \theta_h) \in (X_h, X_h)$ *satisfying,* $\forall (v_h, \psi_h) \in (X_h, X_h)$,

$$\frac{\alpha}{\Delta t}(\varphi_h, v_h) + \nu(\nabla\varphi_h, \nabla v_h) = -(p_h, \nabla \cdot v_h), \tag{6.73}$$

$$\frac{\alpha}{\Delta t}(\theta_h, \psi_h) + \nu_m(\nabla\theta_h, \nabla\psi_h) = -(\pi_h, \nabla \cdot \psi_h). \tag{6.74}$$

4. Find $(\gamma_h, \sigma_h) \in (X_h, X_h)$ *satisfying,* $\forall (v_h, \psi_h) \in (X_h, X_h)$,

$$\begin{aligned}\frac{\alpha}{\Delta t}(\gamma_h, v_h) + \nu(\nabla\gamma_h, \nabla v_h) = \frac{\alpha}{\Delta t}(\varphi_h, v_h) + \nu(\nabla\varphi_h, \nabla v_h)\\ +(\mathcal{U} \cdot \nabla\varphi_h, v_h) - (\mathcal{B} \cdot \nabla\theta_h, v_h),\end{aligned} \tag{6.75}$$

$$\begin{aligned}\frac{\alpha}{\Delta t}(\sigma_h, \psi_h) + \nu_m(\nabla\sigma_h, \nabla\psi_h) = \frac{\alpha}{\Delta t}(\theta_h, \psi_h) + \nu_m(\nabla\theta_h, \nabla\psi_h)\\ +(\mathcal{U} \cdot \nabla\theta_h, \psi_h) - (\mathcal{B} \cdot \nabla\varphi_h, \psi_h).\end{aligned} \tag{6.76}$$

5. Find $(\phi_h, \delta_P, \kappa_h, \delta_\lambda) \in (X_h, Q_h, X_h, Q_h)$ *satisfying,*

$\forall (v_h, q_h, \psi_h, r_h) \in (X_h, Q_h, X_h, Q_h)$,

$$\frac{\alpha}{\Delta t}(\phi_h, v_h) + \nu(\nabla\phi_h, \nabla v_h) - (\delta_P, \nabla \cdot v_h) = 0, \tag{6.77}$$

$$(\nabla \cdot \phi_h, q_h) = -(\nabla \cdot \gamma_h, q_h), \tag{6.78}$$

$$\frac{\alpha}{\Delta t}(\kappa_h, \psi_h) + \nu_m(\nabla\kappa_h, \nabla\psi_h) + (\delta_\lambda, \nabla \cdot \psi_h) = 0, \tag{6.79}$$

$$(\nabla \cdot \kappa_h, r_h) = -(\nabla \cdot \sigma_h, r_h). \tag{6.80}$$

6. *Find* $(u_h, B_h) \in (X_h, X_h)$ *satisfying,* $\forall (v_h, \psi_h) \in (X_h, X_h)$,

$$\frac{\alpha}{\Delta t}(u_h, v_h) + \nu(\nabla u_h, \nabla v_h) + (\mathcal{U}\cdot\nabla u_h, v_h) - (\mathcal{B}\cdot\nabla B_h, v_h) = \frac{\alpha}{\Delta t}(z_h, v_h) + \nu(\nabla z_h, \nabla v_h) + (\mathcal{U}\cdot\nabla z_h, v_h) - (\mathcal{B}\cdot\nabla\omega_h, v_h) + (\delta_P, \nabla\cdot v_h), \tag{6.81}$$

$$\frac{\alpha}{\Delta t}(B_h, \psi_h) + \nu_m(\nabla B_h, \nabla\psi_h) + (\mathcal{U}\cdot\nabla B_h, \psi_h) - (\mathcal{B}\cdot\nabla u_h, \psi_h) = \frac{\alpha}{\Delta t}(\omega_h, \psi_h) + \nu_m(\nabla\omega_h, \nabla\psi_h) + (\mathcal{U}\cdot\nabla\omega_h, \psi_h) - (\mathcal{B}\cdot\nabla z_h, \psi_h) - (\delta_\lambda, \nabla\cdot\psi_h). \tag{6.82}$$

7. *Recover* P_h, λ_h *by setting* $P_h = \delta_P + P^n$ *and* $\lambda_h = \delta_\lambda + \lambda^n$.

We now present a theorem for the error in YUPC scheme.

Theorem 7. *Let* $\hat{u}_h, \hat{P}_h, \hat{B}_h$ *and* $\hat{\lambda}_h$ *be the unapproximated solutions to* (6.12)-(6.15), *with* $\|\hat{P}_h - P^n\| \le C_P\Delta t$, $\|\hat{\lambda}_h - \lambda^n\| \le C_\lambda\Delta t$. *Besides, let* u_h, P_h, B_h, λ_h *be the solutions to Algorithm 6.3.1, i.e., the Yosida-updates pressure corrected solutions. The error satisfies the following bound:*

$$\|\hat{u}_h - u_h\| + \|\hat{B}_h - B_h\| \le \frac{2C_i^4\Delta t^4}{\beta h^4}\Big(C_U + C_B\Big)^2\Big(C_P + C_\lambda\Big)\Big(2C_{PF} + \frac{C_* C_i\Delta t}{h}\Big),$$

where $C_* := \min\{\nu, \nu_m\}$.

Proof. The proof of this theorem is long and technical. However, it follows very closely the structure of the NSE proof, but handling the Maxwell equation just as is done above for the YU analysis. Thus, we omit the proof. □

Just as in the YU case, the stability can be proven using the convergence estimate.

Corollary 2 (Stability of the YUPC scheme)**.** . *Suppose* $\tilde{f} = f + \frac{1}{\Delta t}u^n$, $\tilde{g} = g + \frac{1}{\Delta t}B^n$,

and $\Delta t \leq O(h^{5/4}) \leq O(h)$. *Then the YUPC method is stable, and solutions satisfies*

$$\frac{1}{\Delta t}\left(\|u_h\|^2 - \|u^n\|^2 + \|u_h - u^n\|^2\right) + \frac{1}{\Delta t}\left(\|B_h\|^2 - \|B^n\|^2 + \|B_h - B^n\|^2\right) + \nu\|\nabla u_h\|^2 + \nu_m\|\nabla B_h\|^2 \leq C(data).$$

6.4 Numerical experiment

We now present a numerical experiment to test the predicted convergence rates of the theory above. For the test, we use the viscous Orszag-Tang problem, which is a benchmark MHD test problem studied in [30, 66]. The domain is the periodic box $(0, 2\pi)^2$, and the setup is as follows. We take as the initial conditions

$$u_0 = \langle -\sin(y+2), \sin(x+1.4)\rangle^T, \quad B_0 = \langle -\frac{1}{3}\sin(y+2), \frac{2}{3}\sin(2x+3)\rangle^T,$$

add no external forcing, $f = \nabla \times g = 0$, and allow the flow to evolve. We choose $\nu = \nu_m = 0.01$.

In all of our computations below, we use (P_2, P_1^{disc}) elements for (u_h, p_h) and (B_h, λ_h).

6.4.1 Numerical experiment : Convergence rates

To compute the predicted convergence rates, we compute the unapproximated method for four time steps, the YU method for four time steps, and also for comparison the classical Yosida method (Y), and then compare solutions in the $L^2(\Omega)$ norm. For the first time step of all methods, we use Crank-Nicolson time stepping with an exact linear solver. The subsequent steps use BDF2, and the various solvers. To test the negative scaling with respect to h, we also compute on three different meshes:

barycenter refinements of uniform meshes with $h = \frac{L}{8}, \frac{L}{16}, \frac{L}{32}$, with $L = 2\pi$.

The table below shows the errors in the Y and YU approximations, and the corresponding convergence rates with respect to Δt. Convergence of the usual Y method is clearly observed to be second order. For YU, we observe essentially third order, but with a slight deterioration in the rate as Δt gets smaller. However, this deterioration does not occur until errors approach 10^{-8}, which is at the level where linear solver error can be a factor (10^{-10} is the tolerance for the CG Schur complement solver). We note that YU is clearly much more accurate than Y, and we stress that these two methods require the same amount of work to solve and have exactly the same system matrices.

Regarding the negative scaling with respect to h from the analysis, we do not see a deterioration in the errors as h decreases. However, we do observe a reduced scaling with respect to Δt, which could be related to this issue since the analysis does allow for a tradeoff between better scaling with respect to h and a reduced scaling with respect to Δt. However, the reduced order of convergence is only observed when errors are near .

6.5 Conclusion

In this chapter, we have proposed, analyzed and tested the YU method (and with pressure correction) for MHD. The method provides for very efficient solves of the block saddle point linear systems that arise in MHD, as they decompose the nonsymmetric block Schur complement into 2 Stokes-type Schur complements that are the same at each time step. The method is proven to be third order (fourth order with pressure correction) with respect to Δt, and the analysis is done using the natural norms of the problem. Numerical test was given that show the effectiveness

$h = \frac{L}{8}$

Δt	$\|u_{YU} - u_h\|$	Rate	$\|B_{YU} - B_h\|$	Rate	$\|u_Y - u_h\|$	Rate	$\|B_Y - B_h\|$	Rate
$\frac{0.2}{4}$	2.128e-4		1.232e-4		3.348e-3		1.530e-3	
$\frac{0.2}{8}$	3.137e-5	2.76	1.860e-5	2.73	9.098e-4	1.88	4.218e-4	1.86
$\frac{0.2}{16}$	4.473e-6	2.81	3.103e-6	2.58	2.381e-4	1.93	1.144e-4	1.88
$\frac{0.2}{32}$	6.368e-7	2.81	5.542e-7	2.48	6.108e-5	1.96	3.059e-5	1.90
$\frac{0.2}{64}$	8.918e-8	2.84	9.229e-8	2.57	1.550e-5	1.98	8.102e-6	1.92
$\frac{0.2}{128}$	1.218e-8	2.87	1.400e-8	2.72	3.910e-6	1.99	2.119e-6	1.93
$\frac{0.2}{256}$	1.622e-9	2.91	1.972e-9	2.83	9.826e-7	1.99	5.464e-7	1.96

$h = \frac{L}{16}$

Δt	$\|u_{YU} - u_h\|$	Rate	$\|B_{YU} - B_h\|$	Rate	$\|u_Y - u_h\|$	Rate	$\|B_Y - B_h\|$	Rate
$\frac{0.2}{4}$	2.075e-4		2.075e-4		3.336e-3		1.501e-3	
$\frac{0.2}{8}$	3.100e-5	2.74	1.698e-5	3.61	9.088e-4	1.88	4.138e-4	1.86
$\frac{0.2}{16}$	4.114e-6	2.91	1.975e-6	3.10	2.377e-4	1.93	1.106e-4	1.90
$\frac{0.2}{32}$	5.597e-7	2.88	3.215e-7	2.62	6.087e-5	1.96	2.880e-5	1.94
$\frac{0.2}{64}$	7.817e-8	2.84	6.055e-8	2.41	1.541e-5	1.98	7.368e-6	1.97
$\frac{0.2}{128}$	1.110e-8	2.82	1.077e-8	2.49	3.877e-6	1.99	1.869e-6	1.98
$\frac{0.2}{256}$	1.562e-9	2.83	1.732e-9	2.64	9.726e-7	1.99	4.721e-7	1.98

$h = \frac{L}{32}$

Δt	$\|u_{YU} - u_h\|$	Rate	$\|B_{YU} - B_h\|$	Rate	$\|u_Y - u_h\|$	Rate	$\|B_Y - B_h\|$	Rate
$\frac{0.2}{4}$	1.857e-5		7.683e-5		3.328e-3		1.484e-3	
$\frac{0.2}{8}$	2.878e-5	-0.63	1.301e-5	2.56	9.080e-4	1.87	4.122e-4	1.85
$\frac{0.2}{16}$	3.942e-6	2.87	1.516e-6	3.10	2.377e-4	1.93	1.104e-4	1.90
$\frac{0.2}{32}$	5.213e-7	2.92	1.815e-7	3.06	6.086e-5	1.97	2.873e-5	1.94
$\frac{0.2}{64}$	6.822e-8	2.93	2.762e-8	2.72	1.540e-5	1.98	7.337e-6	1.97
$\frac{0.2}{128}$	9.027e-9	2.92	5.105e-9	2.44	3.875e-6	1.99	1.854e-6	1.98
$\frac{0.2}{256}$	1.234e-9	2.87	9.695e-10	2.40	9.718e-7	2.00	4.662e-7	1.99

of the method.

There are at least two potential future directions for research that comes from this study. The first is testing the YU and YUPC methods efficiency and accuracy against various solvers of MHD systems that do not approximate, but solve with preconditioned iterative solvers. Second, the analysis predicts a potential negative scaling of h^{-3} in the convergence, however the numerical test showed no negative scaling in h. Even for the YU method applied to the incremental NSE, the same h^{-3} is predicted by the analysis, but only a $h^{-1/2}$ is observed in numerical tests [86]. Further study should be done here to see if a sharper analysis with respect to h can be discovered.

Chapter 7

General Conclusions and Directions for Future Research

We proposed, analyzed and tested efficient, decoupled and fully discrete numerical schemes for MHD in Elsässer variables. We proved their stability and convergence theorems, showed the schemes performed well on benchmark problems. Unconditional stability and convergence of these schemes revealed their superiority over the primitive variable schemes. Our analysis and numerical experiments exhibited the superiority of the proposed higher order scheme over the second method of Li and Trenchea [44, 63].

We also proposed and studied an efficient, decoupled algorithm in Elsässer variables for computing flow ensembles of incompressible MHD flows under uncertainties in initial or boundary data. We proved unconditional stability and convergence of the algorithm, and successfully tested it with two numerical experiments.

For future research, we believe that it is necessary to perform more testing on these schemes to verify that they give solutions very similar to primitive variables

schemes with the same mesh and timestep on a wide range of problems. Then the proposed schemes may be an enabling tool to simulate large scale 3D MHD problems much more efficiently than what is currently possible, since they stably decouples the MHD system into two Oseen problems at each timestep that can be solved simultaneously but the schemes in primitive variables require solving very large coupled linear systems (or excessively small timestep sizes) for stable computations. It is worth exploring for MHD problems with higher Reynolds number, reduced order modeling with large eddy simulation or if the schemes can likely be combined with recent stabilization ideas such as in [98], for more accurate large scale simulations that don't have sufficient resolution to fully resolve all active scales. Also, we can extend our proposed ensemble averaging scheme using the ideas herein to the higher order decoupled MHD scheme proposed in [44], which would involve significantly more challenges in the analysis.

As still in some cases, it remains an open question about the boundary conditions on the Elsässer variables, we proposed, analyzed and tested the YU method (and with pressure correction) for MHD in primitive variables. The method is proven to third order (fourth order with pressure correction) accurate with respect to timestep size. In future, we could test the efficiency and accuracy of the YU and YUPC methods against various solvers for MHD systems that do not approximate, but solve with preconditioned iterative solvers. Further study should be carried out to see if a sharper analysis with respect to h can be discovered. We can also propose, analyze and test YU method (and with pressure correction) for MHD in Elsässer variables in future.

Appendix A

Conditional Stability Analysis of MHD Ensemble Algorithm

In this appendix we define the ensemble eddy viscosity term in a different way [52], where

$$\nu_T(u_h^{'}, t^n) := \mu |u_h^{'n}| \Delta x, \text{ where } |u_h^{'n}| = \max_j |u_{j,h}^{'n}| = \max_j |(u_{j,h}^n)^{'}|,$$

and μ is a tuning parameter. This eddy viscosity term leads to a conditional stability of the proposed Algorithm (5.2.1) with respect to the time step size. The stability theorem and its proof is give below.

Theorem 8. *(Conditional Stability) Suppose* $f_{1,j}, f_{2,j} \in L^\infty(0,T;H^{-1}(\Omega)), v_{j,h}^0, w_{j,h}^0 \in H^1(\Omega)$. *Then for any* $\Delta t \leq \min\left\{\frac{4\mu\Delta x}{\|v_h^{'n}\|_{L^\infty}}, \frac{4\mu\Delta x}{\|w_h^{'n}\|_{L^\infty}}\right\}$, *solutions to* (5.12)-(5.13) *satisfy*

$$\begin{aligned}
&\|v_{j,h}^M\|^2 + \|w_{j,h}^M\|^2 + \frac{(\nu-\nu_m)^2}{2(\nu+\nu_m)}\Delta t\left(\|\nabla v_{j,h}^M\|^2 + \|\nabla w_{j,h}^M\|^2\right) \\
&\quad \leq \|v_{j,h}^0\|^2 + \|w_{j,h}^0\|^2 + \frac{(\nu-\nu_m)^2}{2(\nu+\nu_m)}\Delta t\left(\|\nabla v_{j,h}^0\|^2 + \|\nabla w_{j,h}^0\|^2\right) \\
&\quad + \frac{\nu+\nu_m}{2\nu\nu_m}\Delta t\sum_{n=0}^{M-1}\left(\|f_{1,j}(t^{n+1})\|_{-1}^2 + \|f_{2,j}(t^{n+1})\|_{-1}^2\right).
\end{aligned}$$

Proof. Choose $\chi_h = v_{j,h}^{n+1}$ in (5.14), the first nonlinear term vanishes and we obtain

$$\begin{aligned}\frac{1}{\Delta t}(v_{j,h}^{n+1} - v_{j,h}^{n}, v_{j,h}^{n+1}) + \frac{\nu+\nu_m}{2}\left(\nabla v_{j,h}^{n+1}, \nabla v_{j,h}^{n+1}\right) \\ + \frac{\nu-\nu_m}{2}\left(\nabla w_{j,h}^{n}, \nabla v_{j,h}^{n+1}\right) + \left((w_{j,h}^{n} - < w_h >^n)\cdot\nabla v_{j,h}^{n}, v_{j,h}^{n+1}\right) \\ + \left(2\nu_T(w_h^{'}, t^n)\nabla v_{j,h}^{n+1}, \nabla v_{j,h}^{n+1}\right) = \left(f_{1,j}(t^{n+1}), v_{j,h}^{n+1}\right). \end{aligned} \tag{A.1}$$

Using the polarization identity and that

$$\begin{aligned}\left(2\nu_T(w_h^{'}, t^n)\nabla v_{j,h}^{n+1}, \nabla v_{j,h}^{n+1}\right) &= (2\mu\Delta x|w_h^{'n}|\nabla v_{j,h}^{n+1}, \nabla v_{j,h}^{n+1}) \\ &= \int_\Omega 2\mu\Delta x|w_h^{'n}|\,|\nabla v_{j,h}^{n+1}|^2 dx \\ &= 2\mu\Delta x\|\sqrt{|w_h^{'n}|}\,|\nabla v_{j,h}^{n+1}|\|^2,\end{aligned}$$

we get

$$\begin{aligned}\frac{1}{2\Delta t}\left(\|v_{j,h}^{n+1} - v_{j,h}^{n}\|^2 + \|v_{j,h}^{n+1}\|^2 - \|v_{j,h}^{n}\|^2\right) + \frac{\nu+\nu_m}{2}\|\nabla v_{j,h}^{n+1}\|^2 \\ + \frac{\nu-\nu_m}{2}\left(\nabla w_{j,h}^{n}, \nabla v_{j,h}^{n+1}\right) + \left((w_{j,h}^{n} - < w_h >^n)\cdot\nabla v_{j,h}^{n}, v_{j,h}^{n+1}\right) \\ + 2\mu\Delta x\|\sqrt{|w_h^{'n}|}\,|\nabla v_{j,h}^{n+1}|\|^2 = \left(f_{1,j}^{n+1}, v_{j,h}^{n+1}\right)\end{aligned} \tag{A.2}$$

Similarly, choose $l_h = w_{j,h}^{n+1}$ in (5.15), we have

$$\begin{aligned}\frac{1}{2\Delta t}\left(\|w_{j,h}^{n+1} - w_{j,h}^{n}\|^2 + \|w_{j,h}^{n+1}\|^2 - \|w_{j,h}^{n}\|^2\right) + \frac{\nu+\nu_m}{2}\|\nabla w_{j,h}^{n+1}\|^2 \\ + \frac{\nu-\nu_m}{2}\left(\nabla v_{j,h}^{n}, \nabla w_{j,h}^{n+1}\right) + \left((v_{j,h}^{n} - < v_h >^n)\cdot\nabla w_{j,h}^{n}, w_{j,h}^{n+1}\right) \\ + 2\mu\Delta x\|\sqrt{|v_h^{'n}|}\,|\nabla w_{j,h}^{n+1}|\|^2 = \left(f_{2,j}^{n+1}, w_{j,h}^{n+1}\right).\end{aligned} \tag{A.3}$$

Adding equations (A.2) and (A.3) yields

$$\begin{aligned}
&\frac{1}{2\Delta t}\Big(\|v_{j,h}^{n+1}-v_{j,h}^{n}\|^2+\|v_{j,h}^{n+1}\|^2-\|v_{j,h}^{n}\|^2+\|w_{j,h}^{n+1}-w_{j,h}^{n}\|^2\\
&\quad+\|w_{j,h}^{n+1}\|^2-\|w_{j,h}^{n}\|^2\Big)+\frac{\nu+\nu_m}{2}\left(\|\nabla v_{j,h}^{n+1}\|^2+\|\nabla w_{j,h}^{n+1}\|^2\right)\\
&\quad+\frac{\nu-\nu_m}{2}\left\{\left(\nabla w_{j,h}^{n},\nabla v_{j,h}^{n+1}\right)+\left(\nabla v_{j,h}^{n},\nabla w_{j,h}^{n+1}\right)\right\}+\left((w_{j,h}^{n}-<w_h>^{n})\cdot\nabla v_{j,h}^{n},v_{j,h}^{n+1}\right)\\
&\quad+\left((v_{j,h}^{n}-<v_h>^{n})\cdot\nabla w_{j,h}^{n},w_{j,h}^{n+1}\right)+2\mu\Delta x\|\sqrt{|w_h^{'n}|}\,|\nabla v_{j,h}^{n+1}|\|^2\\
&\quad+2\mu\Delta x\|\sqrt{|v_h^{'n}|}\,|\nabla w_{j,h}^{n+1}|\|^2=\left(f_{1,j}^{n+1},v_{j,h}^{n+1}\right)+\left(f_{2,j}^{n+1},w_{j,h}^{n+1}\right).
\end{aligned}\tag{A.4}$$

Using Cauchy-schwarz's inequality and

$$\begin{aligned}
\left((v_{j,h}^{n}-<v_h>^{n})\cdot\nabla w_{j,h}^{n},w_{j,h}^{n+1}\right)&=(v_{j,h}^{'n}\cdot\nabla w_{j,h}^{n+1},-w_{j,h}^{n})\\
&=(v_{j,h}^{'n}\cdot\nabla w_{j,h}^{n+1},w_{j,h}^{n+1}-w_{j,h}^{n})\\
&\le\int_\Omega|v_{j,h}^{'n}|\;|\nabla w_{j,h}^{n+1}|\;|w_{j,h}^{n+1}-w_{j,h}^{n}|d\Omega\\
&\le\|\sqrt{|v_h^{'n}|}\,|\nabla w_{j,h}^{n+1}|\,\|\;\|\sqrt{|v_h^{'n}|}\,|w_{j,h}^{n+1}-w_{j,h}^{n}|\,\|
\end{aligned}$$

yields

$$\begin{aligned}
&\frac{1}{2\Delta t}\Big(\|v_{j,h}^{n+1}-v_{j,h}^{n}\|^2+\|v_{j,h}^{n+1}\|^2-\|v_{j,h}^{n}\|^2\\
&\quad+\|w_{j,h}^{n+1}-w_{j,h}^{n}\|^2+\|w_{j,h}^{n+1}\|^2-\|w_{j,h}^{n}\|^2\Big)+\frac{\nu+\nu_m}{2}\left(\|\nabla v_{j,h}^{n+1}\|^2+\|\nabla w_{j,h}^{n+1}\|^2\right)\\
&\quad+2\mu\Delta x\|\sqrt{|w_h^{'n}|}\,|\nabla v_{j,h}^{n+1}|\|^2+2\mu\Delta x\|\sqrt{|v_h^{'n}|}\,|\nabla w_{j,h}^{n+1}|\|^2\\
&\quad\le\frac{|\nu-\nu_m|}{2}\left(\|\nabla w_{j,h}^{n}\|\,\|\nabla v_{j,h}^{n+1}\|+\|\nabla v_{j,h}^{n}\|\,\|w_{j,h}^{n+1}\|\right)\\
&\quad+\|\sqrt{|v_h^{'n}|}\,|\nabla w_{j,h}^{n+1}|\,\|\;\|\sqrt{|v_h^{'n}|}\,|w_{j,h}^{n+1}-w_{j,h}^{n}|\,\|+\|f_{1,j}^{n+1}\|_{-1}\|\nabla v_{j,h}^{n+1}\|\\
&\quad+\|\sqrt{|w_h^{'n}|}\,|\nabla v_{j,h}^{n+1}|\,\|\;\|\sqrt{|w_h^{'n}|}\,|v_{j,h}^{n+1}-v_{j,h}^{n}|\,\|+\|f_{2,j}^{n+1}\|_{-1}\|\nabla w_{j,h}^{n+1}\|
\end{aligned}\tag{A.5}$$

Using the version of Young's inequality $ab \leq \frac{\epsilon}{2}a^2 + \frac{1}{2\epsilon}b^2$ with $\epsilon = 4\mu\Delta x$ and $\epsilon = \frac{\nu+\nu_m}{2}$ we can write,

$\frac{|\nu-\nu_m|}{2}|\|\nabla w_{j,h}^n\|\,\|\nabla v_{j,h}^{n+1}\| \leq \frac{\nu+\nu_m}{4}\|\nabla v_{j,h}^{n+1}\|^2 + \frac{(\nu-\nu_m)^2}{4(\nu+\nu_m)}\|\nabla w_{j,h}^n\|^2$

$$\|\sqrt{|v_h'^n|}\,|\nabla w_{j,h}^{n+1}|\,\|\;\;\|\sqrt{|v_h'^n|}\,|w_{j,h}^{n+1}-w_{j,h}^n|\,\| \leq 2\mu\Delta x\|\sqrt{|v_h'^n|}\,|\nabla w_{j,h}^{n+1}|\,\|^2 + \frac{1}{8\mu\Delta x}\|\sqrt{|v_h'^n|}\,|w_{j,h}^{n+1}-w_{j,h}^n|\,\|^2.$$

Which reduces (A.5) to

$$\begin{aligned}\frac{1}{2\Delta t}\Big(\|v_{j,h}^{n+1}-v_{j,h}^n\|^2 + \|v_{j,h}^{n+1}\|^2 - \|v_{j,h}^n\|^2 + \|w_{j,h}^{n+1}-w_{j,h}^n\|^2 + \|w_{j,h}^{n+1}\|^2 - \|w_{j,h}^n\|^2\Big)\\ + \frac{\nu+\nu_m}{4}\left(\|\nabla v_{j,h}^{n+1}\|^2 + \|\nabla w_{j,h}^{n+1}\|^2\right) \leq \frac{(\nu-\nu_m)^2}{4(\nu+\nu_m)}\left(\|\nabla w_{j,h}^n\|^2 + \|\nabla v_{j,h}^n\|^2\right)\\ + \frac{1}{8\mu\Delta x}\left(\|\sqrt{|v_h'^n|}\,|w_{j,h}^{n+1}-w_{j,h}^n|\,\|^2 + \|\sqrt{|w_h'^n|}\,|v_{j,h}^{n+1}-v_{j,h}^n|\,\|^2\right)\\ + \|f_{1,j}^{n+1}\|_{-1}\|\nabla v_{j,h}^{n+1}\| + \|f_{2,j}^{n+1}\|_{-1}\|\nabla w_{j,h}^{n+1}\|. \qquad \text{(A.6)}\end{aligned}$$

Again, using Young's inequality $ab \leq \frac{\epsilon}{2}a^2 + \frac{1}{2\epsilon}b^2$ with $\epsilon = \frac{2\nu\nu_m}{\nu+\nu_m}$, we have

$$\|f_{1,j}^{n+1}\|_{-1}\|\nabla v_{j,h}^{n+1}\| \leq \frac{\nu\nu_m}{\nu+\nu_m}\|\nabla v_{j,h}^{n+1}\|^2 + \frac{\nu+\nu_m}{4\nu\nu_m}\|f_{1,j}^{n+1}\|_{-1}^2.$$

Which reduces (A.6) to

$$\begin{aligned}\frac{1}{2\Delta t}\Big(\|v_{j,h}^{n+1}-v_{j,h}^n\|^2 + \|v_{j,h}^{n+1}\|^2 - \|v_{j,h}^n\|^2 + \|w_{j,h}^{n+1}-w_{j,h}^n\|^2 + \|w_{j,h}^{n+1}\|^2 - \|w_{j,h}^n\|^2\Big)\\ + \frac{(\nu-\nu_m)^2}{4(\nu+\nu_m)}\Big(\|\nabla v_{j,h}^{n+1}\|^2 - \|\nabla v_{j,h}^n\|^2 + \|\nabla w_{j,h}^{n+1}\|^2 - \|\nabla w_{j,h}^n\|^2\Big)\\ \leq \frac{\|v_h'^n\|_{L^\infty}}{8\mu\Delta x}\|w_{j,h}^{n+1}-w_{j,h}^n\|^2 + \frac{\|w_h'^n\|_{L^\infty}}{8\mu\Delta x}\|v_{j,h}^{n+1}-v_{j,h}^n\|^2\\ + \frac{\nu+\nu_m}{4\nu\nu_m}\|f_{1,j}^{n+1}\|_{-1}^2 + \frac{\nu+\nu_m}{4\nu\nu_m}\|f_{2,j}^{n+1}\|_{-1}^2. \qquad \text{(A.7)}\end{aligned}$$

We can rewrite (A.7) as

$$\left(\frac{1}{2\Delta t}-\frac{\|w_h'^n\|_{L^\infty}}{8\mu\Delta x}\right)\|v_{j,h}^{n+1}-v_{j,h}^n\|^2+\left(\frac{1}{2\Delta t}-\frac{\|v_h'^n\|_{L^\infty}}{8\mu\Delta x}\right)\|w_{j,h}^{n+1}-w_{j,h}^n\|^2$$
$$+\frac{1}{2\Delta t}\left(\|v_{j,h}^{n+1}\|^2-\|v_{j,h}^n\|^2+\|w_{j,h}^{n+1}\|^2-\|w_{j,h}^n\|^2\right)$$
$$+\frac{(\nu-\nu_m)^2}{4(\nu+\nu_m)}\left(\|\nabla v_{j,h}^{n+1}\|^2-\|\nabla v_{j,h}^n\|^2+\|\nabla w_{j,h}^{n+1}\|^2-\|\nabla w_{j,h}^n\|^2\right)$$
$$\leq\frac{\nu+\nu_m}{4\nu\nu_m}\|f_{1,j}^{n+1}\|_{-1}^2+\frac{\nu+\nu_m}{4\nu\nu_m}\|f_{2,j}^{n+1}\|_{-1}^2 \tag{A.8}$$

we choose, $\Delta t\leq\min\left\{\frac{4\mu\Delta x}{\|v_h'^n\|_{L^\infty}},\frac{4\mu\Delta x}{\|w_h'^n\|_{L^\infty}}\right\}$, to make $\frac{1}{2\Delta t}-\frac{\|w_h'^n\|_{L^\infty}}{8\mu\Delta x}>0$, and $\frac{1}{2\Delta t}-\frac{\|v_h'^n\|_{L^\infty}}{8\mu\Delta x}>0$, and the drop the non-negative terms from left. Next, multiply the both sides by $2\Delta t$ and sum over time steps:

$$\|v_{j,h}^M\|^2+\|w_{j,h}^M\|^2+\frac{\Delta t(\nu-\nu_m)^2}{2(\nu+\nu_m)}\left(\|\nabla v_{j,h}^M\|^2+\|\nabla w_{j,h}^M\|^2\right)\leq\|v_{j,h}^0\|^2+\|w_{j,h}^0\|^2$$
$$+\frac{\Delta t(\nu-\nu_m)^2}{2(\nu+\nu_m)}\left(\|\nabla v_{j,h}^0\|^2+\|\nabla w_{j,h}^0\|^2\right)+\frac{\nu+\nu_m}{2\nu\nu_m}\Delta t\sum_{n=0}^{M-1}\left(\|f_{1,j}^{n+1}\|_{-1}^2+\|f_{2,j}^{n+1}\|_{-1}^2\right) \tag{A.9}$$

This completes the proof. □

Bibliography

[1] https://en.wikipedia.org/wiki/magnetohydrodynamic_generator.

[2] https://en.wikipedia.org/wiki/magnetohydrodynamics.

[3] https://en.wikipedia.org/wiki/solar_wind.

[4] http://www.claymath.org/millennium-problems/navier-stokes-equation.

[5] http://www.intellectualventureslab.com/invent/magnetohydrodynamic-pump.

[6] M. Akbas, S. Kaya, M. Mohebujjaman, and L. Rebholz. Numerical analysis and testing of a fully discrete, decoupled penalty-projection algorithm for MHD in Elsässer variable. *International Journal of Numerical Analysis and Modeling*, 13(1):90–113, 2016.

[7] M. Akbas, S. Kaya, and L. G. Rebholz. On the stability at all times of linearly extrapolated BDF2 timestepping for multiphysics incompressible flow problems. *Numerical Methods for Partial Differential Equations*, in press, 2016.

[8] M. Akbas, M. Mohebujjaman, L. G. Rebholz, and M. Xiao. High order algebraic splitting for magnetohydrodynamics simulation. *Journal of Computational and Applied Mathematics*, 321:128–142, 2017.

[9] M. Akbas, L. Rebholz, and F. Tone. A note on the importance of mass conservation in long-time stability of Navier-Stokes equations. *Applied Mathematics Letters*, 45:98–102, 2015.

[10] O. Al-Habahbeh, M. Al-Saqqa, M. Safi, and T. A. Khater. Review of magnetohydrodynamic pump applications. *Alexandria Engineering Journal*, 55:1347–1358, 2016.

[11] H. Alfvèn. Existence of Electromagnetic-Hydrodynamic Waves. *Nature*, 150:405–406, 1942.

[12] P. Angot, M. Jobelin, and J. Latche. Error analysis of the penalty-projection method for the time dependent Stokes equations. *Int. J. Finite Vol.*, 6:1–26, 2009.

[13] D. Arnold and J. Qin. Quadratic velocity/linear pressure Stokes elements. In R. Vichnevetsky, D. Knight, and G. Richter, editors, *Advances in Computer Methods for Partial Differential Equations VII*, pages 28–34. IMACS, 1992.

[14] W. Bangerth, D. Davydov, T. Heister, L. Heltai, G. Kanschat, M. Kronbichler, M. Maier, B. Turcksin, and D. Wells. The `deal.II` library, version 8.4. *Journal of Numerical Mathematics*, 24(3):135–141, 2016.

[15] L. Barleon, V. Casal, and L. Lenhart. MHD flow in liquid-metal-cooled blankets. *Fusion Engineering and Design*, 14:401–412, 1991.

[16] J. Barrow, R. Maartens, and C. Tsagas. Cosmology with inhomogeneous magnetic fields. *Phys. Rep.*, 449:131–171, 2007.

[17] D. Biskamp. *Magnetohydrodynamic Turbulence*. Cambridge University Press, Cambridge, 2003.

[18] P. Bodenheimer, G. Laughlin, M. Rozyczka, and H. Yorke. Numerical methods in astrophysics. *Series in Astronomy and Astrophysics, Taylor & Francis, New York*, 2007.

[19] S. Börm and S. Le Borne. $\mathcal{H}$-LU factorization in preconditioners for augmented Lagrangian and grad-div stabilized saddle point systems. *Internat. J. Numer. Methods Fluids*, 68(1):83–98, 2012.

[20] S. Brenner and L. Scott. *The Mathematical Theory of Finite Element Methods*, volume 15 of *Texts in Applied Mathematics*. Springer-Verlag, New York, 1994.

[21] S. Brenner and L. R. Scott. *The Mathematical Theory of Finite Element Methods*, volume 15 of *Texts in Applied Mathematics*. Springer Science+Business Media, LLC, 2008.

[22] M. Carney, P. Cunningham, J. Dowling, and C. Lee. Predicting probability distributions for surf height using an ensemble of mixture density networks. *International Conference on Machine Learning*, pages 113 – 120, 2005.

[23] J. Cho and E. T. Vishniac. The Anisotropy of Magnetohydrodynamic Alfvénic Turbulence. *The Astrophysical Journal*, 539:273–282, 2000.

[24] P. A. Davidson. An introduction to Magnetohydrodynamics. *Cambridge Texts in Applied Mathematics, Cambridge University Press, Cambridge*, 2001.

[25] M. Dobrowolny, A. Mangeney, and P. Veltri. Fully Developed Anisotropic Hydromagnetic Turbulence in Interplanetary Space. *Physical Review Letters*, 45:144–147, 1980.

[26] E. Dormy and A. Soward. Mathematical aspects of natural dynamos. *Fluid Mechanics of Astrophysics and Geophysics, Grenoble Sciences. Universite Joseph Fourier, Grenoble*, VI, 2007.

[27] W. M. Elsässer. The hydromagnetic equations. *Phys. Rev.*, 79:183, 1950.

[28] J. A. Font. Gerneral relativistic hydrodynamics and magnetohydrodynamics: hyperbolic system in relativistic astrophysics, in hyperbolic problems: theory, numerics, applications. *Springer, Berlin*, pages 3–17, 2008.

[29] C. J. Freitas. The issue of numerical uncertainty. *Applied Mathematical Modelling*, 26:237–248, 2002.

[30] H. Friedel, R. Grauer, and C. Marliani. Adaptive mesh refinement for singular current sheets in incompressible magnetohydrodynamic flows. *Journal of Computational Physics*, 134:190–198, 1997.

[31] S. Galtier, S. V. Nazarenko, A. C. Newell, and A. Pouquet. A weak turbulence theory for incompressible magnetohydrodynamics. *J. Plasma Physics*, 63(5):447–488, 2000.

[32] P. Gervasio, F. Saleri, and A. Veneziani. Algebraic fractional-step schemes with spectral methods for the incompressible Navier-Stokes equations. *Journal of Computational Physics*, 214:347–365, 2006.

[33] R. Ghanem and P. Spano. *Stochastic Finite Elements: A Spectral Approach*. Dover Publications,, 2003.

[34] V. Girault and P.-A.Raviart. *Finite element methods for Navier-Stokes equations: Theory and Algorithms*. Springer-Verlag, 1986.

[35] V. Girault and P.-A. Raviart. *Finite element approximation of the Navier-Stokes equations*, volume 749 of *Lecture Notes in Mathematics*. Springer-Verlag, Berlin, 1979.

[36] P. Goldreich and S. Sridhar. Toward a theory of interstellar turbulence. II. Strong Alfvènic turbulence. *Astrophysical Journal*, 438(2):763–775, 1995.

[37] M. Gunzburger. *Finite element methods for viscous incompressible flows: A guide to theory, practice, and algorithm (Computer Science and Scientific Computing*. Academic Press Inc.,Boston,MA, 1989.

[38] M. Gunzburger, N. Jiang, and M. Schneier. An Ensemble-Proper Orthogonal Decomposition Method for the Nonstationary Navier-Stokes Equations. *SIAM Journal on Numerical Analysis*, 55(1):286–304, 2017.

[39] M. D. Gunzburger. *Finite Element Methods For Viscous Incompressible Flows: A Guide to Theory, Practice, and Algorithms*. Academic Press, Boston, 1989.

[40] M. D. Gunzburger. Iterated penalty methods for the stokes and navier-stokes equations. *In: Proceedings from Finite Element Analysis in Fluids Conference, University of Alabama, Huntsville*, pages 1040–1045, 1989.

[41] H. Hashizume. Numerical and experimental research to solve MHD problem in liquid blanket system. *Fusion Engineering and Design*, 81:1431–1438, 2006.

[42] F. Hecht. New development in Freefem++. *Journal of Numerical Mathematics*, 20:251266, 2012.

[43] C. Heiles, A. A. Goodman, C. F. McKee, and E. G. Zweibel. Magnetic fields in star-forming regions: Observations. *In: Protostars and planets III (A93-42937 17-90)*, pages 279–326, 1993.

[44] T. Heister, M. Mohebujjaman, and L. Rebholz. Decoupled, Unconditionally Stable, Higher Order Discretizations for MHD Flow Simulation. *Journal of Scientific Computing*, 71:21–43, 2017.

[45] M. Henriksen and J. Holmen. Algebraic splitting for incompressible Navier-Stokes equations. *Journal of Computational Physics*, 175:438–453, 2002.

[46] J. Heywood and R. Rannacher. Finite-Element approximation of the nonstationary Navier-Stokes problem part IV: error analysis for second-order time discretization. *SIAM J.Numer. Anal.*, 27:353–384, 1990.

[47] W. Hillebrandt and F. Kupka. Interdisciplinary aspects of turbulence. *Lecture Notes in Physics, Springer-Verlag, Berlin*, 756, 2009.

[48] P. S. Iroshnikov. Turbulence of a conducting fluid in a strong magnetic field. *Soviet Astronomy-AJ*, 7(4):566–571, 1964.

[49] N. Jiang. A higher order ensemble simulation algorithm for fluid flows. *Journal of Scientific Computing*, 64:264–288, 2015.

[50] N. Jiang. A second order ensemble method based on a blended BDF timestepping scheme for time dependent Navier-Stokes equations. *Numerical Methods for Partial Differential Equations*, 33(1):34–61, 2017.

[51] N. Jiang and W. Layton. An algorithm for fast calculation of flow ensembles. *International Journal for Uncertainty Quantification*, 4:273–301, 2014.

[52] N. Jiang and W. Layton. Numerical analysis of two ensemble eddy viscosity numerical regularizations of fluid motion. *Numerical Methods for Partial Differential Equations*, 31:630–651, 2015.

[53] M. Jobelin, C. Lapuerta, J.-C. Latche, P. Angot, and B. Piar. A finite element penalty-projection method for incompressible flows. *Journal of Computational Physics*, 217:502–518, 2006.

[54] V. John, A. Linke, C. Merdon, M. Neilan, and L. Rebholz. On the divergence constraint in mixed finite element methods for incompressible flows. *SIAM Review*, in press, 2016.

[55] C. A. Jones. Thermal and compositional convection in the outer core. *Treatise on Geophysics*, 8:131–185, 2007.

[56] R. H. Kraichnan. Inertial-Range Spectrum of Hydromagnetic Turbulence. *Physics of Fluids*, 8(7):1385–1387, 1965.

[57] L. Landau and E. Lifshitz. *Electrodynamics of Continuous Media*. Pergamon Press, Oxford, 1960.

[58] W. Layton. *Introduction to the Numerical Analysis of Incompressible Viscous Flows*. Computational Science and Engineering. Society for Industrial and Applied Mathematics, 2008.

[59] W. Layton. *Introduction to the Numerical Analysis of Incompressible Viscous Flows*. SIAM, 2008.

[60] W. Layton, C. Manica, M. Neda, M. A. Olshanskii, and L. Rebholz. On the accuracy of the rotation form in simulations of the Navier-Stokes equations. *Journal of Computational Physics*, 228(9):3433–3447, 2009.

[61] M. Leutbecher and T. Palmer. Ensemble forecasting. *Journal of Computational Physics*, 227:3515–3539, 2008.

[62] J. M. Lewis. Roots of ensemble forecasting. *Monthly Weather Review*, 133:1865 – 1885, 2005.

[63] Y. Li and C. Trenchea. Partitioned second order method for Magnetohydrodynamics in Elsässer fields. *Technical Report 2015, University of Pittsburgh*.

[64] T. Lin, J. Gilbert, R. Kossowsky, and P. S. U. S. COLLEGE. *Sea-Water Magnetohydrodynamic Propulsion for Next-Generation Undersea Vehicles*. Defense Technical Information Center, 1990.

[65] A. Linke, M. Neilan, L. Rebholz, and N. Wilson. A connection between coupled and penalty projection timestepping schemes with FE spacial discretization for the Navier-Stokes equations. *Journal of Numerical Mathematics*, in press, 2016.

[66] J. Liu and W. Wang. Energy and helicity preserving schemes for hydro- and magnetohydro-dynamics flows with symmetry. *Journal of Computational Physics*, 200:8–33, 2004.

[67] O. L. Maître and O. Knio. *Spectral methods for uncertainty quantification*. Springer, 2010.

[68] E. Marsch. *Turbulence in the Solar Wind. In Klare, G. (Ed.)*, volume 4 of *Reviews in Modern Astronomy*. Springer, Berlin, Heidelberg, 1991.

[69] E. Marsch and C.-Y. Tu. Dynamics of correlation functions with Elsässer variables for inhomogeneous MHD turbulence. *J. Plasma Phys.*, 41:479–491, 1989.

[70] E. Marsch and C. Y. Tu. Non-Gaussian probability distributions of solar wind fluctuations. *Annales Geophysicae*, 12(12):1127–1138, 1994.

[71] W. Martin and M. Xue. Sensitivity analysis of convection of the 24 May 2002 IHOP case using very large ensembles. *Monthly Weather Review*, 134:192–207, 2006.

[72] D. L. Mitchell and D. U. Gubser. Magnetohydrodynamic ship propulsion with superconducting magnets. *Journal of Superconductivity*, 1(4):349–364, 1988.

[73] M. Mohebujjaman and L. Rebholz. An Efficient Algorithm for Computation of MHD Flow Ensembles. *Computational Methods in Applied Mathematics*, 17(1):121–137, 2017.

[74] U. Müller and L. Bühler. *Magnetofluiddynamics in Channels and Containers*. Springer Science & Business Media, 2013.

[75] M. Neda, A. Takhirov, and J. Waters. Ensemble calculations for time relaxation fluid flow models. *Numerical Methods for Partial Differential Equations*, 32(3):757–777, 2016.

[76] M. A. Olshanskii and A. Reusken. Grad-Div stabilization for the Stokes equations. *Math. Comp.*, 73:1699–1718, 2004.

[77] P. Olson. Experimental dynamos and the dynamics of planetary cores. *Annual Review of Earth and Planetary Sciences*, 41:153–181, 2013.

[78] J. D. G. Osorio and S. G. G. Galiano. Building hazard maps of extreme daily rainy events from PDF ensemble, via REA method, on senegal river basin. *Hydrology and Earth System Sciences*, 15:3605 – 3615, 2011.

[79] A. F. Palacios. *The Hamilton-Type Principle in Fluid Dynamics. Fundamentals and Applications to Magnetohydrodynamics, Thermodynamics, and Astrophysics*. Springer, Vienna, 2006.

[80] E. N. Parker. *Spontaneous Current Sheets in Magnetic Fields with Applications to Stellar X-rays*. Oxford University Press, 1994.

[81] E. Peralta. Artificial heart using magnetohydrodynamic propulsion, Jan. 11 2007. WO Patent App. PCT/US2005/032,309.

[82] E. R. Priest. *Solar Magnetohydrodynamics*, volume 21. Springer Netherlands, 1982.

[83] B. Punsly. Black hole gravitohydrodynamics. *Astrophysics and Space Science Library, Springer-Verlag, Berlin, Second Edition*, 355, 2008.

[84] J. Qin and S. Zhang. Stability and approximability of the P1-P0 element for Stokes equation. *International Journal for Numerical Methods in Fluids*, 54(5):497 – 515, 2007.

[85] L. Rebholz and M. Xiao. On reducing the splitting error in Yosida methods for the Navier-Stokes equations with grad-div stabilization. *Computer Methods in Applied Mechanics and Engineering*, 294:259–277, 2015.

[86] L. Rebholz and M. Xiao. Improved accuracy in algebraic splitting methods for Navier-Stokes equations. *SIAM Journal on Scientific Computing*, in press, 2016.

[87] F. Saleri and A. Veneziani. Pressure correction algebraic splitting methods for incompresible Navier-Stokes equations. *SIAM Journal on Numerical Analysis*, 43:174–194, 2006.

[88] P. Schmidt. On a magnetohydrodynamic problem of Euler type. *Journal of Differential Equations*, 74:318, 1988.

[89] M. Sermange and R. Temam. Some mathematical questions related to the mhd equations. *Communications on Pure and Applied Mathematics*, 36(5):635–664, 1983.

[90] J. V. Shebalin, W. H. Matthaeus, and D. Montgomery. Anisotropy in MHD turbulence due to a mean magnetic field. *J. Plasma Physics*, 29(3):525–547, 1983.

[91] S. Smolentsev, R. Moreau, L. Buhler, and C. Mistrangelo. MHD thermofluid issues of liquid-metal blankets: Phenomena and advances. *Fusion Engineering and Design*, 85:1196–1205, 2010.

[92] H. Sohr. *The Navier-Stokes Equations: An Elementary Functional Analytic Approach*. Birkhäuser Advanced Texts Basler Lehrbücher. Birkhäauser Basel, 2001.

[93] R. Temam. *Navier-Stokes equations : theory and numerical analysis*. Elsevier North-Holland, 1979.

[94] C. Trenchea. Unconditional stability of a partitioned IMEX method for magnetohydrodynamic flows. *Applied Mathematics Letters*, 27:97–100, 2014.

[95] F. Unger. *Assisted Circulation 4*. Springer Science & Business Media, 2012.

[96] M. K. Verma. Statistical theory of magnetohydrodynamic turbulence: recent results. *Physics Reports*, 401:229–380, 2004.

[97] I. Veselovsky. Turbulence and waves in the solar wind formation region and the heliosphere. *Astrophysics and Space Science*, 277(1):219–224, 2001.

[98] B. Wacker, D. Arndt, and G. Lube. Nodal-based finite element methods with local projection stabilization for linearized incompressible magnetohydrodynamics. *Computer Methods in Applied Mechanics and Engineering*, 302:170–192, 2016.

[99] N. Wilson, A. Labovsky, and C. Trenchea. High accuracy method for magnetohydrodynamics system in Elsässer variables. *Computational Methods in Applied Mathematics*, 15:97–110, 2015.

[100] G. Yuksel and R. Ingram. Numerical analysis of a finite element, crank-nicolson discretization for mhd flows at small magnetic reynolds numbers. *International Journal of Numerical Analysis and Modeling*, 10(1):74–98, 2013.

[101] S. Zhang. A new family of stable mixed finite elements for the 3d Stokes equations. *Mathematics of Computation*, 74:543–554, 2005.

[102] S. Zhang. Quadratic divergence-free finite elements on Powell-Sabin tetrahedral grids. *Calcolo*, 48(3):211–244, 2011.

[103] E. G. Zweibel and C. Heiles. Magnetic fields in galaxies and beyond. *Nature*, 385:131–136, 1997.